NOVEL SYNTHESIS AND PURIFICATION PROCESS FOR PET-RADIOPHARMACEUTICALS FOR RAPID AND CONVENIENT PRODUCTION

By

SAIKAT KUMAR NANDY
Enrollment Number: CHEM012008040018

BHABHA ATOMIC RESEARCH CENTRE

A thesis submitted to the
Board of Studies in Chemical Science Discipline

In partial fulfillment of requirements

For the Degree of

DOCTOR OF PHILOSOPHY
of

HOMI BHABHA NATIONAL INSTITUTE

February, 2013

Homi Bhabha National Institute
Recommendations of the Viva Voce Board

As members of the Viva Voce Board, we certify that we have read the dissertation prepared by **Saikat Kumar Nandy** entitled **Novel Synthesis and Purification Process for PET-Radiopharmaceuticals for Rapid and Convenient Production** and recommend that it may be accepted as fulfilling the dissertation requirement for the Degree of Doctor of Philosophy.

Date:

……..

Chairman: Dr. V. Venugopal

Date:

……..

External Examiner:

Date:

……

Guide /Convener: Dr. M.G.R. Rajan

Date:

……..

Member: Dr. Meera Venkatesh

Date:

……..

Member: Dr. S. Chattopadhyay

Date:

……..

Member: Dr. Sharmila Banerjee

Final approval and acceptance of this dissertation is contingent upon the candidate's submission of the final copies of the dissertation to HBNI.

We hereby certify that we have read this dissertation prepared under my direction and recommend that it may be accepted as fulfilling the dissertation requirement.

Date :

Place: Mumbai

Prof. (Dr.) M.G.R.Rajan
(Guide)

STATEMENT BY AUTHOR

This dissertation has been submitted in partial fulfillment of requirements for an advanced degree at Homi Bhabha National Institute (HBNI) and is deposited in the Library to be made available to borrowers under rules of the HBNI.

Brief quotations from this dissertation are allowable without special permission, provided that accurate acknowledgement of source is made. Requests for permission for extended quotation from or reproduction of this manuscript in whole or in part may be granted by the Competent Authority of HBNI when in his or her judgment the proposed use of the material is in the interests of scholarship. In all other instances, however, permission must be obtained from the author.

Saikat Kumar Nandy

DECLARATION

I, hereby declare that the investigation presented in the thesis has been carried out by me. The work is original and has not been submitted earlier as a whole or in part for a degree / diploma at this or any other Institution / University.

Saikat Kumar Nandy

Dedicated to my Daughter, Wife and Parents

ACKNOWLEDGEMENTS

I wish to record my deep sense of gratitude and sincere thanks to my guide Prof. M.G.R.Rajan of Bhabha Atomic Research Centre (BARC), for his guidance, keen interest, and supports throughout my entire research tenure. I am grateful to him for critically reviewing this thesis.

It is my great privilege to acknowledge Dr. N. V. Krishnamurthy and Dr. A. Korde of Radiopharmaceuticals Division, BARC for their valuable scientific suggestions during the course of this research work.

It is my great pleasure to thank Dr. V. Rangarajan, Head, Bio-Imaging Unit, Tata Memorial Hospital and all his tem members for their help during PET/CT imaging of animals.

Chairman (Prof. V.Venugopal) and members [Prof. (Mrs) Meera Venkatesh, Prof. S. Chattopadhyay, Prof. (Mrs) Sharmila Banerjee] of the doctorial committee are gratefully acknowledged for their critical review and suggestions during progress review and pre-synopsis viva-voce.

It is my pleasure to acknowledge the help rendered by all members of the RMC, BARC at different times. I wish to thank my ex-colleague Mr. D. Y. Mohite, Dr. Tapas Das, RPhD, BARC and Dr. Sisir Kumar Sarkar, BRIT for their moral support, diversified help.

I wish to express my sincere gratitude and indebtedness to my parents, father-in-law, and other family members and all well wishers for their love and blessings on me.

Finally I would like to give credit and love to my wife Sushmita and daughter Srijeeta, for their constant support and allowing me to concentrate on my work beyond office hours and holidays.

February, 2013 **Saikat Kumar Nandy**

RMC, BARC

Contents

SYNOPSIS

SPECT (Single Photon Emission Computed Tomography) and PET (Positron Emission Tomography) have revolutionized nuclear medicine imaging, as they generate three dimensional images of distribution and /or concentration of the radiopharmaceuticals (RPs*) in vivo*. PET imaging, based on the coincidence detection (ACD) of the two collinear 511 keV γ-rays resulting from the mutual annihilation of a β^+ (positron) from the PET-RPs and a β^-(negatron) from the ambient provide us images with much better resolution as well as sensitivity in comparison to SPECT. Another great advancement in the last decade has been the combination of PET and CT in one device which leads to 3D-images with exact morphologic information as well as a physiological and biochemical representation[1]. The combination of PET and MRI is a very recent advancement in molecular imaging. PET radiopharmaceuticals (RPs) are normally present metabolites in the body viz. sugars, amino acids, nucleotides etc., which are labelled with β^+ emitters. The only suitable radioisotopes of Carbon, Oxygen, Nitrogen and Fluorine (a substitute of H) are the short lived ones viz. ^{11}C ($T_{½}$: 20 min) , ^{15}O ($T_{½}$: 2 min), ^{13}N ($T_{½}$: 13 min), ^{18}F ($T_{½}$: 110 min). These are produced in a medical cyclotron. Other PET radioisotopes available from generators are ^{82}Rb ($T_{½}$: 75 seconds) and ^{68}Ga ($T_{½}$: 58 min). The short half-life ($T_{½}$) puts the limitations on the time available as well as strategies for synthesis and quality control (QC) of PET RPs and their clinical use. The attractive advantage of PET RPs is that, they are analogs of common biological molecules, and therefore, truly depict the biological process *in vivo*. This is exemplified by [^{18}F]Fluoro-deoxy-glucose ([^{18}F]FDG), an analog of glucose, used world wide for the detection of tumors and $H_2O[^{15}O]$ for imaging cerebral perfusion. Among the PET radioisotopes, ^{18}F is the most preferred radionuclide for its nuclear and chemical properties and can easily be produced in a medical cyclotron by ^{18}O (p, n) ^{18}F nuclear reaction using $H_2{}^{18}O$

water target. ^{18}F decays 97 % by β^+ emission, 3 % by EC and its $T_{½}$ of 110 minute permits its use for several hours of production, synthesis facilitating kinetic studies [2]. Although, not a natural constituent of metabolic substrates, ^{18}F can be substituted for -H or –OH and does not cause significant sterical changes, although biochemical properties may change and is trapped in the metabolic process ("metabolic trapping") *in vivo*. Further, β^+ of ^{18}F is emitted with fairly low energy (635 keV), having a mean free path of ~ 2.5 mm in tissue and for this reason imaging can be potentially done at quite high resolution.

2-[^{18}F]-fluoro-2-deoxy-D-glicose ([^{18}F]FDG) is to date, the most widely used PET RP (95% of the total PET scans), and the total scenario of diagnosis and management of cancer patients have changed after the wide spread availability and usage of [^{18}F]FDG worldwide and the impact is such that it is adjudged as "the molecule of the millennium" by the father of Nuclear Medicine, Prof. Henry Wagner. However, [^{18}F]FDG has some limitations, for e.g. (1) it is not a highly selective tracer for cancers or active muscles as it is also taken up by macrophages. Macrophages invade tumors and appear in inflammatory lesions, causing false positive results. (2) Decreased uptake is seen in patient with hyperglycemia. (3) Routine whole body [^{18}F]FDG PET lacks sensitivity for imaging brain metastasis because glucose is avidly taken up by the normal brain tissue [3]. (4) [^{18}F] FDG uptake in tumors indicates enhanced metabolism, but does not give any information on the proliferation rate (cell multiplication) of cells in the tumor which is important to determine the aggressiveness of the tumor. In order to overcome these drawbacks, several other bio-molecules like ^{18}F-labeled amino acids [O-(2-[^{18}F]Fluoroethyl)-L-tyrosine] ([^{18}F]FET) [4], 3'-deoxy-3'-[^{18}F]fluorothymidine ([^{18}F]FLT) for imaging cell proliferation [5] etc., have been developed. Other important ^{18}F-labeled PET radiopharmaceuticals are: (a) hypoxia agents: [^{18}F]Fluoromisonidazole ([^{18}F]FMISO)[6] and [^{18}F]-labeled fluoroazomycin arabinoside

([^{18}F]FAZA)[7] (b) receptor radioligands: [^{18}F]flumazenil (central BZ)[8], 6-[^{18}F]fluoro-L-3, 4-dihydroxyphenylalanine (6-[^{18}F]FDOPA), a well-established tracer for Parkinson's disease [9] and many others. In addition to those named above, there are a large number of other ^{18}F-labeled radiopharmaceuticals, which have been reported in the literature.

The success of PET is by and largely dependent on the availability of cyclotron produced radioisotopes and synthesis systems with easy, simplified operations and reliable radiopharmaceutical preparation [10-12]. Computer (PC) and programmable logic controlled (PLC) automation is widely used for this. The rationale for automation of radiopharmaceutical synthesis includes: 1) reduction of radiation exposure to personnel, 2) better reproducibility of the synthetic method and 3) overall cost savings.

Historically, two distinct approaches have been applied to the automation of radiopharmaceutical synthesis, namely, automated modules based on the principle of unit operations and robotics-based system [13, 14]. The unit operations approach is based on the philosophy that a complex process can be reduced to a series of simple operations or reactions, which are identical in fundamentals regardless of the labeled compound being prepared [15, 16]. Synthetic methodologies based on this principle have remained the most popular technique for automation of PET radiopharmaceuticals syntheses [14]. In this approach, a multistep synthetic process is broken down into the required unit operations (e.g., addition of reagent, removal of solvent, solvent extraction, chromatography and sterilization, and so on). These simple unit operations are performed in sequence on a remote, semi automated basis where standard laboratory glassware and equipment are used in conjunction with solenoid valves and fluidics. The interaction of a chemist is entirely remote and involves the addition of reagents, transfer of fluids by application of pressure or

vacuum, and the initiation of each operation by actuating the appropriate combination of electrical switches controlling the solenoid valves.

[^{18}F]FDG synthesis is a classic example to illustrate the versatile concept of a unit operations-based semi-automated synthesis system and its direct extension to a computer controlled fully automated module [17]. A semi-automated system for the synthesis of FDG using the method described in the literature [17] was constructed early on [18] and thoroughly tested before embarking on the automation process. The unit operations are: 1) trapping of [^{18}F]fluoride ion from the irradiated O-18 water target 2) nucleophilic ^{18}F-fluorination of the precursor 3) isolation of the intermediate product 4) acid hydrolysis of protecting groups on the precursor 5) purification of [^{18}F]FDG by a combination of ion exchange chromatography, and reverse phase adsorption to remove impurities and 6) sterilization of [^{18}F]FDG for human use. These unit operations for the synthesis of [^{18}F]FDG were automated under PC control and the resulted fully automated module was termed as Chemistry Process Control Unit (CPCU) [19]. Since 2000, automated [^{18}F]FDG modules based on the principles of unit operations were available from a large number of commercial sources though at considerable expense. Important examples include: TRACERlab Fx $_{FDG}$ (GE Medical Systems, Münster, Germany: former Nuclear Interface module); CPCU, Chemistry Process Control Unit (CTI, Knoxville, TN, USA); EBCO/Jaltech FDG synthesis module (EBCO, Canada); Synchrom (Raytest, Isotopenmeesgerate GmbH, Germany. In the following years, computer-controlled automated synthesizers have made commercially available for a variety of positron-emitter labeled radiopharmaceuticals.

All commercially available automated modules for the synthesis of PET radiopharmaceuticals have certain similarities among them. They are generally compact, and fit inside a compact hot cell less than a square meter footprint. The units are fully controlled by PCs with user-friendly

menu-driven operating systems and allow a graphical visualization of the entire sequence of the synthetic operation. All the reaction parameters of the synthesis and other pertinent data are automatically saved for quality control documentation (cGMP). Further, the software controlling each unit operation is flexible and users, with some understanding, can easily modify and adapt the module for any automation of new syntheses. Most importantly, these automated synthesizers can easily be operated by technicians and are highly suitable for hospital-based PET centers and commercial radiopharmacies for day-to-day routine production of pure, sterile and pyrogen free radiopharmaceuticals.

The chemistry process in most of the automated [^{18}F]FDG synthesizers is based on the nucleophilic synthetic method suggested in 1986 [17] with some modifications [**Fig.1**]. The major steps in this radiochemical synthesis include trapping of [^{18}F]F$^-$ from the irradiated O-18 water in a small anion-exchanger column and recovery of O-18 water, preparation of reactive complex of [^{18}F]fluoride with phase transfer catalyst [Kryptofix 2.2.2 or tetrabutylammonium bicarbonate ($TBAHCO_3$)], its resolubilization in an aprotic dipolar solvent (acetonitrile), nucleophilic displacement reaction with 1,3,4,6-tetra-O-acetyl-2-O-trifluoromethanesulfonyl-D-mannopyranose (mannose triflate), hydrolysis and on-line purification using a solid phase extraction (SPE) technique. The possibility to produce another ^{18}F-labeled radiotracer using commercial [^{18}F]FDG synthesizers allowing economical use of expensive equipment is very attractive for radiochemists. Many radiosyntheses of ^{18}F-labeled compounds comprise sequential steps of direct nucleophilic substitutions of the leaving group in desired molecule and hydrolysis/deprotection. Here the synthetic procedure is similar to that for [^{18}F]FDG. Well-known examples are: (a) hypoxic agents: [^{18}F]Fluoromisonidazole ([^{18}F]

FMISO) and [^{18}F]-labeled fluoroazomycin arabinoside ([^{18}F]FAZA) (b) tumor-seeking agents: 3'-deoxy-3'-[^{18}F]fluorothymidine ([^{18}F]FLT), O-(2-[^{18}F]Fluoroethyl)-L-tyrosine ([^{18}F]FET) (c)

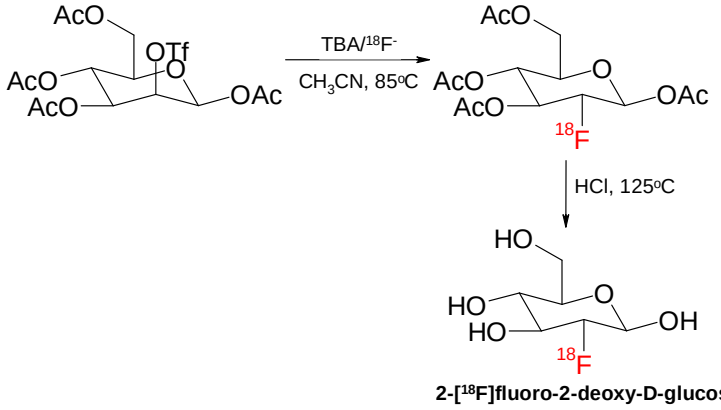

Fig.1 *Synthesis of [^{18}FFDG via nucleophilic substitution reaction*

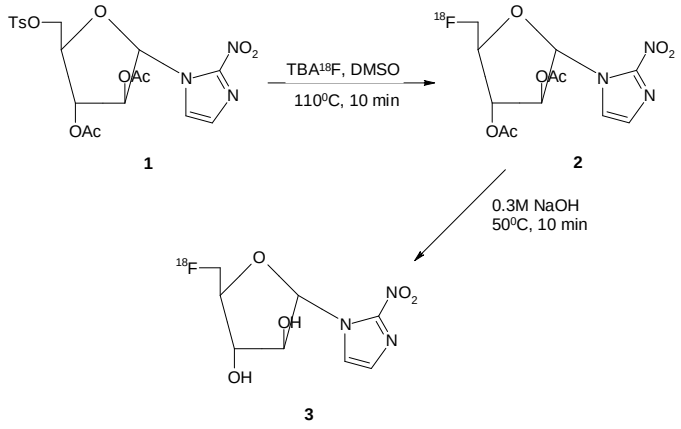

1. 1- (2,3-di-O-acetyl-5-O-tosyl-alpha-D -arabinofuranosyl)-2-nitroimidazole
2. 1- (2,3-di-O-acetyl-5-[^{18}F]-fluoro-5-deoxy-alpha-D-arabinofyranosyl)-2-nitroimidazole
3. 1-(5-[^{18}F]-fluoro-5-deoxy-alpha-D - arabinofuranosyl)-2-nitroimidazole **([^{18}F]FAZA)**

Fig.2 *Schematic of [^{18}F]FAZA synthesis via nucleophilic substitution reaction*

receptor radioligands: [^{18}F] flumazenil (central BZ), [^{18}F]altanserin ($5HT_{2A}$) [20], p-[^{18}F]MPFF ($5HT_{1A}$) [21] and others. As an example, the synthesis scheme for [^{18}F]FAZA is shown in **Fig.2**. Despite the general features in the radiolabeling approach, the synthetic procedure regarding solvents and reaction conditions for a particular compound may be different from [^{18}F]FDG and most significant one from the practical point of view, in contrast to [^{18}F]FDG, for most

radiotracers a semi-preparative HPLC purification has been used by researchers to separate the labelled from the precursor. Therefore, the commercial [^{18}F]FDG module has to be extended to provide an HPLC purification option. The automated injection of the reaction mixture into an HPLC injection loop is not a trivial task. This step is accomplished with losses of the product due to either incomplete delivery of solution into the loop or unavoidable introduction of air, which results in overpressure and plugging of the HPLC column. Thus the practical experience of the production of non-FDG PET RPs using automated module equipped with HPLC is not very encouraging. Further, when large amounts of ^{18}F-tracers are to be prepared, the resin of the column of the semi-preparative HPLC suffers significant radiolytic damage and requires to be changed frequently, which is neither cheap nor easy to do. This problem can easily be solved out provided the automated synthesis procedure of these non-FDG PET RPs are modified and, most importantly, a single combination column or SEP-PAK® cartridge (s) based purification process is developed. This will ensure the production of these non-FDG PET RPs easily and in sufficient quantities for distribution like [^{18}F]FDG.

In this thesis, to be submitted to the Homi Bhabha National Institute for the Doctor of Philosophy (PhD) degree, for convenience of presentation, different aspects of the present work have been discussed in nine different chapters of the thesis. Brief descriptions of the arrangements of different chapters in the thesis are given below.

Chapter 1

Introduction

This introductory chapter begins with the historical developments of the use of radionuclides in life-science and subsequently in nuclear medicine. The differentiation of the non-invasive imaging techniques depending on the type of radionuclide used (SPECT and PET), positron

emission tomography (PET) technique and its superiority over single photon emission computed tomography (SPECT) is discussed in details. A list of important positron emitting radionuclides and their nuclear data is also included. A comparative analysis of the nuclear data of the different positron emitters to show the most ideality of ^{18}F as a PET radionuclide is discussed. Production pathways of important positron emitting radionuclides with a special emphasis of the most four common ones i.e. ^{15}O, ^{13}N, ^{11}C, ^{18}F are described in details. Basic concepts of no-carrier added radio synthesis is briefed. The chapter ends with description of different types of ^{18}F-fluorination techniques with specific examples.

Chapter 2

General Purpose Fluorination Module

This chapter starts describing the need of automation for PET radiopharmacetical production. It further describes the different types of automated synthesis modules commercially available and their merits and demerits. Next, it describes in details the conversion of our existing [^{11}C] Methylation module (Nuclear Interface, Münster, Germany) to a general purpose nucleophilic fluorination one, very similar in principle to the automated FDG synthesis module, is discussed in details. Next, utilization of this adapted module for the production of non-FDG PET-RPs like [^{18}F]NaF, [^{18}F]FMISO, [^{18}F]FAZA , [^{18}F]FLT etc. is thoroughly discussed. For each PET-RP, a synthesis procedure using single column, or a combination column or SEP-PAK® cartridges based purification is developed, very similar to [^{18}F]FDG synthesis.

The facilities available in the original [^{11}C]Methylation module is compared with the GE TRACERlab FX_{FDG} module and then it describes how the various changes to the hardware, routing of the fluidics, reaction vessel, solenoid valves, cooling of the reaction vessel were made, and importantly, the required changes to the software, time list, and on-screen graphics. Each and

every step of [^{18}F]FDG synthesis was performed in standard GE TRACERlab FX_{FDG} module is replicated here. Finally, the detailed arrangement of collection of reaction mixture at different steps of a particular reaction (for standardization of the chemistry) as well as final product through a hatch below the hot cell is described.

Chpater 3

^{18}F-labelled sodium fluoride ([^{18}F]NaF): The PET Radiopharmaceutical for skeletal Imaging

This chapter concentrates on the development of a procedure for the production of pharmaceutical grade ^{18}F- labeled sodium fluoride ([^{18}F]NaF), a PET RP for skeletal imaging. An introduction about the suitability of [^{18}F]NaF as a bone imaging agent and its comparison to its ^{99m}Tc-counterpart, ^{99m}Tc-MDP is given here. The detailed production procedure of the preparation of pharmaceutical grade [^{18}F]NaF utililizing the adapted synthesis module and the details of physico-chemical quality control procedures i.e. the physical appearance, pH, radiochemical purity by radio-TLC (Thin Layer Chromatography), residual solvent analysis by GC (gas chromatography) and radionuclidic purity (RNP) by half-life method are given. Details of microbiological quality control (sterility and bacterial endotoxin) procedure and finally, bio-distribution studies in rabbits and clinical studies in patients are discussed. The last part of this chapter is the "Results and Discussion" part where the quality of the produced [^{18}F]NaF is compared with the quality requirements recommended in USP 31. Gamma spectroscopy analysis of the samples by high purity germanium detector coupled with multi channel analyzer looking for radio-metal ion impurities generating from the radioactivation of Havar® Foil of the cyclotron target is attached. Finally, PET/CT images of [^{18}F]NaF of normal healthy rabbits are shown to show the normal in vivo localization. The chapter ends with some remarkable PET/CT

images of patients with a few skeletal disorders reflecting its importance for the management of cancer patients with skeletal metastasis.

Chapter 4

Development of single column purification method for the production of ^{18}F-labelled misonidazole ([^{18}F]FMISO): The PET Radiopharmaceutical for hypoxia Imaging and optimization of reaction parameters

This chapter is divided into two parts. The first part briefly describes about the method of development of hypoxic regions in tumors and how it affects the management of cancer patients. The importance of *in vivo* imaging with the help of radiolabeled compounds and most importantly, the exploitation of the special property of localization of nitroimidazole based compounds in hypoxic cells are discussed. A survey of the literature for the available production procedures of the ^{18}F-labeled misonidazole ([^{18}F]FMISO), the gold standard for hypoxia imaging agent, is added. The in-house developed, simple and economic procedure for the fully automated production of [^{18}F]FMISO by single neutral alumina column purification using the adapted module is discussed in details along with the quality controls, gas chromatography for residual solvent analysis etc. Data from bio-distribution studies in fibrosarcoma tumor bearing mice and PET/CT imaging studies in rabbit and finally in patients are discussed. The experimental proofs (radio TLC, Radio-HPLC, HPLC by monitoring UV, alumina ion tests, sterility and bacterial endotoxin tests to ensure microbiological quality control) are given in details to ensure that the synthesized [^{18}F]FMISO is of pharmaceutical grade in quality and is free of any radio and non-radioactive impurities. PET/CT images of normal healthy rabbits at different time points are added to show the pharmacokinetics as well as to show its slow clearance through hepatobiliary systems and normal localization in brain as well as slow leaching process through liver due to its

lipophilicity. The first part of the chapter ends with [^{18}F]FMISO PET/CT images of cancer patients suspected to have hypoxic regions in tumour and reflects its usefulness in the management of cancer patients.

The second part of this chapter describes the experiments conducted and results obtained in optimization of the reaction parameters to obtain the maximum radiochemical yield within the shortest synthesis time, minimizing radioactive decay loss and the use of minimum amount of precursor to make the developed process very economic.

Chapter 5

Simple, column purification technique for the fully automated radiosynthesis of [^{18}F]Fluoroazomycinarabinoside ([^{18}F]FAZA)

[^{18}F]FMISO is a well established PET RP for detecting tissue hypoxia and currently widely used for the purpose. The tracer's ([^{18}F]FMISO) primary cellular uptake results from diffusion and partition based retention in lipophilic tissues such as the brain, in addition to hypoxia based retention. Secondly, the excretion of the tracer ([^{18}F]FMISO) is through the billiary system reflecting its higher lipophilic nature. The clearance through liver is also very slow due to its lipophilic nature. Hence, the background remains very high which force to perform the actual imaging late after its administration. For PET tracer, 1-(5-[^{18}F]fluoro-5'-deoxy-α-D-arabinofuranosyl)-2-ntroimidazole ([^{18}F]FAZA) was developed as highly diffusible but less lipophilic radiotracers in order to reduce partition-based uptake. The use is limited because of limited availability due to the absence of simple automated synthesis procedure. This chapter describes in details a very simple production procedure of [^{18}F]FAZA with commercially available single purification cartridge, CHROMABOND® SET V. The details of quality control

of the synthesized [^{18}F]FAZA is given. Finally PET/CT imaging studies in normal healthy rabbit comparing the superiority of [^{18}F]FAZA over [^{18}F]FMISO is included.

Chapter 6

Development of cartridge purification based, simple, fully automated radiosynthesis procedure for the production of 3´-Deoxy-3´-[^{18}F] Fluorothymidine ([^{18}F]FLT)

3´-deoxy-3´-[^{18}F]fluorothymidine ([^{18}F]FLT) is an established PET– radiopharmaceutical to study cell-proliferation rate in tumors. Very low practical yield, requirement of time consuming and less reliable HPLC purification are the main obstacles in routine clinical studies with [^{18}F] FLT. The demand from the medical fertinity for this PET-RP is large as it can rectify the disadvantages of [^{18}F]FDG as discussed earlier in this synopsis and most importantly, its usefulness to detect brain glioma, which is otherwise difficult due to the extensive normal accumulation of [^{18}F]FDG in brain. The first part of this chapter describes an attempt to produce pharmaceutical grade [^{18}F]FLT starting from the precursor 3-N-t-butoxycarbonyl-(5'-O-(4,4'-dimethoxytriphenylmethyl)-2'-deoxy-3'-O-(4-nitrobenzenesulfonyl)-β-D-threo-pento furanosyl) thymine (3N-BOC) and a single column (composed of Ps-HCO_3 and neutral alumina) purification procedure, very similar to [^{18}F]FDG synthesis. Careful analysis of the synthesized [^{18}F]FLT by a variety of radioanalytical techniques including mass spectra, revealed that 4-[^{18}F]Fluoro-benzene-sulphonic acid (4-[^{18}F]FBSA) is present as a radioactive impurity along with [^{18}F]FLT which is not pharmacologically acceptable. The possible reason of competitive radiofluorination of the nosyl moiety of the precursor is confirmed by separately synthesizing 4-[^{18}F]FBSA starting from nosyl chloride. This attempt leads to an important clue that the

pharmaceutical grade [^{18}F]FLT can easily be produced with single column purification technique, provided the precursor does not contain nosyl moiety for competitive radiofluorination. In the second part of this chapter, the details of the synthesis of pharmaceutical grade [^{18}F]FLT with single neutral alumina column purification starting from the anhydro precursor, 5'-O-(4,4'-dimethoxytriphenylmethyl)-2,3'-anhydro-thymidine (DMTThy), where nosyl moiety is absent, is given. Detailed analysis of the radiochemical and chemical purity is described. Bio-distribution studies in normal healthy rabbit showing the localization of [^{18}F]FLT in rapidly proliferating region like bone marrow are included. PET/CT images in healthy human volunteer showing the localization of [^{18}F]FLT in bone marrow and its clearance through kidneys which, is in accordance with the standard published images in literature. Lastly, the images of the cancer patient (mainly brain tumor patients) obtained using [^{18}F]FLT are given. The problem with this developed procedure is that the yield [8.48 ± 0.93 % (n = 5), total synthesis period of 68 ± 3 min] is very less and is not suitable for large scale production.

Chapter 7

Fully automated radiosynthesis of 16-α-[^{18}F]Fluoroestradiol ([^{18}F]FES), using a single neutral alumina column-cartridge for purification

The PET tracer, 16-α-[^{18}F]Fluoroestradiol ([^{18}F]FES) has been shown to be a specific tracer of estrogen receptors in normal breast tissues and in breast cancer. The uptake of [^{18}F]FES in breast tumors correlates with *in vivo* estrogen receptor content of tumors, as assessed by in vitro radioligand assays. The available radiosynthesis procedures published in literature describes the use of HPLC purification in the final stage which is not currently available in our adapted fluorination module. So, development of single column purification based radiosynthesis

procedure is of considerable practical importance. Details of the development of this procedure to synthesize 16-α-[^{18}F]Fluoroestradiol ([^{18}F]FES) is described in this Chapter. Data from elaborate radiochemical and chemical analysis of the synthesized [^{18}F]FES ensuring its quality is provided. Finally, PET/CT images of female rabbit showing prominent uptake of [^{18}F]FES in the mammary gland (organ containing estrogen receptors) are included.

Chapter 8

A Simple, column purification technique for the fully automated radiosynthesis of ethyl [^{18}F]Fluoroacetate ([^{18}F]EFA) as a proradiotracer of [^{18}F]fluoroacetate ([^{18}F]FA) for the measurement of glial metabolism by PET

Glial cells are the main effector cells of innate immune responses to neuronal damage in the central nervous system (CNS). Microglia and astrocytes are strongly activated in response to neuronal damage, producing an array of inflammatory mediators and performing phagocytic functions. Therefore, selective imaging of glial cell activity may be a valuable method to determine the extent and progress of disease and to access a therapeutic intervention. Furthermore, changes in glial metabolism in brain ischemia, Alzheimer's disease, depression, schizophrenia, epilepsy and manganese neurotoxicity have been reported. Undisputedly, the measure of glial metabolism *in vivo* for the elucidation and diagnosis of these diseases has significant importance. ^{18}F-labeled fluoroacetate (FA) has been developed as a PET tracer for imaging of oxidative metabolism in various tissues. For brain studies, however, the low blood-brain barrier (BBB) permeability of anionic form like FA is a fundamental problem. It is well known that ethyl acetate penetrates easily in brain, then, is hydrolyzed to acetate rapidly *in vivo*. Based on these characteristics, ^{18}F-labelled ethyl fluoroacetate (EFA), ethyl-ester of FA, is a potential candidate of PET tracer of oxidative metabolism in brain [22]. In this chapter, a novel

fully automated radiosynthesis procedure for ethyl [^{18}F]fluoroacetate ([^{18}F]EFA) using a commercially available combination column, CHROMABOND® SET V (FDG-BASE-HYDR) for purification in the adapted general purpose fluorination module is described. Detailed analysis of radiochemical and chemical purity is added to demonstrate the efficacy of the developed procedure. A good radiochemical yield 44.0 ±1.5 % (n = 5, without any decay correction) in a reasonably short synthesis period (32 ± 1 minutes) is possible.

Chapter 9

A single column purification technique for the fully automated radiosynthesis of [^{18}F]Fluoroacetate: a potential acetate analog for prostate tumor imaging

PET with ^{11}C-acetate ([^{11}C]ACE) has a high sensitivity for detection of prostate cancer and several other cancers that are poorly detected by [^{18}F]FDG. However, the potential for widespread use of [^{11}C]ACE is limited by short half-life (20.4 min) of ^{11}C, which necessitates production with a cyclotron close to the site of PET-CT. Even with high yield synthesis, only a limited number of patients can be studied from a single-batch production. [^{18}F]-fluoroacetate ([^{18}F]FAC) is an analog of acetate with a longer radioactive half-life (^{18}F =110 min) **[23]**. In this chapter, a novel fully automated radiosynthesis procedure for [^{18}F]-fluoroacetate ([^{18}F]FAC) using a single combination column for purification, composed of neutral alumina and reverse phase resin, is described. The developed procedure is very similar to [^{18}F]FDG synthesis in dedicated FDG module. A considerable radiosynthesis yield [47.2 ± 3.0 %, n =5, without any decay correction] within a short synthesis time (40±1 minutes) is observed.

Chapter 10

A fully automated radiosynthesis of 4-[^{18}F]fluorobenzaldehyde: a synthon for amine-oxi peptide labelling

Direct and fast no-carrier added (n.c.a.) [^{18}F]fluoride labelling may not be always possible especially for large and complex bio-molecules such as peptides. As an alternative, several [^{18}F]fluoride labeled synthons have been developed and applied for conjugation labelling of bio-molecules successfully. More recently, a new fast and straightforward strategy has been published that allows both single step, high-yield synthesis of a [^{18}F]fluoride-labelled synthon with stability against in vivo defluorination and fast, single step, chemoselective conjugation with unprotected peptides in aqueous media. The synthesis consists of a chemoselective oxime formation between an amine-oxy peptide and 4-[^{18}F]fluorobenzaldehyde [24].This methodology has been developed keeping in mind the objective of large scale [^{18}F]fluoride labelled peptides production for clinical routine application. This chapter describes in details a fully automated radiosynthesis procedure of 4-[^{18}F]fluorobenzaldehyde starting from 4-nitro benzaldehyde and single neutral alumina columns purification. Optimization of the radiofluorination conditions and the amount of precursor started with is described. Full scale radiochemical and chemical analysis is described to ensure the quality of the synthesized 4-[^{18}F]fluorobenzaldehyde. A considerable radiosynthesis yield [30.1±1.1 % (n=10, without any decay correction)] within a short synthesis period (35±1 minutes) with the desired purity is observed.

Chapter 11

Studies on a rapid radiosynthesis procedure for [^{18}F]FHBG using a non-HPLC purification technique

9-(4-[^{18}F] Fluro-3-hydroxymethylbutyl) guanine ([^{18}F]FHBG) is an acyclo-guanosine derivative which specifically gets trapped in viral infected cells by phosphorylations by virus specific thymidine kinase. [^{18}F]FHBG is emerging out as a very promising PET-RP for imaging viral infection. Success of gene therapy for tumors in humans depends on *in-vivo* expression of the delivered gene. Noninvasive imaging of transgene expression demands appropriate combination of reporter gene and reporter substrate. Herpes simplex virus type1 thymidine kinase gene (HSV1-tk) is most widely used reporter gene that expresses high level of viral enzyme thymidine kinase (HSV1-TK) which selectively phosphorylates nucleoside analogues such as [^{18}F]FHBG. Hence cellular retention of radioactivity is an indicator of HSV-tk gene expression. When HSV1-tk is linked to another therapeutic transgene, accumulation of [^{18}F]FHBG in tissue can be used to measure the magnitude, time and location of gene expression. Hence PET imaging with [^{18}F]FHBG is going to be useful in evaluation of gene therapy in human. Various research groups have presented methods for the radiosynthesis of [^{18}F] 9-(4 – [^{18}F] Flouro-3-hydroxymethylbutyl) guanine ([^{18}F]FHBG) [25, 26]. However, all the procedures have long radiosynthesis time (60-100 minutes), poor yield (<15% decay corrected) and elaborate purification procedures. Easy, efficient, faster radiosynthesis of [^{18}F]FHBG becomes prime requisite to meet the future demands of [^{18}F]FHBG. In this chapter, preliminary attempts on a fully-automated radiosynthesis of [^{18}F]FHBG with a much shorter synthesis time with a good radiochemical yield is described. The development of purification process based on either

combination-column composed of anion exchanger and neutral alumina or SEP-PAK® cartridges with a view to avoid the cumbersome HPLC method is detailed.

References

1. Pauleit D.; Floeth F.; Hamacher K.; Reimenschneider M. J.; Reifenberger G.; Müller H. –W.; Zilles K.; Coenen H. H.; Langen K. –J. *Brain* , **2005**, *128*,678.

2. Gopal B. Saha. Basics of PET Imaging: Physics, Chemistry, and Regulations. Springer.

3. Varagnolo L.; Stokkel M.P.M.; Mazzi U.; Pauwels E.K.J. *Nucl Med Biol*., **2000**, *27*, 103.

4. Hamacher K.; Coenen H.H. *Appl Radiat Isot*. **2002**, *57*, 853.

5. Shields A.F.; Grierson J.R.; Dohmen B.M.; Machulla H.J.; Stayanoff J.C.; Lawhorn-Crews J.M. *Nature Med*., **1998**, *4*, 1334.

6. Lim J.L.; Berridge M.S. *App. Radia. Isot*., **1993**, *44*, 1085.

7. Kumar P.; Wiebe L.I.; Asikoglu M.; Tandon M.; McEwan A.J. *Appl Radiat Isot*., **2002**, *57*, 697.

8. Ryzhikov N.N.; Seneca N.; Krasikova R.N.; Gomzina N.A.; Shchukin E.; Fedorova O.S.; Vassiliev D.A.; Gulyàs B.; Hall H.; Savic I.; Halldin C. *Nucl Med Biol*., **2005**, *32*, 109.

9. Barrio J.R.; Huang S.-C.; Phelps M.E. *Biochem Pharmacol*., **1997**, *54*, 341.

10. Tilyou S.M. *J Nucl Med*., **1991**, *32*, 15N-26N.

11. Coleman R.E. *J Nucl Med.*, **1993**, *34*, 2269.

12. Deutsch E. *J Nucl Med.*, **1993**, *34*, 1132.

13. Goodman M.M. Automated synthesis of radiotracers for PET applications. In: Hubner K.L.; Collman J.; Buonocore E.; Kablaka G., eds. Clinical Positron Emission Tomography. St. Louis: Mosby Year Book., **1992**, 110-112.

14. Crouzel C.; Clark J.C., Brihaye C.; Langstrom B.; Lemaire, C.; Nebeling B., Stone-Elander S. Radiochemistry automation for PET. In: Stocklin G.; Pike V.W., eds. Radiopharmaceuticals for positron emission tomography. Methodological Aspects. Dordrecht: Kluwer Academic Publishers., **1993**, 45-79.

15. Foust A.S.; Wenzel L.A.; Clump C.W.; Maus L.; Andersen, L.B. Principles of Unit Operations. 2nd ed. New York: John Wiley & Sons; **1980**.

16. McCabe W.L.; Smith J.C.; Harriot P. Unit Operations of Chemical Engineering. 5th ed. New York: McGraw-Hill, Inc.; **1993**.

17. Hamacher K.; Coenen H.H.; Stocklin G. *J Nucl Med*., **1986**, *27*, 235.

18. Satyamurthy N.; Phelps M. E.; Barrio J.R. *Clin Positron Imag*., **1999**, *2*, 233.

19. Padgett H.C.; Schmidt D.G.; Luxen A.; Bida G.T.; Satyamurthy N.; Barrio J.R. *Appl Radiat Isot.*, **1989**, *40*, 433.

20. Lemaire C.; Cantineau R.; Guillaume M.; Plenevaux A.; Christiaens L. *J Nucl Med*, **1991,** *32*, 2266.

21. Schiue C.Y. ; Schiue G.G. ; Mozley P.D. ; Kung, M. ; Zhuang Z. ; Kimn H.J. *Synapse*., **1997**, *25*, 147.

22. Tetsuya M. ; Li-Quan S. ; Masato K. ; Yasushi K. ; Takako F. ; Hidehiko O. ; Yasuhisa F. *J Nucl Med.*, **2007**, *48(Supplement 2)*, 302P.

23. Ponde D. E. ; Dence C.S. ; Oyama N. ; Kim J. ; Tai Y.C. ; Laforest R. ; Siegel B.A.; Welch M.J. *J Nucl Med.*, **2007**, *48*, 420.

24. Bruus-Jensen K., Poethko T., Schottelius M., Hauser A., Schwaiger M., Wester H.J. *Nucl Med Biol*., **2006**, *33*, 5.

25. Alauddin M.M.; Conti P.S. *Nucl Med Biol*., **1998**, *25*, 175.

26. Shiue G.G.; Shiue C.Y.; Lee R.L.; Macdonald D.; Hustinx R.; Eck, S.L.; Alavi A.A. *Nucl Med Biol.,* **2001**, *28,* 875.

LIST OF FIGURES

Page No.

LIST OF TABLES

Page No.

CHAPTER 1

INTRODUCTION

1.1. Radionuclide in Nuclear Medicine

Antonie Henri Becquerel, in 1896, noticed the blackening of photographic films by uranium ore whereby he discovered the radioactivity for which he received the Nobel Prize in Physics in 1903 and this opened a very new window of natural sciences. Consequently, in 1898, the subject of nuclear chemistry was established by the great researcher couple Marie and Pierre Curie, who isolated the radioactive elements polonium and radium from pitchblende[1]. The introduction of radionuclides in life-sciences was opened by Georg de Hevesy in 1920, when he carried out the first *in vivo* investigations [2]. The radiotracer principle which is based on the identical chemical and biochemical behaviour of stable elements and their radioactive isotopes was developed by Hevesy and Adolf Paneth. Since that time, Hevesy is known as the "Grandfather of Nuclear Medicine" and he received the medicine Nobel Prize in 1943 for his life's work.

Till 1930, the radionuclides that were known, were limited to the natural occurring nuclides and only a very few of them were suitable as radiotracers in life-sciences. The development of the first cyclotron (Ernest Orlando Lawrence, 1930), the discovery of the induced nuclear fission (Otto Hahn and Fritz Strassmann, 1938/39, Chemistry Nobel Prize in 1944) and the construction of first nuclear reactor (Enrico Fermi and Leo Szilard, 1942), made possible the production of artificial radionuclides on large scale [3]. Since then, the application of radioactivity in life-sciences have increased rapidly [4]. Today, only, a selected minority of more than 2400 available radionuclides are employed in life-sciences. Their number is strictly limited by special requirements of half-life, achievable chemical and radiochemical purity, type of

radiation and its energy. The field of nuclear medicine calls in particular is very specific about these aspects, more than other domains in life-sciences.

If we consider the applications of radionuclides in Nuclear Medicine, they are generally classified as diagnostic and therapeutic nuclides. For diagnostic investigations *in vivo*, only short-lived single γ photon and positron emitters are used to ensure as small as possible radiation exposure for the patient, but well detectable signals to get the important information [5, 6]. In contrast, for *in vivo* therapeutic use, radioisotopes with half-life of several days to few weeks, high LET (Linear-Energy-Transfer) radiations are in demand with the intention that α and β^- particles accomplish a local degeneration of the pathogen tissues in the short range without damaging neighbouring healthy tissues. Additionally, Auger electron emitting nuclides are also of therapeutic interest, they are capable of causing degeneration in a very small radius of the emitting nuclide. Thus, they are able to induce apoptosis, when they are brought into the cell nucleus and cause radiation damage of DNA [5, 7, 8].

The physiological or pathophysiological processes at a molecular level can easily be visualized by the application of radiolabelled biomolecules or pharmaceuticals with *in vivo* examinations. In addition to *in vivo* techniques, many *in vitro* procedures [e.g. radioimmunoassay (RIA) and autoradiography] have been developed and have become important tools in biochemistry, physiology and pharmacology. The radiotracer method now extends over wide spread fields of physiology and pharmacology and has played a key role e.g. in investigations on metabolic principles, on the function and dysfunction of physiological process and in the development of pharmaceuticals.

1.2. Emission Tomography

In general, the non-invasive imaging techniques like magnetic resonance tomography (MRT) and X-ray computed tomography (CT) give information about tissue structure. Hereby, the MRT includes the sub-fields of magnetic resonance spectroscopy and imaging (MRS and MRI). An enhancement of MRI, the functional MRI (fMRI), is a step to observe specific physiological functions; particularly for brain imaging. fMRI is based on the so-called Bold-effect, an increase in blood flow of a local vasculature that accompanies neural activity in brain. fMRI is versatile tool for mapping the brain and supports the clinical management in neurosurgery [9].

In comparison to the above mentioned methods, the emission tomography shows special advantages of visualizing pathophysiological, physiological and metabolic processes. The use of compounds, which are involved in this biochemistry and labelled with suitable radionuclides, helps to understand the mechanisms and processes such as Alzheimer's , Parkinson's and Huntington's disease. Furthermore, radiotracers have got widespread applications in diagnosis as well as for controlling and monitoring endoradiotherapy in oncology. As an added advantage, the very sensitive traceability of radioactivity and radiotracers with high specific activities allow the use of substrate quantities in sub-nanomolar scales. In considerations of this fact, the implementation of highly potent or even toxic compounds is possible without any pharmacodynamic effects and a physiological or pathophysiological system can be studied without disturbance [10-13].

Emission tomography is possible as single photon emission tomography (SPET) and positron emission tomography (PET). Both are routinely used in nuclear medicine and pharmacological research.

SPECT is the more popular technique so far, as the requirement here is the artificial radionuclide, ^{99m}Tc. ^{99m}Tc has favourable properties: a monoenergetic 140 keV single photon emission and an appropriate half-life of 6 hours, all suitable for low radiation exposure to the patient. Further, the major advantage is the ready availability of ^{99m}Tc generator system and thus its application is independent of nearby cyclotrons or reactors.

Moreover, the easy and commercially available one-step-labeling systems (so-called 'cold kits') containing precursors and all necessary reagents make the practical applications very convenient. Other single photon emitting radionuclides such as ^{111}In, ^{123}I and ^{201}Tl are also in routine use for SPECT, but not to the extent of ^{99m}Tc.

Even in recent years SPECT has continued to become more developed and attempts at software sophistications have been made for quantitative image analyses, PET is still an advanced technology. PET shows a higher sensitivity (more than 100-fold of SPECT) and its quantitation methods are very elaborate. The special characteristics of the positron decay itself establishes the basis for a sensitive and quantitative measurement of radioactivity with remarkable spatial resolution. Nonetheless, an exact independent transmission measurement and attenuation correction is necessary. With this combination, radiotracer concentrations and their kinetics in organs and the regions of interests can be measured quantitatively and used with appropriate bio-mathematical models to evaluate (patho) physiological processes [14].

Short-lived, neutron deficient positron emitters are of primary interest for labeling PET radiotracers. From the decaying nucleus, a positron (β^+) and a neutrino (ν) are emitted synchronously by the conversion of a proton into a neutron. Neutrinos show practically no interaction with matter and PET cameras are not able to detect them [15]. The positron loses its kinetic energy by interactions with matter within a very short distance. The range depends on the

β^+ energy, which is specific for the employed isotope. **Table 1.1.** shows the β^+_{max} energies of important positron emitters used for PET and ranges from one mm to several millimeters. When the positron is nearly at rest, it is able to interact with an electron, its anti-particle. Positron and electron form an intermediary positronium, an exotic atom showing similarities to hydrogen. In the positronium, the proton in the hydrogen's nucleus is replaced by a positron. Positronium atom exists as para-positronium in a singlet state (antiparallel spins, angular momentum: 0, mean life: $1.25X10^{-10}$ s) or as ortho-positronium in a triplet state (parallel spins, angular moment: $\hbar = h/2\Pi$, mean life: $1.39X10^{-7}$ s). In the positronium, the particles "spiral" closer to each other until they are terminated by annihilation. By annihilation, two γ-rays are released with a total energy of 1.022 MeV (the sum of the masses of positron and electron) and of 511 keV each. As a result of conservation of energy, parity and angular momentum, the singlet state emits two γ-rays and the triplet state emits three γ-rays. The two γ-rays from the singlet state show a nearly 180˚ distribution. Due to the different number of quantum states of ortho and para – positronium, their possibility of creation is 3:1. However, in matter, the ortho-positronium merges into para-positronium by the so-called pick-off process, where it interacts with electrons of its environment. In matter, the high efficiency of the pick-off processes leads to a strong depression of the triplet state, thus only the two γ-rays annihilation is relevant here and the three γ-rays annihilation is negligible [16].

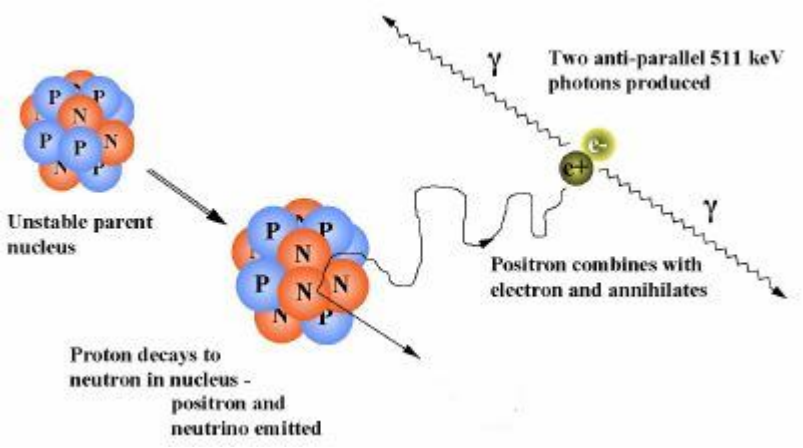

Fig. 1.1. *Positron emission and annihilation. After travelling a few millimetres in tissue the positron collides with an electron and they annihilate. In the annihilation process two photons are emitted. P = proton, N = neutron, e^+ = positron, e^- = electron, γ = photon* [5]

The annihilation of the para-positronium and the resulting two body-penetrating photons provide the basis of PET [**Fig. 1.1.**]. The PET camera consists of circularly arranged scintillator detectors. In these rings of detectors, every pair of opposite detectors is connected for coincidence measurement. As a result, the two γ-rays of the annihilation process will be detected and registered to have originated from the same radioactive atom if they hit both opposite detectors within a time window of few nanoseconds (generally ~ 12 ns). If we assume that both detected photons results from an event, the positron emitter must be located on or nearby the connection line of the detector pair. But, the spatial resolution depends on both the distance between origin and annihilation of the positron and the size of the detector crystals. As the distance of the positron from emission to annihilation is dependent on its β^+ energy, which is again specific for decaying isotopes, PET nuclides should emits positrons with an energy as low as possible to increase the spatial resolution and also to reduce the radiation dose. Besides, other uncertainties based on individual attenuation can be avoided by an attenuation factor, which is developed by an accurate independent transmission measurement. For this purpose, a ^{68}Ge source is generally used in PET machines and a CT in PET/CT machines to correct adsorption

and scattering affects before the real tracer will be injected. Finally, the distribution of radioactivity quantity in the object tissues can be measured preciously [14].

Computer-aided image reconstruction of the data of several transversal measurement planes allows the output of 3D-images of region of interest. These can be obtained with spatial resolutions down to ~ 3 mm and accuracy in quantity down to nano- and picomolar concentrations. Furthermore, physiological and pharmacological processes can be acquired in combination with a bio-mathematical model by dynamic studies with a longer span of time. With such methods and an accurate quantification, information about transport processes, metabolic rates and concentrations become accessible depending on the specific radiotracer used. Modern scanners that combine PET and MRT/CT in one device, which leads to 3D-images with exact morphologic information as well as a physiological and biochemical representation. Those procures are highly relevant in e.g. the clinical management of oncologic therapy [17].

Due to the fact, that, PET is a powerful tool in pharmacology and physiological research, special small animal PET scanners were developed in recent years [18]. Animal PET cameras make repeatable drug trials in one animal possible, without the need for vivisection and therefore costs and expanses for (radio) pharmaceutical development can be reduced [19, 20]. One of the latest innovations in this field is the so-called RatCAP, a small, head mounted PET system, the main item of which is a 4 cm diameter ring consisting of 12 crystal detectors. Those systems allow PET measurements of the brain of an awake rat without the need of anaesthesia, which actually make studies of behaviour or severely depressed brain functions impossible [21].

1.3. Radionuclide and Tracers for Positron Emission Tomography (PET)

As mentioned earlier, PET represents an excellent imaging technique with its advantages of very high sensitivity, good spatial resolution and the ability to identify (patho) physiological processes and functions and to quantify them accurately. Enhancement of the devices and combined scanner systems made strong contributions to the understanding of metabolic functions and processes. But it should be kept in mind that not only the progress of the technical equipment has achieved these but also a steady improvement and advanced development of suitable and high specific radiotracers that were needed.

To develop the right radiotracer molecule, the designated physiology to be studied and the related bio-chemistry have to be investigated. When it comes to new radiotracer development, the choice of biochemical or physiological concept is only the first step and many more considerations are essential. One of the very important considerations is the choice of the radionuclide with a suitable half-life (cf. Table 1.1), which is affected by the radiosynthesis as well as the characteristic of the finally studied bio-chemistry. A comprehensive pharmacological evaluation of the radio-labelled compound covering its *in vitro*, *ex vivo* and *in vivo* localization and metabolic pathways, dosimetry and toxicology studies is unavoidable. Before starting the routine use of a new radiopharmaceutical, a rigorous quality management should be completed in terms of automation and up-scaling (GBq range) of the radiosynthesis as well as validation of the bio-mathematical modelling for quantitation.

Table 1.1. Important positron emitters used for PET and their nuclear data [6, 12]

Nuclide and Its use in	Half-life	Decay Mode (%)	$E_{\beta+,max}$ [keV]
Organic Bio-molecules			
^{11}C	20.4 min	β^+ (98.8) EC (0.2)	960
^{13}N	9.96 min	β^+ (100)	1190
^{15}O	2.03 min	β^+ (99.9) EC (0.1)	1720
^{30}P	2.5 min	β^+ (99.8) EC (0.2)	3250
Analogue to Organic Biomolecules			
^{18}F	109.6 min	β^+ (97) EC (3)	635
^{75}Br	98 min	β^+ (75.5) EC (24.5)	1740
^{76}Br	16.1 hour	β^+ (57) EC (43)	3900
^{73}Se	7.1 hour	β^+ (65) EC (35)	1320
^{120}I	1.35 hour	β^+ (64) EC (36)	4100
^{124}I	4.18 day	β^+ (25) EC (75)	2140
Metallic as free cationic tracers or in complexed form (Radiolabeled peptides)			
^{38}K	7.6 min	β^+ (100)	2680
^{62}Cu	9.7 min	β^+ (98) EC (2)	2930
^{64}Cu	12.7 min	β^+ (18) β^-(37) EC (45)	655
^{68}Ga	68.3 min	β^+ (90) EC (10)	1900
^{82}Rb	1.3 min	β^+ (96) EC (4)	3350
^{86}Y	14.7 min	β^+ (34) EC (66)	1300
^{94m}Tc	52 min	β^+ (72) EC (28)	2470
^{72}As	26 hour	β^+ (88) EC (12)	2515

Carbon, hydrogen, oxygen, nitrogen sulphur and phosphorous are the main elemental constituents of biomolecules (e.g. glucose, amino acids, fatty acids enzymes, etc) and pharmaceuticals. Obviously, the short-lived positron emitting isotopes of these elements are ideal to achieve so-called authentic labelling. The so-called "organic" PET nuclides -^{11}C, ^{15}O, ^{13}N and ^{30}P allows the authentic labelling without any changes in (bio) chemical and physiological behaviour or properties of the labelled compounds. But, unfortunately, the very short half-lives of these isotopes from two to twenty minutes severely limit their practical applicability. In case of ^{15}O ($T_{½}$ = 2 min) and ^{13}N ($T_{½}$ = 10 min), only fast, accessible, very simple compounds such as [^{15}O]H_2O, [^{15}O]C_4H_9OH and [^{13}N]NH_3 as blood flow tracer, [^{15}O]O_2 as indicator of oxygen metabolism and [^{15}O]glucose as indicator for glucose uptake can be synthesized [22].

The moderately higher half-life of ^{11}C ($T_{½}$ = 20.4 min) provides the possibility of multi-step radiosynthesis and allows PET investigations of slower physiological processes. If we consider the cyclotron production of carbon-11, the primary labelling precursor [^{11}C]CO_2 is available, which finds very rare application for direct labelling reaction of organic molecules. Nonetheless, [^{11}C]CO_2 can easily be transformed to many precursors, which offer versatile ^{11}C-labeling pathways [23]. The most important synthon is [^{11}C]CH_3I, which enables ^{11}C-methylations of organic compound with very high specific activity [24]. For those radiotracers, rapid automated radiosynthesis procedures were developed and the ^{11}C-labelled products, such as amino acid L-[methyl-^{11}C] methionine [25] or the dopamine D_2 receptor ligand [^{11}C]raclopride [26] are routinely prepared as PET radiopharmaceuticals for nuclear medicine diagnosis.

If the radiosynthesis procedure is a multi-step and time-consuming one or the physiological process to be investigated is very slow in nature, the very short-lived organic positron emitters do not meet the demands. The solution of these problems is the introduction of longer-lived radionuclides into the tracer molecule. The so-called “analogue” radiotracers are commonly labelled with ^{18}F, [75, 76] Br, ^{73}Se and [120,124] I. The very wide range of half-life from 1.35 hour (^{120}I) to 4.15 days (^{124}I) allows more elaborate radiosynthesis as well as PET investigations of kinetically slow bio-chemical processes. While developing analogue tracers, the most important consideration is the similarity in steric demand and/or in the electronic character of the substituted atom or function. For example, methyl groups can easily be substituted by [75, 76] Br and [120,124] I due to the similarities in bulkiness as well as electronic characters [27, 28]. Since, ^{73}Se is the next homologue to sulphur; their steric and chemical properties are similar. So, sulphur can be successfully replaced by ^{73}Se, e.g. in the labelling of *L*- [^{73}Se] selenomethoinine [29], and *L*-homocystine [$^{73, 75}$ Se] selenolactone [30].

Mostly, the incorporation of foreign isotopes lead to only small, insignificant structural differences, but the resulting changes in overall electronic environment as well chemical reactivity can be important. Higher radio-halogen substituted radiotracers often exhibit higher lipophilicity leading to higher non-specific binding. In particular, radioiodine labelled molecules show frequently strong deviations in specificity, and even end with completely non-specific compounds. So, the bio-chemical behaviour of the analogous labelled molecules has to be tested for change in characteristics in each individual case.

The most ideal analogue isotope is ^{18}F, which is very similar to hydrogen atom from steric point of view (Van der Waals radii of fluorine is 1.35 Å, and of hydrogen is 1.20 Å), but differs widely in electronic character. Nevertheless, the steric factor predominates and ^{18}F is successfully incorporated in many organic molecules in place of hydrogen, hydroxyl or some other functional groups without creating much significant changes in the steric atmosphere. If we consider the example of analogue tracer for the amino acid, tyrosine, *L*-2-[^{18}F] fluorotyrosine, the ^{18}F-radiotracer has identical metabolic behaviour with the mother compound, tyrosine and is bound to tRNA and into proteins while the 3-isomer does not and is very toxic [31]. A recently developed and better version amino acid analogue radiotracer for tumour imaging especially brain tumour is O-(2-[^{18}F] fluoroethyl)-*L*-tyrosine [32]. In spite of the fact that this amino acid is not incorporated into proteins, uptake by tumour cells is stereo specific and mediated by amino acid transporters [17, 33, 34].

One more examples is 2-[^{18}F] fluorodeoxygluocose ([^{18}F]FDG), which is the most widely used PET radiopharmaceutical. Similar to the very first steps of glucose metabolism, FDG is accepted as glucose analogue and taken up into the cells by glucose transporters. In cells, it is metabolized to 2-[^{18}F] fluorodoxyglucose-6-phosphate by the cytoplasmic enzyme hexokinase, but the ^{18}F-

for-OH substitution in the 2-position of the original glucose leads to interruption of the metabolism further, as 2-[^{18}F] fluorodoxyglucose-6-phosphate is not a substrate of the next step enzyme, phosphor-fructo-isomerase; leaving the phosphorylated FDG in the cell unaltered. This effect is known as metabolic trapping and PET images of regional glucose uptake can be obtained. Additionally, with the help of a suitable bio-mathematical three-compartmental model, the regional glucose metabolism can be quantified [35]. Besides, FDG helps to study brain and myocardial metabolism and function; it is also the most trusted and widely used tracer for detection of tumours and metastases, whose cells exhibit an increased glucose uptake and metabolism [36, 37].

The suitable chemical and nuclear properties of fluorine-18 are behind the success of it as routine PET nuclide and in diagnosis and pharmacological research. Fluorine-18 can be produced in good yields, even with low-energy cyclotrons. As mentioned earlier, the half-life of 109.7 min allows both time-consuming multi-step radiosynthesis up to several hours and extended PET studies of slower bio-chemical process. Because of the handy half-life, shipment is possible within a range that can be covered in a few hours ensuring the supply to the clinics without on-site cyclotron in a so-called "satellite" concept [38]. ^{18}F has a low β^+ energy of 635 keV, besides ^{64}Cu the lowest of the PET nuclides, which promises a very high resolution of down to 1mm in PET images and assures minimum radiation doses to the patients.

A third group of suitable positron emitters for PET is represented by the metallic isotopes (cf. Table 1.1). In contrast to the "organic" and "analogue" PET radionuclides, a few metallic isotopes are achievable by generator systems (e.g. ^{82}Rb, ^{62}Cu and ^{68}Ga) which make them available in places without an on-site cyclotron [39].For *in vivo* studies, they are applied as free cationic tracers or in complexed form (e.g. ^{68}Ga-DOTATOC). For example, rubidium-82 has

been evaluated as a myocardial perfusion tracer because of its similarities to the potassium cation and is routinely employed in its free cationic form [40]. Cyclotron produced positron emitters like ^{94m}Tc and ^{86}Y are also of interests. ^{94m}Tc offers the possibility of use of PET for quantifying the uptake kinetics of γ-emitting ^{99m}Tc-labelled SPECT radiopharmaceuticals. Similarly, ^{86}Y is the PET radionuclide of interest for the quantitative access to the pharmacokinetics of therapeutic ^{90}Y-agents for palliative treatment [28].

Production pathways of important positron emitting radionuclides

Positron emitters are neutron deficient radionuclides and in general they are produced by bombardment of stable isotopes by small charged particles mainly protons, deuterons and alphas in accelerators. The knowledge of nuclear data, such as cross sections and excitation functions are essential for optimal results in production. The final chemical form of the product depends on the type of nuclear reaction and mostly on the target (e.g. target body, target volume, maximum permissible beam current), the physical state (e.g. gas, liquid and solid) and the chemical form of the target material.

For fluorine-18, more than twenty nuclear reactions are known as production routes. The most common nuclear reactions of ^{18}F-production are listed in Table 1.2. The use of ^{18}O(p, n)^{18}F (Ep = 16 → 3 MeV) reaction on ^{18}O-enriched water is the most commonly used and an effective method of production of [^{18}F]fluoride with very high specific radioactivity. Thus, even with low energy cyclotrons, under optimal conditions, high activities of [^{18}F]fluoride can easily be produced within one hour irradiation. Fluorine-18 can be produced by two different, double stage reactions in a nuclear reactor. One method uses a target consisting of (enriched) Lithium - 6 oxide (oxygen, 99.75% ^{16}O). Lithium-6 can absorb a neutron and give rise to a triton

[tritium (^{3}H) nucleus] and an alpha particle (^{4}He nucleus). Both the triton and the alpha have a lot of kinetic energy. The triton has enough kinetic energy that it can interact with a ^{16}O nucleus, be absorbed and give rise to fast neutron, leaving behind ^{18}F [$^{6}Li(n, \alpha)^{3}H/^{16}O(^{3}H, n)\ ^{18}F$]. The major problems with this method are, firstly, it allows activity production of < 1 GBq only and secondly, the target ends up with fair amount of tritium (radioactive hydrogen) as waste which is a concern from radio-waste management point of view. In a light water reactor, fission neutrons will occasionally collide with hydrogen (^{1}H) nuclei giving up most or all of their kinetic energy. This means we have a reasonable number of high speed protons in the reactor water. If one of these high speed protons interacts with an O-18 nucleus (stable, 0.20% abundance), a (p, n) reaction results in the formation of ^{18}F.

Table1.2. Most common nuclear reactions for production of fluorine-18 [6, 41, 42, 43]

Reaction	**$^{18}O(p,n)^{18}F$**	**$^{16}O(^{3}H,n)^{18}F$**	**$^{20}Ne(d,\alpha)^{18}F$**	**$^{18}O(p,n)^{18}F$** [c]
Target	$H_2{}^{18}O$[a]	H_2O	Ne (0.1-0.2% F_2)[b]	$^{18}O_2$, Kr (1%F_2)
Particle Energy	16→3	36→0	14→0	10→0
Main product form	$^{18}F_{aq}^-$	$^{18}F_{aq}^-$	$[^{18}F]F_2$	$[^{18}F]F_2$
Yield [GBq/μAh]	2.22	0.26	0.37-0.44	~ 0.37
Specific Activity [Bq/mmol]	≤ 3.7 X10 ^{15}	≤ 3.7 X10 ^{15}	3.7 X 10 $^{10\text{-}11}$	3.7-185X10 ^{10}

[a] Ti-target, Ti-window [b] passivated Ni-target [c] two steps process

For the incorporation of ^{18}F in the radiotracer by electrophilic fluorination method, molecular radioactive fluorine, $[^{18}F]F_2$ is needed. ^{20}Ne and $^{18}O_2$ gas are the targets of choice. The major problem faced in both the cases is the deposition of the produced fluorine-18 on the target walls. So, the addition of elemental fluorine to the target gas is mandatory for isotopic exchange of the absorbed fluorine-18. As a result, high molar activities can not be achieved. Since two consecutive irradiations are necessary with the $^{18}O_2$-target, for saving enriched material, the ^{20}Ne

(d, α)^{18}F reaction is the most practical and well-established process for electrophilic fluorine-18, although production rates are slow.

The general production method of carbon-11 is through the ^{14}N(p, α)^{11}C nuclear reaction route.^{14}N gas targets bombarded by protons in the energy range of 15→7 MeV is used for this purpose and is feasible even with low energy cyclotrons. Small portions of oxygen added to the target gas cause [^{11}C]CO_2 formation and in case of hydrogen addition, [^{11}C]CH_4 is the product form [44].^{13}N results from the ^{16}O(p, α)^{13}N reaction on a natural water target [45]. ^{15}O is regularly achieved from a natural nitrogen target via the ^{14}N(d, n)^{15}O reaction [46] (cf. Table 1.3).

Table 1.3. Production routes of the four most common PET radionuclides

Radionuclide	Half-life	Production Reaction
^{15}O	2.04 min	^{14}N(d,n)^{15}O
^{13}N	9.96 min	^{16}O(p,α)^{13}N
^{11}C	20.4 min	^{14}N(p,α)^{11}C
^{18}F	109.7 min	^{18}O(p,n)^{18}F (nucleophilic) [^{18}O-water target]
		^{20}Ne (d,α)$^{18}F_2$ (electrophilic)
		^{18}O(p,n)$^{18}F_2$(electrophilic) [^{18}O-O_2 gas target]

1.4. Basic aspects of reactions under no-carrier added conditions

The extremely high sensitivity of detection of the short-lived radionuclides is the greatest advantage when it comes to its use in nuclear medicine. Consequently, they are produced and employed in quantities at a subnanomolar range.

The amount of material can only be determined by the number of decays, thus the activity of 55 GBq (average production at a small cyclotron) ^{18}F is equivalent to 8.8 X 10^{-10} mol fluorine. Since it is always desirous to use the radiotracer as minimum as possible, a very fundamental criterion of the quality of a radiotracer is its specific activity (A_s), which depends on the amount of stable isotopes present (carrier). “Carriers” can be subdivided into two different categories; one is isotopic carrier i.e. isotopes of the same element as the radionuclide; and the

other is non-isotopic carrier meaning isotopes of other elements mostly with very similar chemical properties to the radionuclide.

In this context, the mass related activity, the specific activity, in chemistry, more relevant than the activity itself [47]:

$$A_s = A/m \text{ [Bq/g]}$$

Where 'A' is the activity, 'm' is the mass of radioactive material including all impurities and carrier, respectively. In practical sense, the specification related to mass is very inconvenient in chemistry; more practical and informative is the use of molar activity, thus A_s is usually expressed on the molar basis:

$$A_s = A/n \text{ [Bq/mol]}$$

here the mass 'm' is replaced by 'n'; the number of moles of the substance. The theoretically achievable maximum molar activity, $A_{s,\ max}$ (assuming the absence of impurities and carrier) equals to:

$$A_{s,\ max} = N_A\ (\ln 2/\ T_{½}) \text{ [Bq/mol]}$$

where N_A is the Avogadro's number and $T_{½}$, the half-life of the radionuclide. Most of the applications in molecular imaging look for high molecular activity. So, it is relevant to know the maximum achievable molar activities. For the most prevalently used PET nuclides, ^{18}F and ^{11}C, they amount to 6.3 X 10^{10} GBq/mol and 3.4 X 10^{11}GBq/mol, respectively. Since the stable isotopes of these radionuclides are present in nature, only a 10^3 - 10^5 fold less A_s is actually attainable in practice. However, though the quantity of material becomes higher by the natural isotopic carrier, but it is still in nano- to picomolar scale.

The presence of stable elements reduce the molar activities, but in some cases, either for increasing the yields or in case of cyclotron production of $[^{18}F]F_2$ for electrophilic fluorination reaction, it is unavoidable, to add carrier purposefully. Otherwise, PET investigations with very low concentrations in the target tissue (e.g. substrate of enzymes, receptor ligands and uptake inhibitors) demands for radionuclide of very high specific activity. In general, for radiochemical practice, the radiosynthesis can be classified as:

i. Carrier-free (c.f.)

ii. No-carrier-added (n.c.a.)

iii. Carrier-added (c.a.)

Ideally, carrier-free systems are only achieved when artificial radio elements are used in the absence of longer-lived isotope of that element. In very early days, ^{99m}Tc was adjudged as radionuclide providing almost carrier-free radiosynthesis, but in recent years, the production of this radionuclide has increased tremendously keeping in pace of its extensive use in nuclear medicine. Due to this fact, its very long-lived isomer ^{99}Tc ($T_{½} = 2.1 \times 10^5$ years) become more and more in the environment achieving the status of a "natural-occurring" isotope, which scales down the radiochemistry of ^{99m}Tc almost to n.c.a. level.

Without any doubt, in radiosynthesis with cyclotron –produced radionuclides of natural-occurring elements, traces of stable isotopes of these elements are omnipresent and act as isotopic carrier. Even, when utmost care is taken in operational methods; this effect can not be avoided. Sources of natural isotopic carrier are the air, water target and reaction vessel materials, chemicals and solvents. Such contamination in solvents and chemicals are below the normal chemical purification limits, but they are still in the quantities that are in excess of the radionuclides. As mentioned earlier, radiosynthesis under this condition are referred to as no-

carrier-added (n.c.a.) and represents a state of practically highest attainable A_s. On the contrary, under some circumstances, addition of weighable quantities of stable isotopes is unavoidable. Principally, carrier addition is employed to increase the radiochemical yields or to make certain labelling reaction possible, but for other reasons such as for electrophilic ^{18}F, when n.c.a. $[^{18}F]F_2$ is too reactive to remove it from the walls of targets and tubing. This method is known as carrier-added (c.a.).

Labelling reactions and radiosynthesis on the n.c.a. scale mean to work at subnanomolar level. Naturally, the course of the reaction is totally different from that of a classical reaction of equimolar stoichiometric ratios. Such reactions, under non-equilibrium conditions, generally proceed according to pseudo-first-order kinetics, since the concentration of the precursor to be labelled is in a very high excess to the n.c.a. radionuclide and can be approximately set as constant. For a reaction of the form A + B → C, where A is the precursor, B the radionuclide and C the labelled product and the starting concentration of B is $[B]_0$, the concentration of C after the reaction time t can be presented as:

$$[C]_t = [B]_0 \, (1\text{-}e^{-k't}) \; [mol/l]$$

where k' is the rate coefficient of pseudo-first-order type and contains [A] as constant factor [48]. The decay-corrected yield, i.e. the radiochemical yield (RCY) is related to the starting activity. So, the RCY increases with proceeding reaction time 't' and increasing precursor concentration [A] and shows a hyperbolic character in a plot versus time. The final saturation yield ideally equals to $[B]_0$ and is achieved often within few minutes, due to the high excess of the precursor. Furthermore, the radionuclide and the labelled product both exist on the n.c.a. scale thus a

consecutive labelling reaction or other interaction of the two radioactive species can statistically be excluded.

In comparison to classical equimolar chemistry, some special points are to be considered in case of radiochemistry. Firstly, slightest impurities can easily reach the concentration level of the n.c.a. radionuclide; to that reason highest purity grade of solvents and substrates, especially precursor should be used. Secondly, the incorporation of the radionuclide into the designated molecule should occur in the latest possible step (so-called last-step labelling) to avoid multi-step synthesis with radioactive intermediates which will minimise the final yield of activity but maximizes the radiation exposure burden. Finally, the whole preparation of radiopharmaceutical including labelling reaction, purification , isolation and quality control should be finished within three half lives of the radionuclide.

1.5. Radiolabelling with fluorine-18

Depending on the production procedure of fluorine-18 (cf. Table 1.3), the fluorine-18 will be available in different chemical forms for the labelling reaction. Generally, the ^{18}F-labelling methods can be defined into three main categories:

(a) Nucleophilic ^{18}F-fluorination (b) Electrophilic ^{18}F-fluorination and (c) ^{18}F-fluorination via prosthetic group.

The first two procedures are the direct fluorination methods, while in the third one, first an ^{18}F-labelled prosthetic group or synthon is synthesized and in the next step it is suitably coupled with the molecules of interest that has the limitations of direct labelling with ^{18}F.

Nucleophilic ^{18}F-fluorination

At present, the aliphatic and aromatic nucleophilic fluorination with n.c.a. [^{18}F]fluoride is the only way suitable for preparing high specific activity ^{18}F-labelled tracers. The [^{18}F] fluoride, commonly produced by $^{18}O(p, n)^{18}F$ nuclear reaction on highly enriched [^{18}O]H_2O, is in aqueous solution. Due to its high electronegativity, it is strongly hydrated ($\Delta_{hydration}$ = 506 kJ/ mol) and very poor nucleophile. As a strong base, it is protonated in the presence of acidic protons to form H[^{18}F] (E_B = 565 kJ/mol), thus it is unavailable for further reaction. Furthermore, n.c.a. [^{18}F]fluoride has the tendency to adhere or to get absorbed on the reaction vessel walls. Thus, several major aspects have to be considered for successful nucleophilic fluorinations. Therefore, n.c.a. [^{18}F]fluoride must be activated and water removed before radiolabelling. For this purpose, for nucleophilic ^{18}F-fluorination, water is ideally replaced by dipolar aprotic solvents such as acetonitrile (MeCN), dimethyl sulfoxide (DMSO), dimethyl formamide (DMF), dimethyl acetamide (DMAA) because of their ability to solubilize the fluoride salts and most of the organic compounds used as precursor and their corresponding [^{18}F]fluorinated intermediate. Very recently, nucleophilic radio fluorination has been carried out successfully in polar protic solvent (t-BuOH, t-Amyl alcohol, 3, 3 –Dimethyl-2-butanol) instead of conventional polar aprotic solvent such as CH_3CN with increased fluorination yield with low amount of precursor and at a lower fluorination temperature [49, 50]. Compared with [^{18}F]fluorination using ionic liquids [51], the use of protic solvent provided higher yields without an additional separation procedure before high-performance liquid chromatography (HPLC) purification. Furthermore, alcohol was removed easily by evaporation due to lower boiling temperature (~ 100˚C) [52]. In routine production, anion activation phase transfer catalyst (PTC) like tetraalkylammonium carbonates ($TBAHCO_3$), hydroxides or mainly aminopolyethers such as Kryptofix® 2.2.2 (4,7,13,16,21,24-

hexaoxa-1,10-diazabicyclo[8.8.8] hexasone) in combination with potassium carbonate or oxalate as base are employed [53 - 55]. While the amino poly ether complexes the potassium ion and composes a $[K/2.2.2]_2CO_3$ cryptate system, the [^{18}F]fluoride ion is non-hydrated and available with very high nucleophilicity. If the solubility product of the cryptate system is not exceeded in this procedure, the losses by the wall–adsorption are negligibly small [56]. Further, the proper ^{18}F-labelling reaction must be carried out in absence of positive ions e.g. metallic cations, which would also inactivate the naked [^{18}F]fluoride.

The direct nucleophilic ^{18}F-fluorination of aliphatic compounds proceeds according to S_N2-mechanism. The leaving groups in the precursor molecules can be, for example, mesylate (methane sulphonate), tosylate (p-toluene sulphonate), nosylate (p-nitro benzene sulphonate) or triflate (trifluoromethane sulphonate) [53] [**Fig. 1.2.**].

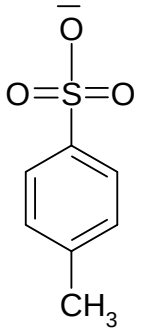

p-toluenesulfonate (Tosylate)

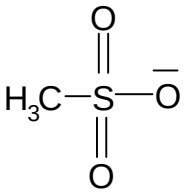

Methanesulfonate (Mesylate)

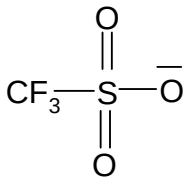

Trifluoromethane sulfonate (Triflate)

Fig. 1.2. *Structures of the leaving groups generally introduced in the precursor molecule for the ^{18}F-fluorination of aliphatic compounds*

Generally, triflate precursors give the best results [57, 58]. Halogen also in some cases serves the purpose of successful leaving groups. Among halogens, bromine (Br) has shown the best leaving group characteristics, for example, the preparation of ω-[^{18}F]fatty acids or their analogues [59, 60]. The incorporation rate of ^{18}F-fluoride is not the only important factor when choosing the appropriate leaving group. The choice also depends on the stability of the precursors, the ease of the subsequent purification process, or the formation of the side products.

When the leaving group is replaced by the [^{18}F]fluoride, the stereochemistry is changed by the concertedly proceeding Walden Inversion according to the stereo specific S_N2 mechanism. In this way, the most widely used radiopharmaceutical, [^{18}F]FDG (2-[^{18}F]fluoro-2-deoxy-D-glucose) is synthesized starting from the completely acetylated mannose precursor, mannose triflate (1,3,4,6-tetra-O-acetyl-β-D-mannopyranose) by a ^{18}F-for-triflate exchange and subsequent hydrolysis [61][**Fig. 1.3.**]. The overall average synthesis yield including purification proceeds in about 45-50%.

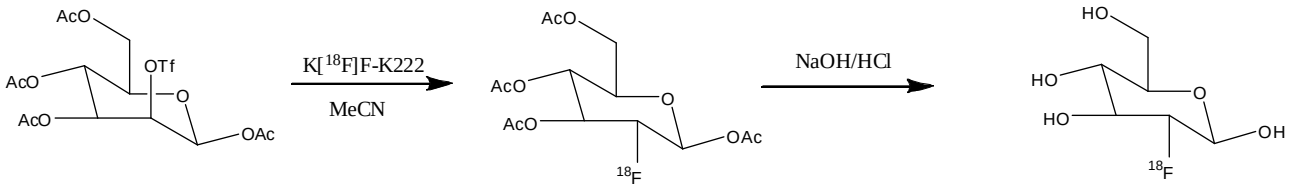

Tf = Triflate ($-SO_2CF_3$)

Ac= Acetyl group

Fig.1.3. *Radiosynthesis of [^{18}F]FDG. The synthesis is carried out by first a nucleophilic substitution of triflate by [^{18}F]fluoride, and second hydrolysis of the acetyl groups resulting in the formation of [^{18}F]FDG* [61]

Additionally, the nucleophilic aromatic n.c.a. [^{18}F]-fluorination is of great importance for the development of ^{18}F-labelled radiopahrmaceuticals. Besides, multiple possible aromatic radiotracers, the generally good metabolic stability of the resulting ^{18}F-labelled aromatic compounds is a major advantage. Consequently, nucleophilic aromatic substitution where ^{18}F is substituted for a proper leaving group has become a method used widely in ^{18}F-chemistry [62] . Aromatic rings themselves are not suitable for nucleophilic substitution with fluoride, but if the aromatic ring is activated by the presence of one or more electron-withdrawing groups in *ortho*- or *para*- positions to the leaving group, a direct mucleophilic exchange is possible [63-65].

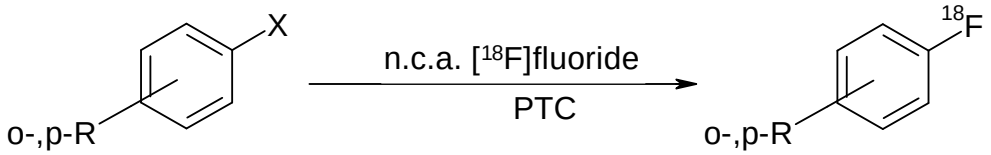

Fig. 1.4. *Nucleophilic aromatic ^{18}F-fluorination with activated arenas, X = Br, Cl, I, NO_2, $N(CH_3)_3^+$ (counter ions: TfO^-, TsO^-, ClO_4^-, I^-); R = NO2, CN, CHO, RCO, COOR, Cl, Br, I; PTC = $[K/222]_2CO_3$, $[K/222]_2C_2O_4/CO_3$, R_4N^+, Cs^+, Rb^+* [66]

Substituents such as NO_2, CN, CHO or $COCH_3$ can function as strong electron-withdrawing groups [66]. A variety of leaving groups are used, but the nitro and tetra methyl ammonium groups

are the most used and efficient in aromatic substitutions with ^{18}F-fluoride [67] [**Fig.1.4**].Simple isotopic exchange substitution between ^{18}F-fluoride and ^{19}F-fluoride can be rapid but results in low specific activity and is therefore not suitable in cases where high specific activity is needed. A direct one-pot nucleophilic ^{18}F-for-NO_2 substitution of the nitro precursor is often well suited for routine preparation of radiotracers such as [^{18}F]aryl fluorides, [^{18}F]altanserin [68] [**Fig.1.5.**] and [^{18}F]butyrophenone neuroleptics [69] [**Fig. 1.6.**].

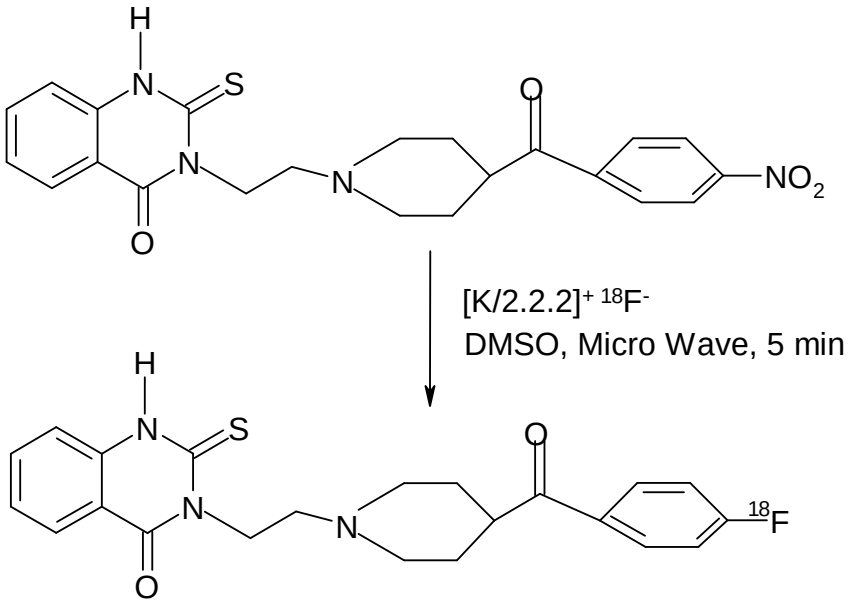

Fig. 1.5. *Radiolabeling of [^{18}F]Altanserin starting from its nitro precursor* [68]

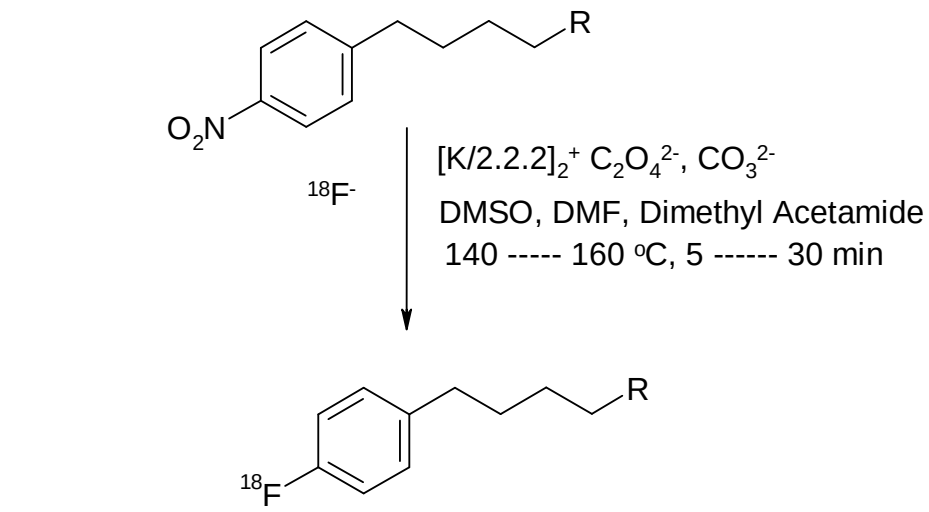

Radiochemical Yield
25 -------- 35 %

R =

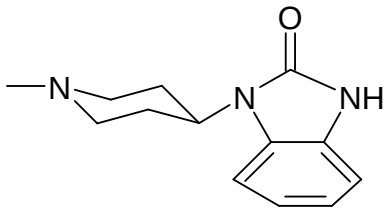

Benperidol

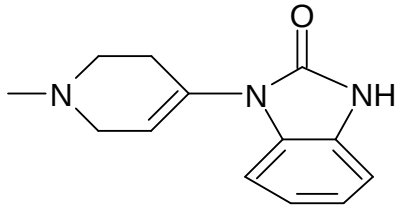

Droperidol

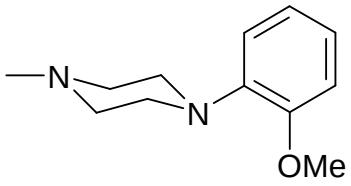

Fluanisone

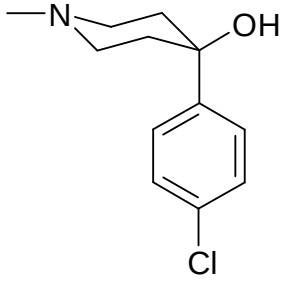

Haloperidol

Fig.1.6. *General labeling conditions for direct nucleophilic ^{18}F-fluorination of butyrophenone neuroleptics*.

Electrophilic ^{18}F-fluorination

Electrophilic ^{18}F-fluorination is characterized by the reaction of highly polarized fluorine with an electron rich reactant, e.g. an aromatic system, an alkene or a carbanion. [^{18}F]F_2, the simplest electrophilic fluoro-species, is obtained directly from the irradiated target. Other reagents have to be prepared in subsequent steps, either from carrier-added (c.a.) [^{18}F]F_2, or no carrier-added (n.c.a.) fluoride. [^{18}F]XeF_2 can be obtained in target via the ^{19}F(p, pn)^{18}F process on XeF_2, by the reaction of Xe and [^{18}F]F_2 or by isotopic exchange of XeF_2 with [^{18}F]HF. Synthesis of another important reagent, [^{18}F]acetylhypofluoride ([^{18}F]AcOF) can be carried out by passing dilute fluorine-18 gas through a solution of ammonium acetate in glacial acetic acid [70], or via an on-column gas-solid phase reaction by passing F_2 diluted in N_2 through columns containing complexes of alkali metal acetates with acetic acids [71-73].

Due to the necessary carrier addition in the [^{18}F]F_2 production and the fact that every [^{18}F]F_2 molecule carries on an average only one ^{18}F atom, the theoretical achievable maximum radio chemical yield in electrophilic ^{18}F – substitution is limited to 50%. This also applies to all other electrophilic reagents, because they are either produced via [^{18}F]F_2 or by isotopic exchange. Furthermore, the products are c.a. with maximum specific activities in the range of 0.04-0.4 GBq/µmol. Consequently, this method is limited to the production of a tracer (a) which competes to a high concentration of endogenous analogues *in vivo*, e.g. amino acids (b) which bind to molecular targets of low saturability, e.g. enzymes or transporter substrates. Due to the high reactivity of electrophilic ^{18}F-labelling agents, their selectivity is rather low and undesired radical side reactions and those with solvents take place. Therefore, electrophilic methods call for extensive purification procedures to meet the requirements of very high purity of radiopharmaceuticals.

Regioselective aromatic fluorinations can be achieved using [^{18}F]fluorodemetallation reaction. Suitable organometallic precursors are aryltrimethyltin, aryltrimethylgermanium and aryltrimethylsilicon compounds, whereas the organotin moiety shows the best result [74,75].For example, Hess et al.[76] has recently described the synthesis of 2-[^{18}F]fluoro-L-tyrosine ([^{18}F]FET) via regioselective destannylation of O, N-di-Boc-2-trimethylstannyl-L-tyrosine-ethylester with 42% radiochemical yield [**Fig. 1.7.**].

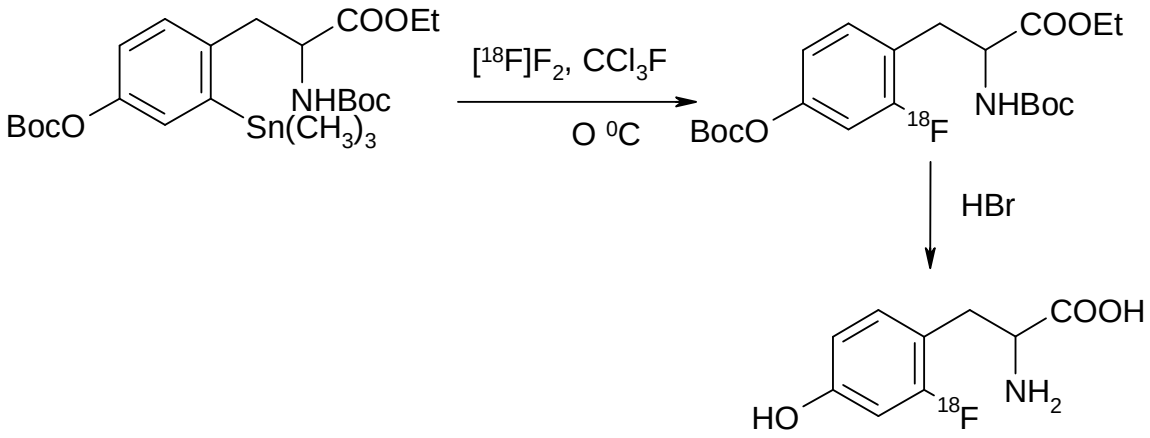

Fig.1.7. *Synthesis of 2-[^{18}F]fluoro-L-tyrosine via destannylation* [76]

However, for complex molecules including sensitive functional groups, those may have to be protected before radiofluorination and further radiosynthetic steps become necessary for the deprotection. As a first example, ^{18}F-labeling via an organotin precursor led to 25% RCY in case of 4-[^{18}F]fluoro-L-Phenylalanine [77], while direct electrophilic labeling causes isomeric mixtures of aromatic fluoroamino acids [78]. One more relevant PET radiopharmaceutical produced *via* electrophilic substitution is 6-[^{18}F]fluoro-3, 4-dihydroxyl-L-phenylalanine (6-[^{18}F]fluoro-L-DOPA). 6-[^{18}F]fluoro-L-DOPA is a radiotracer for the dopamine anabolism in the brain and is employed for the diagnosis of patients with neurodegenerative diseases (Parkinson's disease) and recently also in oncology due to its high tumor uptake. In clinical routine, 6-[^{18}F]fluoro-L-DOPA

is produced *via* ^{18}F-flourodestannylation, although the maximum RCY is only 30% and the specific activities are low [79, 80]. The lack of an efficient and simple automated nucleophilic methods for 6-[^{18}F]fluoro-L-DOPA requires the electrophilic path way. The reported nucleophilic methods still involves a multi-step radiosynthesis including chiral auxiliaries, and therefore complicates the automation and reduces the RCY [64].Very recently, "one pot" and "automation" friendly synthesis procedure of 6-[^{18}F]fluoro-L-DOPA has been reported which is based on isotopic exchange concept [81]. In the reported procedure, the new precursor, (2S,5S)-*tert*-butyl-5-(4-benzyloxy-2-fluoro-5-formylbenzyl)-2-*tert*-butyl-3-methyl-4-oxoimidazolidine-1-carboxylate enables the radiosynthesis of 6-[^{18}F]fluoro-L-DOPA by an isotopic exchange reaction with ^{18}F-fluoride. Thereafter, only, two further radiosynthesis steps, namely, Baeyer-Villiger oxidation with mCPBA followed by hydrolysis with HBr, the desired L-isomer of c.a. 6-[^{18}F]fluoro-L-DOPA is isolated at an enantiomeric purity of more than 99%. The complete preparation and isolation of c.a. 6-[^{18}F]fluoro-L-DOPA under the conditions optimized gives about 22% yield after a synthesis period of 105 min [**Fig. 1.8.**].

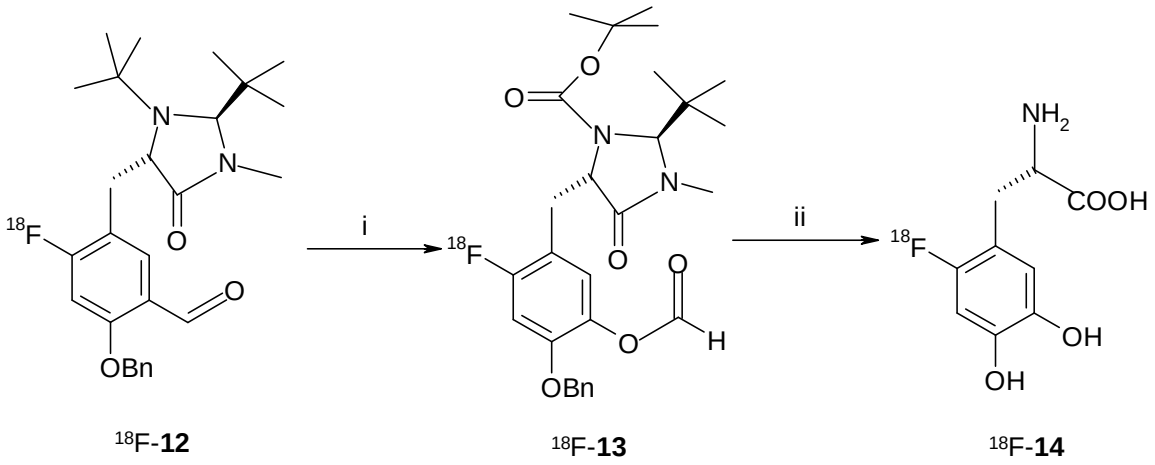

^{18}F-**12** ^{18}F-**13** ^{18}F-**14**

Fig.1.8. *Radiosynthesis of 6-[^{18}F]fluoro-L-DOPA (^{18}F-14) by Bayer-Villiger oxidation of(^{18}F-12) and subsequent acid hydrolysis (i) mCPBA, $CHCl_3$, 60°C, 20 min (ii) HBr(47%), 150°C, 30 min* [From [81]]

^{18}F-fluorination via prosthetic groups

Direct nucleophilic substitution is in many cases difficult and sometimes impossible to carry out in complex and multisubstituted molecules that have not been activated with a good leaving group. The ^{18}F-fluorination via prosthetic groups is an indirect method. This means a primary ^{18}F-fluorinated labelling group is coupled with a second molecule to form the product molecule. Important procedures via prosthetic groups are ^{18}F-fluoroalkylation [82, 83], ^{18}F-fluoroacylation [84, 85], and ^{18}F-fluoroamidation [86] [**Fig.1.9**]. Application of these ^{18}F-labelling pathways via prosthetic groups are wide spread and can be applied with almost every molecule carrying a protic function such as thiol, amino or hydroxyl group. In practice, several bio-relevant molecules e.g. receptor ligands of the dopamine system [87] and the serotonin system [88], benzodiazepines [89], amino acids [33] and analogues of cocaine [90] are ^{18}F-labelled via ^{18}F-fluroalkylation. In contrast, ^{18}F-fluoroacylation and ^{18}F-fluoroamidation are of great interest for the ^{18}F-labelling

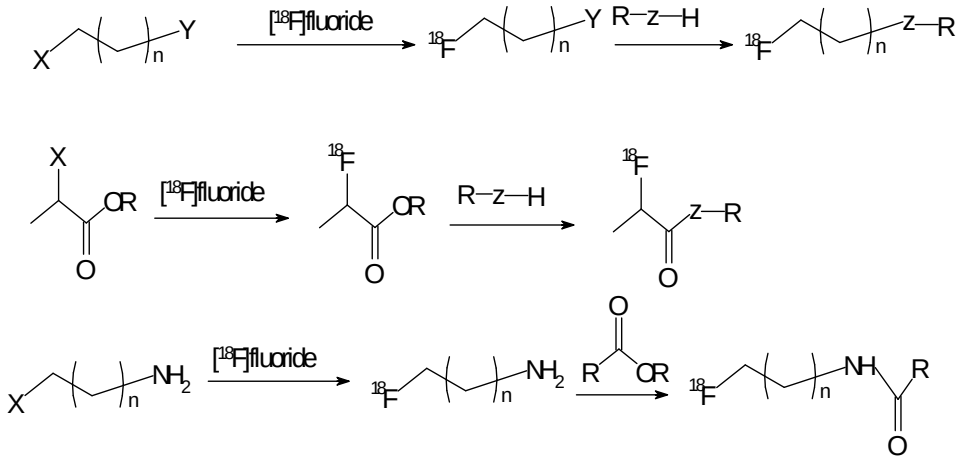

Fig.1.9. *^{18}F- fluorination via prosthetic groups, top: ^{18}F-fluoroalkylation; middle: ^{18}F-fluoroacylation; bottom: ^{18}F-fluoroamidation (X, Y = Br, I, OTs, OTf; Z = N, O, S; R = alkyl, aryl)*

of proteins and peptides since they allow radio syntheses under amide-bond formation in aqueous system [91]. As a result, β-^{18}F-labelled ester were successfully coupled e.g. biotin [92] and the protein octreotide, the first ^{18}F-labelled peptide [93].

CHAPTER-2
Adapted General Purpose Synthesis Module for Radiofluorination

2.1.
Automation of PET Radiotracer Synthesis

The motivation for the development of automated systems is clear and compelling since unique operational and safety requirements of PET radiotracer synthesis is essential. These unique constraints include short synthesis (within 2 or 3 half-lives of the radioisotope used) and control from behind bulky shielding structures that make both access to, and visibility of, radiochemical process and equipment difficult. Often tens of GBq (Curie) levels of positron emitting nuclides are required for synthesis of PET radiopharmaceuticals, making this potential source of unacceptable radiation exposure for a radio-chemist involved. The use of short half-lived radionuclides also necessitates that the PET radiotracer (particularly those labeled with ^{11}C, ^{13}N and ^{15}O) be synthesized more than once during the day, each dose being produced separately just before administration. Radiotracer synthesis must be reliable and efficient to keep the costs of the PET studies low and affordable for the patient. Furthermore, radiotracer synthesis procedures for human use must follow pharmaceutical quality assurance and be well documented and as per the requirements of the existing rules and regulations of the country where the work is carried out. Automation can help in fulfilling these obligations by overcoming the limitations of human errors possible in routine work. PET research institutions overcome all these potential limitations. In the span of last ten years, the automation of PET radiotracer synthesis has developed tremendously and presently several types of automated synthesis modules for various PET radiotracer synthesis are commercially available from large number of companies.

2.2.

Automated PET Radiotracer Synthesis Modules

The automated synthesis device, often called a *black box*, is a unit controlled by microprocessors and software programmes (**time lists**) to carry out the sequential physical and chemical steps to accomplish the entire synthesis and purification of a radiolabeled product. The unit consists of templates or vials pre-filled with required chemicals attached to the apparatus via tubing that are connected to solenoid valves to switch on and off as needed. Most black boxes are small enough to be placed in hot cells 20 X 20 X 20 inches (inner dimensions) and are designed for cleaning and sanitizing by simple procedures. In some cases, disposable cassettes are employed so that new clean and sterile cassettes can be used for each new synthesis. Various parameters for synthesis such as time, pressure, volume and other requisites are well controlled by a remote computer. In all the cases, the synthesis modules are kept inside air-tight appropriate lead shielded hot cells (having negative pressure inside). In cassette based synthesis module, once the cassette which comes with pre-filled reagents is plugged and programme initiated, the whole synthesis will finish at a stretch. The difficulty with this type of synthesis module is that there is no provision of manual intervention if any step of the synthesis goes wrong, leading to failure of the whole production. The advantage is from its operational simplicity and non-requirement of specialist radiochemist. The advantage of the non-cassette type of synthesis module is that the synthesis can be paused at a particular step if it goes wrong and subsequent steps can be carried out manually and can successfully save the production. Further, reagent quantities can be optimized as per the previous yield obtained. However, the availability of an experienced PET radiochemist is a must. Normally, simple two step radiosynthesis procedure like the case of [^{18}F]FDG synthesis from mannose triflate (first step: selective radiofluorination of the specially

designed precursor molecule and subsequently, in the next step removal of the blocking groups either by acid or alkali hydrolysis) are preferred one for the routine production. Now, if the purification is manageable by solid phase extraction cartridges either commercially available or assembled in-house, then simple GE Tracerlab FX_{FDG} type synthesis module (single reaction vessel) is sufficient. But if the chemistry is a multistep process (like the attachment of a ^{18}F-labelled synthon to a biomolecule, ^{18}F-peptide labeling via ^{18}F-SFB etc) and the purification needs semi preparative HPLC (high performance liquid chromatography), then a synthesis module with minimum two reaction vessels equipped with semi-prep HPLC purification facility is needed for e.g. Tracerlab FX_{F-N}. This type of module is also a must for R&D of the development of new ^{18}F-labeled PET Radiotracer.

In our facility, we have two dedicated [^{18}F]FDG synthesis modules (Originally procured from Nuclear Interface, Münster, Germany, now branded as GE Tracerlab FX_{FDG}) and one [^{11}C] Methylation module [Model No. 14369, Nuclear Interface, Münster, Germany] for the synthesis of [^{11}C] Methoinine. The very limited use of this module for the purpose it was procured and the chemistry process used together with the non-availability of chemicals gave us the idea to modify it in such a manner so that it could be used as a basic nucleophilic fluorination synthesis module. The modification is also planned in such a manner that by any time it can be revert back to the original [^{11}C]Methylation module. The ultimate goal was to use this module to synthesize many other useful non-FDG PET radiopharmaceuticals like Na[^{18}F], [^{18}F]FMISO, [^{18}F]FAZA, [^{18}F]FLT etc by developing a solid phase purification procedure like [^{18}F]FDG, since in all the cases the basic outline of the nucleophilic fluorination strategy is similar.

2. 3.

Conversion of [^{11}C]Methylation Module for [^{18}F]FDG synthesis using SPE (Soild Phase Extraction) purification cartridges

2.3. a.

Rearrangement of tubing connection

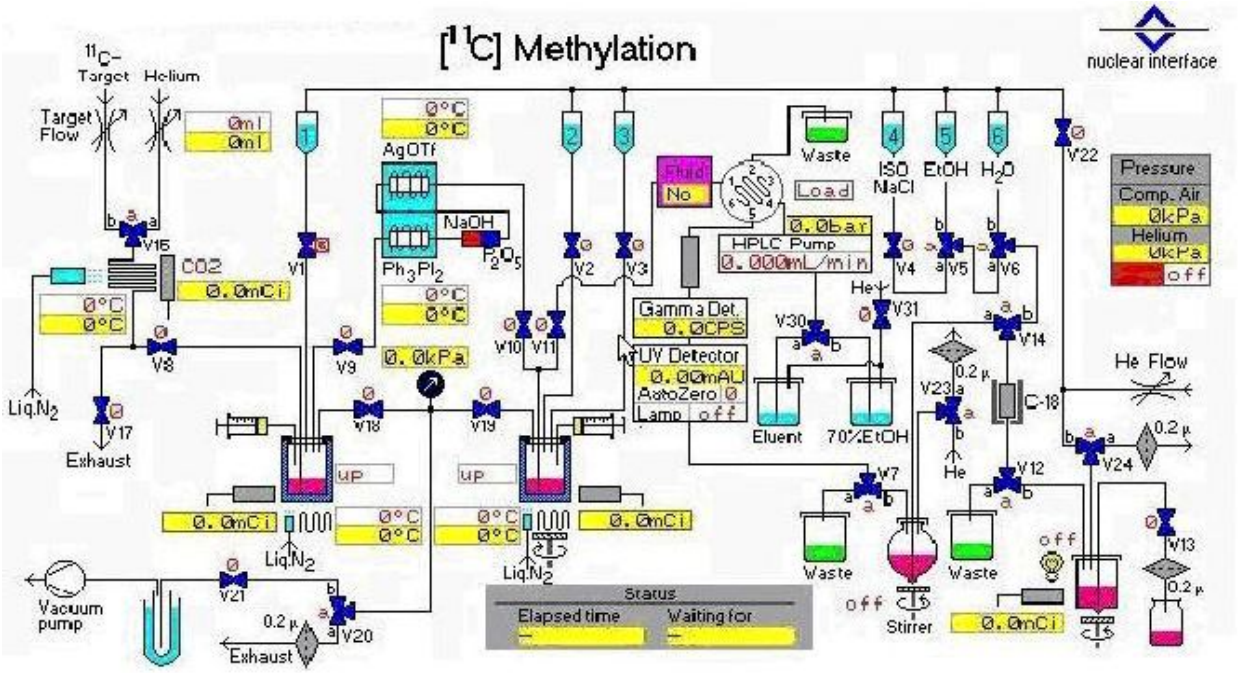

Fig.2.1. *Control Screen of [^{11}C]Methylation Module*

The original [^{11}C]Methylation module [**Fig.2.1.**] was having two reactors i.e. reactor-1 and reactor-2. The reactor-1 was having a heating facility through a sensor controlled heater. For cooling, liquid nitrogen cooling facility was available. This was required to condense the ^{11}CO & $^{11}CO_2$ produced by the cyclotron irradiation and send through Tefzel tubing to the module for further chemical process. There was no provision for compressed air cooling. There was no facility of stirring the reaction through magnetic stirrer. One GM counter was attached to reactor-1 to read the radioactivity value. The reaction vessel was of conical shape and made of glass with a volume capacity of 1.5 ml. The reaction vessel is attached with a PEEK reactor head which is having total four ports for the connections of tubing through standard connectors [**Fig.2.2**].

Transfer of reaction mixture is through PEEK tube is connected to the bottom of the reaction vessel through a pneumatic mechanism which enables the movement of the PEEK tube up and down inside the reaction vessel.

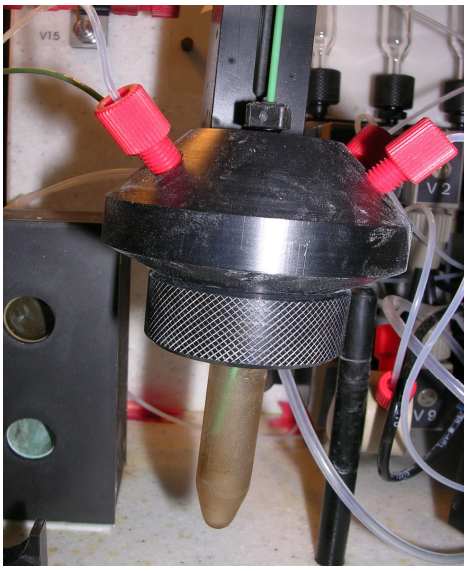

Fig.2.2. *Photograph of reactor-1 with a conical shaped glass made reaction vessel with the PEEK REACTOR HAED having four ports for connection of tubing through standard chromatography fittings. The Green PEEK tube is the "REACTION NEEDLE".*

The reaction [^{11}C]Methylation module was converted to receive the irradiated O-18 water from the cyclotron. So the existing reactor-1 of the [^{11}C]Methylation module was utilized in this purpose. The three ports are connected to three tubing to collect the irradiated O-18 water from three different targets (Target 1, Target 4 and N-13 target respectively, all of which are liquid targets). The remaining port is connected to exhaust to take care of helium pressure development during delivery of the irradiated O-18 water from the cyclotron.

For [^{18}F]FDG synthesis in the standard FDG module, the irradiated O-18 water is first passed through an anion exchanger (PS-HCO_3^-) to trap ^{18}F and the O-18 water is collected in the O-18 water recovery vial. If we look at the tubing connection details, the PS-HCO_3 column is in between two 3/2 way solenoid valves (V7 & V8). One port of V7 (Normally Closed, "N/C") is

connected to target vial. The other port (Normally Open, "N/O") is connected with a 2/2 way solenoid valve (V1) which is connected to the reservoir meant for $TBAHCO_3$ solution, the eluting solvent of [^{18}F]fluoride in the from of radioactive tetra butyl ammonium fluoride ($TBA^{18}F$) from the PS-HCO_3 column. The common port ("C") is connected to the top of the PS-HCO_3 column through a male nut. Of the two tubings coming out from V8, one ("N/C") is connected to the $H_2{}^{18}O$ recovery vial. The common port ("C") of the V8 is used to make connection with the bottom of the PS-HCO_3 column. The "N/O" port is connected to the reaction vessel through a 2/2 way solenoid valve (V9).The $H_2{}^{18}O$ recovery vial is connected to vacuum through V19 (2/2 way solenoid valve) via a three way connector. The third port of the three way connector is connected to V20 (3/2 way solenoid valve). One port (N/C) of this 3/2 way solenoid valve is connected to exhaust and the other port (C) is connected to the central reaction vessel through V18 (2/2 way solenoid valve) for creating vacuum inside the reaction vessel whenever required. In between V18 and V20 one pressure gauge is attached to show the pressure inside the reaction vessel throughout the synthesis [**Fig.2.3.**]. Solenoid valves control or, in the case of three way valves, redirect the passage of the fluid. A 2/2 way solenoid valves (**Bürkert, IN 120721**) is normally closed when there is no electrical input; it is actuated upon the arrival of 24-V input from the control box, allowing an open path for the fluid being transferred. On the contrary, in idle 3/2 way valve (**Bürkert, IN 120433**), has a flow path between the common port, or simply called "the common"(C), and one of the other two ports. In the actuated state, the valve opens the normally closed port (N/C) and blocks the normally open (N/O) one, redirecting the flow into or out of the common [**Fig.2.4.**].

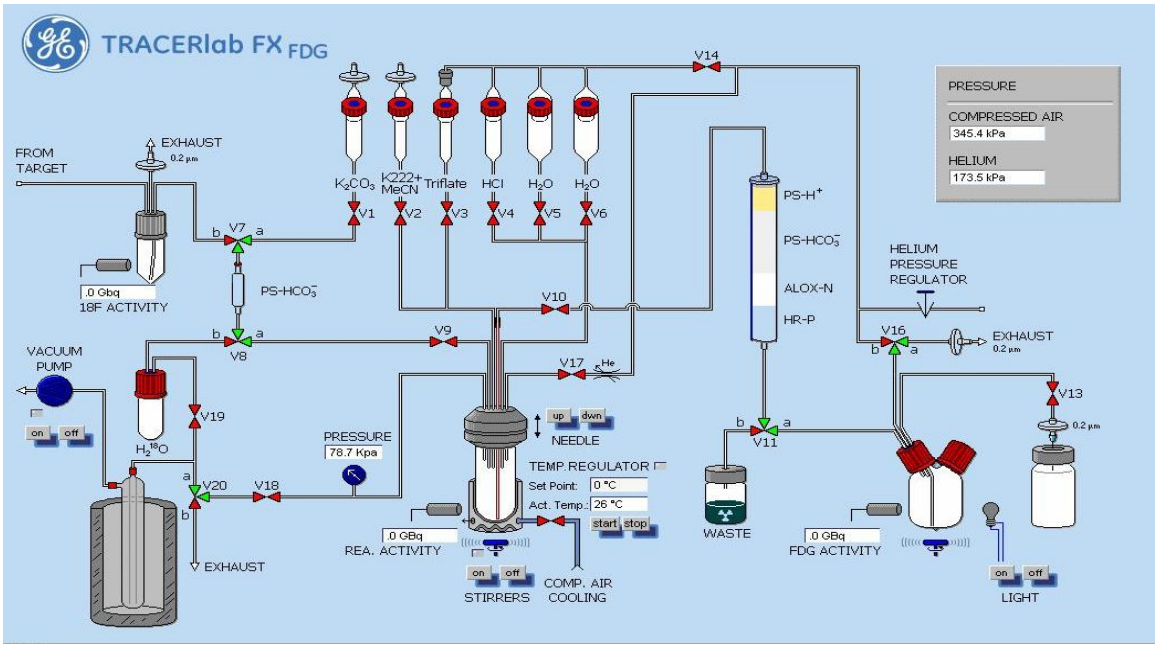

Fig. 2.3. *Showing Default Operating Position of V7, V8, V20, V11, V16 (All 3/2 way solenoid valves, Green = Open, Red = Closed)*

Fig.2.4. *Bürkert 3/2 way valve showing Common (C), Normally Open (N/O) and Normally Closed (N/C) ports. In idle position, "C" and "N/O" ports are open. When 24 V input comes from the control panel, "C" and "N/C" ports are opened. Automatically "NO" port remains closed. Thus, correctly selecting the ports, liquid can be transferred in different directions using the same valve.*

Now, for the conversion of [^{11}C]Methylation module to a FDG synthesis module, we have to make similar type of arrangement. The existing [^{11}C]Methylation module did not have such provision for housing a PS-HCO_3 and collection vial for collection of recovered O-18 water. So,

stand was fabricated and used in this purpose [**Fig.2.5.**]. Of course it was modified to suit the purpose and fit inside the module. The tubings and the valves were reoriented to achieve the same chemical process that takes place in the Tracerlab FX_{FDG} module. The existing glass reagent reservoirs were changed with ones of the required volumes, which were fabricated in our glass blowing section and tested for air-tightness before fitting. For creation of vacuum inside the recovery vial for efficient passage of irradiated O-18 water through the column, one thick hypodermic needle is used in the recovery vial and the other end is directly connected to vacuum line through appropriate valves.

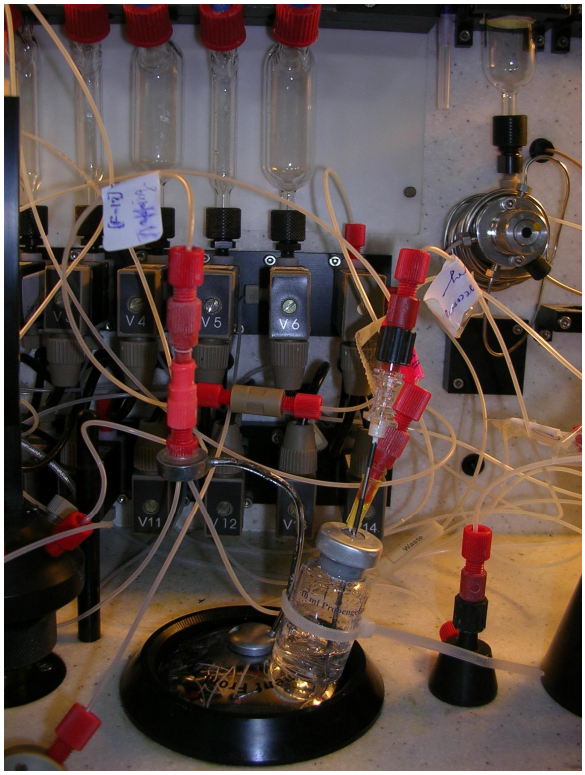

Fig.2.5. *Stand fabricated for housing PS-HCO_3 column and O-18 recovery vial*

An important step in [^{18}F]FDG synthesis is the transfer of the reaction mixture through the purification cartridge and elution of the product from the purification cartridge. For this the practice is to add large volume (normally 12 ml) of eluting solvent to the reaction vessel from

one of the reservoir (reservoir 6, **Fig. 2.1.**) and then pump the liquid from the reaction vessel through the purification column and collect the eluent coming out of the column to the product vial. A similar arrangement was made to guide the eluting solvent to pass through the purification column and the liquid coming out of the purification column is collected in the product vial. After carrying out all these modification and rearrangement of the existing C-11 methylation module, it was transformed to a fluorination module suitable for FDG type reaction and purification through a solid phase purification cartridge [**Fig.2.6.**].

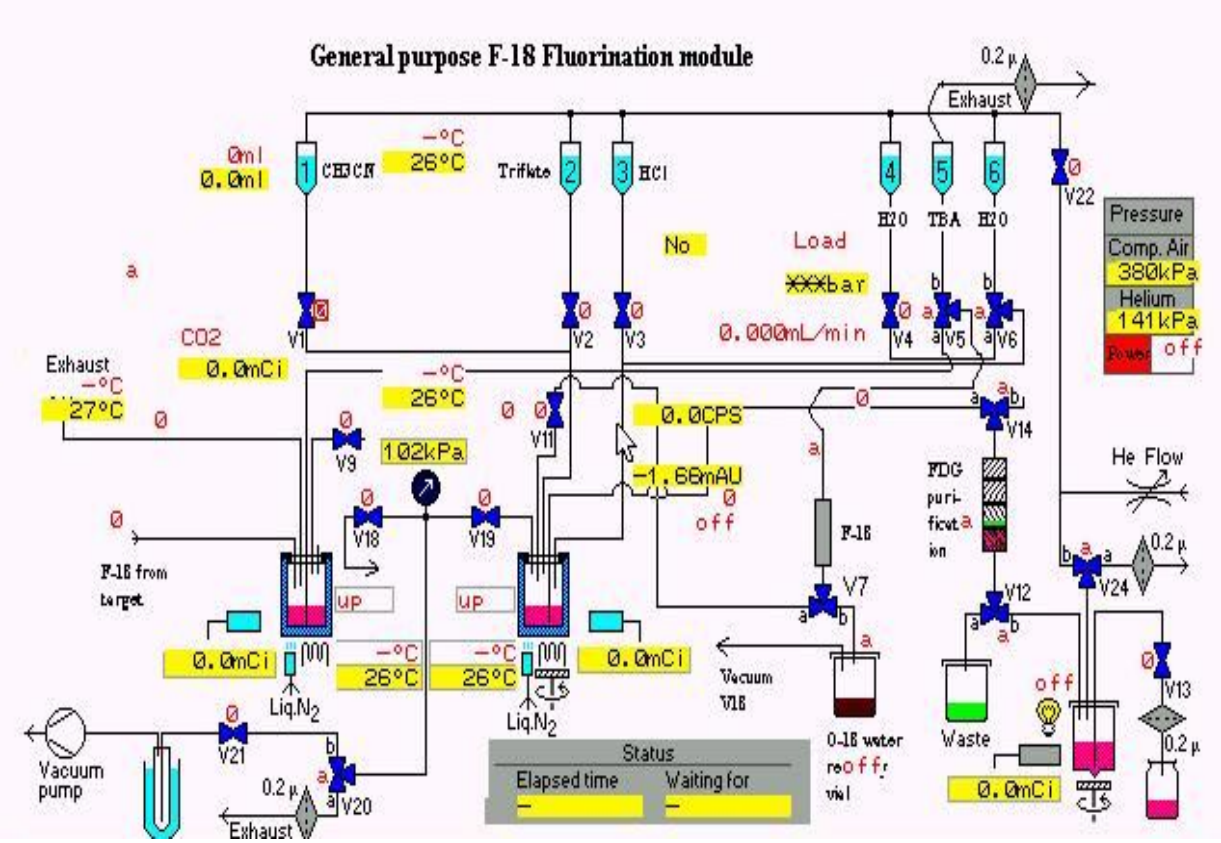

Fig.2.6. *Control Screen of General Purpose Fluorination Module*

2.3. b. Helium and Compressed Air Connection

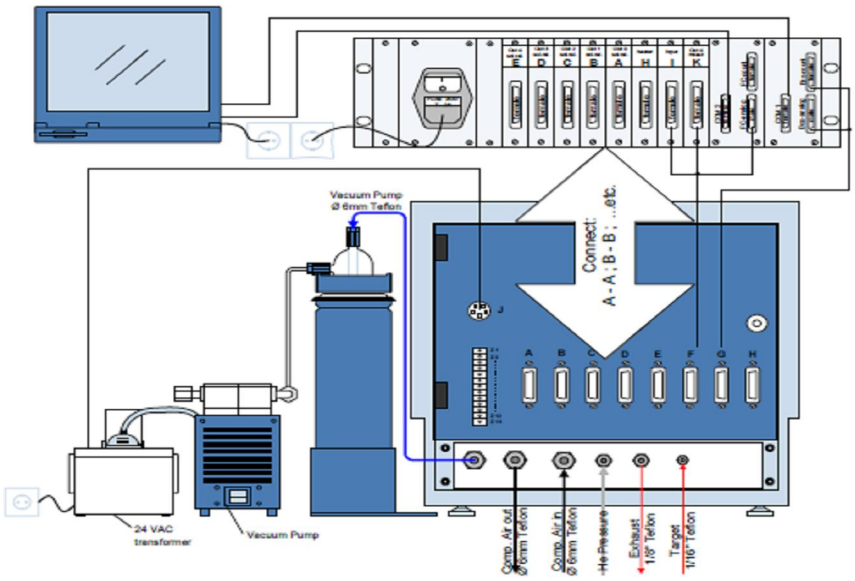

Fig.2.7. *Schematic diagram of the synthesizer back door showing the connections of compressed air (in and out), helium gas, vacuum and exhausts*

External to the module, the source of compressed air and helium gas is connected to the synthesizer through metal connectors provided at the back side of the synthesizer [**Fig.2.7.**]. The regulators [**Fig. 2.8**.] for both the compressed air and the helium gas is inside the synthesizer and accessible by opening the back door. The helium pressure was suitably adjusted to 100 ± 10 kPa (14.5 ± 1.45 psi), and similarly, the compressed air supply was adjusted to 400±50 kPa (58 ± 7.25 psi).

Fig. 2.8. *The helium pressure regulator inside the synthesizer which is accessible after opening the back door of the synthesizer*

2.3. c. Heating arrangement for the reaction vessel

The radiofluorination of mannose triflate, the precursor of [^{18}F]FDG is carried out at 85°C for 5 min and subsequently the acid hydrolysis takes place at a much higher temperature of 125°C for 5 min. The heater assembly is mounted at the base of the synthesizer [**Fig.2.9. & 2.10.**], and the glassy carbon reaction vessel goes into the groove of the heater and silicone oil is added as a conducting medium between the metallic groove of the heater and the glassy carbon vessel [**Fig. 2.11.**].

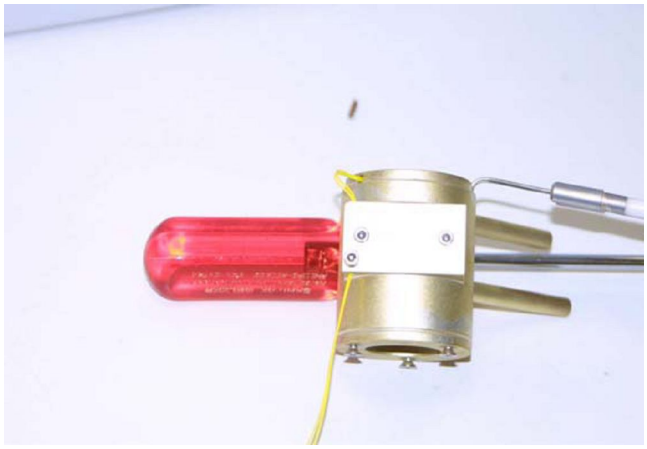

Fig.2.9. *Dismounted Heater Assembly showing the grove for housing the glassy carbon reaction vessel, thermocouple for heating arrangement and a thermocouple sensor (Yellow one) for temperature control*

Fig.2.10. *The mounted heater assembly at the base of the synthesizer*

Fig.2.11. *The attached glassy carbon reaction vessel on the reactor head and the cavity of the heater. The glassy carbon fits exactly inside the cavity of the heater.*

The reaction vessel is a glassy carbon tube (SPI-Glas™ Brand) with internal diameter of 20 mm and 100 mm longer. Glassy Carbon Reaction Tubes exhibit some very unusual properties which make them suitable for the purpose.

a. High Purity;
b. High thermal conductivity;
c. Corrosion resistance;
d. Impermeability to gas and liquids;
e. High hardness and strength, almost like that of a ceramic;
f. Low density;
g. High surface quality with excellent polishing characteristics (a black mirror reflective finish);
h. No adhesion;
i. Good resistance to thermal shock;
j. Biocompatibility;
k. Physical and chemical properties are isotropic.

For example, the SPI-Glas™ Brand Glassy Carbon Test Tubes, relative to quartz test tubes, exhibit far higher thermal conductivity and show very little adhesion. Thermal cycling times are reduced, sometimes substantially. This also means that the heater coils can be operated at lower temperatures than would otherwise be mandated if ceramic or quartz test tubes were being used. Because of the lack of any porosity and high purity, and high temperature properties, glassy carbon is the ideal material for fabrication into evaporation boats. Its non-wetting characteristics make it the ideal approach for certain otherwise difficult –to-evaporate materials. In our case,

since the reaction mixture is heated by heat transfer by silicone oil which is primarily getting heated by the heater arrangement, glassy carbon is the ideal material for reaction vessel.

The existing reactors of the [^{11}C]Methylation module were made of quartz [**Fig.2.12.**] and of smaller dimension than the standard glassy carbon reaction tube available. Further, the [^{11}C]Methylation module does not have the "compressed air blast" cooling mechanism as in Tracerlab FX_{FDG} ; but it gets cooled by cold helium gas which, in the [^{11}C]Methylation module, is cooled by liquid N_2 kept in a large Dewar flask. Cooling of the reaction vessel is essential to avoid any kind of thermal degradation and hence we need a reaction vessel of better thermal conductivity. Secondly, because of the smaller size, we had restriction of the quantities of reagent to be used during the reaction. Lastly, the use of a magnetic stirrer inside the reaction vessel for homogeneous heating and cooling is essential. These above three conditions could not be met because of the smaller size of the quartz glass reaction vessel and most importantly, because of the conical ("V") shape at the bottom, the use of a magnetic stirrer was almost impossible. All these reasons guided to change the reaction vessel to a standard glassy carbon one, similar to Tracer lab FX_{FDG}. To do this, the cavity of the heater assembly in the original [^{11}C] Methylation module [**Fig.2.13.**], which was of smaller dimension was changed to fit with the bigger OD glassy carbon vessel.

Fig.2.12. *The glassy carbon reaction vessel (black one, normally used in Tracer lab FX_{FDG}) and the existing quartz glass reaction vessel of the [^{11}C]Methylation module*

Fig. 2.13. *Dismounted heater assembly of the [^{11}C]Methylation module. The "cavity" inside the heater can only house the quartz reaction vessel not the bigger dimension glassy carbon one.*

For the same reason, the reactor head, which was fit for the small quartz reaction vessel of the [^{11}C]Methylation module [**Fig. 2.14. & 2.15.**] was changed with the other one fit for the glassy carbon one [**Fig. 2.16. & 2.17.**].

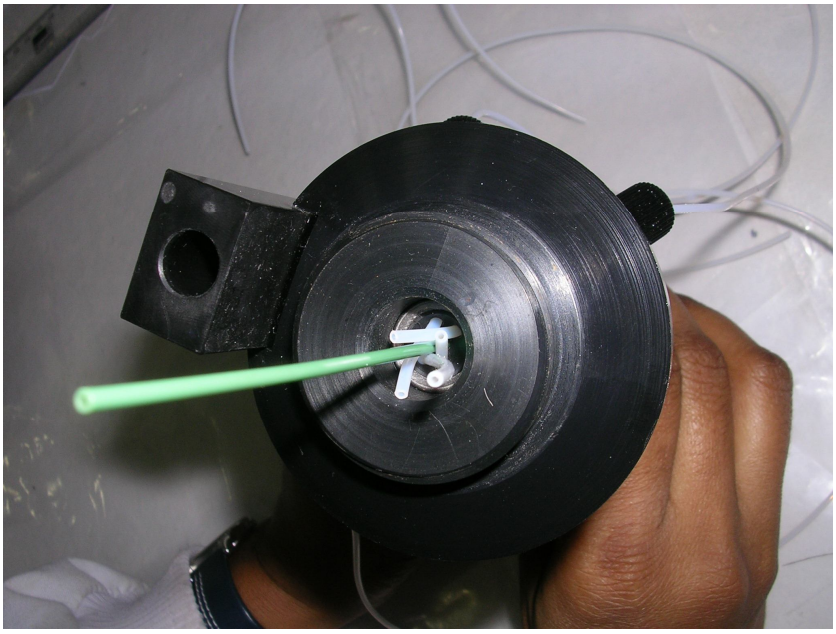

Fig.2.14. *The reactor head cavity for holding the quartz reaction vessel of [^{11}C]Methylation module (Bottom View)*

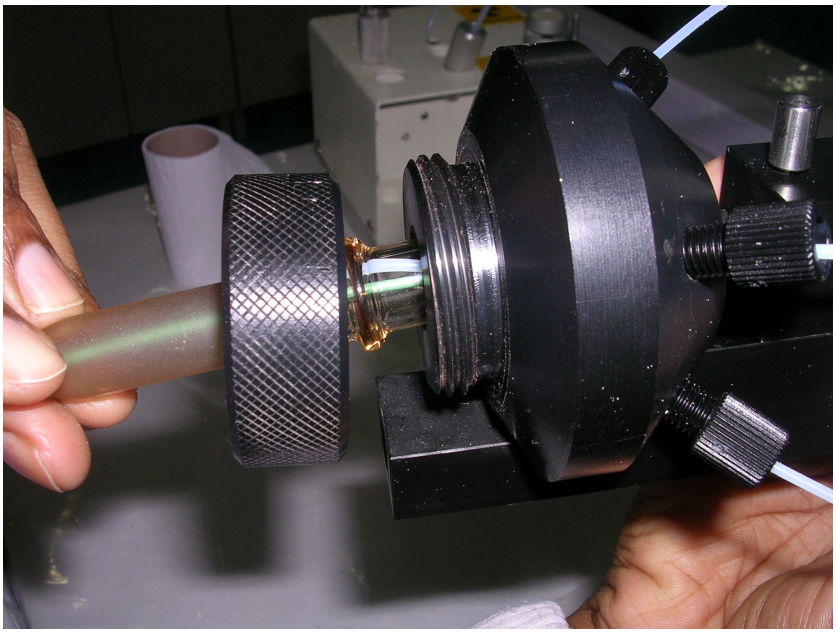

Fig.2.15. *The attachment assembly of the quartz glass reaction vessel with the reactor head of the [^{11}C] Methylation module*

Fig. 2.16. *Reactor head of standard Tracer lab FX$_{FDG}$ synthesizer*

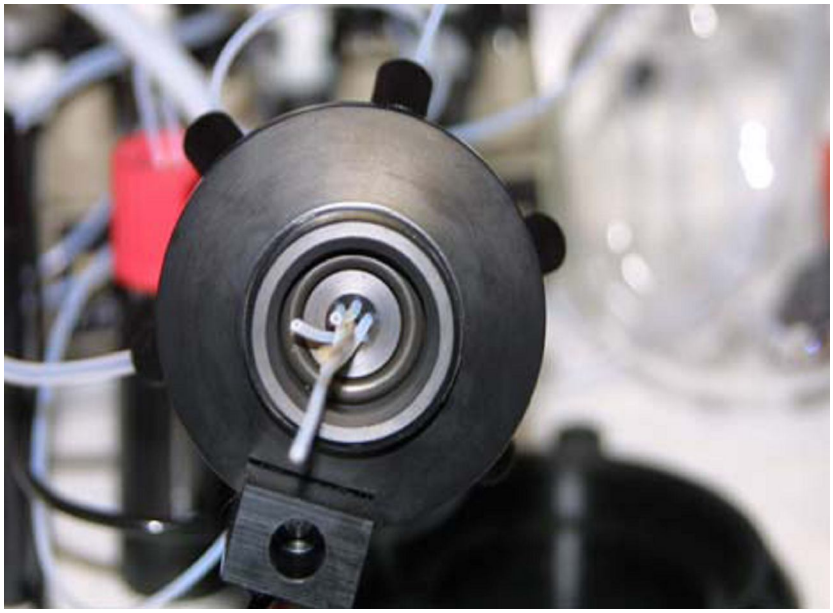

Fig.2.17. *Reactor head of standard Tracerlab FX_{FDG} (Bottom View) showing the arrangement for attaching bigger glassy carbon reaction vessel*

2.3. d. The reaction vessel cooling arrangement

In the original [^{11}C]Methylation module, for cooling the reaction vessels, chilled pressurized helium is utilized. Pressurized helium, through a coil, flow inside a tightly closed Dewar tank filled with liquid nitrogen. The Dewar Tank [**Fig.2.18.**] is kept outside the hot cell and the piping connection enters into the hot cell through a hole provided at the bottom of the hot cell. In case of [^{11}C]Methylation, the purpose of using liquid nitrogen is first to condense the ^{11}CO or $^{11}CO_2$ as fast as possible as they are the radioactive species obtained from cyclotron irradiation, Secondly, the cooling process must be very fast considering the very short half-life of ^{11}C (half life: 20 min) so that the overall synthesis time remains as short as possible ensuring minimum loss for radioactive decay. For nucleophilic radio-fluorination reactions, such rapid cooling is not necessary.

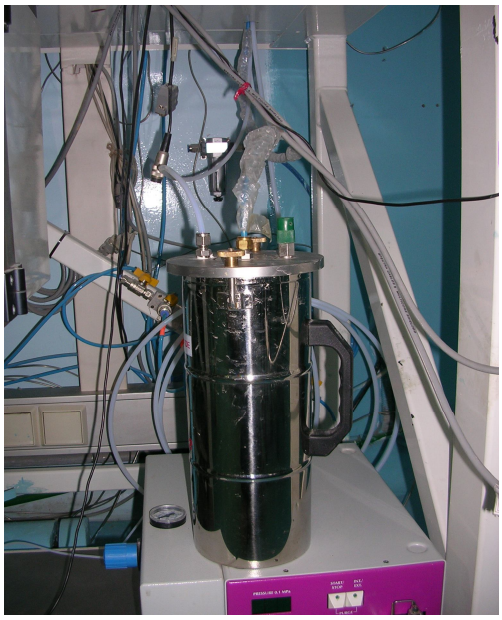

Fig.2.18. *The Dewar Tank out side the hot cell for liquid nitrogen storage*

Hence, instead of liquid nitrogen, dry ice or normal ice is filled into the Dewar, and then closed tightly ensuring no leakage. Now, when helium is pumped into the Dewar, it gets cooled in contact of dry ice or normal ice and then this cooled helium gas is sufficient to effectively cool the reaction vessel.

2.3. e. The "Time Lists" for the Radiosynthesis

The synthesis module is controlled by the DOS based computer programme NINA® which was provided along with the original [^{11}C]Methylation module by Nuclear Interface, Münster, Germany. Any fully automated radiosynthesis through this type of module is based on a "time list" [**Fig. 2.19.**] which is basically the sequence of operation to be performed during the whole synthesis process including heating, cooling, transfer of radioactivity from the target vial to the reaction vessel etc. and works on the temperature and pressure sensors attached with the reaction vessel. The propagation of the reaction can be monitored by the online graph showing the temperature and pressure change of the reaction vessel at each step as well as monitoring the

radioactivity at different vessels i.e. “target vial”, “reaction vessel” and “the product vial” [**Fig. 2.20.**]. This “on line display” is very helpful to diagnose any problem during the radiosynthesis leading to a failure.

SKN-HDR synthesis program Page 1

No.	Time	Event type	Value	Unit
1	00"00	Vac.pump/heater	on	
2	00"00	V21 Vac. Reac	1	
3	00"00	V20 Exh. Reac	b	
4	05"00	V7 Waste	b	
5	06"00	V5 Vial 5	a	
6	07"00	Reac 1 needle	down	
7	08"00	V18 Vac. Reac.1	1	
8	01'50	V18 Vac. Reac.1	0	
9	01'52	Reac 1 needle	up	
10	01'52	V7 Waste	a	
11	01'52	V11 Reac. 2 Out	1	
12	01'52	V5 Vial 5	b	
13	01'53	V19 Vac. Reac.2	1	
14	02'30	V5 Vial 5	a	
15	02'31	V11 Reac. 2 Out	0	
16	02'32	V1 Vial 1	1	
17	02'52	V22 Helium Vial	1	
18	03'00	Reactor 2	55	°C
19	03'00	Wait for event	T React2	
20	T1+ 06'00	Reactor 2	95	°C
21	+ 06'00	Wait for event	T React2	
22	T2+ 02'00	V1 Vial 1	0	
23	+ 03'30	Reactor 2	65	°C
24	+ 03'30	Wait for event	T React2	
25	T3+ 00"00	V20 Exh. Reac	a	
26	+ 05"00	V2 Vial 2	1	
27	+ 15"00	V2 Vial 2	0	
28	+ 15"00	V20 Exh. Reac	b	
29	+ 15"00	V21 Vac. Reac	0	

Fig.2.19. *The “Time List” of a radiosynthesis showing the sequence of operations to be performed during the synthesis*

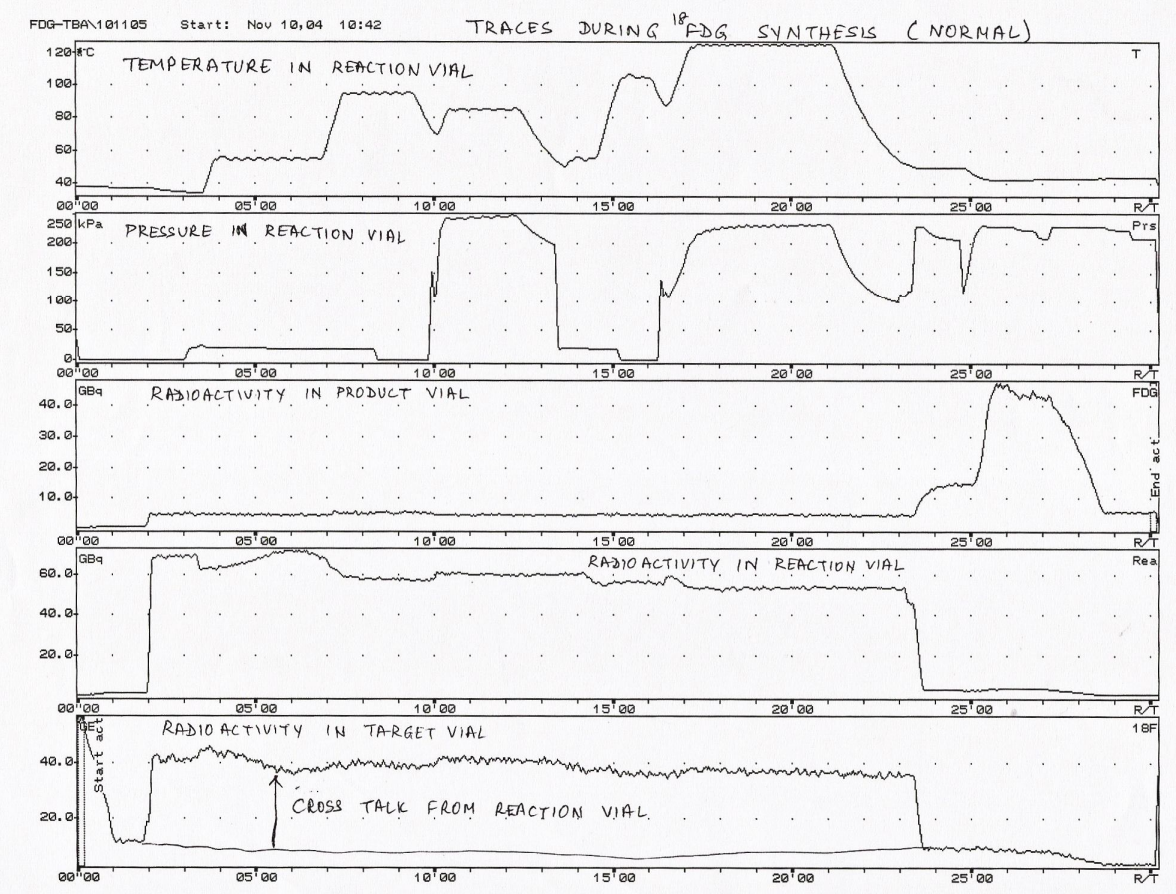

Fig. 2.20. *Radiosynthesis monitoring graph: the temperature and pressure profile of the reaction vessel and shifting of the radioactivity at the three vessels (Target Vial, Reaction Vessel and the Product Vial) are displayed.*

So, after transforming the existing [^{11}C]Methylation module to a module in which nucleophilic fluorination by solid phase extraction (SPE) purification can be carried out, the next task was to standardize the "time list" for the synthesis of different PET Radiopharmaceutical like [^{18}F]FDG, Na[^{18}F], [^{18}F]FLT, [^{18}F]FMISO, [^{18}F]FAZA etc suitable for the modified module and the "time lists" are optimized and standardized.

2.3. f. Arrangement of dispensing and reaction mixture collection

Since it is a transformed module, so the "time list" can only be optimized after analyzing the reaction mixture at different stages of the reaction as well the final product by radio analytical techniques like radio TLC (Thin Layer Chromatography) or radio HPLC (High Performance

Liquid Chromatography). This needs the collection of the reaction mixtures at different stages of the reaction. So that, provision has to be made to take out the reaction mixture from the reaction vessel out of the hot cell in which the synthesis module is housed. So provision has been made to collect the reaction mixture as well as product out of the hot cell through tubing coming out of the hot cell directly from the product vial. The reaction mixture can also directly be collected by small rearrangement of the tubing connection [**Fig. 2.21. & 2.22.**].

Fig.2.21. *The tubing coming out of the hot cell into the hatch for collection of reaction mixture as well as product*

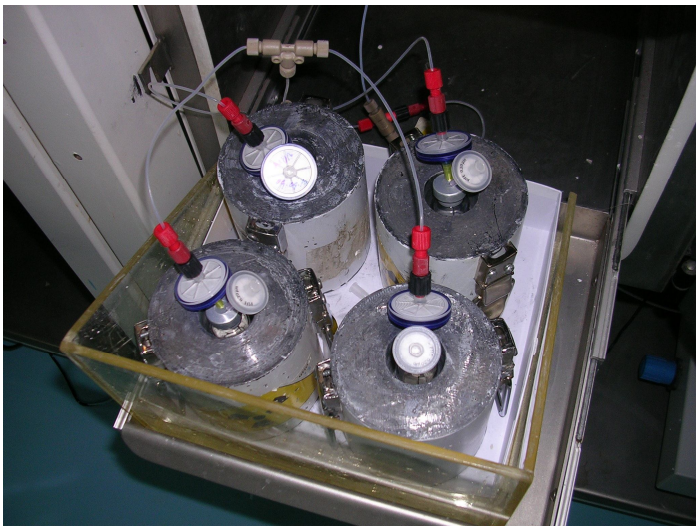

Fig. 2.22. *The product collection assembly inside lead hatch using a manifold*

The use of this in-house developed module and time-list programme will be elaborated in detail in subsequent chapters describing the synthesis / production of the ^{18}F-labelled PET radiopharmaceuticals other than [^{18}F]FDG.

CHAPTER 3

^{18}F-labelled sodium fluoride ([^{18}F]NaF): The PET Radiopharmaceutical for Skeletal Imaging

3.1. Introduction

Way back in 1972, several decades before the introduction of modern PET systems, ^{18}F-labeld NaF was recognized as an excellent radiopharmaceutical for skeletal imaging [94]. ^{18}F-Fluoride has the desirable characteristics of high and rapid bone uptake accompanied by very rapid blood clearance, which results in a high bone-to-background ratio in a short time. After intravenous administration, ^{18}F-fluoride diffuses through the bone capillaries into the bone's extracellular fluid (ECF). From the bone ECF, ^{18}F-fluoride ions exchange with hydroxyl groups in the hydroxyapatite at the surface of bone crystals forming fluoroapatite mainly at sites of bone remodeling with high turnover. Therefore, uptake of ^{18}F-fluoride reflects blood flow and osteoblastic activity [95]. Because of its very fast bone uptake and very rapid blood clearance, high-quality images of the skeleton can be obtained less than one hour after the intravenous administration of [^{18}F]NaF. [^{18}F]NaF became widely used for skeletal scintigraphy after its introduction by Blau and others in the early 1960s [96] and was approved by the U.S. Food and Drug Administration (FDA) in 1972. Rectilinear scanners were used to image the location of [^{18}F]NaF, one to three hours post administration.

In the early 1970s, ^{99m}Tc-labeled polyphosphates and then ^{99m}Tc-labeled pyrophosphate were introduced as bone-imaging agent. With readily available ^{99m}Tc through ^{99}Mo/^{99m}Tc generator, bone scintigraphy quickly became one of the most commonly performed nuclear medicine

imaging procedure [97]. When it became apparent that pyrophosphate impurities or degradation products were responsible for most of the bone-imaging properties of ^{99m}Tc-labeled polyphosphates, ^{99m}Tc-polyphosphates were abandoned in favour of ^{99m}Tc-pyrophosphate [98]. However, skeletal imaging with ^{99m}Tc-pyrophosphate was limited by prolonged clearance from the circulation. During this same period, ^{99m}Tc-labeled diphosphonates were introduced for skeletal scintigraphy. These compounds demonstrated higher skeletal uptake, faster blood-pool clearance, and better in vivo stability than did either polyphosphates or pyrophosphate. With the successful development of kit-based ^{99m}Tc-diphosphonate radiopharmaceuticals and the increased availability of Anger-type γ-cameras, ^{99m}Tc-diphosphonates, particularly ^{99m}Tc-methylene diphosphonates (MDP), which demonstrated faster blood-pool clearance than most other ^{99m}Tc-labeled diphosphonates, became adopted as the standard agent for skeletal scintigraphy [97, 98.] In direct comparison, the plasma clearance of [^{18}F]NaF is more rapid than that of ^{99m}Tc-MDP, and its single-passage extraction efficiency is higher because of its smaller molecular weight and the fact that its protein binding is negligible whereas binding of ^{99m}Tc-MDP to plasma protein varies from 25% after injection to 70%, 12 hours after injection. In the blood, approximately 30% of ^{18}F-Fluoride is transported by erythrocytes. The single-pass extraction of ^{18}F-fluoride, is, however, almost 100% as the red blood cell ^{18}F-Fluoride, is available for clearance to bone [99-101]. Bone uptake of ^{18}F-Fluoride is 2-fold greater than that of ^{99m}Tc-MDP [94, 102, 103]. Currently, the use of ^{99m}Tc-MDP is being looked into given the advantages of PET imaging and the limited global supply of ^{99m}Tc [104].

Combining the favourable pharmacokinetic characteristics of ^{18}F-fluoride with the high performance of positron emission tomography (PET) technology, ^{18}F-fluoride is a valuable imaging modality of the skeleton. Quantitative methods of ^{18}F-fluoride PET imaging allow

dynamic measurement of the tracer uptake and regional characterization of metabolic bone lesion, monitoring their response to therapy, and separation between uneventful and impaired healing processes of bone fracture, osteonecrosis and graft incorporation. Static ^{18}F-fluoride PET is highly sensitive for detection of malignant and benign bone abnormalities. As various pathological bone conditions are associated with increased uptake of ^{18}F-fluoride, PET findings often require morphological characterization for accurate diagnosis. This is now easily achieved by using hybrid PET/computed tomography (CT) systems [105].

Despite the high performance of ^{18}F-fluoride PET/CT, it is not widely used. The tracer is not always commercially available, and the number of available PET/CT systems is still smaller than the number of gamma cameras. ^{18}F-fluoride PET or PET/CT is reserved for selected patients, either high-risk cancer patients or patients who are suspected clinically to have malignant or benign skeletal problems even though conventional imaging modalities and/or bone scan are negative or nonconclusive. It is reported that ^{18}F-fluoride imaging is expected to replace bone scintigraphy completely within several years [106]. However, the decision to use ^{18}F-fluoride PET or PET/CT routinely warrants meticulous cost-effectiveness analysis. In a report by Hetzel and coworkers [107] on 103 patients with lung cancer, the cost-effectiveness of ^{18}F-fluoride PET was compared with that of bone scintigraphy with SPECT of the spine. Such analysis should compare the cost-effectiveness of PET/CT to separate performance of bone scan and correlative CT, which at present, is the commonly applied imaging algorithm in patients with suspected bone abnormality.

Given the applicability of [^{18}F]NaF for bone imaging has been confirmed, the objective was to develop a fully automated production procedure to obtain high quality product.

The adapted general purpose fluorination module described in the previous chapter is used for this purpose. Microbiological, physical-chemical and biological quality control tests were performed, and the [^{18}F]NaF injectable solution met the quality control requirements contained in the United States Pharmacopoeia (USP 31). After obtaining required regulatory clearance, it is now supplied to various hospitals from our centre. Advantages are manifold [107, 108]. [^{18}F]NaF is less cumbersome to prepare and more easily available. The patient has to wait shorter time after injection in comparison to ^{99m}Tc-MDP for its bio-distribution, thereby, reducing the radiation exposure problem. It provides better target to non target ratio. It also provides better count rate as uptake of [^{18}F]NaF is almost twice than ^{99m}Tc-MDP. [^{18}F]NaF is very effective in detecting both lytic and sclerotic metastases. The [^{18}F] Fluoride scans are much more accurate than ^{99m}Tc-MDP scans. The requirement for repeat CT and MRI studies is less. It shows improved sensitivity for detection of metastasis. It is also having a better diagnostic capability because of fusion imaging which will help in distinguishing benign bone damages from metastatic lesions. PET as well as PET/CT machine always provides better resolution [109] in comparison to SPECT machine due to the latter's method of imaging (99% in case of PET and PET/CT, 94% for SPECT). The widespread re-adoption of [^{18}F]NaF as a bone imaging agent, however, has been limited by longstanding familiarity with ^{99m}Tc-diphosphonate scintigraphy and, possibly, by concerns about insurance reimbursement for [^{18}F]fluoride PET.

In this Chapter, the production procedure of pharmaceutical grade [^{18}F]NaF using the adapted general purpose fluorination module, production details, QC results, bio distribution studies by PET/CT imaging of rabbit and finally PET/CT imaging studies of human volunteers are discussed. The Radiopharmaceutical Committee (RPC) clearance was obtained in 2007 and from then [^{18}F]NaF is routinely supplied to various hospitals.

3.2.

Materials & Methods

$H_2{}^{18}O$ of 95% enrichment (Isotopic) is procured from ROTEM Industries. ^{18}F separation cartridges (CHROMAFIX® PS-HCO_3^-) in HCO_3^- (bi-carbonate) form was obtained from Macherey-Nagel. Sterile, pyrogen-free and pharmaceutical grade isotonic saline solution, pharmaceutical grade ethanol (EtOH) and sterile and BET free water were obtained from ABX Advanced Biochemical Compounds, Germany. Sterile, non-pyrogenic, hypodermic, single use, 0.2µ syringe filter was procured locally. Sterile, pyrogen-free, evacuated vials of capacity 10 ml (Pyrovac®) were procured from ACILA AG, Germany and were used for dispensing. H^+ (proton beam) is produced by Medical Cyclotron (GE PET Trace, 16.5 MeV Proton & 8.5 MeV deuteron). Silver Cavity Target with Havar® Foil combination is used for the production of ^{18}F via $H_2{}^{18}O$ (p, n) ^{18}F nuclear reaction.

3.2.1.

a. Conditioning of CHROMAFIX® PS-HCO_3^- anion exchanger column

Chromafix 45-PS-HCO_3 is a solid phase extraction (SPE) cartridge filled with strong basic anion exchange resin based on polystyrene-divinylbenzene in HCO_3^- form, 45 mg ±10% packed in polypropylene case and fitted with 20 µm polyethylene frits. 1 ml absolute ethanol is first passed through it followed by rinsing with 1 ml sterile and BET free water. It is then dried by applying Helium (He). Drying should be such that it will have little bit of moisture content left as it permits the maximum elution of $[^{18}F]F^-$ form the anion exchanger column.

b. [^{18}F]NaF Production Procedure

[^{18}F]Fluoride was produced on a 16.5 MeV Cyclotron PETtrace® (GE Healthcare) by the $^{18}O(p,n)^{18}F$ nuclear reaction. The silver target is filled with enriched $H_2{}^{18}O$ and irradiated with H^+. The proton beam current and the duration of irradiation, both, were decided according the required final radioactivity. The solution ($H^{+18}F^-$ in $H_2{}^{18}O$ water) containing [^{18}F]fluoride was transferred into the adapted automatic general purpose fluorination module. [^{18}F]fluoride ions were trapped into the Chromafix 45-PS-HCO_3 anion exchange column via anion exchange with HCO_3^- and the irradiated water was collected in the recovery vial. [^{18}F]fluoride was eluted with 2.0 ml of physiological saline (0.9% NaCl solution) and then diluted with extra 10 ml physiological saline. Finally, the resulting 12 ml of [^{18}F]NaF was dispensed into sterile, pyrogen-free vials, through 0.2 µm filter, in an automated dispensing unit [110].The whole production process is fully automated and is carried out inside the fluorination module controlled by the "time-list" (menu driven software programme) suitable for [^{18}F]NaF production. After dispensing, if necessary, the vials were autoclaved tray and autoclaved using a short cycle (Flash Autoclave, 134°C, 3.5 bar pressure, 5 minutes) . Finally, the vials are taken out of the dispenser one by one with the help of a robotic arm and stored into LP-30 (lead thickness: 30 mm) lead pots.

c. Physical-Chemical quality control

The final [^{18}F]NaF solution was checked for clarity i.e. it should be colourless and free of any suspended particle or any colloidal particle by visual inspection through naked eye. The pH value of [^{18}F]NaF was measured using pH papers of 0-14 and 4-8 range. The results were compared with colour chart on the pH paper strip and estimated value was registered.

Radiochemical purity (RCP) of [^{18}F]NaF was confirmed by thin layer chromatography (TLC) [111].

The TLC stationary phase was silica gel and the mobile phase was acetonitrile: water (95:5 % v/v). The radioactivity was determined by scanning the TLC SG plate with a suitable collimated radiation detector (*Minigita BGO-V-detector*, Raytest®). The main peak was analyzed to define the retention factor (R_f) value and the radioactivity related to the sample, that must lie between 0.0-0.01 and be not less than 95%, respectively.

Since the synthesis procedure is fully automated, the module needs to be cleaned to maintain the aseptic conditions and normally before [^{18}F]NaF production, the module is thoroughly cleaned using 70% ethanol. It is then possible that the final product, [^{18}F]NaF may contain some traces of ethanol as a residual solvent impurity. In order to check the level of ethanol in the final [^{18}F]NaF, gas chromatography of the decayed samples were carried out.

The residual solvent analysis was carried out using a Gas Liquid Chromatography (GLC) equipped with a flame ionization detector (FID) using a PEG capillary column (BP-20 from SGE, Australia). Sealed samples from each synthesis of [^{18}F]NaF were stored at room temperature and analyzed later for the residual solvents. The GC column was maintained at a temperature of 50°C during the operation. An aqueous solution containing 200 ppm each of ethanol and acetonitrile was used as the standard solution. [^{18}F]NaF sample (1 µl), after radioactive decay, was injected and compared against the calibration data obtained from 1 µl injection of the standard solution.

Radionuclidic purity was evaluated by gamma-ray spectrometry (Eurisys Mesures, France; Multichannel Analyzer). Half-life of ^{18}F was calculated after measuring the radioactivity decay of the sample over 30-minute period in a radioisotope dose calibrator (Capintec CRC® -15 PET) after three measurements at 10 minutes interval. The equation used is shown below:

$$\ln A = \ln A_0 - \lambda t \text{ --------- (1)}$$

Considering the first reading of the dose calibrator as the reference, at each five minutes interval, the activity figure is noted and the natural logarithm of the activity figure (lnA) is calculated. Each figure (Y axis) is then plotted against the reference time (t)(X axis). As the equation (Eqn.1) above shows, a straight line with a negative slope (equal to λ) and an intercept equal to $\ln A_0$ is obtained. The half-life ($T_{½}$) is calculated using the following equation and it must be within a range of 110±5 minutes.

$$T_{(1/2)} = 0.693/\lambda \text{ ---------- (2)}$$

Where: A_0 = initial activity; A = activity measured after t minutes; t = time interval (in minutes) between the two measures (t_A-t_{A0}); $T_{(1/2)}$ = half-life, λ = radioactive decay constant

d. Microbiological quality control

Since the [^{18}F]NaF is to be used intravenously in patients, quality control for biological contaminations i.e. sterility and bacterial endotoxin tests are carried out on the samples (post radioactive decay) of each batch according to the standard procedure as used for [^{18}F]FDG. This is done considering the radioactive decay loss due to short half-life of ^{18}F.

Sterility tests were performed in accordance with the Indian Pharmacopoeia, 1996 and addendum 2005 protocol. In this test, 1 ml of the [^{18}F]NaF sample after radioactive decay was inoculated in fluid thioglycollate medium at 37°C for 14 days to observe the growth of aerobic and anaerobic bacteria. Similarly, 1 ml of the [^{18}F]NaF sample was also inoculated in soybean casein digest medium at 22-25°C for 14 days to detect fungal growth.

The bacterial endotoxin test was performed in accordance with USP XXX1. The test was based on the formation of gel clot in the sample by Limulus Amoebocyte Lysate (Sensitivity: 0.125 EU/ml) reagent.

e. Bio-distribution and Patient Studies

About 111-148 MBq of [^{18}F]NaF in a volume of 1 ml was administered to rabbits (Avg. wt ~ 2.5 Kg, maintained in our animal house facility and on normal diet) through *IV (Intravenous)* injection After one hour, images were taken on a PET/CT machine (Discovery ST, GEMS, GE, USA). PET/CT images of few patients with osteochondroma problem, osteoporotic changes etc. were studied using approximately 370 MBq of [^{18}F]NaF per patient. Images were taken one hour post injection. For performing the clinical trials in patient, regulatory clearance from the Tata Memorial Hospital (TMH) Ethics Committee was obtained (This was a collaborative project with the Bio-Imaging Unit, TMH where the clinicians of the particular unit were also involved).

f. Radiation Dosimetry

Radiation exposure of [^{18}F]NaF skeletal imaging is very well documented and a large number of references are already available. This is discussed in details in Results and Discussion section of this chapter.

3.3.

Result and Discussion

3.3.1. [^{18}F]NaF Production

Enriched $H_2{}^{18}O$ water was successfully irradiated in the cyclotron. $^{18}F^-$ fluoride was produced by the nuclear reaction $^{18}O(p,n)^{18}F$, by irradiation with protons for 10 minutes at the intensity of 25 μA. Around 10 -15 GBq of Fluorine-18 is produced in the cyclotron. Since the underlying principle of [^{18}F]NaF production is trapping of ^{18}F-fluoride ion in an anion exchange and then simple elution by physiological saline, the overall yield is almost 100% and the total production

time is around five minute. The total production process can be monitored by the online graphs as shown in **Fig. 3.1**.

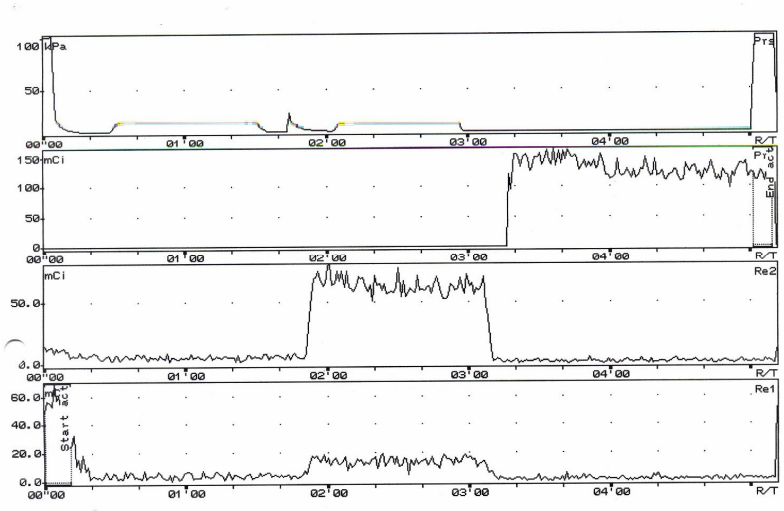

Fig. 3.1. *The reaction profile of [^{18}F]NaF production. The last channel shows the radioactivity of the target vial. At the first step, ^{18}F is delivered to the target vial of the synthesis module. So, we can observe a total accumulation of radioactivity. Subsequently, ^{18}F is trapped in the anion exchanger explaining the total loss of radioactivity in the target vial as shown in the graph. After trapping, the whole ^{18}F radioactivity in the form of Na^{18}F is eluted in the reaction vessel which is shown by the peak in the second bottom channel. We can also observe a very small peak in the target vial which is generating for a "cross talk" due to insufficient shielding provided between the target vial and the reaction vial. In the final step, the whole radioactivity is pumped to the product vial from the reaction vial. The huge peak in the second channel from the top represents the same.*

Finally, [^{18}F]NaF is transferred to an automated dispenser unit and dispensed into sterile, bacterial endotoxin free vial through 0.2μ filtration in a class 100 area [**Fig. 3.2.**]. As an

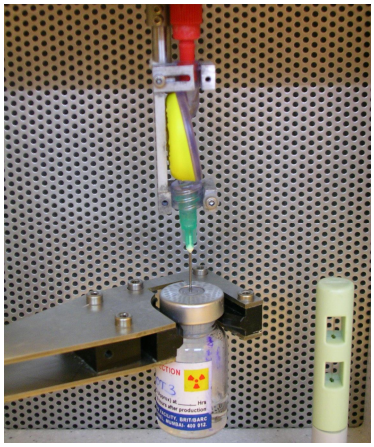

Fig. 3.2. *Automated dispensing unit: Vials are getting dispensed through 0.2µ filter one by one in Class-100 area*

additional safety, if necessary, the vials after dispensing, is autoclaved at 134°C for four minutes [**Fig. 3.3.**] (@ 3.0 bar), also built-in inside the dispenser. Once the fluorine-18 is received from the cyclotron into the synthesizer, the production of sterile, injection grade [^{18}F]NaF, hardly takes 15 minutes.

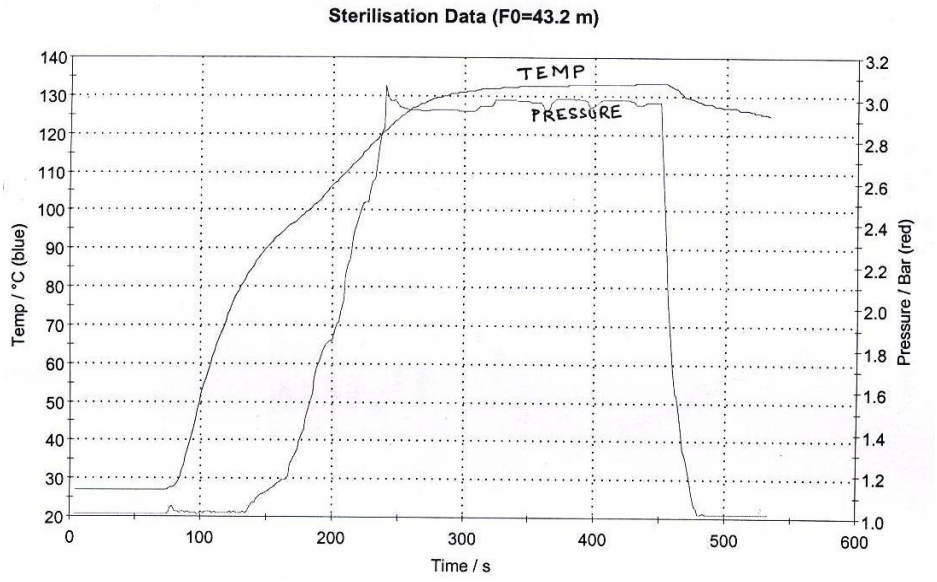

Fig.3.3. *Graphical Representation of the autoclave process*

3.3.2 Physical-chemical and microbiological quality control

[^{18}F]NaF physical-chemical and microbiological characteristics were evaluated. The analyses described earlier determined its radiochemical identity and purity, radionuclidic identity and purity, pH, bacterial endotoxins and sterility.

The quality requirements used for [^{18}F]NaF were in accordance with those found in the United States Pharmacopeia (USP 31) as presented in **Table 3.1**.

Table 3.1. Results obtained after testing [^{18}F]NaF microbiological, physical-chemical and biological properties

Tests	Quality Requirements (USP 31)[112]	Results
pH	**Between 4.5 and 8.0**	**7.0 ± 0.2 (n = 10)**
Radiochemical Identity	**0.00< R_f > 0.12**	**0.06 ± 0.02 (n = 10)**
Radiochemical Purity	**≥ 95 %**	**99.5 ± 0.01(n = 10)**
Radionuclidic Identity	**$T_{(1/2)}$ = 110 ± 5 minutes**	**109.8 ± 2.8 (n = 10)**
Radionuclidic Purity	**Main Peak = 0.511 MeV**	**Main Peak = 0.511 MeV**
Bacterial Endotoxin	**≤ 25 EU. mL^{-1}**	**≤ 25 EU.mL^{-1}**
Sterility	**Sterile**	**Sterile**

Radiochemical purity of the [^{18}F]NaF solution was assessed by thin layer chromatography (TLC). The product migration profile was determined by scanning the chromatogram plate with a suitable collimated detector [**Fig. 3.4.**]. R_f of [^{18}F]NaF is measured as 0.01 in 95:5 MeCN: H_2O solvent.

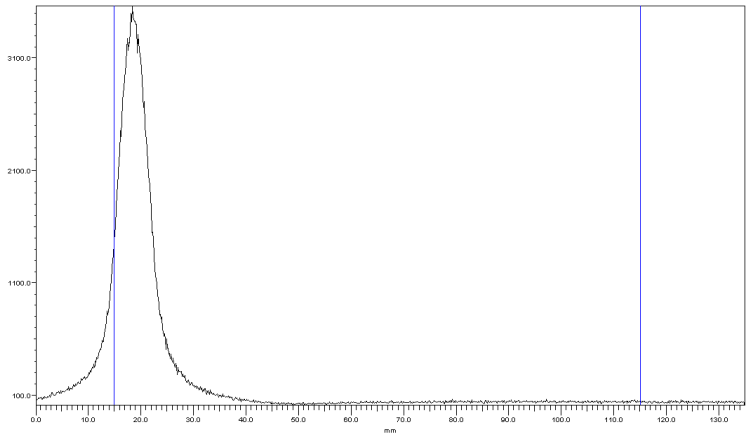

Fig. 3.4. *Radio TLC of [^{18}F]NaF in MeCN: H2O (95:5). R_f of Na^{18}F is 0.02*

The proton beam hits the target material (here $H_2{}^{18}O$) inside the cavity of the cyclotron target by passing through an entrance foil. The material used for the entrance foil is Havar, which is a high tensile strength (1860 MPa), non-magnetic alloy (Co 42%, Cr 19.5%, Fe 19.3%, Ni 12.5%, W 2.6%, Mo 2.2%, Mn 1.7% and C 0.2%) with a high melting point (1480°C) and a moderate thermal conductivity (14.7 W/m/K at 23°C). However, it has been observed that the use of this material for a long time irradiations has led to the formation of water soluble contamination (**Table 3.2, Fig. 3.5.**)[113].

Table 3.2. Radionuclidic impurities and possible nuclear reaction [113]

Product	$T_{(1/2)}$	Reaction	Threshold (MeV)
^{55}Co	17.5 h	^{58}Ni(p,α)	1.36
^{56}Co	77 d	^{56}Fe(p,n)	5.44
^{57}Co	272d	^{57}Fe(p,n)	1.65
		^{60}Ni(p,α)	0.27
		^{58}Ni(p,2p)	8.31
^{58}Co	71d	^{58}Fe(p,n)	3.14
^{57}Ni	35.6 h	^{58}Ni(p,pn)	12.43
^{51}Cr	27.7d	^{52}Cr(p,pn)	12.27
^{52}Mn	5.6d	^{52}Cr(p,n)	5.60
^{95}Tc	20 h	^{95}Mo(p,n)	2.50
^{181}Re	19.9 h	^{182}W(p,2n)	10.65
^{93m}Mo	6.85h	^{93}Nb(p,n)	3.60

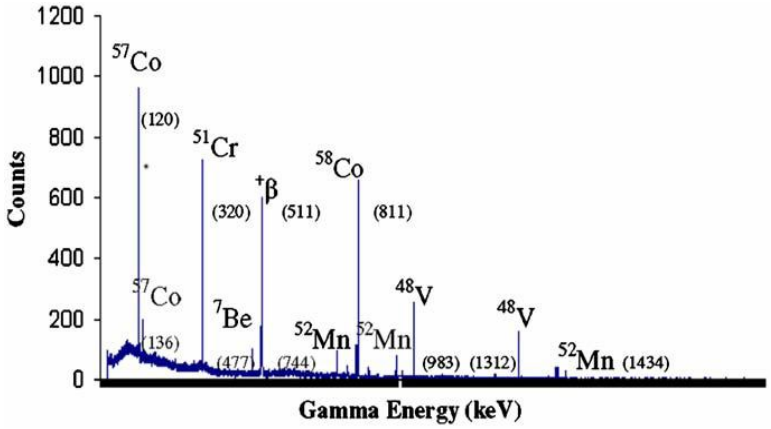

Fig. 3.5. *Gamma-ray spectrum showing the presence of radioactive metal ions produced due to radio activation of metal target housing. The figure within small bracket represents the gamma energy associated with the corresponding radio metal ion [114]*

Ion-exchange column based chromatography is the principal method used in the separation of metal impurities including ^{56}Co, ^{57}Co, ^{58}Co, ^{51}Cr, ^{52}Mn, ^{54}Mn, ^{48}V and ^{7}Be from enriched target $[^{18}O]H_2O$ [115].

So, as a very valid reason, the $[^{18}F]NaF$ produced was analyzed using high purity germanium detector (HPGe) coupled with a multi channel analyzer for a sufficiently long period of 6 to 7 hours. The gamma spectrum showed 511 keV as the major peak [**Fig. 3.6. & 3.7.**] ensuring the radionuclidic purity.

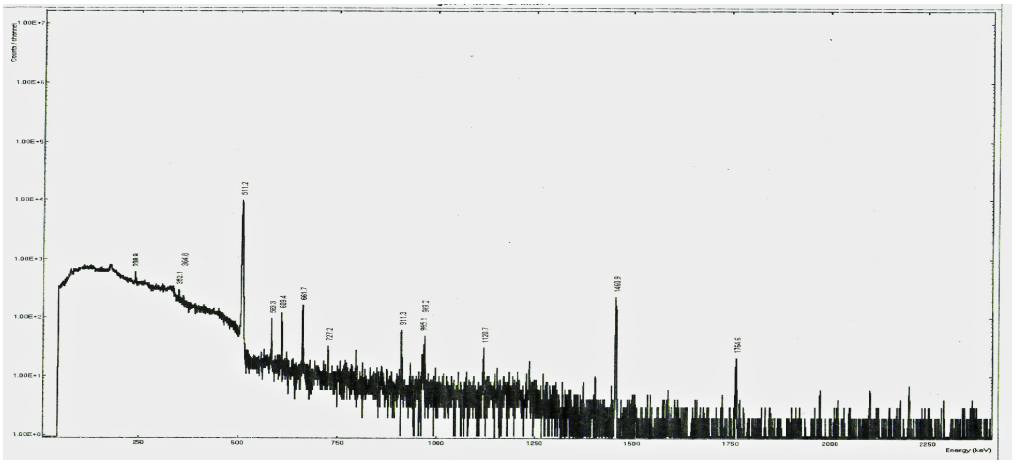

Fig. 3.6. *γ-ray spectrum of $[^{18}F]NaF$ showing 511keV as the major peak*

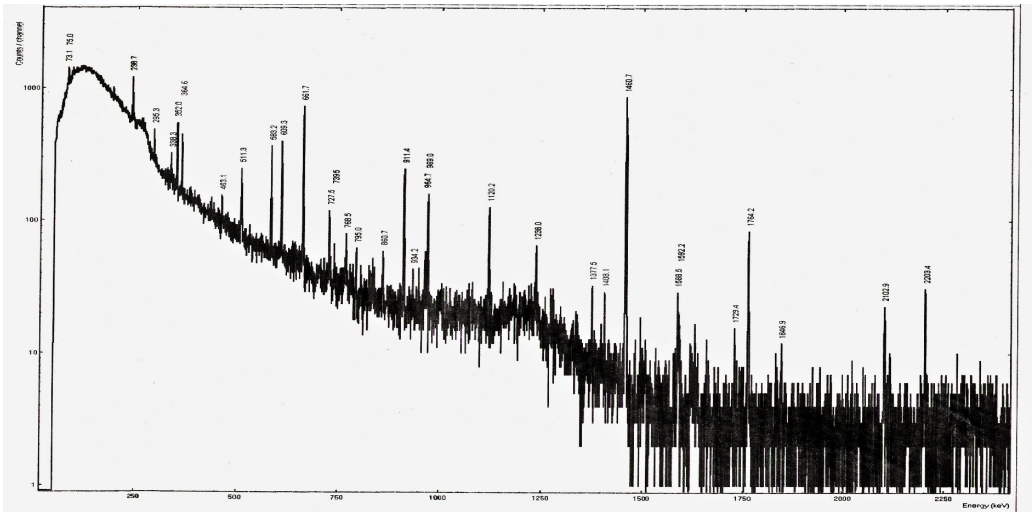

Fig. 3.7. *γ-ray spectrum of the background recorded before the analysis of $[^{18}F]NaF$*

Since the contaminant radio metal ions are cationic in nature, it is expected that the contaminant radio metal ions will not be trapped in the anion exchanger and will be collected in recovery vial along with the recovered irradiated $H_2{}^{18}O$. Subsequently, when the trapped ^{18}F-fluoride will be eluted from the column with physiological saline, which is again an anion exchange process, it is very unlikely that the final [^{18}F]NaF will be contaminated with the presence of the radio metal ions. There are hardly any reports of generation of anionic impurity containing the radio metal ions. There are few reports of the presence of anionic impurities like nitrate and nitrite [116] originating from the radiolysis of water as well as halogens [117] probably originating through a leaching mechanism from the metal parts of the target handling system or from organic halogen compounds present in the target water, which are broken down during the irradiation. To ensure that there is no anionic impurities, for a safer side, the small anion exchange column can be washed with 2 ml of water after trapping ^{18}F-fluoride ensuring the removal of loosely bound anionic impurities if present and then ^{18}F-fluoride can then easily be eluted with physiological saline. Practically, the 'washing process' of the anion exchange column after ^{18}F-fluoride trapping is associated with small loss of ^{18}F-fluoride (0.5-1.0 %) which will cause insigficant loss of the total [^{18}F]NaF production making the process economically also acceptable.

As discussed earlier, the synthesis module is cleaned thoroughly with 70% ethanol for maintaining the aseptic condition prior to [^{18}F]NaF production. So, the presence of ethanol in the final [^{18}F]NaF is measured by GC and found to be below the acceptable limit (< 5000 ppm) [**Fig. 3.8.**].

The results of the bacterial endotoxin tests performed compliance with the requirement established by USP 31.

All the samples assayed for sterility were observed for 14 days and none showed evidence of microbiological growth. Therefore, the [^{18}F]NaF solutions were considered sterile.

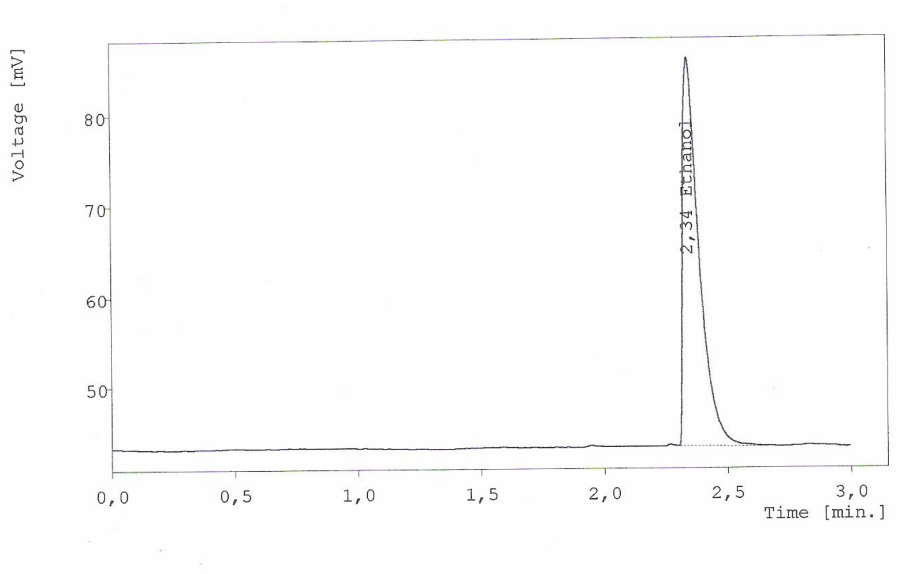

Result Table - Calculation Method Norm

Peak No.	Reten. time	Area [mV.s]	Amount [ppm]	Amount [%]	Peak Type	Component Name
1	2,343	196,6271	1983,2939	100,000	Ordnr	Ethanol
-	Total	196,6271	1983,2939	100,000		

Fig. 3.8. *Gas chromatogram of [^{18}F]NaF showing the presence of ethanol within the permissible limit*

3.3.3 Bio-distribution in rabbit

Fluoride ions usually accumulates in the skeleton in an even fashion, with greater deposition in the axial skeleton (e.g. vertebrae and pelvis) than in the appendicular skeleton, and greater deposition in the bones around joints than in the shafts of long bones. Following, intravenous administration, about 50 % of the ^{18}F-fluoride is rapidly taken up by the skeleton where it remains for the entire periods of its radioactive decay [118]. The remainder of the ^{18}F-fluoride is distributed in the extra cellular fluid and eliminated by renal excretion within a few hours. The PET/CT images of rabbit are shown in **Fig. 3.9. & 3.10.** As expected, higher deposition of ^{18}F-fluoride is observed in vertebrae and pelvis and joints. Accumulation of radioactivity is observed

in urinary bladder which is a very common feature of a radiopharmaceutical excreted through renal system. The images are remarkable for the resolution and sensitivity.

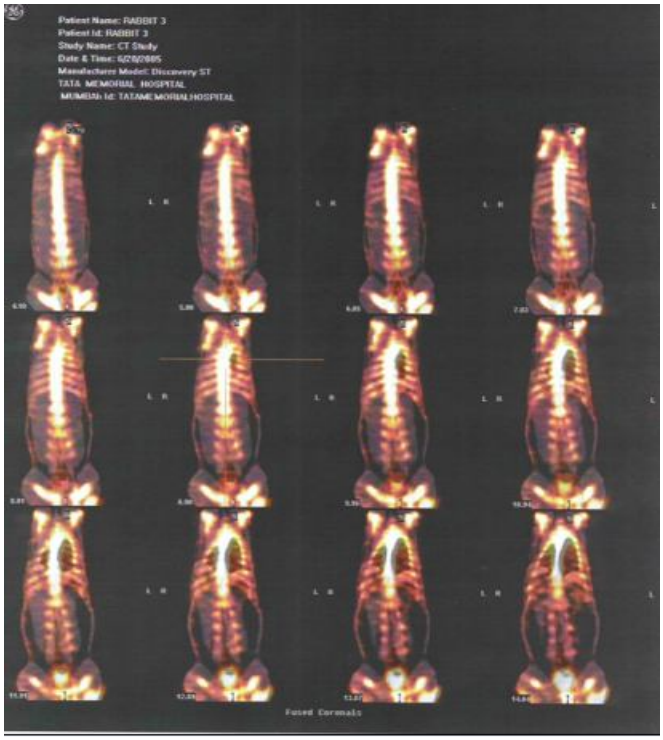

Fig.3.9. *[^{18}F]NaF PET/CT Scan of rabbit, Coronal*

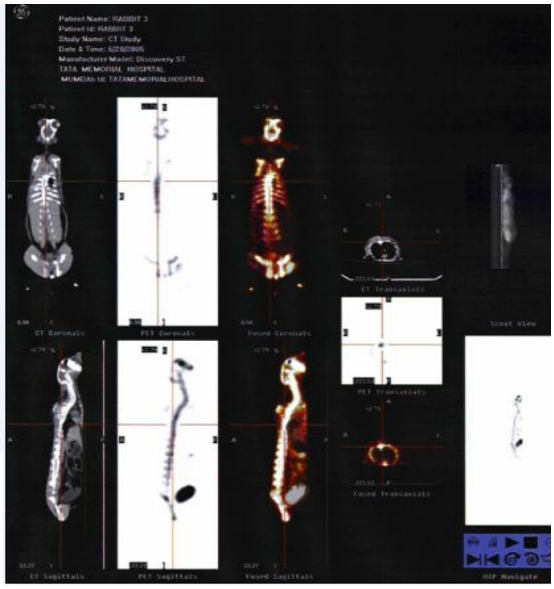

Fig.3.10. *[^{18}F]NaF PET/CT Scan of rabbit, Sagittal*

3.3.4 Evaluation in human volunteers

After obtaining the clearance from all regulatory and ethics committee, around 100 patients having different types of problems associated to bone, including patients having bone cancer, bone metastasis , breast cancer etc were evaluated in a collaborative project with Bio-Imaging Unit, Tata Memorial Hospital, India. **Fig. 3.11., 3.12., 3.13., 3.14.** are PET/CT images of patients having different types of skeletal problem.

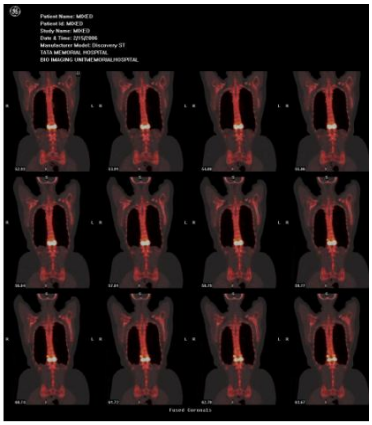

Fig.3.11. *[^{18}F]NaF PET/CT image (coronal) of a patient having changes In vertebra due to osteoporosis.*

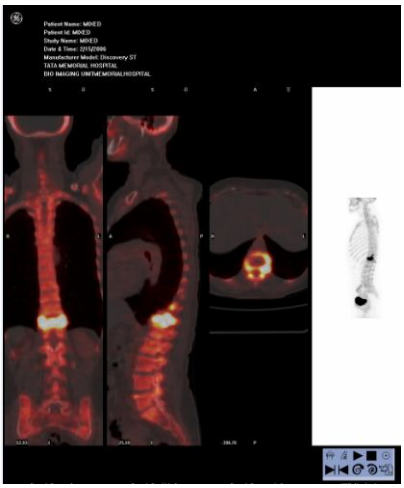

Fig. 3.12. *[^{18}F]NaF PET/CT image (sagittal) of a patient having changes in vertebra due to osteoporosis*

Fig. 3.11. & 3.12. were the [^{18}F]NaF PET/CT images of a patient having changes in the vertebra due to osteoporosis. The location as well as the changes in the vertebra is clearly evident.

Fig. 3.13. & 3.14. were the [^{18}F]NaF PET/CT images of a patient having osteochondroma. The images very precisely locate the osteochondroma sites.

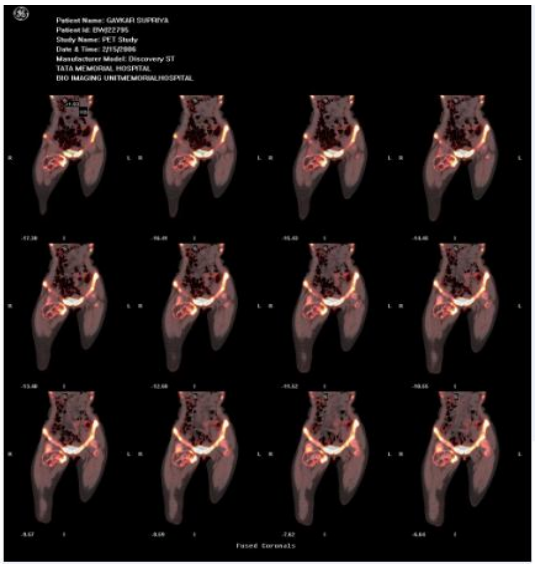

Fig: 3.13. *[^{18}F]NaF PET/CT image (coronal) of a patient having osteochondroma.*

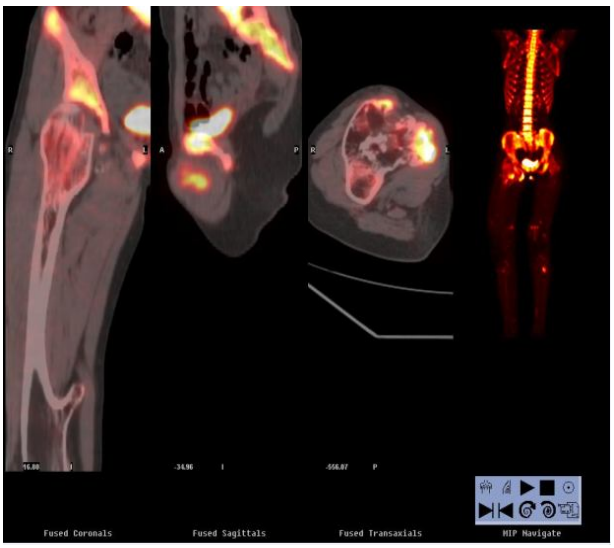

Fig.3.14. *[^{18}F]NaF PET/CT fused image precisely locating the site of osteochondroma.*

Fig. 3.15. is the [^{18}F]NaF PET/CT scan of a breast cancer patient looking for the involvement of bones as a secondary effect which is very much susceptible in this type of cancer. The image showed normal distribution of [^{18}F]NaF ruling out bone involvement very precisely.

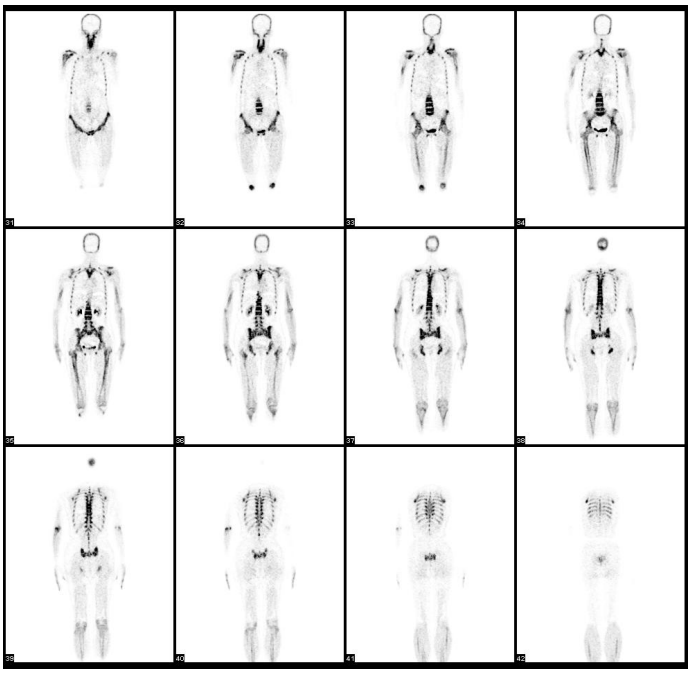

Fig.3.15. *[^{18}F]NaF PET/CT image of a breast cancer patient*

3.3.5 Radiation Dosimetry [95]

Several factors affect the radiation dose of ^{18}F relative to that of single-photon emitters (such as ^{99m}Tc). With a positron emitter such as ^{18}F, energy is delivered by the positron itself (mean energy, 250 keV) and by the two 511 keV annihilation photons, whereas ^{99m}Tc emits a single 140 keV γ-ray. These differences affect the relative internal dosimetry of ^{18}F and ^{99m}Tc. The ^{18}F positron will deposit essentially all its kinetic energy in the source organ, whereas the different energies of 511 and 140 keV photons results in different patterns of internal radiation dose. The soft-tissue half-value layers for the 511 and 140 keV photons are 7.3 and 4.6 cm, respectively, so that 511 keV photons can deliver their energy to organs distant from the source organ, whereas the 140 keV photons will deliver more of their energy to organs near the source organ. On the

other hand, the half-life of ^{18}F is 110 minute, compared with 6 hour of ^{99m}Tc, leading to a shorter exposure period and , in turn, to a reduced radiation dose for ^{18}F.

With consideration of all these factors, the radiation dosimetry for both [^{18}F]NaF and ^{99m}Tc-MDP was calculated using the data provided by reports 53 and 80, respectively, of the International Commission on Radiological Protection (ICRP) [118, 119]. The effective dose per unit of administered activity for [^{18}F]NaF and ^{99m}Tc-MDP were calculated, as was the radiation dose to several individual organs (**Table 3.3.**). Also listed in this table are the absolute doses for patients of different sizes for injected activities of 2.11 and 7.40 MBq/kg for [^{18}F]NaF and ^{99m}Tc-MDP, respectively. At the prescribed administered activities, the effective dose for [^{18}F]NaF and ^{99m}Tc-MDP are similar for most patients (4.0 and 3.0 mSv, respectively, for a 70 kg patient). For patients, weighing less than 20 kg, the effective dose is relatively less with ^{99m}Tc-MDP (2.0 mSv) than with [^{18}F] NaF (approximately 3.5 mSv). The bone surface dose is higher for ^{99m}Tc-MDP relative to that of [^{18}F] NaF (32.6 and 5.9 mGy, respectively, for a 70 kg patient), whereas the dose to the bladder wall is slightly higher for [^{18}F] NaF than for ^{99m}Tc-MDP (32.6 and 24.9 mGy, respectively for a 70 kg patient). Thus to minimize the radiation absorbed dose to the bladder, adequate hydration should be encouraged to stimulate frequent voiding during the first few hours after intravenous administration. Therefore, there is little overall difference in the estimated radiation dose for [^{18}F] NaF and ^{99m}Tc-MDP scintigraphy.

The toxicology of [^{18}F]NaF injection will be the same as that of non-radioactive compound, except for the radiation exposure. However, the amount of fluoride ions in [^{18}F]NaF injection, at the indicated dose, is very low (less than one nano-gram), and provides assurance that toxic effects will not be observed.

Table 3.3. Radiation Dosimetry of ^{99m}Tc-MDP Scintigraphy vs. [^{18}F]NaF PET[95]

Type of Imaging	Adult (70 kg)	15 Y Old Child (55 kg)	10 Y Old Child (32 kg)	5 Y Old Child (19 kg)	1 Y Old Child (9.8 kg)
^{99m}Tc-MDP*					
Administered Activity (MBq)	518	407	237	141	73
Effective dose in mSv/MBq (mSv)	0.0057 (3.0)	0.0070 (2.8)	0.0110 (2.6)	0.0140 (2.0)	0.0270 (2.0)
Bladder wall in mGy/MBq (mGy)	0.048 (24.9)	0.060 (24.4)	0.088 (20.9)	0.073 (10.3)	0.130 (9.5)
Bone Surface (mGy)	0.063 (32.6)	0.082 (33.4)	0.130 (30.8)	0.220 (31.0)	0.53 (38.7)
Red marrow (mGy)	0.0092 (4.8)	0.010 (4.1)	0.017 (4.0)	0.033 (4.7)	0.067 (4.9)
[^{18}F]NaF#					
Administered Activity (MBq)	148	116	68	40	21
Effective dose in mSv/MBq (mSv)	0.027(4.0)	0.034 (3.9)	0.052 (3.5)	0.086 (3.4)	0.170 (3.6)
Bladder wall in mGy/MBq (mGy)	0.22 (32.6)	0.27 (31.3)	0.40 (27.2)	0.61 (24.4)	1.10 (23.1)
Bone Surface (mGy)	0.040 (5.9)	0.050 (5.8)	0.079 (5.4)	0.130 (5.2)	0.300 (6.3)
Red marrow (mGy)	0.040 (5.9)	0.053 (6.1)	0.088 (6.0)	0.180 (7.2)	0.380 (8.0)

*** Derived from ICRP Report 80. Ann ICRP. 1999; 28:75**

 # Derived from ICRP Report 53. Ann ICRP. 1987; 17:74

Values in the parentheses are doses in mGy (mSv for effective dose) for administered activity listed in table for that patient size

Conclusion

[^{18}F]NaF, although one of the early bone-scanning agents, was displaced by the arrival of ^{99m}Tc-MDP, which is available in convenient kit form for labeling with generator-produced ^{99m}Tc and produced better images on the commonly used , Anger-style, γ-cameras. The widespread availability of modern PET scanners permits high-quality skeletal imaging with [^{18}F]NaF, which has the favourable characteristics of highly specific bone uptake, rapid clearance from the blood pool (because of minimal protein binding) and dosimetry similar to that of ^{99m}Tc-MDP. The commercial FDG synthesis module can also used for efficient production of [^{18}F]NaF as demonstrated in this chapter of this thesis. It is now feasible to perform high-quality [^{18}F]NaF bone scans in most nuclear medicine departments having a PET or PET/CT. Numerous recent studies have compared [^{18}F]NaF PET to ^{99m}Tc-MDP scintigraphy. These studies have demonstrated that [^{18}F]NaF PET is more accurate than planar imaging or SPECT with ^{99m}Tc-MDP for localizing and characterizing both malignant and benign bone lesions. The addition of correlative imaging such as CT, MRI, or hybrid imaging with PET/CT, further improves the specificity and accuracy of [^{18}F]NaF skeletal PET. Direct correlation of [^{18}F]NaF PET and anatomic imaging using either fusion software or hybrid imaging probably will become the routine clinical practice in nearly all cases. The clinical usefulness of [^{18}F]NaF PET has been demonstrated for a wide range of clinical indications for oncology and for benign diseases of bone. Although not yet in routine clinical use, quantitative [^{18}F]NaF PET may prove useful for the assessment of metabolic bone disorders such as renal osteodystrophy, osteoporosis, or Paget's disease.

[^{18}F]NaF PET offers the additional advantages of faster study times, improved workflow in the nuclear medicine clinic, and increased convenience to the patient, and rapid turnaround of results to the referring physicians. The wide spread readoption of [^{18}F]NaF

as a bone imaging agent, however, has been limited by longstanding familiarity with ^{99m}Tc-MDP scintigraphy and by issues related to cost of [^{18}F]NaF PET. The higher-quality imaging, increased diagnosis making greater convenience to the patient and referring physician, all indicate the need to reconsider the use of [^{18}F]NaF PET for imaging benign and malignant diseases of the skeleton.

The fully automated synthesis of [^{18}F]NaF and is availability was successfully accomplished using a general purpose fluorination module. The [^{18}F]NaF product obtained was of high quality in accordance with the requirements of the USP 31. Obtaining the approval from the Radiopharmaceutical Committee (RPC) and commercial production in 2007, ensured regular availability to nuclear medicine centers and its large scale clinical use.

CHAPTER 4

Development of single column purification method for the production of ^{18}F-labelled misonidazole ([^{18}F]FMISO): The PET Radiopharmaceutical for hypoxia Imaging and optimization of reaction parameters

PART-I

4.1. Introduction

In tumors, cells proliferate more rapidly than the vasculature because of rapid growth. A larger solid tumor usually contains a necrotic centre resulting from the vascular inadequacy as well as several layers of hypoxic cells adjacent to the necrotic region [**Fig. 4.1**.]. Hypoxia in solid tumors appears to accelerate malignant progression and the metastatic potential of the primary tumor and consequently, leads to resistant against

Fig.4.1. Tumor growth and development of hypoxic region (Red coloured region) [121] *Cell division is essential for healthy growth of an organism. A complex biochemical pathway switches the cell division **'on'** or '**off**' at the appropriate time for normal development. This mechanism is uncontrolled in Cancer, when the cells begin to divide uncontrollably often resulting in malignant tumours. The malignant growth sustain themselves by stimulating **angiogenesis**, by secreting vascular endothelial growth factors that prompts the growth of blood vessel (angiogenesis) to supply the tumour with oxygen and nutrients. When the angiogenesis is not able to keep pace with the tumour growth, or when the tumour growth constricts the blood supply to the inner regions of the tumour, then a region of **hypoxia** (inadequate oxygen supply) develops within the tumour.*

***Tumor Hypoxia** can be defined as a situation where cells have severely reduced access to oxygen due to the inability of tumor vasculature to supply blood and oxygen to all parts of the fast growing tumor*

anticancer drugs and radiotherapy [120]. Direct invasive measurements with oxygen electrodes are technically difficult and limited to superficial tumors [122]. It is well known that the nitroimidazole class of radiosensitizers act by mimicking the oxygen effect [123] forming molecular adducts under the reducing conditions of viable but hypoxic cells. The reductive binding (adduct formation) of nitroimidazoles [**Fig.4.2.**] not only increases the sensitivity of hypoxic cells to low LET ionizing radiation through this oxygen- mimicking process, but also results in their hypoxia-selective accumulation in hypoxic cells [124]. This special property of oxygen-dependent covalent binding of the nitroimidazole, misonidazole (1-(2-nitroimidazolyl)-2-hydroxy-3-methoxy propane, MISO) in cells, multicellular spheroids, and tumors has stimulated interest in using this drug or a congener as an imaging agent for hypoxia in malignant tumors, myocardial infarct, or cerebral ischemia [124-128]. Therefore, selective accumulation of a radiotracer based on nitroimidazoles in hypoxic tissues should be the key idea to be explored for the development of radiotracer for non-invasive imaging of hypoxia. Non-invasive assessment of tumor hypoxia with a specific radiotracer, prior to radiation therapy should provide a rational means for selecting patients for treatment with bio-reductive drugs and chemical radio sensitizers. In addition, it is possible to differentiate radiation therapy modalities (neutron versus photon) by correlating results with labeled markers of hypoxic cells with tumor response. The potential advantage of neutron over conventional photon radiation is the former's reduced dependence on oxygenation of the tumor and less variability of cell sensitivity to neutrons around the cell cycle [129]. Consequently, the

Fig. 4.2. *Nitroimidazoles undergo a series of one electron reductions in hypoxic cells and get irreversibly bound to the cellular components. This property is exploited to selectively target hypoxic cells. The first step is reversible under oxygenated condition. So the reduction chain will not continue in normal cells which are well oxygenated. However, in hypoxic cells, reduction continues till the ring gets fragmented and the reactive fragments get bound to the cellular components*

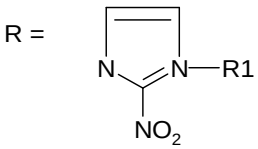

R1 = Alkyl side chain suitably modified to hold the radiotracer

radio labeled analogues of MISO and its derivatives are used as markers of hypoxic tissues [130-137]. PET imaging with [^{18}F]FMISO can help to estimate the oxygenation status of tumors in any part of the body [138]. The tracer has also been used to study the relative hypoxic volume of tumors during the course of radiation treatment. Recently, improvement in response to treatment with new selective experimental chemotherapy agents has been observed by using [^{18}F]FMISO and PET [139]. The tracer's ([^{18}F]FMISO) primary cellular uptake results from diffusion and partition based retention in lipophilic tissues such as the brain, in addition to hypoxia based retention. Secondly, the excretion of the tracer ([^{18}F]FMISO) is through the billiary system reflecting its higher lipophilic nature. The clearance through liver is also very slow due to its lipophilic nature. So, the background remains very high which requires that the imaging be done late after its administration. Despite these disadvantages, [^{18}F]FMISO is, still the most used radiotracer in hypoxia studies in humans and it is in high demand for PET oncology studies [132, 140-144].There are reports of the use of a more hydrophilic derivative of FMISO *viz*., fluoroerythronitroimidazole, FETNIM [129,136]. In addition to, a large number of ^{18}F labeled analogues have been developed

such as [^{18}F]FETA [145], [^{18}F]EF1 [146], [^{18}F]EF5 [143, 147-149] and [^{18}F]FAZA [150], although the data regarding their use in humans is limited.

The most commonly used route for the synthesis of [^{18}F]FMISO, to date, is the nucleophilic substitution of the tosylate-leaving group by [^{18}F]fluoride on the tetrahydropyranyl-protected precursor 1-(2'-nitro-1'-imidazolyl)-2-O-tetrahydropyranyl-3-O-toluenesulphonylpropanediol (NITTP) followed by the hydrolysis of the protecting group [151,152]. The synthesis procedure is summarized in **Scheme IV.I.**

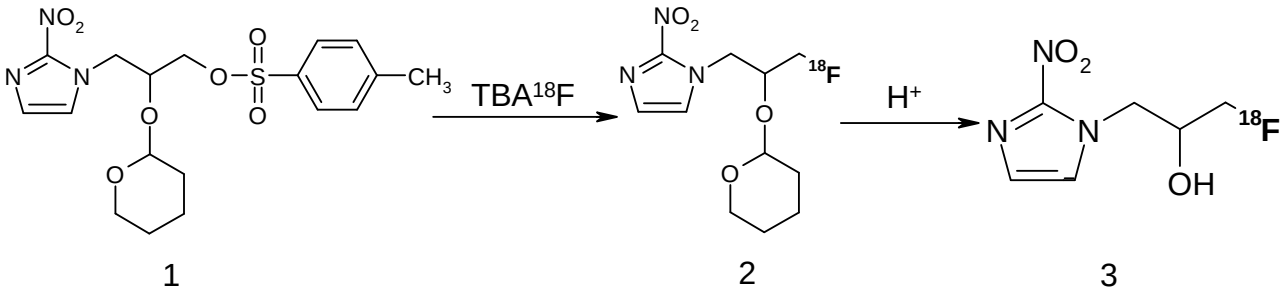

1: 1-(2´-nitro-1´-imidazolyl)-2-O-tetrahydropyranyl-3-O-toluenesulphonyl prapanediol (NITTP)
2: 1H-1-(3-[18F]fluoro-2-hydroxypropyl)-2-nitroimidazole
3: [18F]-FMISO

Scheme IV.I. *Synthesis scheme of [^{18}F]FMISO from the precursor, NITTP*

Recently, a fully automated synthesis of [^{18}F]FMISO using HPLC purification with a radiochemical yield more than 60% in a synthesis time of approximately 60 min has been reported [152]. [^{18}F]FMISO radiosynthesis using Sep-Pak® purification with more than 40% radiochemical yield (without decay correction) in about 40 minutes has also been reported [153]. The possibility of producing a ^{18}F-labeled PET radiotracer other than [^{18}F]FDG using a commercial [^{18}F]FDG synthesizer, allowing economical use of an expensive equipment is very attractive for radiochemists. Many radiosynthesis of ^{18}F-labeled compounds comprise of direct

nucleophilic substitutions of the leaving group in desired molecule followed by hydrolysis/deprotection. [^{18}F]FMISO belongs to the same category [154]. However, [^{18}F]FMISO production using semi-preparative HPLC purification can not be adapted in a commercial [^{18}F]FDG synthesis module but the same is easily possible if a method is developed to produce [^{18}F]FMISO using a single column purification .Semi-preparative HPLC purification for routine production of [^{18}F]FMISO is quite complicated and significantly adds to the synthesis time. Considering all these facts and since an semi-preparative HPLC equipped synthesis module was not readily available, a simple, fully automated radiosynthesis procedure of [^{18}F]FMISO employing a neutral alumina column purification using a general purpose fluorination module was attempted [155-157]. Details of the synthesis procedure, analysis of chemical and radiochemical impurities, PET/CT imaging study in normal healthy rabbit to visualize the distribution *in vivo* and finally bio-distribution studies in fibrosarcoma tumor model to confirm tumor localization are described in this chapter in the first part (**Part I**).The second part (**Part II**) describes the optimization of reaction parameters i.e. the radiofluorination temperature and time, the hydrolysis condition, to shorten the total production time to minimize the radioactive decay loss, as well as minimal usage of the costly precursor to make the production procedure much more economical.

4.2 **Materials & Methods**

4.2.1. Reagents and apparatus

NITTP, FMISO reference standard, 75mM $TBAHCO_3$ solution, molecular-grade acetonitrile, 10% NaCl, 1M HCl, 1M NaH_2PO_4 buffer, sterile and pyrogen-free water for injection and pharmaceutical grade ethanol were procured from ABX Advanced Biochemical Compounds,

Germany. Fluorine-18 separation cartridge, Chromafix 45-PS-HCO_3, was obtained from Marcherey-Nagel, Germany. Aluminium oxide active (neutral, activity I-II) for column chromatography was procured from MERCK, India. Evacuated 10 ml vials (sterile and pyrogen free) were obtained from ACILA AG, Germany. Minisart 0.2µ filters were purchased from Sartorius. Sterility tests were carried out in-house using standard protocol [Indian Pharmacopoeia (IP, 1996: IP, addendum 2005 protocol)]. Pyrogenicity was verified by LAL test using Endosafe Reagent Kits from Charles River Laboratory, USA (US License No: 1197). Radioactivity was measured using an ion chamber (Capintec CRC-15R). Radiofluorination and conversion of NITTP to [^{18}F]FMISO was carried out in a general-purpose fluorination module (Nuclear Interface, Münster, Germany) which features similar to GE TRACERlab FX_{FDG} [**Fig.4.3.**]. Radio-HPLC analysis was carried out in a Knauer system (Germany) with a tunable UV absorption detector and a radiometric detector system using a C-18 reverse phase analytical column (Nucleosil, 5µM, 250 × 4 mm). The UV absorption was monitored at 254 nm. Radio TLC was carried out on Silica Gel 60, 20 × 20 and Silica Gel 60 F_{254}, 20 × 20 (Merck, Germany) and scanned using a RayTest TLC scanner with a BGO scintillation detector and spectrum analyzed with GINA® software. The residual solvent analysis was carried out using a semi-automatic Gas Chromatograph from Chemito, India equipped with a flame ionization detector (FID) using a PEG capillary column (BP-20 from SGE, Australia). Alizarin Red S was procured from Sigma. Microquant® Aluminium-Test Kit (Sensitivity: 0.1-6µg/ml) was procured from Merck, India. All other chemicals used were of either HPLC or analytical grade and procured locally. All animal experiments were carried out as per guidelines set for animal experiments and after approval from BARC Animal Ethics Committee.

4.2.2 Automated synthesis of [^{18}F]FMISO

The fully automated synthesis of [^{18}F]FMISO consists of three main steps. 1) Nucleophilic fluorination of NITTP 2) Deprotection and 3) Purification through a neutral alumina column. [^{18}F]fluoride from the cyclotron is first trapped on a Chromafix 45-PS-HCO_3 anion exchange cartridge [**Fig.4.4.**]. This is then eluted from the column using 0.4 ml of 75mM $TBAHCO_3$ into the reaction vessel. The [^{18}F]TBAF fluoride was then dried by azeotropic distillation with acetonitrile (0.8 ml). To this, the NITTP precursor (varying amounts i.e. 25mg, 10 mg and 5 mg respectively were tested) dissolved in acetonitrile (0.6 ml) was added and the S_N2 fluorination reaction carried out at 110°C for 15 min. The acetonitrile was then evaporated from the reaction mixture and acid hydrolysis was carried out by the addition of 1N HCl (1 ml) at 105°C for 10 min. The reaction mixture was cooled to 50°C and the reaction mixture is passed through a neutral alumina column.

4.2.3. [^{18}F] FMISO purification column

The [^{18}F]FMISO purification column is a ready to use column composed of only neutral alumina, active, grade I-II (Brockmann) [**Fig. 4.4.**] packed in-house in our lab. In brief, neutral alumina (dry weight) was taken and most of the fines are removed by adding water and stirring vigorously, and after a while, when most of the alumina settles, the supernatant with fines in suspension, is decanted off. This is repeated thrice. The sedimented alumina is kept at 60°C (overnight) till it dries to a free flowing powder. This is stored in an airtight container. Whenever a column is required, 7.7 g of the washed and dried neutral alumina is packed inside a polypropylene cartridge barrel (6.5 cm × 1.2 cm) taking care to pack uniformly without any cavities. The top and bottom of the column were attached with 20-µm-polyethylene frits. The

column was washed and sanitized by passing 20 ml of ethanol and 50 ml of sterile and bacterial endotoxin free distilled water before use. The reaction mixture is loaded to the column. The reaction vessel was rinsed with 1.5 ml of 5% ethanol containg water, and the rinsing passed through the column and the eluent directed to waste. [^{18}F]FMISO was finally eluted using 10% ethanol (12 ml) and is collected in the product vial containing 10% NaCl (1.7 ml) and 1M NaH_2PO_4 (0.7 ml) to make the final product isotonic. [^{18}F]FMISO collected in the product vial is then transferred to an automated dispensing unit and dispensed into different vials in a class 100 area through a 0.2 µM filter. The [^{18}F]FMISO was obtained as a clear, colorless, sterile solution and free of any suspended particles.

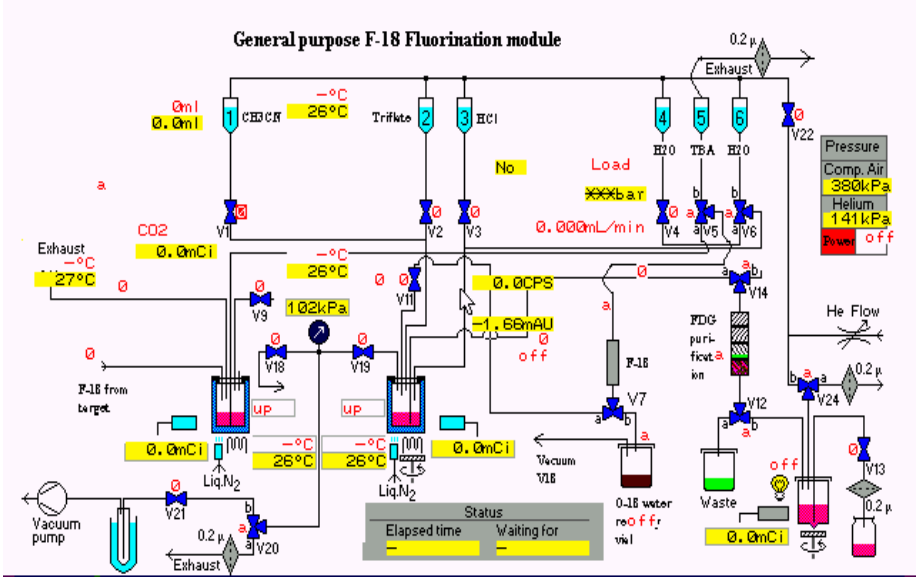

Fig.4.3. *Schematic representation of general purpose fluorination module*

Fig. 4.4. *^{18}F-trapping column (Ps-HCO_3) and neutral alumina purification column*

4.2.4. Quality control and stability

The pH of [^{18}F]FMISO was checked with pH test paper strip since as in [^{18}F]FDG , the acceptable range is wide. The radiochemical purity was first checked by radio-TLC using a silica gel 60-coated plate developed in methanol/ammonia (95:5, v/v) solvent system. The reference standard FMISO was also chromatographed identically and stained with iodine vapour for comparison. Additionally the chemical and radiochemical purity were also analyzed using an analytical HPLC by monitoring the UV absorbance (λ = 254 nm) as well as the radioactivity profile. The mobile phase consisted of 70% MeOH and 30% water and HPLC carried out in an isocratic system at a flow rate of 0.5 ml/min. The presence of non-radioactive impurities was also verified under similar HPLC conditions by analyzing pure NITTP, reference-standard FMISO and a mixture of the two. Finally [^{18}F] FMISO prepared was confirmed by co-eluting peaks (radioactive as well as UV) in HPLC analysis and comparing the UV peak of [^{18}F] FMISO with that of cold reference standard of FMISO. Radiochemical stability was checked with a 10

ml solution [9 ml saline + 1 ml [^{18}F] FMISO (10% ethanol)] using radio TLC and analytical HPLC upto 8 hrs post synthesis.

4.2.5. Gas chromatography analysis

Sealed samples from each synthesis of [^{18}F]FMISO were stored at room temperature and analyzed later for the residual solvents, mainly the presence of toxic acetonitrile, using gas chromatography [158]. The GC column was maintained at a temperature of 50°C during the operation. An aqueous solution containing 200 ppm each of ethanol and acetonitrile was used as the standard solution. [^{18}F]FMISO sample (1 µl) after radioactive decay was injected and compared against the calibration data obtained from 1 µl injection of the standard solution.

4.2.6. Test for aluminum ions

The aluminum ion (Al^{3+}) test was performed using the following two methods: (1) The Alizarin Red S method [159] In a test tube containing 50 µl of the sample, 50 µl of a 10% ammonia solution and then 50 µl of an aqueous solution of Alizarin Red S were added. The colour developed (Wine Red in presence of Al^{3+}) was compared by unaided eye with that of standard Al^{3+} aqueous solutions treated similarly. Additionally, for confirmation of results, the colour change of the mixture (light red in presence of Al^{3+}) was also compared with the standards after further adding 500 µl of 1N acetic acid solution. Standard solutions (0, 5, 10 and 20 µg/ml Al^{3+}) were tested. The samples were also analyzed by Microquant® Al test kit as per standard protocol for confirming the exact Al^{3+} concentration.

4.2.7. Sterility and bacterial endotoxin analysis

Sterility tests were performed in accordance with IP (Indian Pharmacopoeia), 1996: IP, addendum 2005 protocol. In this test, 1 ml of the [^{18}F]FMISO sample after radioactive decay was inoculated in fluid thioglycollate medium at 37°C for 14 days to observe the growth of aerobic

and anaerobic bacteria. Similarly, 1 ml of the decayed [^{18}F] FMISO sample was also inoculated in soybean casein digest medium at 22-25°C for 14 days to detect fungal growth. The bacterial endotoxin test was performed in accordance with USP XXV. The test was based on the formation of gel clot in the sample by Limulus Amoebocyte Lysate (sensitivity: 0.125 EU/ml) reagent.

4.2.8. Biodistribution

Biodistribution of [^{18}F]FMISO was performed in Swiss mice bearing fibrosarcoma tumors (developed by subcutaneous injection of 10^6 cells per animal). After 14 days of the injection of the cells, a tumor diameter of 1-2 cm was observed. [^{18}F]FMISO as prepared in 4.2.2 was administered to three groups of mice [mean wt. ~ 25g] with four animals in each group. Around 100 KBq in 0.3 ml was administered per animal (considering the small size and weight of the animals only 100 KBq) intravenously through the tail-vein and sacrificed at 30, 120 and 240 min. The various organs and blood were removed, tissue excised, weighed and counted for radioactivity. The percentage of injected dose per gram of tissue weight was determined.

4.2.9. PET/CT imaging study in rabbit

The normal biodistribution of [^{18}F]FMISO in normal healthy rabbit (~ 2.5 Kg) was studied by PET/CT (Discovery ST, GEMS, GE, USA) by imaging after over night fasting. [^{18}F]FMISO (~111 MBq / 1.0 ml) was injected intravenously through the ear vein. Images were recorded after 1 hr and 4 hrs post injection after standard anesthesia administration.

4.2. 10. Patients Study

PET/CT images of a number of cancer patients with suspected tumor hypoxia, were studied using approximately 370 MBq of [^{18}F]FMISO per patient. Images were taken one hour post

injection. For performing the clinical trials in patient, regulatory clearance from the Tata Memorial Hospital (TMH) Ethics Committee was obtained (This was a collaborative project with the Bio-Imaging Unit, TMH where the clinicians of the particular unit were also involved) [155-157].

4.3. Results and Discussion

Starting from the precursor, NITTP, [^{18}F]FMISO was prepared in the adapted general purpose fluorination module with features very similar to GE TRACERlab FX_{FDG} as discussed in **Ch.2**. Purification was achieved using a single neutral alumina column. The radiochemical yield obtained (without decay correction) was 23.40 ± 0.65% (n = 3) with 5 mg NITTP, 37.49 ± 1.68 % with 10 mg NITTP (n = 3) and 34.1 ± 3.2 (n = 5) with 25 mg of NITTP (**Table 4.1.**). The radiochemical yield was expressed as the percentage of radioactivity finally obtained as [^{18}F]FMISO compared with the total ^{18}F activity obtained in the reaction vessel without applying decay correction. Within the range of precursor used, the highest yield was obtained with 10 mg of precursor. Within 5 mg and 10 mg, the radiochemical yield appears to be directly proportional to the amount of the starting material NITTP taken. Beyond 10 mg of NITTP, the yield does not increase linearly. The final [^{18}F]FMISO obtained was clear, colourless and free of any suspended particles. pH observed was in the range of 6.5-7.0. The entire synthesis was monitored by TLC at the three important steps, viz (1) after radio fluorination of the precursor, NITTP (2) after acid hydrolysis of the ^{18}F-substituted NITTP and finally (3) after purification through single neutral alumina column and elution with 10% ethanol containing water. The TLC of the radiofluorinated NITTP showed the presence of free [^{18}F]fluoride with a R_f of 0.04 whereas the radiofluorinated NITTP was observed as a broad peak with a R_f of 0.85 as shown in **Fig. 4.5(a).**. The TLC pattern of acid hydrolyzed radiofluorinated NITTP was also of similar nature showing two peaks one corresponding to free fluoride and another to [^{18}F]FMISO **Fig. 4.5(b).**. The TLC of the final

purified [^{18}F]FMISO showed only one prominent peak with an R_f of 0.69 as shown in **Fig. 4.6(a)..** The difference in the R_f value of the THP-protected reaction product, [^{18}F]NITTP and [^{18}F]FMISO were in accordance with their polarity. The R_f value of [^{18}F]FMISO was further verified by TLC of the reference standard FMISO in the same solvent system and then staining with iodine vapor [**Fig. 4.6(b).**]. The R_f value of [^{18}F]FMISO exactly matched with that of reference standard FMISO after iodine staining. The HPLC chromatogram of [^{18}F]FMISO is shown in **Fig. 4.7..** From the chromatogram

Table 4.1.Dependence of Radiochemical Yield on amount of precursor (Reaction Condition: Radiofluorination at 110°C, 15 min, Acid hydrolysis at 105°C, 10 min)

S. No	Amount of precursor , NITTP (mg)	Radiochemical Yield* (%) (Individual Synthesis)	Radiochemical Yield* (%) (Average)
1	5	24.0	23.40 ± 0.65
		22.7	
		23.5	
2	10	39.2	37.49 ± 1.68
		35.8	
		37.5	
3	25	34.3	34.10 ± 3.20
		30.6	
		31.5	
		38.4	
		35.6	

*Without decay correction

it is seen that the retention time of [^{18}F]FMISO is 7.9 min and the corresponding retention time from the UV chromatogram is 10.04 min. The difference in the retention times of radioactivity and UV peak may be attributed to the dead volume of the tubing between the UV detector and radioactivity detector attached externally [In our HPLC system, the sample is first detected by the radioactivity detector and then by the UV detector The length of the tubing, connecting the two detectors is quite large, approximately 1 meter. This always shows up as a difference in the

retention time of the radioactivity peak and the UV peak]. The retention time of [^{18}F]FMISO was validated using a reference FMISO standard [**Fig.4.8.**]**.** The presence of UV active non-radioactive impurities was also examined. The precursor, NITTP shows a retention time of 15.13 min [**Fig.4.9.**]. When a

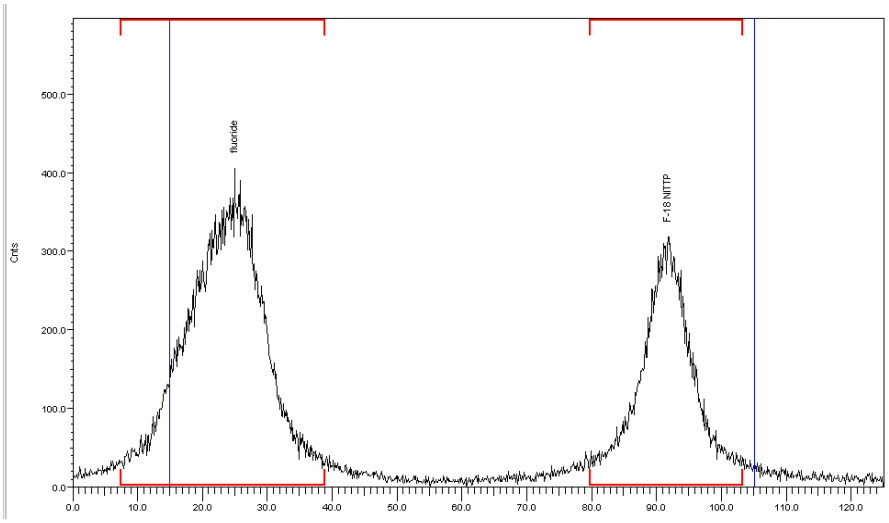

Fig. 4.5(a). *Radio TLC of fluorinated NITTP, Free [^{18}F]F$^-$ comes at point of spot with an R_f value of 0.09. Radiofluorinated NITTP appears with an R_f value of 0.85*

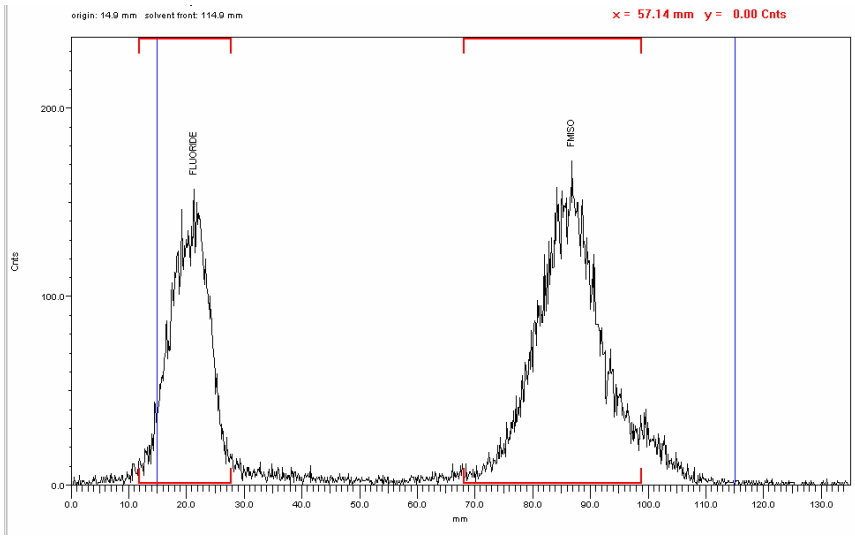

Fig. 4.5(b). *Radio TLC of the reaction mixture of NITTP after acid hydrolysis in 95:5 MeOH/NH_3 solvent. Free [^{18}F]F$^-$ appears with an R_f value of 0.05-0.06 and [^{18}F]FMISO appears with an R_f value of 0.69-0.72.*

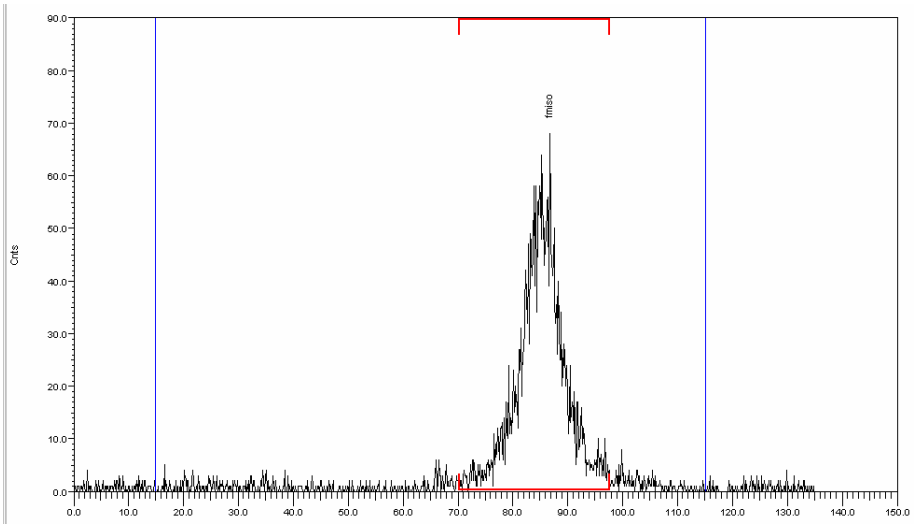

Fig. 4.6(a). *Radio-TLC of [^{18}F] FMISO in 95:5 MeOH/NH_3 solvent, R_f (max) is 0.7*

Fig. 4.6(b). *TLC of reference standard FMISO visualized by iodine staining*

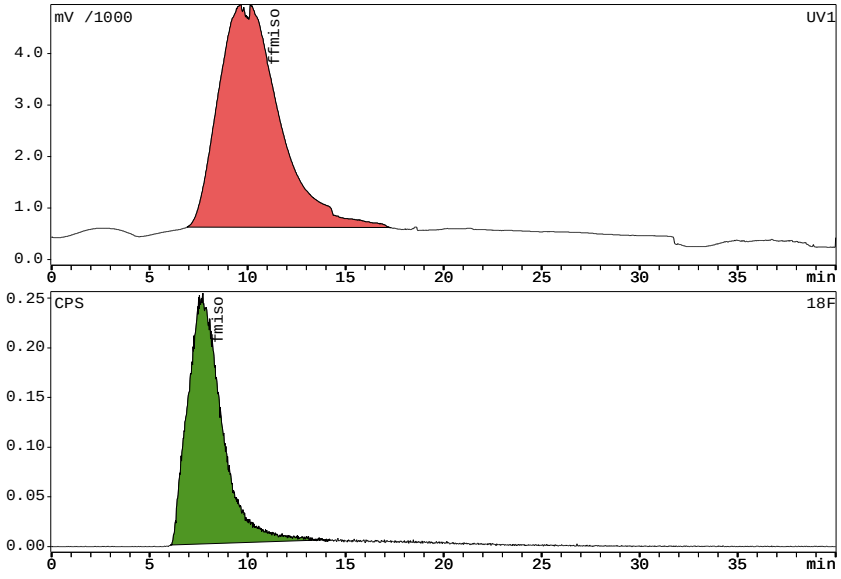

Fig. 4.7. *Analytical HPLC of [^{18}F] FMISO*
[Radioactivity (green peak) & UV (red peak, λ = 254 nm)]

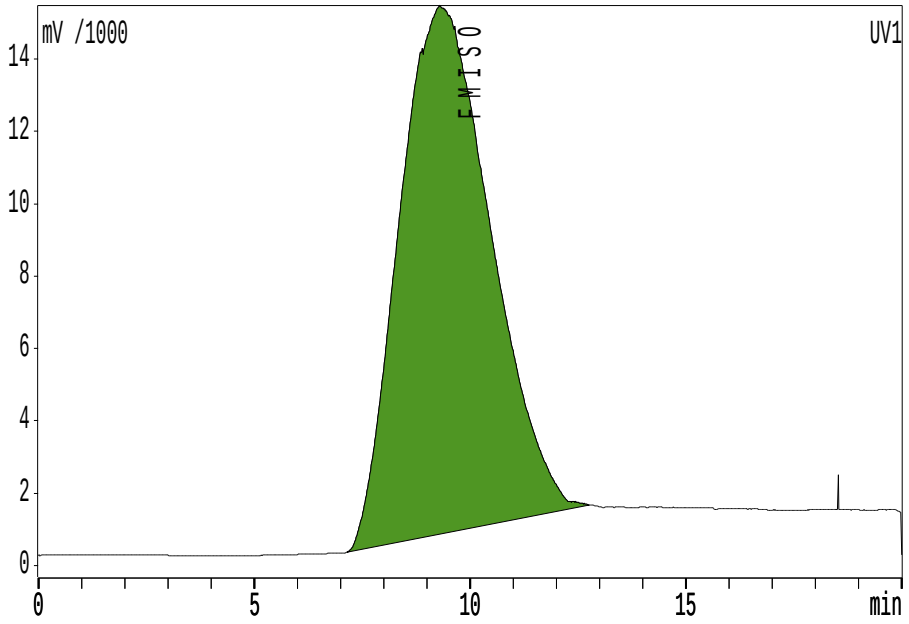

Fig. 4.8. *HPLC Chromatogram of Ref. Std. FMISO (UV only, λ = 254 nm)*
Retention time (t_R) : 9.3 min

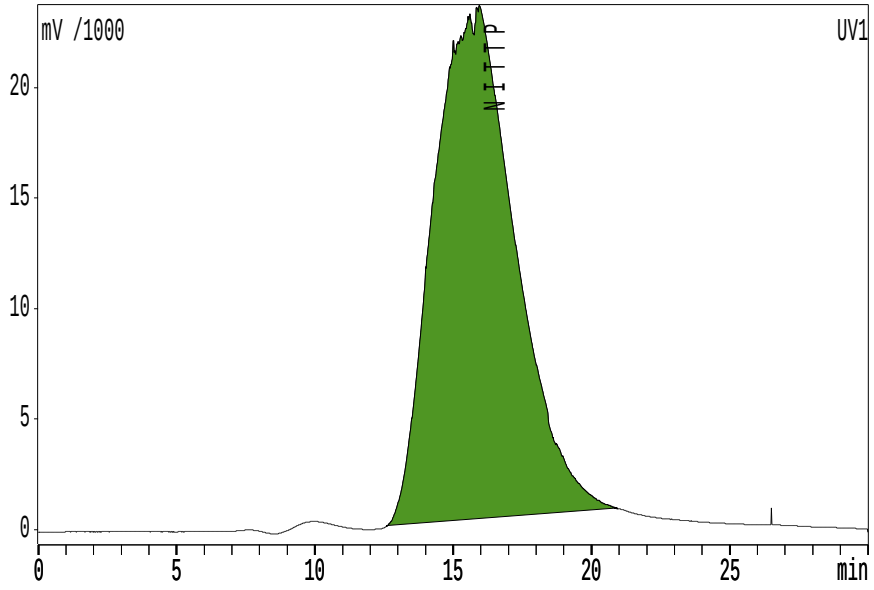

Fig.4.9. *HPLC Chromatogram of the precursor, NITTP (UV only, λ = 254 nm)*
t_R : 15.1 min

mixture of NITTP and reference standard FMISO were analyzed and two well resolved peaks were obtained at 9.13 min (FMISO) and 15.80 min (NITTP) respectively [**Fig.4.10.**] The HPLC

analysis of the radio fluorinated NITTP precursor showed two UV peaks at 10.13 min and 16.2 min respectively but a single radioactive peak at 10.40 min [**Fig.4.11.**]. By comparing this with the retention times of FMISO and NITTP standards, it is apparent that the first UV peak could be that of [^{18}F]NITTP whereas the second one that of unreacted NITTP, which is comparatively more non-polar due to the presence of THP moiety. Free $^{18}F^-$ did not elute out under the HPLC condition and this was verified by

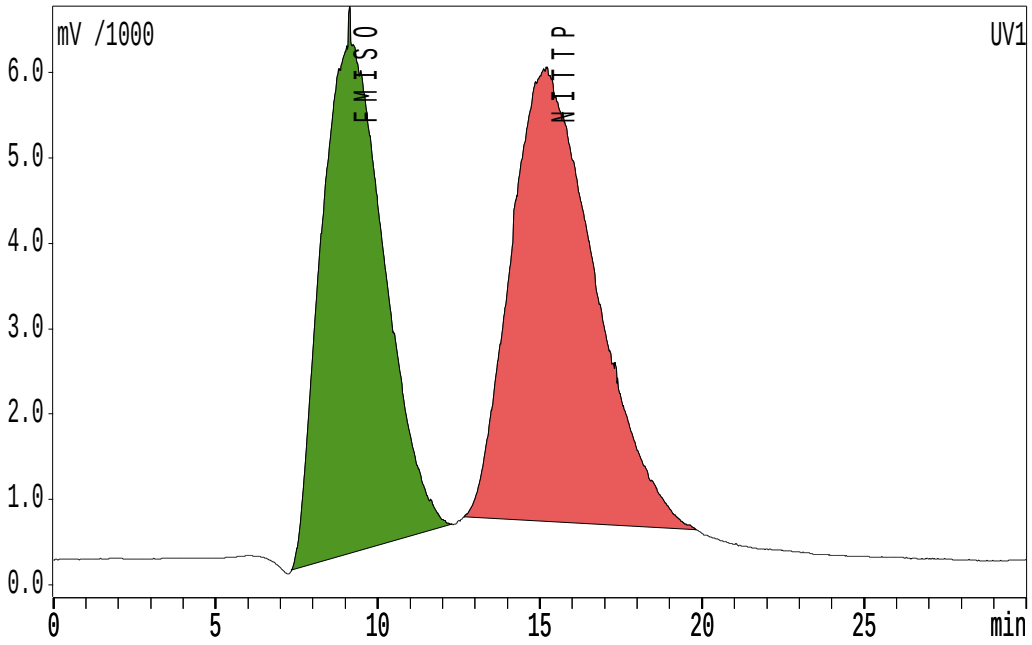

Fig. 4.10. *Mix. of NITTP & Ref. Std. FMISO t_R (Ref. Std. FMISO):9.1 min, t_R (NITTP):15.8 min*

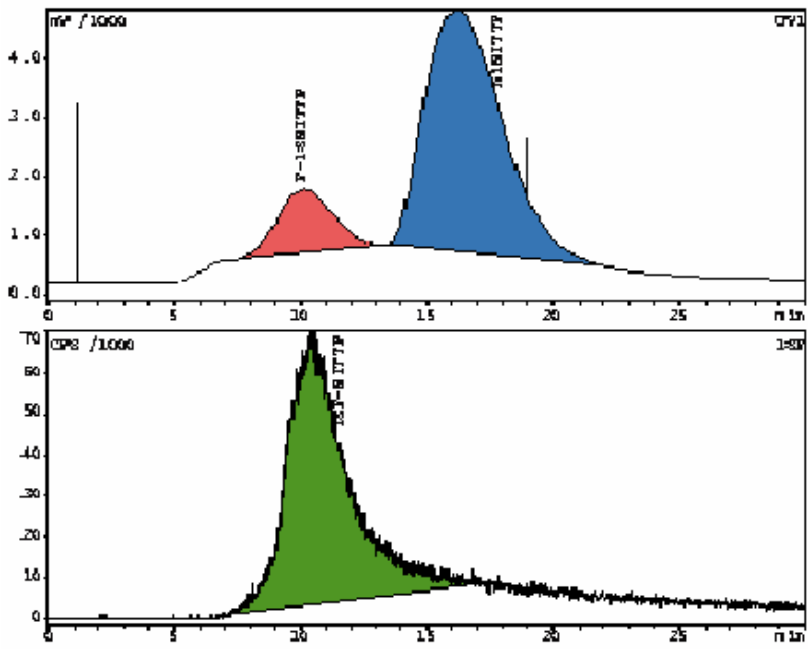

Fig.4.11. *HPLC of the Reaction Mixture after radiofluorination (After S_N2)*

carrying out HPLC of free $^{18}F^-$. The HPLC of the [^{18}F]FMISO showed only one UV peak and one radioactive peak. Hence, it could be concluded that the final [^{18}F]FMISO was free from any kind of non-radioactive impurity. The formation of MISO, which is reported to show some neurotoxicity at therapeutic doses, is virtually impossible under the experimental conditions employed. Since it has to be produced by the hydrolysis of the precursor NITTP followed by the etherification of the –OH generated from the tosyl group. GC analysis showed no traces of acetonitrile in the final [^{18}F]FMISO. However, ethanol is present as expected since the product is obtained from the alumina column by elution with 10% ethanol in water . The Alizarin Red S method detects Al^{3+} on the basis of color development reactions between aluminum hydroxide (formed from Al^{3+} in the presence of ammonium base) and Alizarin Red S. The limit of Al^{3+} in standard aqueous solution is 5µg/ml [159] which can be detected by the Alizarin Red S method and the coloured product is visible to the unaided eye. The test for Al^{3+} in a sample of [^{18}F]FMISO, post radioactive decay, analyzed by Alizarin S method shows that the Al^{3+} ion concentration is

below the allowed limit of 5µg/ml. Further analysis with Microquant® Al^{3+} test kit (sensitivity 0.1-6µg/ml) based on Chromazurol S method confirmed that Al^{3+} in the final [^{18}F]FMISO was in the range of 3-4µg/ml. The biodistribution study in fibrosarcoma tumor bearing mice [**Fig.4.12.**] showed maximum uptake in tumor two hours post injection (% injected dose/g: 7.8 ± 2.7) (**Table 4.2**)

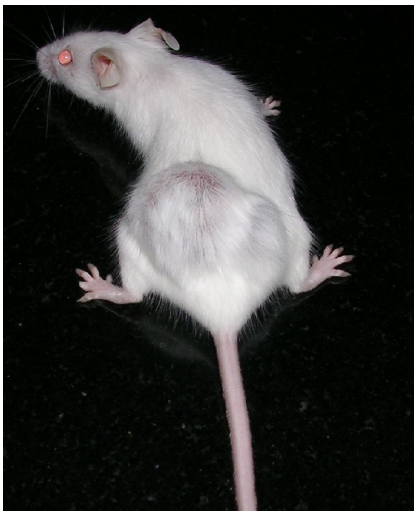

Fig. 4.12. *Fibrosarcoma tumor bearing Swiss Mice*

(**Table 4.2**) but decreased at four hour post injection (% Injected dose/g: 4.48 ± 0.89). Bone uptake showed marginal increment when compared half an hour and four hours post injection results. The biodistribution result was in accordance with the findings by Yang et al [129]. PET/CT images of the rabbit were recorded one hour and four hours post injection and are shown in **Fig. 4.13.a.** and **4.13.b.**. There is significant uptake in organs involved in the metabolic pathway of MISO like liver, GI tract etc. Uptake in brain is also observed as expected (% Injected dose/g: 2.75 ± 0.23 at four hours post injection as obtained in bio-distribution study).

Table 4.2. Bio-distribution in fibro sarcoma tumor model

Organ	% Injected Dose per gm tissue		
	30 min (n = 4)	120 min (n = 3)	240 min (n = 4)
Blood	4.45±2.22	1.42±0.19	1.70±1.07
Bone	1.84±0.18	2.29±1.06	2.90±1.07
Muscle	2.18±0.16	1.45±1.00	1.44±0.88
Liver	4.59±0.24	5.34±1.60	1.92±0.34
Intestine + Gall bladder	4.58±1.86	5.04±1.51	11.34±4.72
Fibro sarcoma Tumor	2.19±0.48	7.77±2.66	4.48±0.89

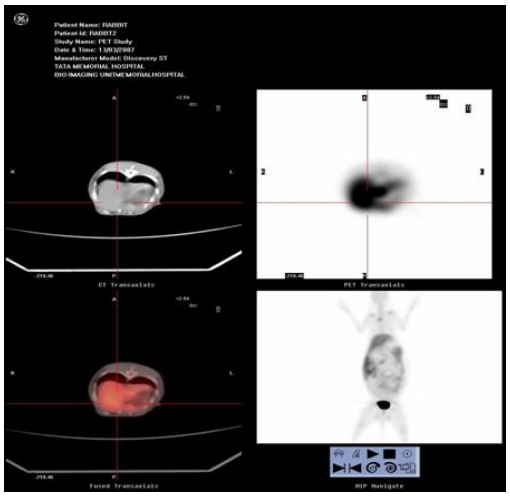

Fig.4.13.a. *[^{18}F] FMISO PET/CT scan of rabbit (One hour post Injection) showing liver uptake*

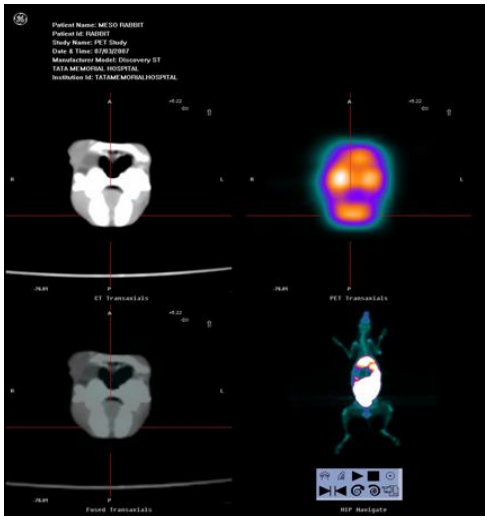

Fig.4.13.b. *[^{18}F] FMISO PET/CT scan of rabbit (Four hours post Injection) showing brain uptake and huge accumulation of activity in the billiary system*

The underlying principle by which the single neutral alumina column purification procedure is developed is *flash chromatography* technique. This is a "state of art" application of traditional column chromatography (where the solvent is allowed to flow down the column by gravity, or by percolation; also known as gravity column chromatography) used by the organic chemists for separating components from a reaction mixture. The difference is that, the solvent is forced down the column by positive gas (helium in our case) pressure (around 1 to 4 atmosphere) in this case. This technique is very useful and widely used in almost all organic chemistry labs now a days as it is more efficient and gives higher resolution than conventional chromatography at atmospheric pressure and is completed in a relatively shorter time. In PET radiopharmaceutical production process, it is ideally suitable considering short half life of the PET radionuclides, ease of operation (no need of specialist chemist!) and most importantly, easy to use in the fully automated synthesis module. It is needless to mention that the flash column (here the neutral alumina column) or if we say more precisely, the adsorbent material packed inside the column is the 'heart" of the whole purification process. Since the solvent is forced through the column, in order to make the flow rate slow, fine adsorbent particles (smaller particle, 0.040-0.063 mm, higher mesh size) of mesh size 230-400 are normally used in flash chromatography. For the same reason as mentioned above, how the adsorbent are tightly packed inside the column is also an important factor. The more tightly it is packed, the better separation is the result. Air bubble formation while packing the adsorbent material is to be strictly avoided. Alumina (Al_2O_3) is one the two most frequently used adsorbent for column chromatography. Alumina is quite sensitive to the amount of water which is bound to it: the higher its water content, the less polar sites it has to bind organic compounds, and thus the less "sticky" it is. This stickiness or activity is designated as I, II or III, with I being the most active. Alumina is usually purchased as activity I

and deactivated with water before use by keeping it suspended for several hours and then making it dry. This conditioning involves skill and has to be mastered. By this process, alumina turned to be activity grade II to III. Alumina is available in three different forms: acidic, neutral and basic. The neutral form of activity II or III, 150 mesh, is most commonly employed. In specific use, if the column length is to be shortened, higher mesh (smaller particle) neutral alumina is preferable. The polarity of the eluting solvent which is passed through the column affects the relative rates at which compounds move through the column. Polar solvents can more effectively compete with the polar solute molecules in the mixture for the polar sites on the adsorbent surface and will also better solvate the polar constituents. Consequently, a highly polar solvent will move even highly polar molecules rapidly through the column. If a solvent is too polar, movement becomes too rapid, and little or no separation of the components of a mixture will result. If the solvent is not polar enough, no compounds will elute from the column. Proper choice of an eluting solvent is thus crucial to the successful application of column chromatography as a separation technique.

In case of [^{18}F]FMISO synthesis, the two radioactive impurities are unreacted [^{18}F]F^{-} and the radiofluorinated intermediate generating from radiofluorination of the precursor NITTP followed by incomplete hydrolysis. Of the two, the major one and present in maximum percentage in the reaction mixture is unreacted [^{18}F]F^{-} and activated alumina is a well known adsorbent for it [160]. Considering very low concentration (normally in pico molar range) of unreacted [^{18}F]F^{-}, the big neutral alumina column is sufficient to adsorb it. If we carefully consider the two radio TLCs [**Fig. 4.5(a) & 4.5(b)**], it is very evident that the acid hydrolysis of the [^{18}F] - NITTP to produce [^{18}F]FMISO is complete thereby making the presence of the of this particular radiofluorinated intermediate negligible. Secondly, by carefully optimizing the polarity of the eluting solvent, [^{18}F]FMISO can be selectively eluted out. The major non-radioactive impurity we should be

concerned is the hydrolysis product of the unreacted precursor [1-(2'-nitro-1'-imidazolyl)-2, 3-propanediol. Alumina column has been successfully used for this purpose [154]. Thus a suitably conditioned pre-packed neutral alumina column is successfully used for the production of [^{18}F]FMISO as well making use of a standard [^{18}F]FDG synthesizer-an equipment.

The clearance for regular clinical use and commercial production using the method developed was obtained in January 2010 and the routine production as well as clinical use started from May 2010. A variety of patients suspected of tumor hypoxia are screened by [^{18}F] FMISO PET/CT images for further treatment strategies [**Fig. 4.14.a. & 4.14.b.**].

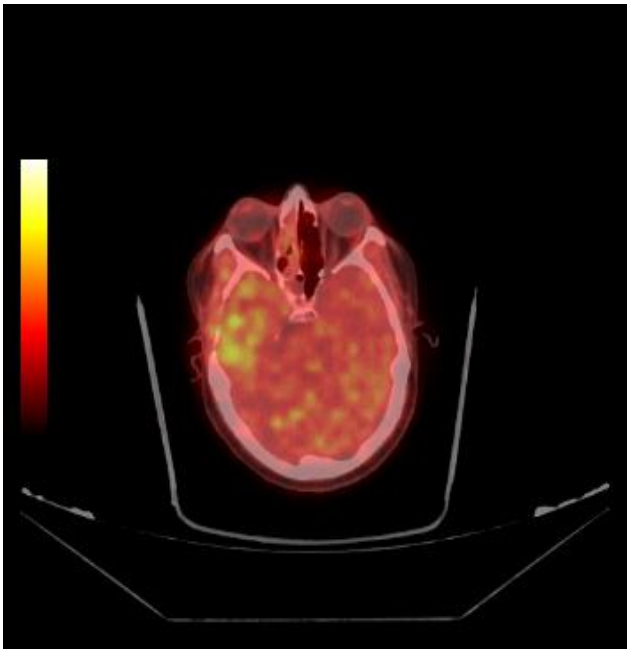

Fig.4.14.a. *[^{18}F]FMISO scan of radiation necrosis patient*

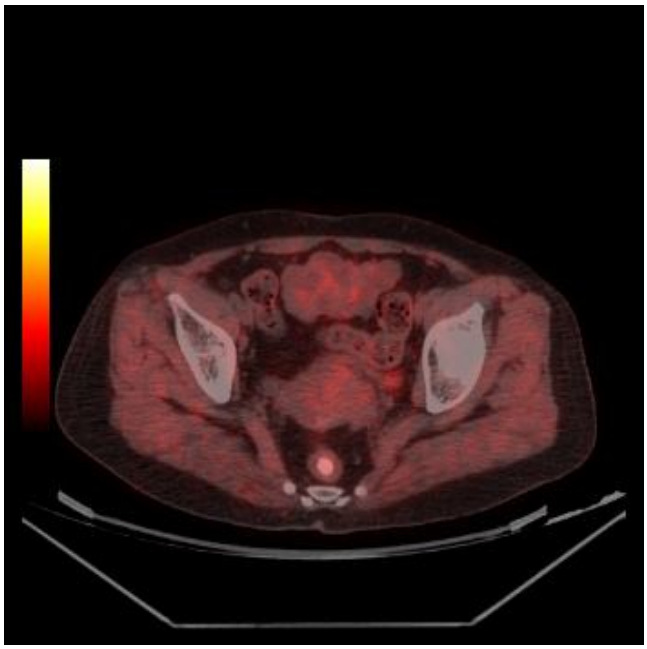

Fig.4.14.b. *CA cervix patient, [^{18}F]FMISO Scan, Negative, Good response in chemotherapy and radiotherapy*

Conclusion

A fully automated radio synthesis procedure for [^{18}F]FMISO achieving satisfactory chemical and radiochemical purity using a neutral alumina purification column instead of semi preparative HPLC has been developed. Further, this is achieved in a fluorination module configured for [^{18}F]FDG synthesis, very similar to GE TRACERlab FX_{FDG}. A moderately good yield of 37.49 ± 1.68 % (without decay correction) with 10 mg NITTP precursor has been obtained in 40 ± 1minutes. The synthesis procedure is fast, reliable, and very similar to that routinely used for [^{18}F]FDG synthesis. We obtained a product with consistent radiochemical yield, and the product also fulfills the criteria of radiopharmaceutical quality. The regulatory clearance for the routine production and clinical use was obtained in January 2010 and from May 2010, routine production and clinical use is started. This new procedure can easily be used for the routine production of [^{18}F]FMISO using commercially available FDG synthesis modules from different vendors.

PART-II

Fully automated radiosynthesis of [^{18}F]Fluoromisonidazole with single neutral alumina column purification: Optimization of reaction parameters

4. II.1 Introduction

In Part-I of this chapter, a very economic, and simple [^{18}F]FMISO synthesis procedure is described. By using just a single, neutral alumina column for the purification step, we have demonstrated that the production of [^{18}F]FMISO can be similar to that used for [^{18}F]FDG. As the main purpose was to demonstrate that single alumina column purification is indeed possible, much importance has not been given on the optimization of the reaction parameters (the radiofluorination and acid hydrolysis temperature and duration) as well as the amount of precursor used. In this chapter, the optimization of the reaction parameters for the fully automated synthesis of [^{18}F]FMISO developed by us using general purpose fluorination module (described in Chapter 2) and a single neutral alumina column purification step. Optimization is done on the amount of NITTP precursor required, the radio-fluorination temperature / time and the acid hydrolysis conditions to achieve the maximum possible radiochemical yield in the shortest synthesis time. Radio-fluorination was attempted at four different conditions and their efficiency was compared.

4. II. 2. Materials & Methods

4.II.2.a. Reagents and apparatus

1-(2'-nitro-1'-imidazolyl)-2-O-tetra-hydropyranyl-3-O-tosyl-propanediol (**NITTP**), precursor for synthesis, reference standard fluoromisonidazole, $TBAHCO_3$ solution (75mM), molecular-grade anhydrous acetonitrile, ^{18}F trapping column ($PS\text{-}HCO_3$), 10% NaCl, 1.0 M HCl, 1.0 M NaH_2PO_4 buffer, sterile and pyrogen-free water for injection and pharmaceutical grade ethanol were procured from ABX Advanced Biochemical Compounds, Germany. Aluminum oxide (neutral, Activity I-II) was purchased from Merck, India. Evacuated 10 ml vials certified for sterility and pyrogen free were obtained from ACILA AG, Germany. Minisart 0.2μ filters were purchased from Sartorius. All other chemicals used were of HPLC and AR grade.

HPLC analysis was carried out using a Knauer HPLC system equipped with a variable wavelength UV detector and a radioactive detector in series. The analysis was carried out using a C-18 reverse phase analytical column (Nucleosil, 5μ, 250 X 4 mm) and the elution was carried out with methanol/water (70:30) at a flow rate of 0.5 ml/min. The elution was monitored at a wavelength of 254 nm followed by radioactivity level. Radiochemical purity was evaluated by thin layer chromatography (Silica gel 60, Merck) using methanol/ammonia (95:5) as the mobile phase and the radiochromatogram acquired and analyzed using a RayTest TLC scanner (Model No. BGO-V-Detector) and GINA® software provided with the scanner.

4.II.2.b Radiochemistry

All radio-fluorination studies as well as conversion of NITTP to [^{18}F]FMISO whenever required were carried out in a Nuclear Interface Module (Münster, Germany) configured for general-purpose fluorination and extensively used for [^{18}F]FDG synthesis. The method of fully automated radio synthesis of [^{18}F]FMISO by single neutral alumina column purification is

described in the previous chapter and reported by us [156]. To optimize the use of NITTP precursor and maximize the yield, the parameters studied were (i) varying amounts of precursor- 2.5, 5, 10 and 20 mg (ii) S_N2 reaction condition - 110˚C,15 min; 125˚C,7min; 135˚C, 5 min and 145˚C, 3 min (iii) acid hydrolysis to remove the protecting groups - 105˚C, 10 min ; 110˚C, 7 min ; 115˚C, 5 min and 125˚C, 3 mins. Whenever required, the synthesis is stopped after the radio-fluorination step and a sample from the reaction mixture was analyzed by radio-TLC to determine the radio-fluorination efficiency. Similarly, the reaction mixture was also sampled after the hydrolysis step and analyzed by radio-TLC to compare the efficiency of hydrolysis under different conditions. The radiochemical yield was expressed as the percentage of radioactivity finally obtained as [^{18}F]FMISO compared with the total ^{18}F activity started with in the reaction vessel, without applying correction for radioactive decay.

4.II.2.c Radio-analytical Analysis

The reaction mixtures sampled at different radio- fluorination conditions were analyzed by radio-TLC. Area under the peak in the radio-TLC were directly considered as the quantity of that particular radiolabeled moiety in the reaction mixture and expressed as percentage. Similarly, the reaction mixtures after hydrolysis step also were analyzed by radio-TLC to compare the efficiency of hydrolysis. The radiochemical purity of the finally synthesized [^{18}F]FMISO for each parameter was first checked by radio-TLC under identical conditions. This was parallelly verified by running the TLC of the reference standard FMISO under identical condition and developing the spot by iodine staining. Finally, the radiochemical purity was also checked by analytical HPLC. Twenty-five micro liter of the test solution was injected into the HPLC column and the eluate was monitored by UV absorbance (λ = 254 nm) as well as radioactivity profile.

The [^{18}F]FMISO synthesized was confirmed by comparing the retention time of the UV peak of reference standard FMISO with the radioactive peak of the test solution.

4. II.3 Results and Discussion

The amount of precursor used clearly affected the overall yield. The yield is expressed as the percent ratio of [^{18}F]FMISO obtained to the amount of [^{18}F]F$^-$ used without correcting for decay losses due to synthesis time, as this represents the actual amount of product available for use.

As shown in **Table 4.II.1.**, the highest overall yield (48.4 ± 1.18 %) was obtained with 10 mg of precursor reacted for 3 min at 145°C and was nearly twice the yield obtained with 5mg (25.3 ± 0.6 %). At other reaction conditions too, the yield with 10 mg precursor was more than 5 mg but much less than double. Higher amount of precursor, 17.5 mg and 25 mg did not yield more than that of 10 mg as would have been expected [**Fig. 4.II.1.**]. This showed that it was not economical to use more than 10 mg precursor. Our study with 2.5 mg NITTP, though at only one reaction condition of 145°C for 3 min, gave a very low yield (6.5 ± 0.3%), lower than what was proportionally expected. The R_f (max) values of free $^{18}F^-$, [^{18}F] fluorinated intermediate (**2** in **Scheme 4.II.1**) and [^{18}F] FMISO (**3** in **Scheme 4.II.1**) were 0.04, 0.85 and 0.69 respectively [161]. Lim et al. [153] first reported the affect of temperature and reaction time on the over all yield. According to their study, a small improvement in yield was observed with increasing the radiofluorination temperature from 80°C to 100˚C and time from 10 to 15 min. The optimized condition according to them was 5 mg of precursor and a 10 min reaction at 100˚C with a decay uncorrected yield of nearly 50 %. At about same time, Patt et al.[151] reported the influence of radiofluorination time on the overall labeling efficiency. Highest yield of about 60% were obtained after 10 and 15 minutes, but surprisingly the yield decreased with longer reaction times resulting in a yield of 38 ±13 % (n =5) at 30 minutes and 18 ± 10% (n = 5) at 60

minutes, indicating a thermal instability of the [^{18}F] fluorinated reaction intermediate **2** (the experiments were performed with 5 mg NITTP in a reaction volume of 2.5 ml acetonitrile). Based on their result, they fixed the radiofluorination time to 10 min and optimized the radiofluorination temperature. They studied three different temperatures i.e. 80˚C, 100˚C and 120˚C respectively. The highest yield (60 ±14 %, n = 5) was obtained at 100˚C, but lower yield (46 ±11%, n =3) at lower temperature of 80˚C. Low yield (29 ± 14%, n =3) was also observed at higher reaction temperature of 120˚C. The significant decrease of the yield at 120˚C can be interpreted as another hint suggesting assumed thermal instability of the reaction intermediate. A very fundamental question arises from the results summarized above. Which factor is responsible for the thermal instability of the [^{18}F]fluorinated intermediate **2**, the radiofluorination temperature or the duration of radiofluorination? In order to come to a conclusion, the radiofluorination reaction was carried out at four different conditions; gradually increasing the radiofluorination temperature but reducing the duration as shown in **Table 4.II.2.**. The radio-TLC pattern of the reaction mixtures were shown in **Fig. 4.II.2 (a&b)..** Comparing the radio-TLC pattern of the radiofluorinated NITTP at a temperature of 145˚C for 3 minutes, with the same at 110˚C for 15 min (this condition is identical with the optimized one by Patt et al.; in both the cases the precursor amount was 10 mg), the former showed a radiofluorination efficiency of about 84% (the peak area within the R_f range of 0.8-0.9 was 84%), the thermally degraded product was amounting to 9.9 % (the peak area within the R_f range of 0.4-0.7, the peak area upto R_f range of 0.2 was considered to be free $^{18}F^-$).On the other hand the radio-TLC of the latter, showed only 34.4% radiofluorination efficiency with a very significant 46.7% thermally degraded

Table 4.II.1. Dependence of overall [^{18}F]FMISO yield on reaction parameters and the amount of NITTP started with

	Reaction Parameters				Overall Yield (%) (Without Decay Correction)					
	Radiofluorination		Acid Hydrolysis		Amount of Precursor (NITTP) (mg)					
	Temp (˚C)	Duration (min)	Temp (˚C)	Duration (min)	2.5	5.0	10.0	17.5	25.0	Total Syn Time (min)
1	110	15	105	10	-	23.4 ± 0.6 (n = 3)	37.4 ± 1.7 (n = 3)	35.7 ± 0.5 (n =3)	34.1±3.2 (n = 5)	40±1
2	125	7	110	7	-	23.4±0.5 (n = 3)	34.5±0.3 (n = 3)	32.7±0.6 (n = 3)	38.7±0.2 (n = 3)	38±1
3	135	5	115	5	-	24.3±0.1 (n = 2)	40.7±0.2 (n = 2)	38.8±0.6 (n = 2)	39.1±0.2 (n = 2)	35±1
4	145	3	125	3	6.5±0.3 (n = 2)	25.3±0.6 (n = 3)	48.4±1.2 (n = 3)	45.9±0.7 (n = 3)	46.8±1.6 (n = 3)	32±1

product. This clearly proves that the duration of radiofluorination not the radiofluorination temperature is responsible for the thermal degradation of the radiofluorinated intermediate **2** thereby reducing the overall yield. Keeping the NITTP amount fixed at 10 mg, radiofluorination of NITTP at higher temperatures like 155˚C, 165˚C and at 175˚C (DMSO as reaction medium) for a fixed period of 3 min were also studied. The results (not shown) did not show much

variation in the percentage of radiofluorination efficiency as well as the percentage of thermally degraded product. So 145˚C was chosen as the optimized radiofluorination temperature. The acid hydrolysis of the THP protecting group of the [^{18}F] fluorinated intermediate **2** to obtain [^{18}F]FMISO proceeded rapidly with quantitative yield in all the four different hydrolysis conditions.

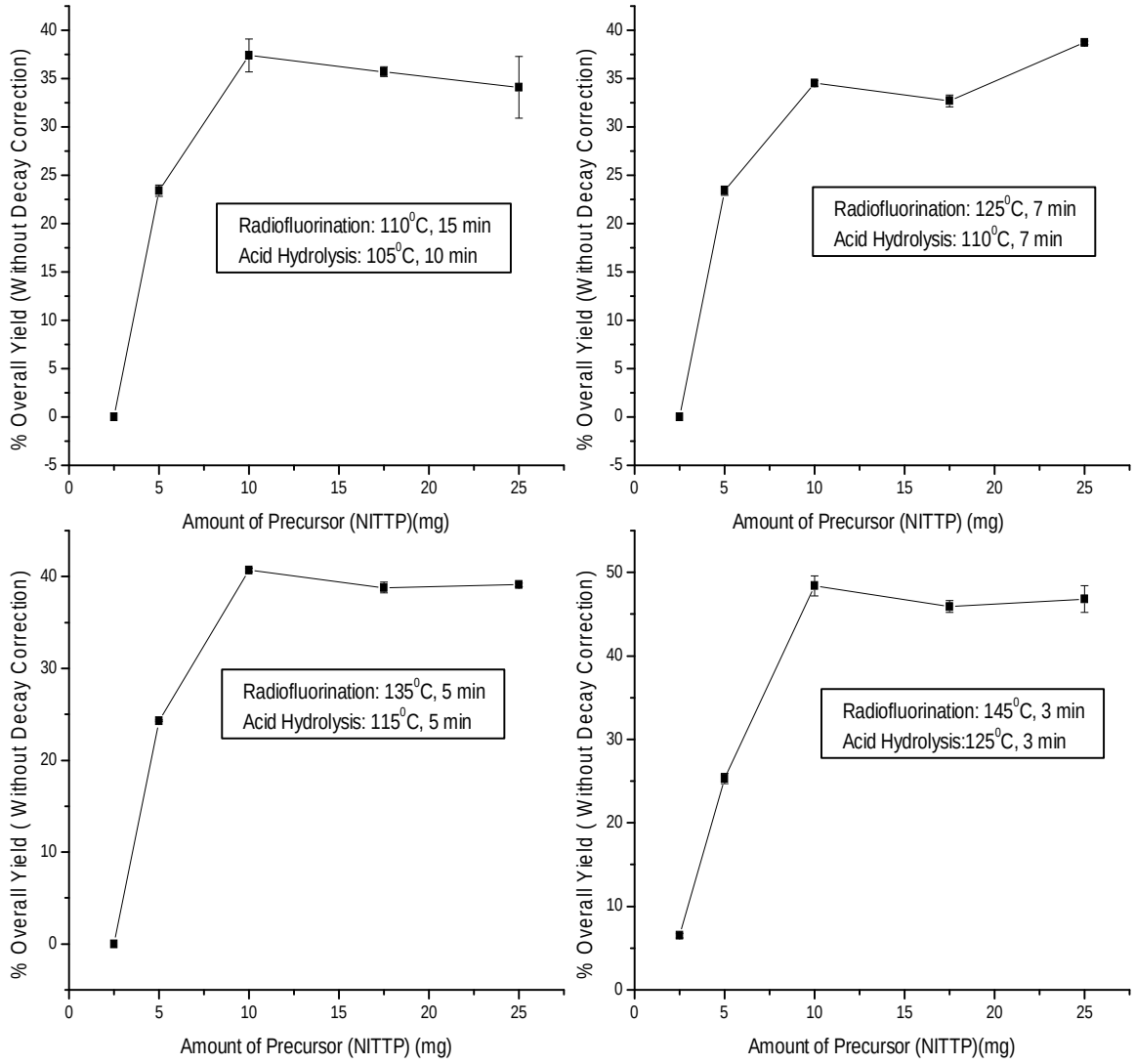

Fig. 4.II.1. *Dependence of precursor (NITTP) amount on the overall yield of [^{18}F]FMISO at different reaction conditions (Data from Table.1 were used)*

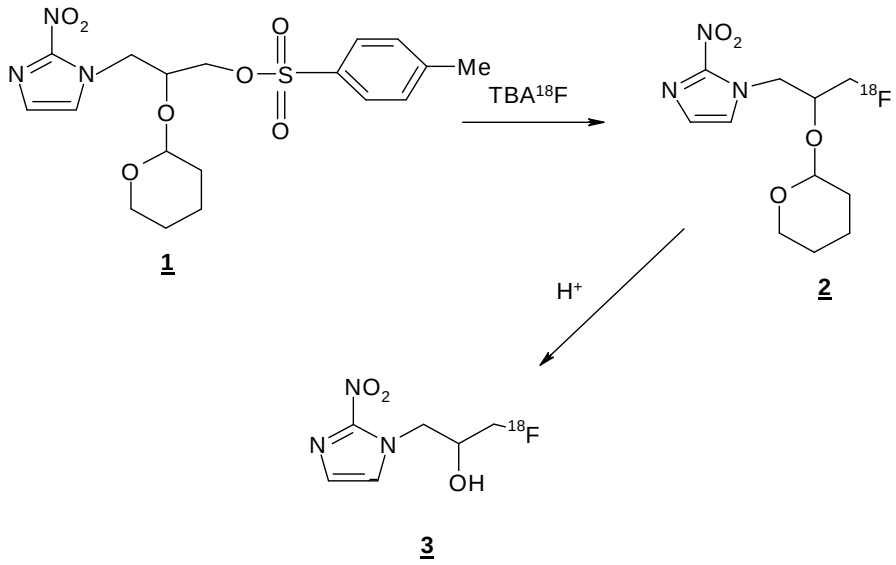

1 1-(2'-nitro-1'-imidazolyl)-2-O-tetrahydropyranyl-3-O-toluenesulphonylpropanediol (NITTP)
2 [^{18}F]fluorinated intermediate
3 1H-1-(3-[^{18}F]fluoro-2-hydroxypropyl)-2-nitroimidazole ([^{18}F]FMISO)

Scheme 4.II.1. *Schematic representation of synthesis of [^{18}F]FMISO starting from NITTP*

Table 4.II.2. Radio-fluorination efficiency at different radio-fluorination conditions [10 mg NITTP Used, Directly calculated from the peak area of radio-TLC, Mean± SD (n = 3)]

Sr. No	Radio fluorination Condition		Radio fluorination Efficiency			
	Temperature (˚C)	Duration (min)	Radio-fluorinated Intermediate **2** (%)	Thermally degraded Product (%)	Free $^{18}F^-$ (%)	Others (%)
1	110	15	34.4±0.9	46.7±0.6	13.6±0.2	5.0±.1
2	125	7	26.0 ± 0.5	52.7±1.3	14.2±0.5	7.1±0.1
3	135	5	76.4±1.5	13.2±0.9	8.3± 0.1	1.8±0.2
4	145	3	84.7±0.5	9.9±1.1	4.3±0.1	1.2±0.2

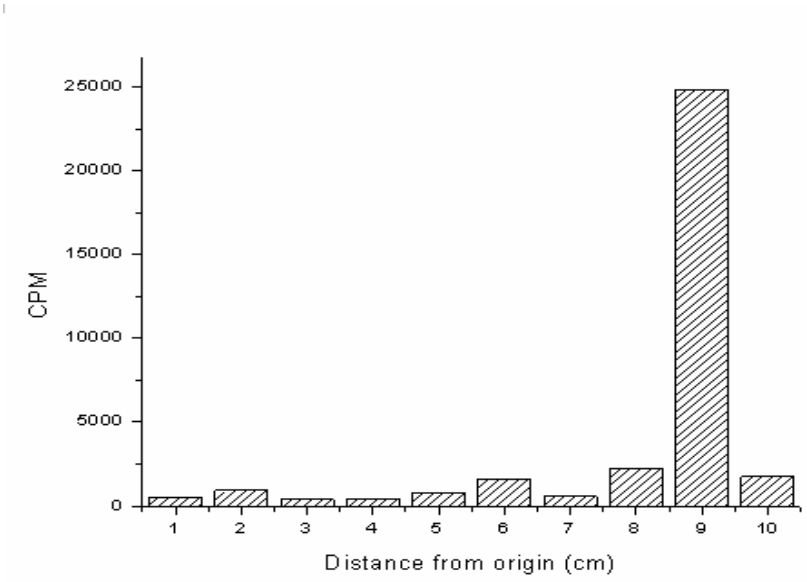

Fig.4.II.2.a. *Radio-TLC pattern of radio fluorinated NITTP (10mg) at 145˚ C for 3 minute*

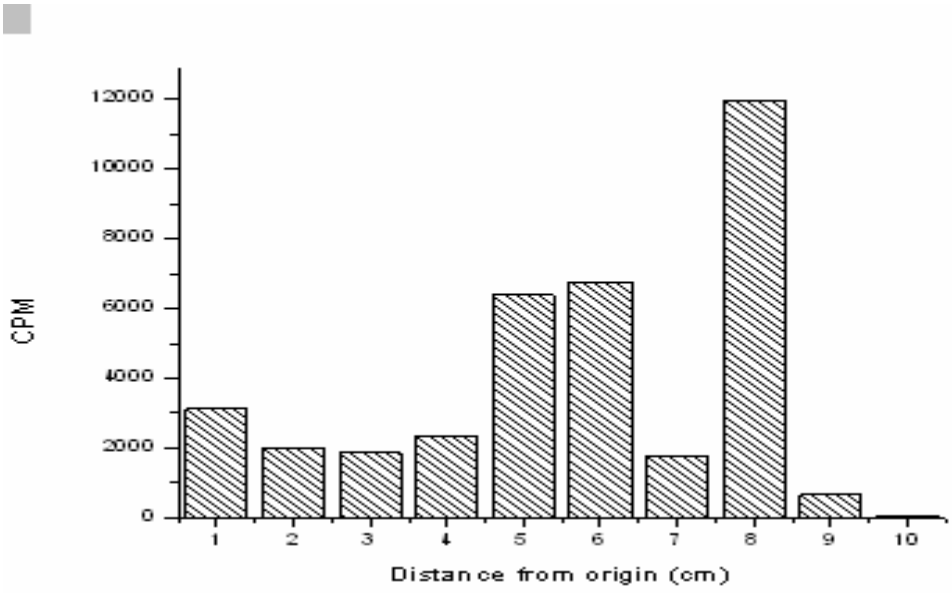

Fig. 4.II.2.b. *Radio-TLC pattern of radio-fluorinated NITTP (10mg) at 110˚C for 15 min*

It was observed that much longer reflux time generating significant amount of an un-characterized labeled polar byproduct which may originate from the reaction of [^{18}F]FMISO with excess of NITTP or its hydrolyzed product, 1-(2'-nitro-1'-imidazolyl)-2,3-propanediol.This observation is in agreement with the observations reported by Lim et al.[153]. So, hydrolysis at a temperature of 125˚C for 3 min with 1N hydrochloric acid was considered as the optimum. Setting the reaction parameters at an elevated temperature with shorter duration has profound effect on the total synthesis time. Adapting these new optimized reaction conditions, the total synthesis time was reduced to 32±1 min from the earlier reported value of 40±1 min [156], minimizing the radioactive decay losses. To my best knowledge, this is the fastest fully automated synthesis procedure of [^{18}F]FMISO so far reported. Alkali hydrolysis generally gives the opportunity to be performed at room temperature helping in reducing the total synthesis time further. With the aim to reduce further the total synthesis time, alkali hydrolysis was tested out but with expected failure as the electronegativity of the ^{18}F and the oxygen atom holding tetrahydropyran (THP) were not sufficient enough to create the nucleophilic centre on the carbon atom to be attacked by OH^- . Even if there was evidence of formation of radio labeled thermally degraded products, [^{18}F]FMISO obtained after single neutral alumina column purification was free of any radioactive as well as cold impurity as confirmed by HPLC [**Fig.4.II.5.**] **.**

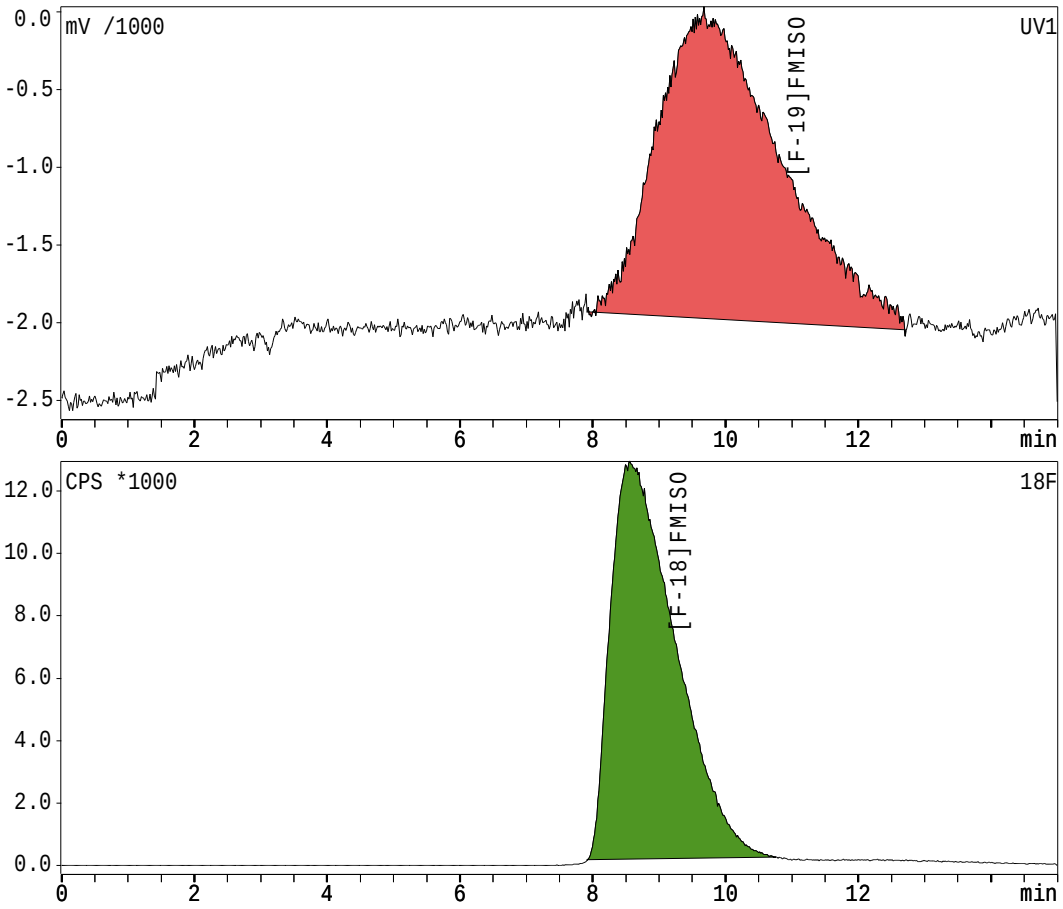

Fig. 4.II.5. *HPLC Chromatogram of [^{18}F]FMISO doped with reference standard FMISO, [^{18}F] FMISO Peak (green): 8.58 min , Reference Standard FMISO peak (red): 9.7 min*

4.II.4. Conclusion

The fully automated radiosynthesis procedure for the synthesis of [^{18}F]FMISO starting form the tosylate precursor, NITTP and single neutral alumina column purification within the shortest synthesis time of 32±1 min with considerable good yield of 48.4±1.18% (without decay correction) in a module configured for [^{18}F]FDG production was optimized. Starting with 10 mg

NITTP, radiofluorination at 145˚C for 3 minutes followed by acid hydrolysis for 3 minutes at 125˚C emerged out as the optimized conditions assuring the maximum yield. The duration of radiofluorination as well as hydrolysis was responsible for the thermal degradation of the [^{18}F] fluorinated intermediate **2**, not the temperature within the investigated range. Even if, there was evidence of formation of a little bit thermally degraded product at the optimized condition, the single neutral alumina column purification was adequate enough to remove all the radioactive as well as non-radioactive impurities. The synthesis procedure is very simple, fast, reliable and very similar to [^{18}F]FDG synthesis procedure with consistent radiochemical yield. This new radiosynthesis procedure can easily be implemented in a regular [^{18}F]FDG synthesis module without the need for additional automation for the HPLC purification.

CHAPTER 5

Simple, column purification technique for the fully automated radiosynthesis of [^{18}F]Fluoroazomycinarabinoside ([^{18}F]FAZA)

5.1. Introduction

In non-invasive molecular imaging of cancer, one of the current major goals is the prediction of the fractional hypoxic volume in a tumour, i.e. the portion of hypoxic cells within a solid tumor[136]. In both rodent and human tumors, hypoxic cells are known to be more than three fold resistant than those with normal oxygenation levels [124,126]. It is also strongly believed that hypoxia is linked with malignant progression leading to increased invasive potential and metastasis [162]. Thus the identification and quantification of tumor tissue hypoxia may have a significant influence on individual treatment planning and monitoring as well as predicting prognosis [163]. Radiolabeled 2-nitroimidazole was proposed for non-invasive hypoxia imaging by Chapman[164, 128]. ^{18}F-labeled fluoromisonidazole (1H-1-(3-[^{18}F]fluoro-2-hydroxypropyl)-2-nitroimidazole), ([^{18}F]FMISO) is an established positron emission tomography (PET) radiopharmaceutical for detecting tissue hypoxia and currently widely used for the purpose and has also been produced by our centre as discussed in Chapter-4-I and Chapter-4-II [131, 165]. The tracer's primary cellular uptake results from diffusion and partition based retention in hypoxic tissues and in lipophilic tissues such as brain [166]. The azomycin nucleosides were developed as highly diffusible but less lipophilic radiotracers in order to reduce partition-based uptake. The most well known example of this class is 1-(5-[^{123}I]iodo-5-deoxy-α-D-arabinofuranosyl)-2-nitroimidazole ([^{123}I]IAZA) [167,168]. For PET application, 1-(5-[^{18}F]fluoro-5'-deoxy-α-D-arabinofuranosyl)-2-ntroimidazole ([^{18}F]FAZA) was developed [169]. The value of [^{18}F]FAZA as a

new class of PET tracer for tumor hypoxia imaging is demonstrated by animal studies [170, 171]. Sorger et al. [172] methodically compared the uptake of [^{18}F]FAZA with the established tracer [^{18}F]FMISO both *in vitro* and *in vivo* and demonstrated the superiority of the former for the visualization of tumor hypoxia. Routine clinical studies with any radiotracer requires a ready and consistent supply, which requires a reliable fully automated synthesis procedure with short production time and consistent high yield. The originally reported method for the synthesis of [^{18}F]FAZA is lengthy, since it requires semi preparative HPLC purification, and gives yields of about ~12% [173], which is low. No reported procedure till date is available for the fully automated radiosynthesis of [^{18}F]FAZA by non-HLPC column purification.

2-deoxy-2-[^{18}F]fluoro-D-glucose ([^{18}F]FDG) is routinely prepared, worldwide, by nucleophilic fluorination of the mannose triflate precursor followed by either acid or alkali hydrolysis to remove the protective acetyl groups. [^{18}F]FDG is purified from the reaction mixture using a series of Sep-Paks containing cation exchanger, anion exchanger, neutral alumina and reverse phase resin respectively or with the same in a combination column [61,174 -176].This played a major role in simplifying the automated production of [^{18}F]FDG. As shown in **Scheme 5.1**, the synthesis of [^{18}F]FAZA from its precursor is very similar to [^{18}F]FDG synthesis by alkali hydrolysis procedure except for the temperature and duration of radiofluorination and hydrolysis step. Since, the blocking of the hydroxyl groups (-OH) of the ribose is by acetyl groups in the [^{18}F]FAZA-precursor, it is expected that the by products generated will be from the hydrolyzed acetyl groups. Hence, the suitability of using a combination column in the purification step in the [^{18}F]FAZA synthesis was tested, starting from the FAZA precursor, 1-(2,3–di-*O*-acetyl-5-*O*-tosyl-α-D-arabinofuranosyl)-2-nitroimidazole (**Scheme 5.1**)[177]. The combination column consists of cation exchanger, anion exchanger, neutral alumina and reverse phase resin, and is

commercially available as Chromabond® Set V (FDG-Base-Hydr). Analysis of radioactive and non-radioactive impurities in the product was carried out. The aim of the study was to observe if the automated radiosynthesis procedure could be readily implemented in any [^{18}F]FDG synthesis module.

5. 2. Materials & Methods

5.2.1. Reagents and apparatus

FAZA precursor, FAZA standard, $TBAHCO_3$ solution (75 mM), molecular-grade anhydrous acetonitrile, ^{18}F trapping column (PS-HCO_3) and Chromabond® Set V (FDG-base-hydr), 10% NaCl, 1.0 M NaH_2PO_4 , sterile and pyrogen-free water for injection and pharmaceutical grade ethanol were procured from ABX, Advanced Biochemical Compounds, Germany. Di-methyl sulfoxide (DMSO), sodium hydroxide pellets (NaOH) were obtained from Aldrich, USA. Evacuated 10 ml vials certified for sterility and pyrogen free were obtained from ACILA AG, Germany. Minisart 0.2μ filters were purchased from Sartorius. Sterility testing was carried out in-house using standard approved protocol. Pyrogen testing was done by LAL test using Endosafe Reagent Kits from Charles River Laboratory, USA (US License No. 1197). Radioactivity was measured using a calibrated ion chamber (Capintec CRC-15R). All other chemicals used were of HPLC and AR grade. The Chromabond® Set V from ABX, is composed of cation exchanger (PS-H^+, 920mg), anion exchanger (PS-HCO_3, 910 mg), neutral alumina (ALOX N, 1520 mg) and reverse phase (HR-P, 680 mg). The columns were conditioned first by passing 20 ml ethanol followed by 100 ml of sterile and bacterial endotoxin free water before use.

HPLC analysis using a C-18 reverse phase analytical column (LIChroCART® 250-4, HPLC cartridge, LIChrospher® 100, RP-18, 5 μm) was done on a Knauer HPLC system equipped with a

radiometric detector followed by a variable wavelength UV detector. Radiochemical purity was also evaluated by thin layer chromatography (Silica gel 60, Merck) using a RayTest TLC scanner (Model No. BGO-V-Detector) and GINA® software provided with the scanner.

Analysis of the decayed samples of [^{18}F]FAZA for identifying the presence of non- radioactive impurities was carried out in JASCO V-530 UV/VIS SPECTROPHOTOMETER, Synergy HT ELIZA PLATE READER (200-600 nm) and Nano Drop® ND-1000 Spectrophotometer.

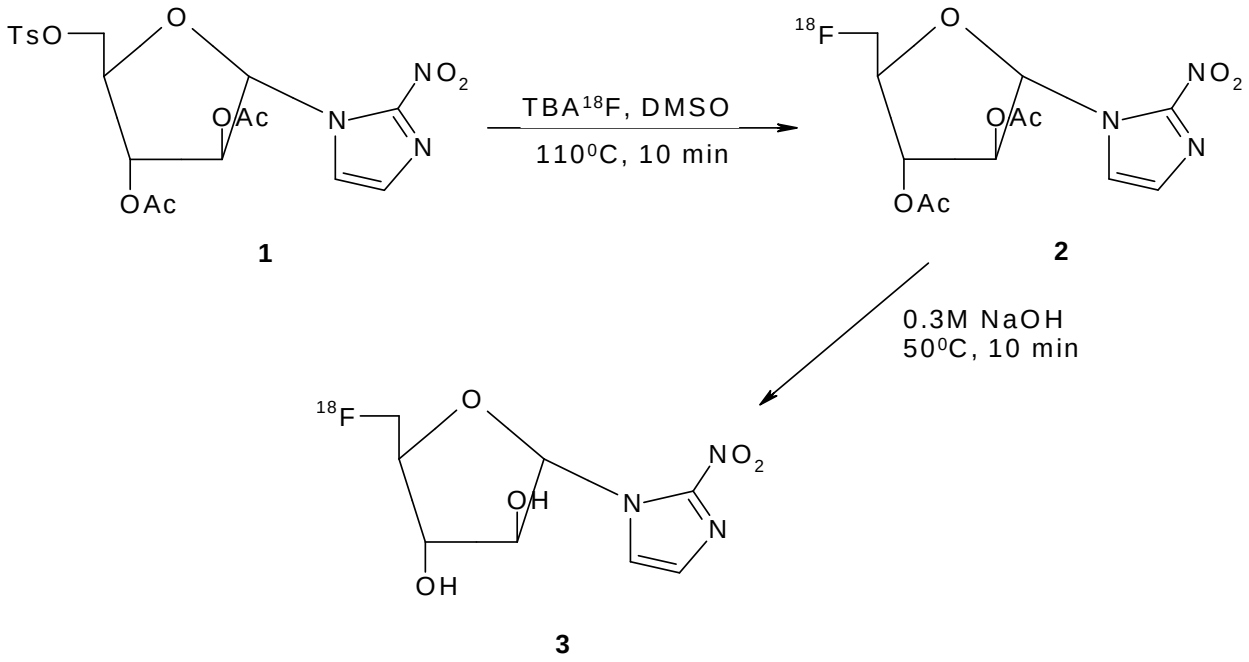

1

2

3

1. 1- (2,3-di-O-acetyl-5-O-tosyl-alpha-D -arabinofuranosyl)-2-nitroimidazole
2. 1- (2,3-di-O-acetyl-5-[^{18}F]-fluoro-5-deoxy-alpha-D-arabinofyranosyl)-2-nitroimidazole
3. 1-(5-[^{18}F]-fluoro-5-deoxy-alpha-D - arabinofuranosyl)-2-nitroimidazole **([^{18}F]FAZA)**

Scheme 5.1. *Schematic representation of synthesis of [^{18}F]FAZA starting from 1-(2,3–di-O-acetyl-5-O-tosyl-α-D-arabinofuranosyl)-2-nitroimidazole*

5.2.2. Automated Radiosynthesis of [^{18}F]FAZA

Radiofluorination and conversion of the FAZA precursor to [^{18}F]FAZA was carried out in a Nuclear Interface Module (Munster, Germany) configured for general-purpose fluorination like that of GE TRACERlab FX_{FDG} and extensively used for [^{18}F]FDG synthesis as described in Chapter 2 . The steps in the fully automated radiosynthesis of [^{18}F]FAZA are summarized in **Table 5.1**. Finally the synthesized [^{18}F]FAZA in buffered saline was sent to an automated dispensing unit and dispensed into vials in a class 100 environment through a 0.2μ filter. The radiochemical yield was expressed as the percentage of radioactivity finally obtained as [^{18}F]FAZA compared with the ^{18}F activity used without applying correction for radioactive decay during the synthesis. In order to determine the R_f value of the [^{18}F] fluorinated intermediate **2** (**2**, according to scheme 5.1), the reaction is terminated after the radio fluorination step and the reaction mixture is analyzed by radio-TLC.

5. 2.3. Quality Control

The synthesized [^{18}F]FAZA was checked for clarity, colour and presence of any suspended particle. The pH was checked with broad (0-14) and narrow (4-8) range pH test paper strip. The radiochemical purity was first checked by radio-TLC followed by analytical HPLC. Twenty-five μl of the test solution was injected into the HPLC column and the eluate was monitored for UV (λ = 254 nm) absorbance as well as radioactivity. The mobile phase for eluting consisted of 70% MeOH (solvent A) and 30% Water (solvent B) with 0.5ml/min flow rate in an isocratic system. The presence of non-radioactive impurities was also checked under the same HPLC conditions. Finally [^{18}F]FAZA prepared was confirmed by comparing the retention time of the UV peak of reference standard FAZA with the radioactive peak of the test solution.

Thin layer chromatography using acetonitrile/water (95:5) as the mobile phase was also done and the radiochromatogram acquired and analyzed.

5.2.4. Sterility and Bacterial Endotoxin Tests

Sterility tests were performed in accordance with the Indian Pharmacopoeia, 1996 and addendum 2005 protocol. In this test, 1 ml of the [^{18}F]FAZA sample after radioactive decay was inoculated in fluid thioglycollate medium at 37°C for 14 days to observe the growth of aerobic and anaerobic bacteria. Similarly, 1 ml of the [^{18}F]FAZA sample after radioactive decay was also inoculated in soyabean casein digest medium at 22-25°C for 14 days to detect fungal growth.

The bacterial endotoxin test was performed in accordance with USP XXV. The test was based on the formation of gel clot in the sample by Limulus Amoebocyte Lysate (Sensitivity: 0.125 EU/ml) reagent.

Table 5.1. Flow chart of [^{18}F]FAZA radiosynthesis scheme

Step I: Nucleophilic fluorination of the FAZA precursor i) [^{18}F] fluoride trapped on a Chromafix 45-PS-HCO_3 anion exchange cartridge ii) [^{18}F] fluoride eluted from the column using 75mM $TBAHCO_3$ (0.5 ml, Vial V5) to the reaction vessel iii) Tetrabutyl ammonium fluoride [^{18}F] dried by azeotropic distillation with acetonitrile (1.0 ml, Vial V1) iv) FAZA precursor (10 mg) dissolved in DMSO (1.0 ml, Vial V2) added to the reaction vessel. v) S_N2 fluorination reaction carried out at 110°C for 10 minutes
Step II: Deprotection i) The reaction mixture was cooled to 50°C ii) 0.3 M NaOH (1ml, Vial V3) was added to the reaction vessel. iii) Base hydrolysis carried out at 50°C for 10 minutes iv) Reaction mixture was cooled to 40°C
Step III: Purification through CHROMABOND® SET V Column i) The reaction mixture was passed through the CHROMABOND® SET V Column ii) The reaction vessel was rinsed with 80% ethanol (2.0ml, Vial V4) and the column was first washed with this solvent. iii) [^{18}F]FAZA was eluted using 15% ethanol (12ml, Vial V6) and is collected in the product vial containing 10% NaCl (1.7ml) and 1M NaH_2PO_4 (0.7ml)

5.2.5. Analysis of non-radioactive impurities

The presence of non-radioactive toxic impurities in the final [^{18}F]FAZA product, is checked by analyzing the samples after radioactive decay using UV-Visible spectroscopy. The samples were scanned over 200-700 nm where the absorbance from the probable impurities are expected. It

was further validated by the absorption spectrum obtained using Synergy HT ELIZA PLATE READER (200-600 nm).

5.2.6. PET Imaging Studies

The bio-distribution of [^{18}F]FAZA in normal healthy rabbits was studied with the GE Advance PET scanner system. The rabbits weighing approximately 2.5 Kg, were maintained on our animal house and fed standard animal house diet. The animals were administered [^{18}F]FAZA (~ 185 MBq / 2.0 ml) intravenously through the ear vein. The images were acquired 150 minutes post injection after standard anesthesia procedure. Approval from BARC Animal Ethics Committee was taken for the animal studies.

5.3. Results and Discussion

Starting from the precursor, 1-(2,3–di-*O*-acetyl-5-*O*-tosyl-α-D-arabinofuranosyl)-2-nitroimidazole, [^{18}F]FAZA was synthesized and purified by passing the reaction mixture through a properly conditioned commercially available combination column, Chromabond® Set V [**Fig. 5.1.**]. The radiochemical yield (without decay correction) was 21.98 ± 1.40 % (**Table. 5.2.**). The synthesized [^{18}F]FAZA was clear, colourless and free of any suspended or colloidal particle and had a pH between 6.5 to 7.0. Prior to hydrolysis, the radio-TLC of the radio-fluorinated precursor in 95:5: MeCN: H_2O solvent showed free $^{18}F^-$ peak at an R_f (max) of 0.01 (peak area 25.2%) whereas the radio-fluorinated precursor peaked at R_f of 0.7 (peak area 54.8%) [**Fig. 5.2.**]. The TLC of the final purified [^{18}F]FAZA showed a very prominent peak at R_f (max) of 0.47 [**Fig.5.3.a.**]. The R_f value of [^{18}F]FAZA was further verified by TLC of the reference standard FAZA in the same solvent system and then staining with iodine vapour [**Fig. 5. 3. b.**].

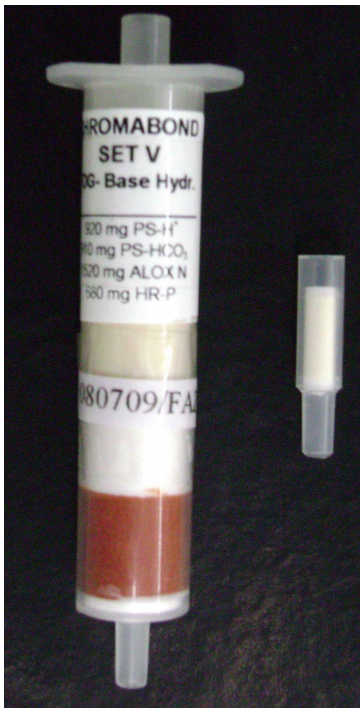

Fig.5.1. *CHROMABOND® SET V Combination Purification and ^{18}F trapping columns*

Table 5.2. Radiochemical yield of [^{18}F]FAZA

S. No	^{18}F in the reaction vessel (MBq)	[^{18}F]FAZA produced (MBq)	% Yield*
1	4588	943.5	20.56
2	4070	895.4	22.00
3	5920	1313.5	22.06
4	2368	573.5	24.22
5	3700	777.0	21.00

* Without decay correction

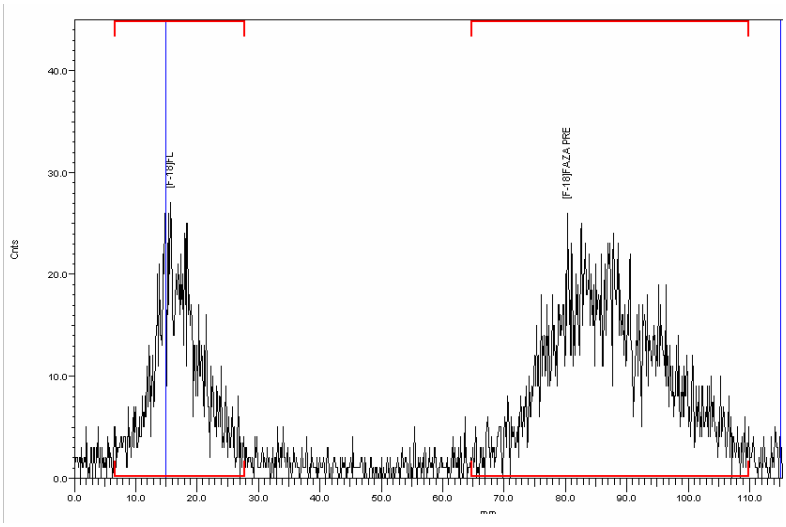

Fig.5.2. *Radio TLC of the radio fluorinated reaction mixture of FAZA precursor, Solvent: 95/5. (MeCN/H_2O). Free fluoride comes at point of spot (R_f of 0.01, peak area 25.2%), [^{18}F]-Fluorinated Intermediate 2 (2, according to scheme 1) comes with an R_f of 0.72 (peak area: 54.8%)*

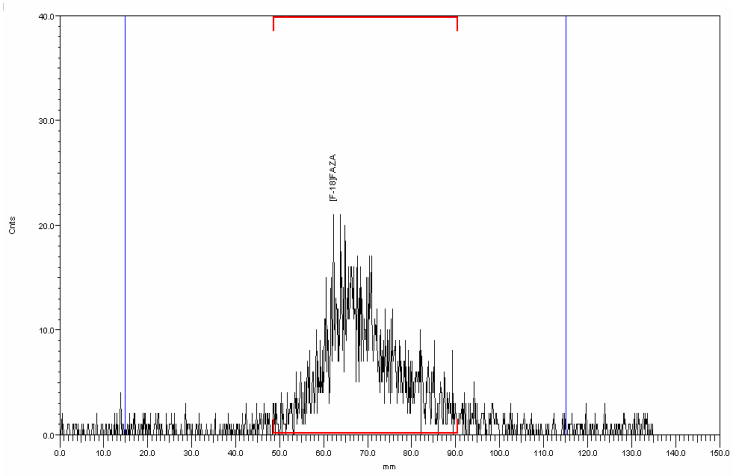

Fig.5.3.a. *TLC of [^{18}F] FAZA in MeCN: H_2O (95:5), R_f value of [^{18}F] FAZA: 0.47*

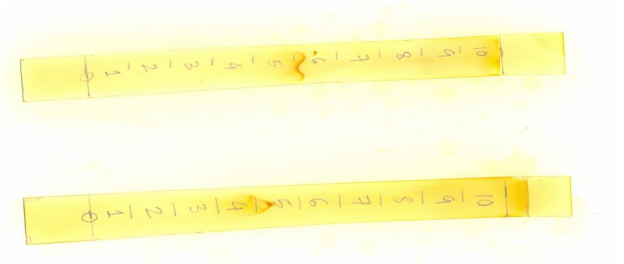

Fig.5.3.b. *TLC of reference standard FAZA in MeCN: H_2O (95:5) Coloured by iodine vapour, R_f (range): 0.45-0.55*

The HPLC chromatogram of the synthesized [^{18}F]FAZA doped with reference standard FAZA is shown in **Fig. 5.4**. From this figure it is observed that the radiochromatogram displays single radioactive peak at 8.83 min, and a single UV peak at 10.45 min. The difference in the retention times of the radioactivity peak and UV peak is due to the dead volume of the tubing connecting the lead-shielded radioactivity detector attached externally, to the UV detector in the HPLC.

The UV component at 10.45 min corresponds to reference standard FAZA as confirmed by HPLC separately [**Fig.5.5.**]. The co-elution of the radioactivity peak along with the UV peak of the reference standard FAZA confirmed that the single radioactive peak corresponds to [^{18}F]FAZA. The presence of UV active non-radioactive impurities was also examined.

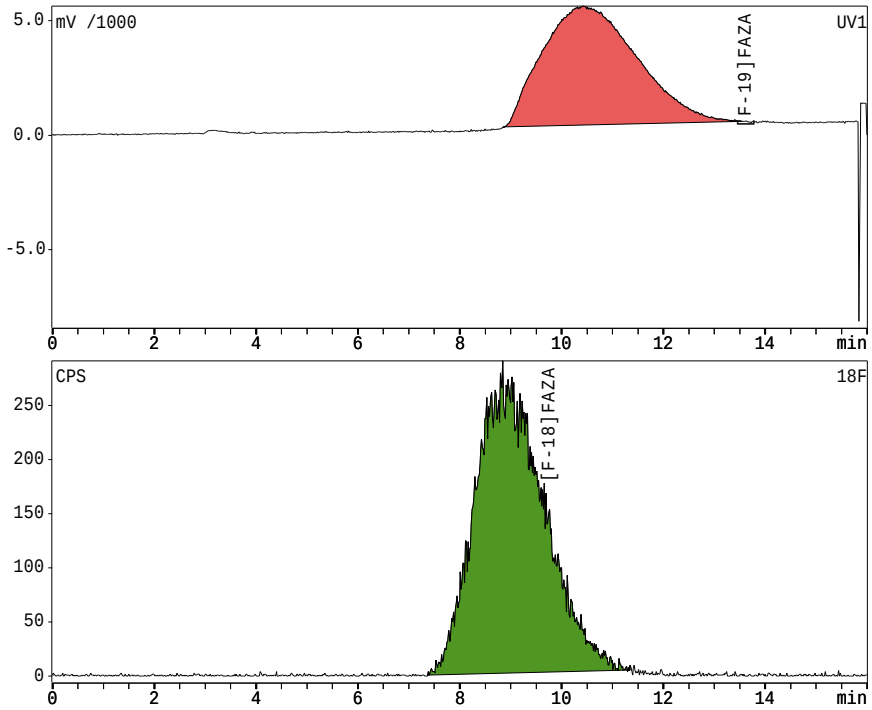

Fig.5.4. *HPLC chromatogram of [^{18}F]FAZA doped with reference standard FAZA (Green peak = [^{18}F]FAZA, Red peak = Reference standard FAZA)*

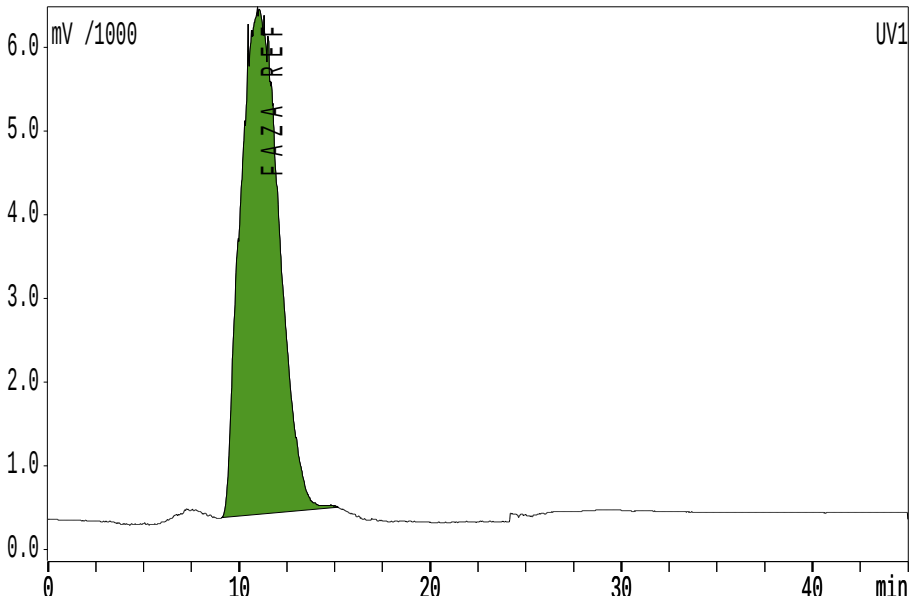

Fig.5.5. *HPLC chromatogram of reference standard FAZA (UV, λ = 254 nm)*

The precursor of FAZA shows a retention time of 17.57 min under identical HPLC conditions. Any other UV peak except the peak of the reference standard FAZA was observed. So, it may be assumed that the synthsized [^{18}F] FAZA is free of any significant non-radioactive impurities. The presence of non-radioactive impurities is further cross checked by analyzing the decayed samples in UV-VIS spectrophotometer over 200-700 nm range [**Fig. 5.6.**]. Now if the spectra are compared, it is very clear that DMSO is the only non-radioactive impurity present in the [^{18}F]FAZA. Since DMSO is a liquid with a boiling point of 189°C and the temperature at which the radiosynthesis is carried out is 110°C, it is logical to expect some vapours of DMSO to be carried forward into the subsequent steps and finally eluted out with [^{18}F]FAZA. From toxicity point of view, DMSO belongs to solvents in Class 3 (Solvents with Low Toxic Potential) according to the European Agency for the Evaluation of Medicinal Products (EMEA 2000) and the acceptable limit as residual solvent is 5000 ppm or higher [178].

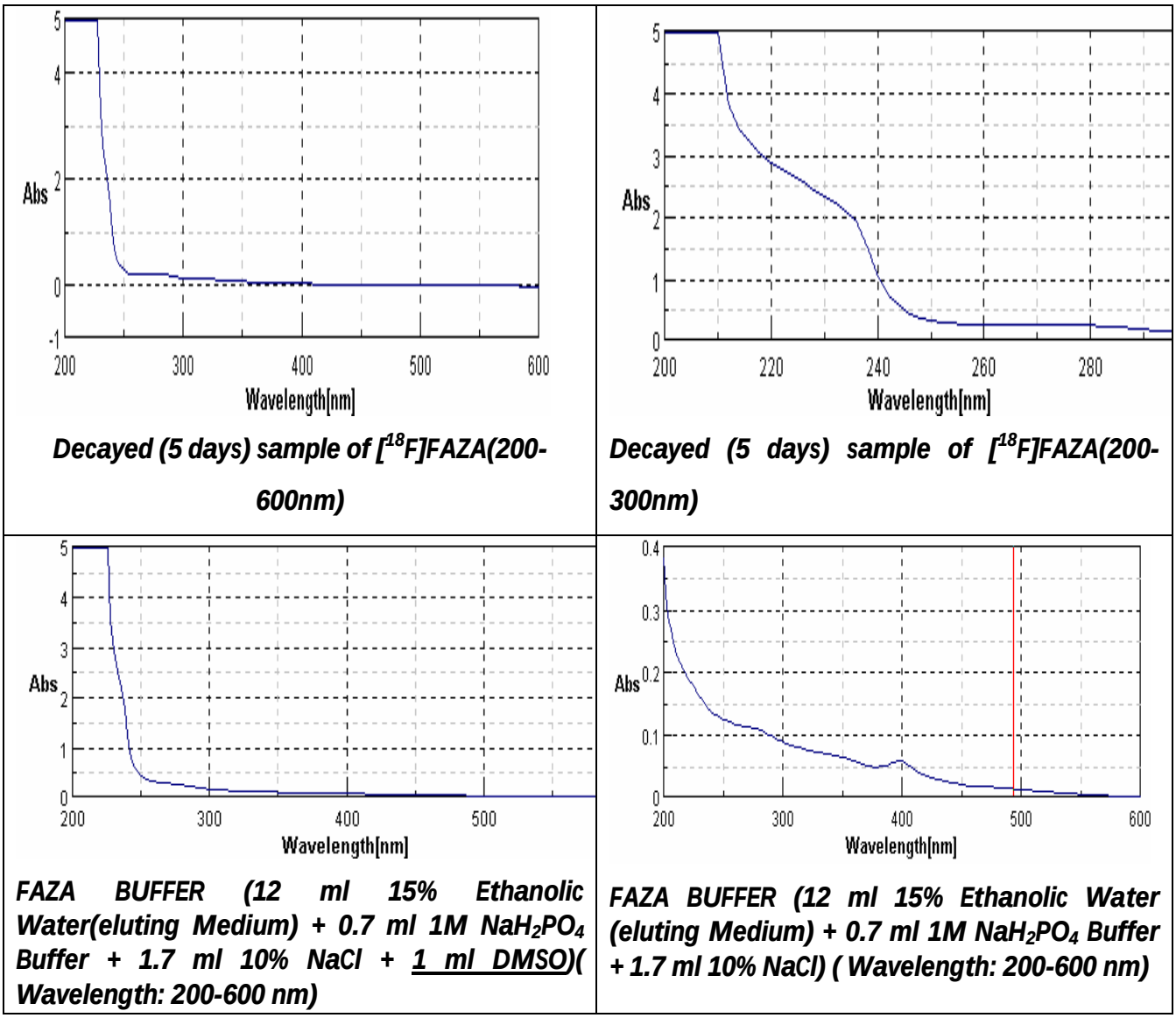

Decayed (5 days) sample of [^{18}F]FAZA(200-600nm)

Decayed (5 days) sample of [^{18}F]FAZA(200-300nm)

FAZA BUFFER (12 ml 15% Ethanolic Water(eluting Medium) + 0.7 ml 1M NaH_2PO_4 Buffer + 1.7 ml 10% NaCl + 1 ml DMSO)(Wavelength: 200-600 nm)

FAZA BUFFER (12 ml 15% Ethanolic Water (eluting Medium) + 0.7 ml 1M NaH_2PO_4 Buffer + 1.7 ml 10% NaCl) (Wavelength: 200-600 nm)

Fig.5.6. *UV-VIS spectra (200-600 nm)*

The LD_{50} in rats (orally administered DMSO) is also very high (14,500 mg/kg). The experiment was repeated with Synergy PLATE READER (200-600 nm) [**Fig.5.7.**] and the spectra look identical. The purification of [^{18}F]FAZA using the same column used for FDG base hydrolysis procedure is successful mainly because of the very simple structure of the FAZA precursor and most importantly

the blocking groups are also identical as in the FDG precursor, mannose triflate. Further, the C-N bond linking the arabinofuranosyl moiety to the nitroimaidazole group is not broken under the

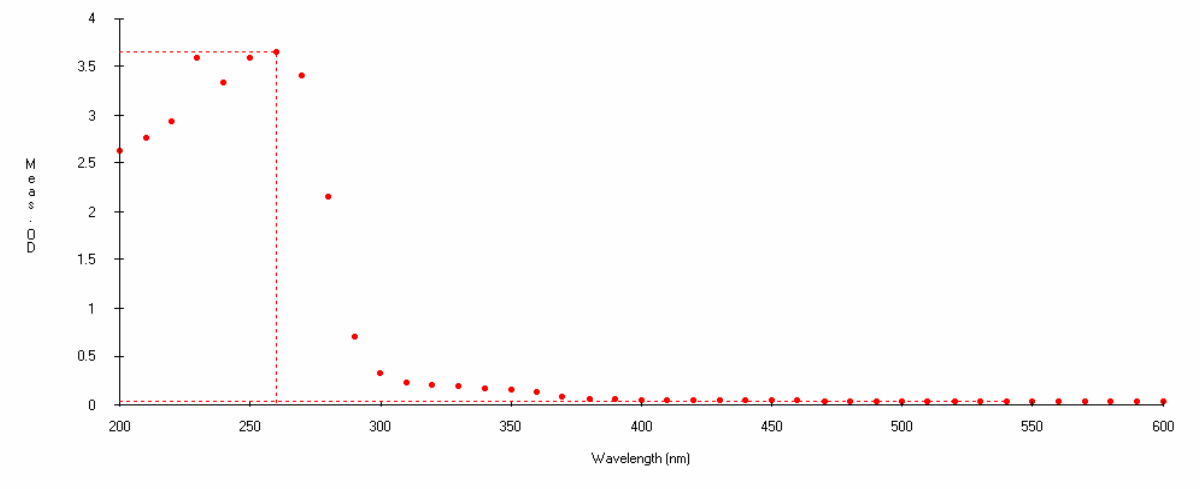

FAZA BUFFER (12 ml 15% Ethanolic Water + 1.7 ml 10% NaCl + 0.7 ml 1M NaH_2PO_4 Buffer) +GREINER 96 WELL PLATE (Wavelength Increment by10 nm)

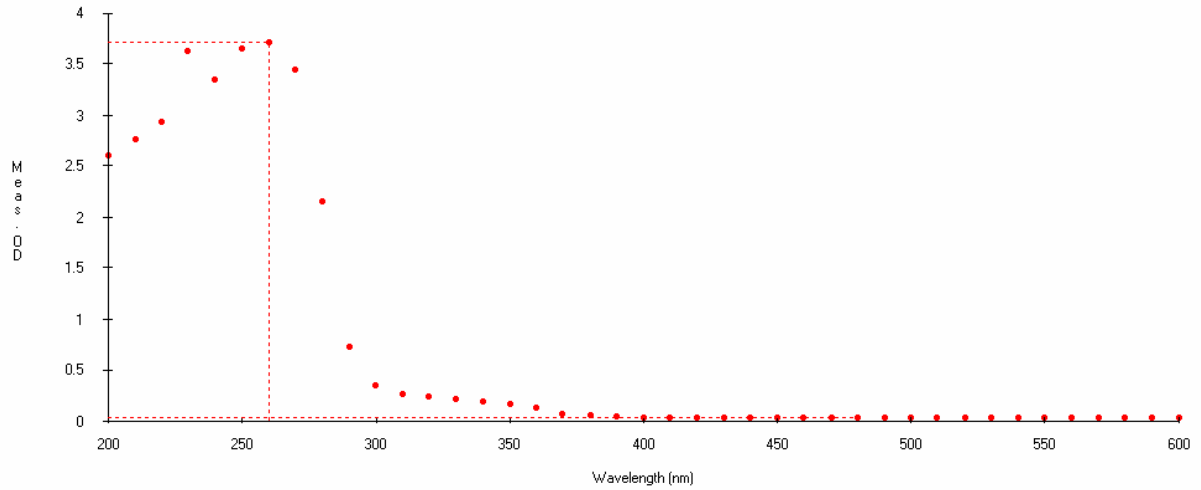

[^{18}F]FAZA DECAYED (5 days) SAMPLE [UV (λ: 200 - 600 nm)] (Increment by 10 nm)

Fig.5.7. *Spectrum of radioactive decayed sample of [^{18}F]FAZA and FAZA buffer*

conditions used, eliminating the possibilities of 5-[^{18}F]-fluoro-5-deoxy-alpha-D-arabinofuranose and 2-nitro imadazole impurities. As in the case of [^{18}F]FDG, the formation of the radiofluorinated but

unhydrolysed product is a possibility, but not detected it on radio-HPLC. Final product sterility was achieved by 0.2 μ filtration. All the trial batches passed the BET tests.

PET images of the bio-distribution of [^{18}F]FAZA in normal rabbits at 150 min post injection is shown in **Fig. 5.8**. The PET image of [^{18}F]FMISO rabbit scan done at our Centre (Chapter 4) is also included for one-to-one comparison. Importantly, the most noticeable difference in the images is that the [^{18}F]FAZA image (150 min post injection) does not show any brain uptake whereas as the [^{18}F]FMISO image shows significant brain uptake (240 min post injeaction). This is as expected and it is to eliminate brain uptake that [^{18}F]FAZA was designed. Additionally, there was no significant bone uptake, which confirms the insignificant free $^{18}F^-$ in the [^{18}F]FAZA preparation as seen in the radio-TLC. It is known that [^{18}F]FAZA clears primarily from rest of the body via renal system reflecting its higher hydrophilic nature. Hence, a high accumulation of radioactivity in kidneys and bladder but very low uptake in liver was observed. In contrast, the excretion of [^{18}F]FMISO, is through the billiary system reflecting its higher lipophilic nature. A high accumulation of radioactivity both in the liver and billiary system [**Fig.5.9.**] in [^{18}F]FMISO rabbit image can be seen.

5.4. Conclusion

A fully automated radiosynthesis procedure for the synthesis of [^{18}F]FAZA starting form the precursor, 1-(2,3–di-*O*-acetyl-5-*O*-tosyl-α-D-arabinofuranosyl)-2-nitroimidazole and single combination purification column is developed. The purification of [^{18}F]FAZA using the same column used for the base hydrolysis procedure for [^{18}F]FDG is successful mainly because of the very simple structure of the FAZA precursor and most importantly the blocking groups are also identical as in mannose triflate, the FDG precursor. The radiochemical purity is more than 95%

and the synthesized [^{18}F]FAZA is free of any non-radioactive impurity. Further, we could do this in a module configured for FDG synthesis with considerable yield of 21.98 ± 1.40 % (n = 5) without decay correction in 51 ± 1 min. The synthesis procedure is very simple, fast, reliable and very similar to [^{18}F]FDG synthesis procedure with consistent radiochemical yield. This new radiosynthesis procedure can easily be implemented in any regular [^{18}F]FDG synthesis module.

Fig.5.8. *[^{18}F]FAZA PET scan of rabbit, 150 minute post injection*

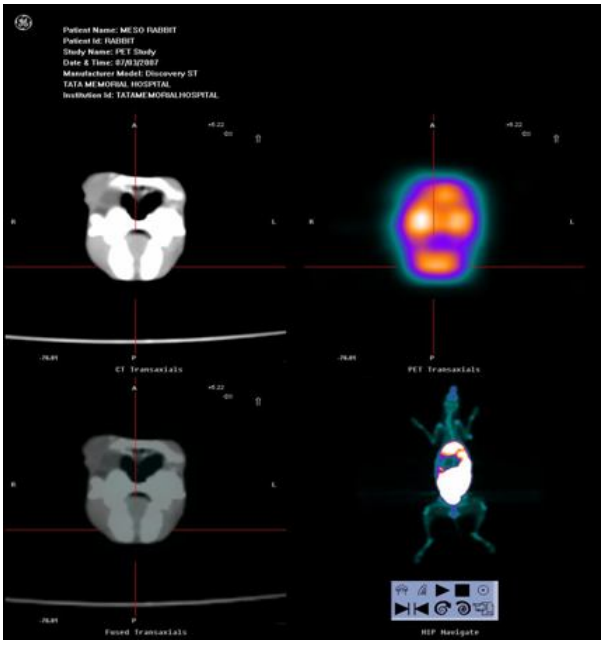

Fig.5.9. *[^{18}F]FMISO rabbit PET scan (240 minutes post injection) showing considerable brain uptake and accumulation of radioactivity in the hepatobiliary system*

CHAPTER 6

Development of cartridge purification based, simple, fully automated radiosynthesis procedure for the production of 3´-Deoxy-3´-[^{18}F] Fluorothymidine ([^{18}F]FLT)

6.1. Introduction

2-deoxy-2-[^{18}F]fluorodeoxyglucose ([^{18}F]FDG) is by far the most widely used positron emitting tomography (PET) radiopharmaceutical in clinical oncology. Over the last two decades this agent has proven to be an almost universally applicable imaging agent in oncology [179]. The growth of [^{18}F]FDG in clinical oncology has resulted from a combination of clinical demand, based on its accepted value in the detection and assessment of cancer and wide spread availability. The advent of clinical instruments that combine PET Imaging with X-ray tomography scans (PET-CT) has added additional impetus for the growth of [^{18}F]FDG PET Imaging. Modern PET-CT instrumentation allows fused images that provide an exquisite combination of anatomical and functional information.

Notwithstanding the widespread use of [^{18}F]FDG and its accepted utility in tumor imaging, there are some limitations in several clinical conditions and, hence, there are research efforts to identify additional PET tracers for oncology. With the power of [^{18}F]FDG PET in oncology, one might ask why there is a need to expend effort to find additional agents. We can identify two incentives that encourage the search for novel PET tracers. The limitations of [^{18}F]FDG in tumor imaging include [180];

(i) Normal uptake of [^{18}F]FDG in metabolically active tissues including the brain makes tumors in or near these structures difficult to evaluate.

(ii) Tumors that are slow growing or highly differentiated often do not take up [^{18}F]FDG adequately to permit definitive imaging. This has been noted with prostate tumors and with a number of neuroendocrine tumors [181-183].

(iii) [^{18}F]FDG is excreted through the kidneys and urinary bladder making tumors in these organs hard to assess. This also complicates attempts to image prostate tumors.

(iv) A number of hepatocellular carcinomas show relatively low uptake of [^{18}F]FDG related to the levels of cellular transport of the sugar by the GLUT transport system [184] or elimination of [^{18}F]FDG through upregulation of the intracellular glucose-6-phosphate enzyme [185].

(v) [^{18}F]FDG is relative non-specific and also accumulates at sites of inflammation and infection. Although in the proper context this increases the imaging indications for this radiopharmaceutical[186], it can be a significant complication in oncologic imaging in a number of settings including in post surgery assessment of residual tumor where inflammation and or infection are likely to be present [187].

The second limitation of [^{18}F]FDG relates to its restricted applications in the growing field of molecular medicine. Molecular medicine is defined by the National Library of Medicine [188] as "A science that seeks to comprehend disease causes and mechanisms at the molecular level and to apply this basic research to the prevention, diagnosis and treatment of diseases and disorders". Molecular medicine seeks to individualize patient treatment by creating a genetic and molecular profile specific to individual pathological processes in the body at a cellular level, which can

then be used to tailor disease therapy. Molecular imaging using PET is acknowledged to have a valuable role to play in this patient oriented science. In this context [^{18}F]FDG provides some very specific information about cellular dynamics related to energy requirements. The process of cellular transport and metabolism of glucose and [^{18}F]FDG [**Fig.6.1.**] has been extensively studied. [^{18}F]FDG uptake is a measure of tissue and cell glucose utilization (glycolysis). More specifically it can be regarded as a molecular imaging probe of hexose entry into cells mediated by GLUT facilitative transporters as well as an indicator of cellular hexokinase enzyme activity. Gene mediated regulation of GLUT transporters and

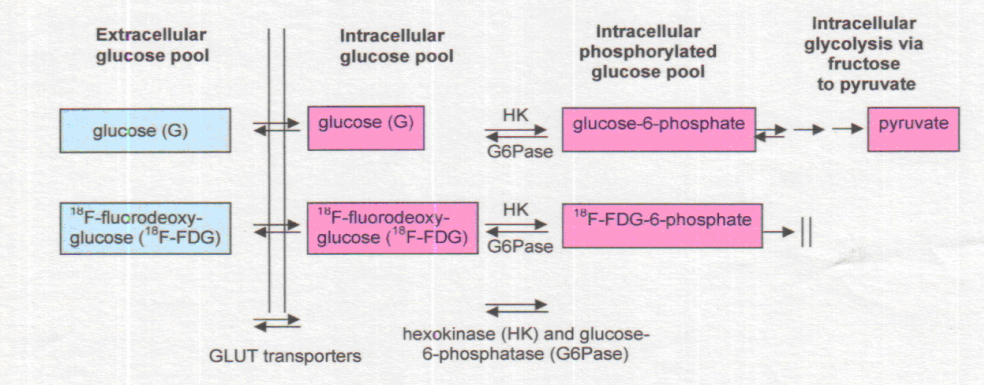

Fig. 6.1. *The transport and metabolism of glucose and 2-deoxy-2-^{18}F-Fluoro-D-glucose*

hexokinase activity contributes to the increased accumulation of [^{18}F]FDG in tumor cells relative to normal tissues. An important distinction must be made between the behaviour of [^{18}F]FDG and glucose at the cellular level. [^{18}F]FDG is metabolically trapped after phosphorylation to [^{18}F]-FDG-6-phosphate. Unlike glucose it is not a substrate for the subsequent enzymatic conversion to fructose-6-phosphate by phosphohexose isomerase and thus does not further participate in the glycolytic pathway. Subtle differences between glucose and [^{18}F]FDG may also be expected when they are transported by GLUTs and phosphorylated by hexokinase. [^{18}F]FDG

must be regarded as a surrogate marker for glucose although for some processes (transport and phosphorylation), the two molecules have very similar behaviour.

There are many molecular targets relevant to cancer that are not measured or assessed by [^{18}F]FDG. Several recent reviews have addressed this issue [189, 190]. One of the special class is the labeled nucleoside analogs for measurement of cellular nucleic acid utilization and cell proliferation.

6.2. [^{18}F]FLT as an Imaging probe for cellular proliferation

Cell proliferation requires the expansion of nucleic acid content in the cell prior to division. This is accomplished by the transport of nucleosides or their de novo synthesis as building blocks of DNA. Thymidine is a recognized marker for cell proliferation being moved into cells by the nucleoside transport system and being rapidly incorporated into DNA. Additionally thymidine, unlike the other three-nucleosides building blocks is incorporated into DNA but not into RNA making it an accurate probe for DNA replication. ^{11}C-thymidine was first described as an *in vivo* marker of DNA synthesis in 1972 [191] and it has been used sporadically as a clinical measure of cell proliferation. Because it is modified only by the substitution of ^{11}C for ^{12}C it will behave identically to the native nucleoside [192]. The major problems encountered with ^{11}C-thymidine relate to the short half-life of ^{11}C and to the catabolism of thymidine, mediated by the enzyme thymidine phosphorylase, leading to the production of ^{11}C-labeled metabolites [**Fig. 6.2.**].

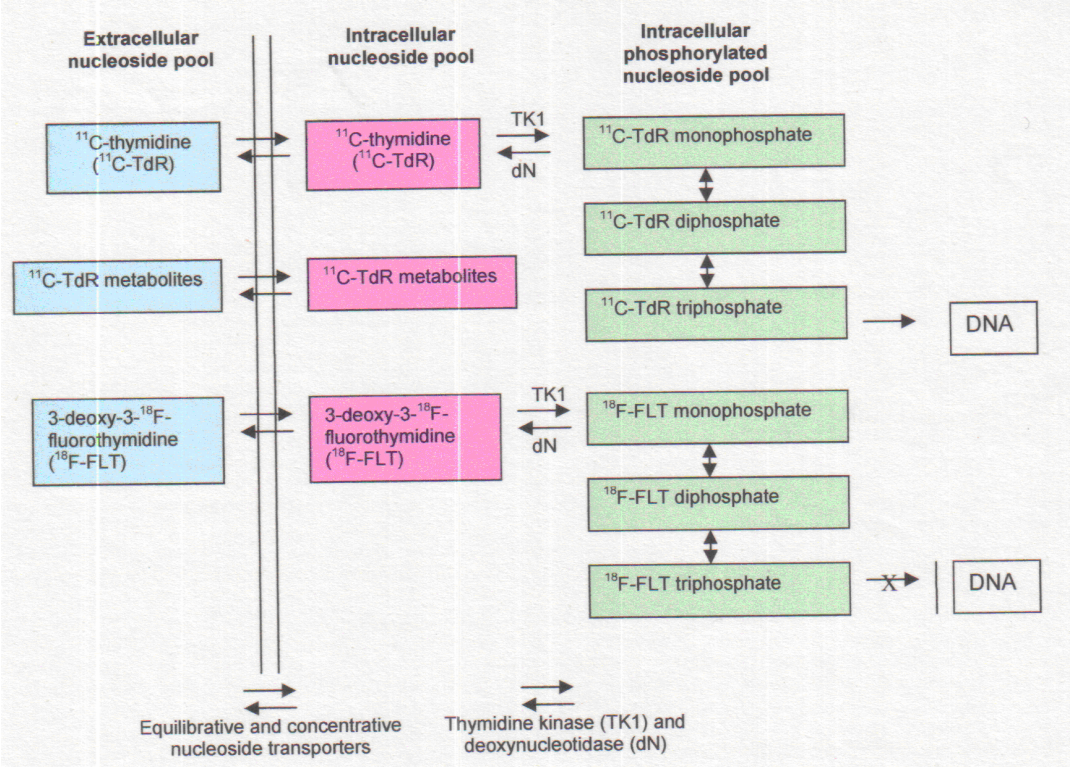

Fig. 6.2. *The transport and cellular utilization of thymidine and 3'-deoxy- 3'-[^{18}F]fluorothymidine ([^{18}F]FLT)*

The most promising ^{18}F-fluorinated analogue of thymidine, 3'-deoxy-3'-[^{18}F]fluorothymidine ([^{18}F]FLT), has eliminated some of the problems encountered with ^{11}C-labeled nucleoside analogs by having a longer radionuclide half-life and by not being a substrate for enzymatic catabolism [193-196]. FLT, unlike thymidine, is not measurably incorporated into DNA. FLT uses the nucleoside transport system and is a substrate for thymidine kinase (TK) but very little of the FLT-phosphate pool becomes incorporated into DNA [197]. Despite the trapping of FLT at the phosphate stage a number of studies have shown that [^{18}F]FLT accumulation in tissue corresponds to the proliferation rate of the tissue [198, 199]. What is actually measured by [^{18}F]FLT uptake into tissues is cellular nucleoside transport and phosphorylation by thymidine kinase with a strong correlation with TK levels in cells [197, 199].

6.3. Challenges of fully automated radiosynthesis of [^{18}F]FLT

The first report to label FLT with ^{18}F came in 1991 [200], but the radiochemical yield was very low. A considerably improved method was reported by Grierson and Shields [195], but it was found to be very demanding especially regarding the purification of the [^{18}F]fluoride/1-(2-deoxy-3-O-nosyl-5-O-DMT-β-D-*threo*-pentafuranosyl)-3-DMBn-thymine reaction mixture [201]. Martin et al.[202] reported an automated radiosynthesis procedure based on 3-N-BOC-1-[5-O-(4,4'-dimethoxytrityl)-3-O-nosyl-2-deoxy-β-D-lyxofuranosyl] thymine with improved radiochemical yield. This approach was remarkable since it could be easily adapted in an automated synthesis module equipped with a semi-preparative HPLC. Machulla et al.[203] reported a simplified labeling approach for synthesizing [^{18}F]FLT using 2,3'-anhydrothymidine (AThy) and an improved version with the '5' position –OH group protected, viz., 5'-O-(4,4'-dimethoxytriphenylmethyl)-2,3'-anhydrothymidine (DMTThy). Inspite of all these attempts, the synthesis of [^{18}F]FLT has remained tedious. The real fact is that the yields in practice are low (5-20%, uncorrected for decay) and all described procedures require time consuming and tricky semi-preparative HPLC purification, not conducive for the routine production of [^{18}F]FLT [204].

The presence of organic solvents often used as the reaction medium like dimethyl sulfoxide (DMSO), acetonitrile (CH_3CN) or N, N'-dimethyl formamide (DMF) etc., and the pH of the reaction mixture to be loaded on to the HPLC column, have a huge influence in the elution and retention time of [^{18}F]FLT. These facts make the purification of [^{18}F]FLT very difficult and in obtaining a sufficiently radio chemically pure product.

The synthesis methods for [^{18}F]FLT reported so far, show a common approach. Semi-preparative HPLC purification is needed only to remove the products resulting from the blocking groups used in the precursor either in the radiofluorination step or in the hydrolysis step. If these

products can be avoided, [^{18}F]FLT synthesis could be achieved with a combination column purification technique very similar to [^{18}F]FDG. A precursor with minimum-blocking groups holds the key to an HPLC-free radiosynthesis procedure.

Guided by this concept, development of a simplified radiosynthesis procedure of [^{18}F] FLT starting with FLT-BOC precursor [**Fig.6.3.**] which, by virtue of it structure is expected to give a high radiochemical yield due to higher level of radiofluorination in comparison to DMTTHy.

The first part of this chapter is a detailed analytical analysis of the radio synthesized [^{18}F]FLT using FLT-BOC precursor and single purification column consisting of neutral alumina and anion exchanger has been attempted [205].

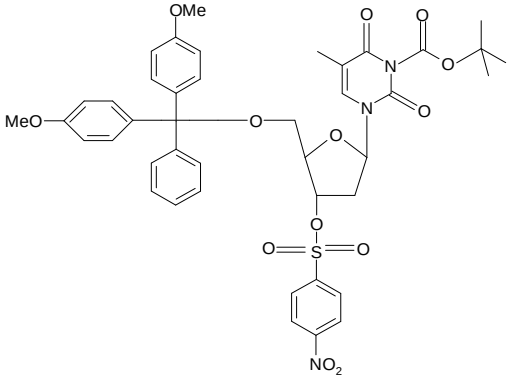

3-N-BOC-1-[5-O-(4, 4'-dimethoxytrityl)-3-O-nosyl-2-deoxy-β-D-lyxofuranosyl] thymine (FLT-BOC Precursor)

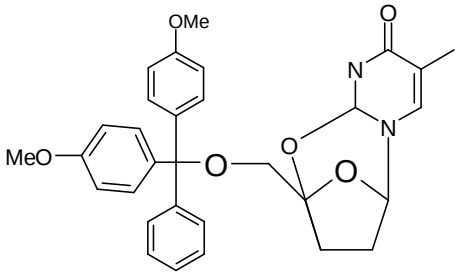

5'-O-(4, 4'-dimethoxytriphenylmethyl)-2, 3'-anhydrothymidine (DMTThy) (FLT anhydro precursor)

Fig.6.3. *Different precursors for [^{18}F]FLT synthesis*

The second part of this chapter describe the details of a fully automated radiosynthesis procedure of [^{18}F]FLT. This fully automated radiosynthesis procedure can be readily implemented in any [^{18}F]FDG synthesis module without the need for additional automation for the HPLC purification and has been developed using the adapted general purpose fluorination module described in details in Chapter 2.

PART-I

Evaluation of the radiochemical impurities arising during the competitive fluorination of nosyl group during the synthesis of 3'-Deoxy-3'-[^{18}F] Fluorothymidine with FLT-BOC precursor and a combination column composed of neutral alumina and anion exchanger

6.I.1.

Introduction

A variety of precursors have been reported for the synthesis of [^{18}F]FLT [195, 200, 202-204] The most commonly used precursor is 3-N-4-butoxycarbonyl-(5'-O-4,4'-dimethoxytriphenylmethyl)-2'-deoxy-3'-O-(4-nitrobenzenesulfonyl)-β-D-threopentofuranosyl) thymine (BOC precursor) (**I**) reported by Yun *et al* [206], though better alternatives and the synthesis of 3'-sulfonyl esters have been reported [204]. The synthetic pathway is summarized in **Scheme 6.I.1.**

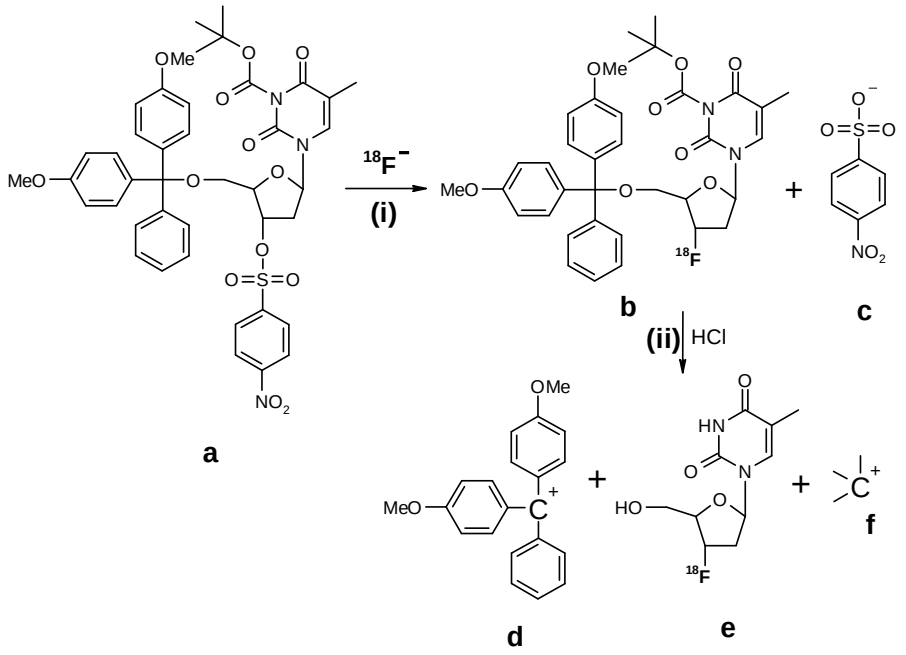

(a) 3-N-Boc-5'-O-Dimethyltrityl-3'-deoxy-3'-O-nosyl-thymidine (BOC precursor)
(b) 3-N-Boc-5'-O-Dimethyltrityl-3'-deoxy-3'-fluorothymidine
(c) Nosylate ion
(d) Dimethoxytrityl cation
(e) 3'-deoxy-3'-fluorothymidine
(f) t-butyl cation

(i) CH_3CN, 130°C, 6 min
(ii) 105°C, 5 min

Scheme 6.I.1. *Schematic representation of synthesis of [^{18}F]FLT from FLT-BOC precursor*

The routine use of [^{18}F]FLT for imaging cell proliferation is restricted by the difficulties in the synthetic procedure. Compared to [^{18}F]FDG, the reaction conditions are more demanding, yield is quite low and final purification of the product is carried out by a cumbersome semi-preparative HPLC. Hence, the automation of the procedure is complicated. The need for a simple column based purification procedure for the synthesis of [^{18}F]FLT is emphasized in this chapter and attempts have been made to produce [^{18}F]FLT without the need for semi-preparative HPLC purification [207]. In an attempt to simplify the synthetic procedure, a simple cartridge (composed of neutral alumina and anion exchanger) based purification step, so that the entire [^{18}F]FLT synthesis can be carried out in a [^{18}F]FDG synthesis module. To evaluate the adequacy of this cartridge based purification, studies have been carried out to identify the presence of the possible

chemical impurities, generated during the synthesis of [^{18}F]FLT starting from the BOC precursor. During the course of our work, there has been a curiosity to evaluate the source of chemical impurities, and their bio-distribution, particularly, if these impurities are labeled with ^{18}F, since they could produce artifacts during PET Imaging.

6.I.2 Materials & Methods

6.I.2. a. Reagents and apparatus

FLT-BOC precursor, Fluorothymidine standard, $TBAHCO_3$ solution (75 mM), molecular-grade anhydrous acetonitrile, 10% NaCl, 1.0 M HCl, 1.0 M NaH_2PO_4 buffer, sterile and pyrogen-free water for injection and pharmaceutical grade ethanol were procured from ABX Advanced Biochemical Compounds, Germany. Nosyl chloride, Dimethoxytrityl chloride and thymidine were obtained from Aldrich, USA. Aluminum oxide (neutral, Activity I-II) was purchased from Merck, India. All other chemicals used were of HPLC and AR grade.

HPLC analysis was carried out using a Knauer HPLC system equipped with a variable wavelength UV detector and a radiometric detector. The analysis was carried out using a C-18 reverse phase analytical column (Nucleosil, 5 μM, 250 x 4 mm). The elution profile was monitored at a wavelength of 254 nm. Radiochemical purity was evaluated by thin layer chromatography (Silica gel 60 and Silica Gel 60 F_{254}, Merck) using methanol/ammonia (95:5) as the mobile phase and the radiochromatogram acquired using a RayTest TLC scanner equipped with a BGO scintillation detector. The radiochromatogram was analyzed with the GINA software provided with the scanner. Additionally, the radiochemical and chemical purity were also determined by reverse phase HPLC. The elution was carried out using methanol/water (70:30) solvent at a flow rate of 0.5 ml/min. Mass spectra were recorded by Electron spray ionization-Mass spectrometry (ESI-MS) (Q-TOF micro YA-105, Micromass).

6.I.2. b. Radiosynthesis of [^{18}F]FLT and 4-[^{18}F]Fluoro benzene sulphonic acid ([^{18}F]FBSA)

The radiosynthesis of [^{18}F]FLT was carried out according to the optimized procedure [205] and based on **Scheme 6.I.1**. The optimized procedure is described in details in **Table 6.I.1** and carried out using the adapted general purpose fluorination module.

Table 6.I.1. Flow chart of [^{18}F]FLT radiosynthesis scheme

Step I: Nucleophilic fluorination of FLT-BOC Precursor
i) [^{18}F] fluoride trapped on a Chromafix 45-PS-HCO_3 anion exchange cartridge ii) [^{18}F] fluoride eluted from the column using 75mM $TBAHCO_3$ (0.5 ml, Vial V5) to the reaction vessel iii) Tetrabutyl ammonium fluoride [^{18}F] dried by azeotropic distillation with acetonitrile (1.0 ml, Vial V1) iv) FLT-BOC precursor (20 mg) dissolved in dry MeCN (1.0 ml, Vial V2) added to the reaction vessel. v) Radiofluorination (S_N2) reaction carried out at 130°C for 6 minutes
Step II: Deprotection
i) The reaction mixture was cooled to 50°C ii) 1N HCl (1ml, Vial V3) was added to the reaction vessel. iii) Acid hydrolysis carried out at 105°C for 5 minutes iv) Reaction mixture was cooled to 50°C
Step III: Purification through single combination column
i) The reaction mixture is passed through a single combination column ii) The reaction vessel was rinsed with 10% ethanol (1.5ml, Vial V4) and the column was first washed with this solvent. iii) [^{18}F]FLT was eluted using 10% ethanol (12ml, Vial V6) and is collected in the product vial containing 10% NaCl (1.7ml) and 1M NaH_2PO_4 (0.7ml)

The radiofluorination of nosyl chloride instead of BOC precursor (**Scheme 6.I.2**) under identical conditions yields 4-[^{18}F]Fluoro benzene sulphonic acid. The final product was collected after filtration through a 0.2 μM filter.

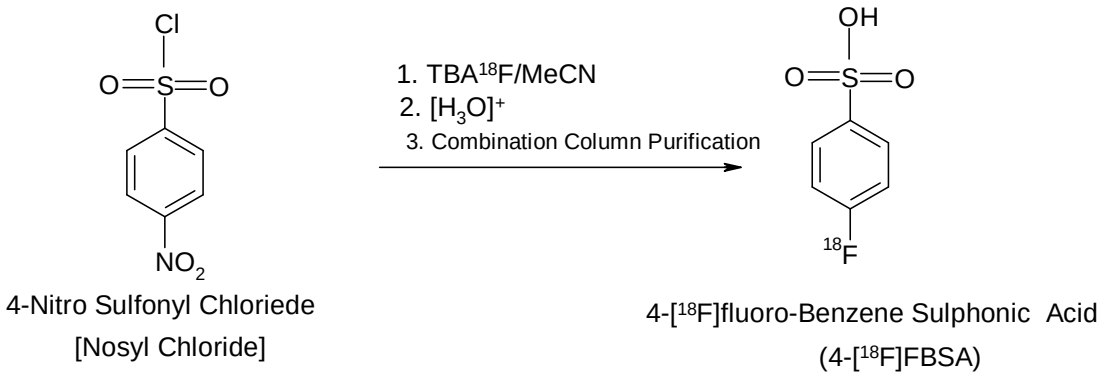

Scheme 6.I.2. *Schematic representation of the synthesis of [^{18}F]FBSA from nosyl chloride*

6.I.2. C. PET/CT Imaging Studies

The normal bio-distributions of [^{18}F]FLT and 4-[^{18}F]FBSA in healthy rabbits were studied by the Discovery ST PET Scanner from GE Medical Systems. The rabbit (~2.5 Kg) maintained in our animal house was maintained on our standard animal house diet. [^{18}F]FLT and 4-[^{18}F] FBSA (~ 111 MBq / 1.0 ml) were injected intravenously through ear vein in separate animals. The images were acquired 90 minutes post injection after standard anesthesia procedure.

6.I.3 Results and Discussion

The HPLC chromatogram of the synthesized [^{18}F]FLT is shown in **Fig. 6.4**. From this figure it is observed that the radiochromatogram displays two peaks at 8.63 and 40.15 min, but only a single UV component at 14.5 min. The majority of the radioactivity is contained in the second peak and corresponds to [^{18}F]FLT, which is confirmed by the retention time of standard FLT measured under similar conditions and which was found to be 40 min**.** HPLC analysis of the final product after allowing the sample to decay for a period of 7 days displays a UV peak at 7.82 min

whereas the peaks corresponding to [^{18}F]FLT (40.15 min) and the other radioactive peak at 8.63 min is not observed.

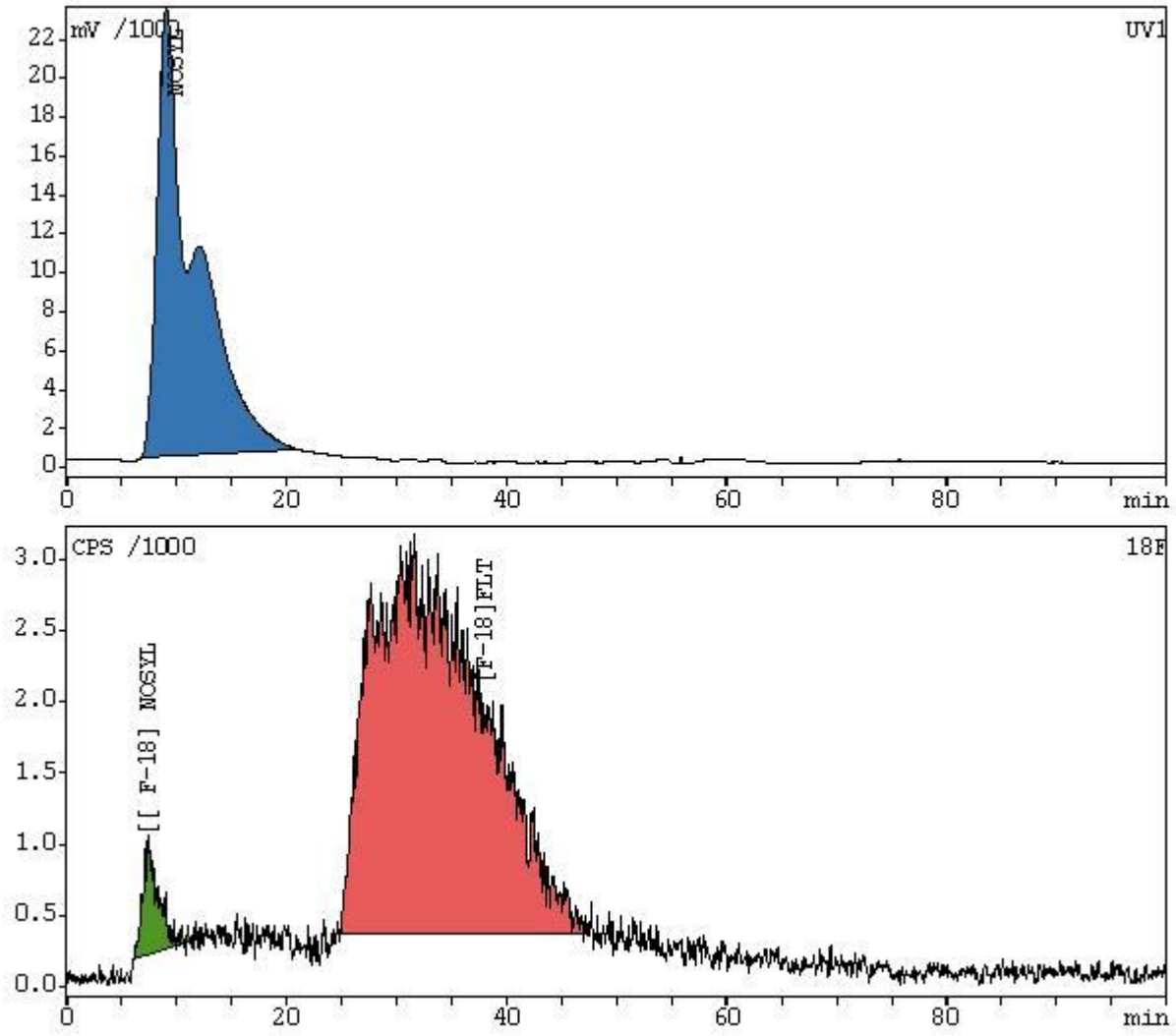

Fig.6.4. *HLPC chromatogram of the synthesized [^{18}F]FLT [Radioactivity & UV (λ = 254 nm)]*

This result suggests that except [^{18}F]FLT, some other ^{18}F- labeled compound is also getting generated which has a very strong absorbance at 254 nm. The possible origin of this compound could be one of the constituents groups of the precursor i.e. thymidine, t-BOC, DMT or nosylate. Of these, t-BOC doesn't contain a chromophoric group and hence will not show any significant UV absorbance at 254 nm. DMT is a highly colored compound, which absorbs strongly at 498

nm[208] [**Fig.6.5.**]. UV-Vis absorbance of the final product doesn't show any absorbance corresponding to this wavelength which rules out the presence of DMT.

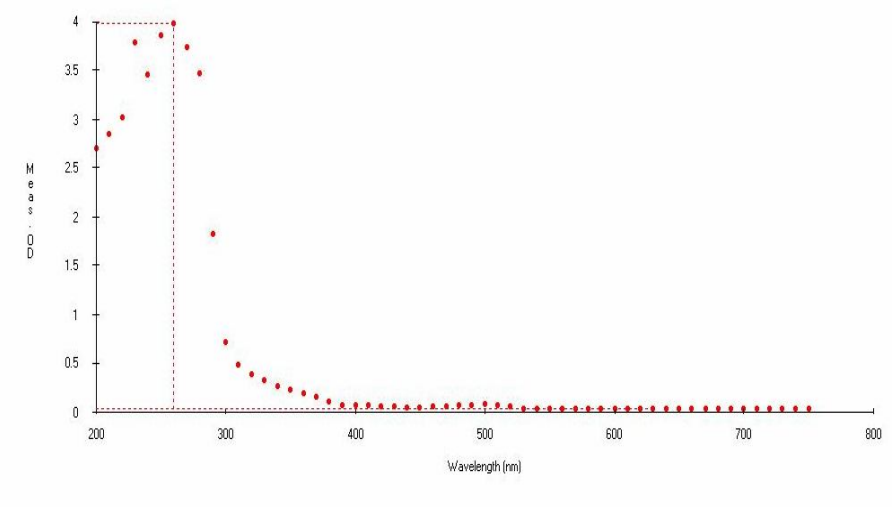

Absorbance spectrum of DMTrCl, 200-700 nm

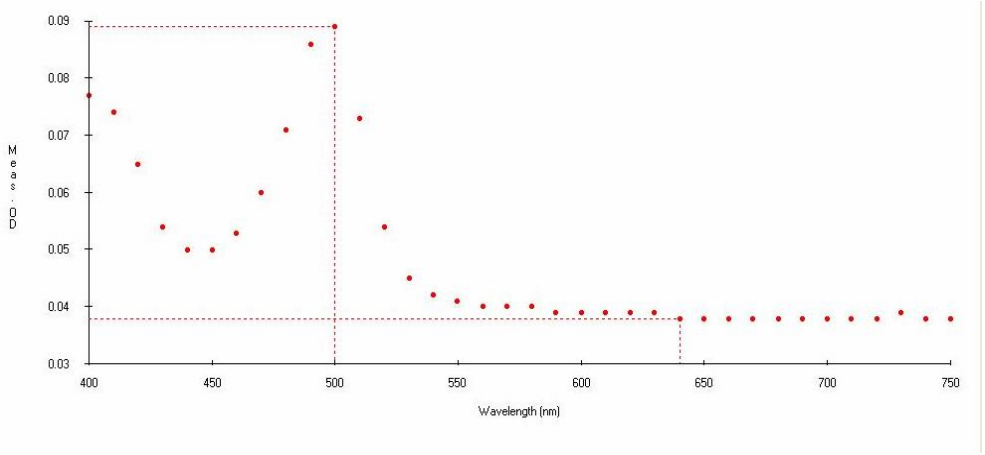

Absorbance spectra of DMTrCl (400-700 nm, shows the presence of additional absorbance peak at 500 nm)

Fig. 6.5. *Absorbance spectrum of DMTrCl (200-700 nm, the one below is from 400-700 nm, showing strong absorption at 500 nm)*

The possibility of the radioactive impurity arising from the non-specific labeling of the 5'-OH group of the furanosyl ring was considered by Yun *et al* [206]. However, the retention time of this compound is markedly different from that of the observed impurity and this was ruled out.

Thymidine, the possible product after removing the blocking groups (DMTr- & t-BOC) as well as the nosyl moiety from the FLT-BOC precursor, has a retention time of 26.97 min (UV, λ = 254 nm) [**Fig.6.6.**] under identical HPLC condition. The HPLC spectrum of [^{18}F]FLT does not show any UV peak around retention time 27 min. So, the presence of thymidine as a radiochemical impurity was ruled out.

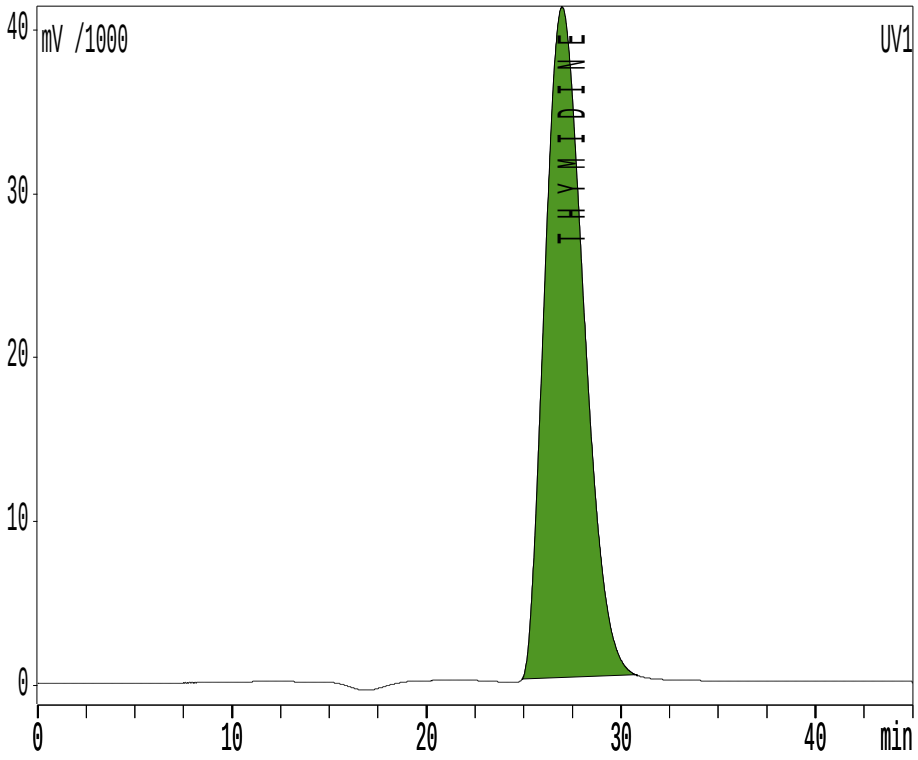

Fig.6.6. *HPLC (UV, λ = 254 nm) chromatogram of thymidine, R_t = 26.97 min*

Hence, it can be concluded with a high degree of certainty that the impurity is a nosyl derivative. This could arise from the competitive nucleophilic substitution at the para position of the aromatic ring by the fluoride with the nitro group acting like a leaving group [**Scheme 6.I.3.**].

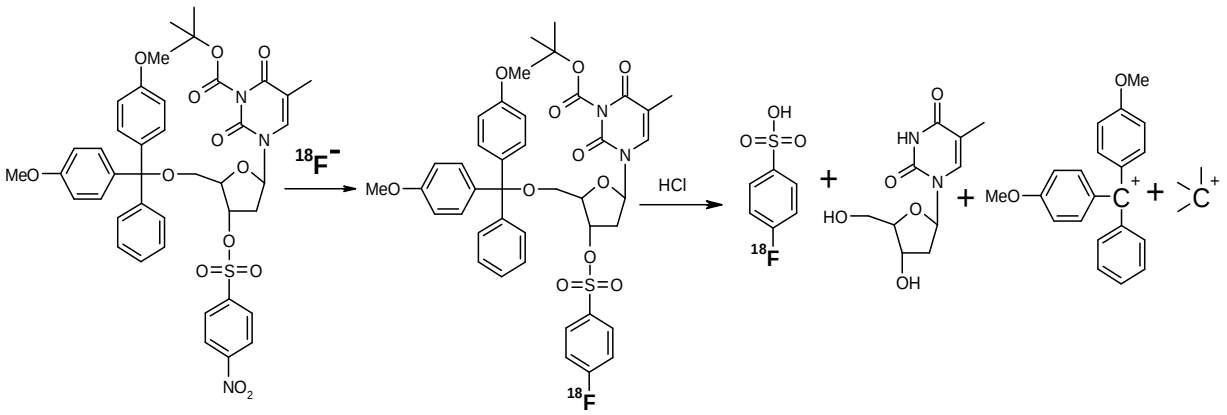

Scheme 6.I.3. *Mechanism of formation of radiofluorinated impurities during [^{18}F]FLT synthesis*

Nucleophilic substitution reactions are the most commonly used method for the radiolabeling using cyclotron produced [^{18}F] fluoride [209]. Nucleophilic substitution reactions of carbohydrates are preferably carried out using sulfonic esters because of their reactivity and their ease of preparation. The most commonly used activating groups are the sulfonic acid derivatives, triflic anhydride, mesityl chloride, tosyl chloride, and nosyl chloride derivatives of the hydroxyl group of the carbohydrate of interest. The efficacy of these derivatives as efficient leaving groups have been studied and it has been observed that the most efficient leaving group is the triflate, followed by the nosylate [210].

The synthesis of [^{18}F]FLT has been carried out using a variety of precursors and a comparison of various precursors and their radiochemical yields have been carried out by Tewson *et al* [211]. The chemical impurities formed during the synthesis of [^{18}F]FLT have been investigated. An expected impurity is 2', 3'-didehydro-3'-dideoxythymidine (Stavudine) [**Fig. 6.7.**] used as antiviral drug arising from the competitive base catalysed β-elimination reaction. The cellular toxicity of the compound makes it mandatory for final preparations to be free of Stavudine [212]. However, it is observed that the generation of Stavudine is through the base catalyzed elimination and is dependant on the concentration and also the time of exposure to the

base [213]. Hence, this is one of the major byproducts in the synthesis of [^{18}F]FLT using the Kryptofix-K_2CO_3 method [214].

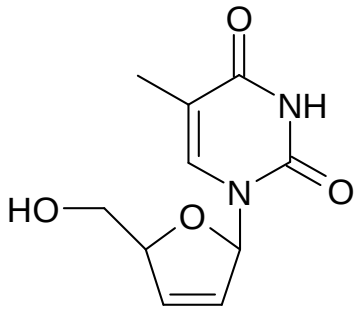

Fig.6.7. *2', 3'-didehydro-3'-dideoxythymidine (Stavudine)*

Tewson *et al* [211] have reported the formation of a radio fluorosulfonate derivate as an impurity which is obtained due to the competitive fluorination of the nosyl derivative with the nitro group acting as a leaving group (**Scheme 6.I.2**). The possibility of this impurity in the synthesis of [^{18}F]FLT was confirmed by its anionic nature and could possibly be [^{18}F] 4-fluorobenzenesulfonic acid ([^{18}F]FBSA). The aromatic nature of the fluorine atom was confirmed by the ^{19}F NMR analysis based on the chemical shift of the fluorine atom. Thus, there is a competitive nucleophilic substitution reaction possible at the 4-nitro position of the benzene ring of the nosyl group in addition to the 3' hydroxyl position of the furanosyl ring. A similar impurity was also reported by Yun *et al* with the nosylated anhydro precursor [206]. Though our initial suspicion was the formation of 4-nitrobenzenesulfonyl group, it was ruled out by carrying out a HPLC analysis of the commercially available standard compound. Similarly, the fluorination of the 5' position of the ribose ring is ruled out as it is not feasible. Hence, a conclusion similar to that of Tewson *et al* [211] was arrived at and was confirmed by synthesizing 4-[^{18}F] fluorobenzene sulphonic acid and comparing the retention times by HPLC. The reasoning

provided for such a reaction to occur was based on the enhanced susceptibility of the nitro group for nucleophilic substitution rather than the 3' OH group.

Aromatic nucleophilic substitutions involving nitro as the leaving group have been widely studied [215]. The nucleofugicity of the nitro group is enhanced by decreased electron density at the reaction center, which is made possible by an electron withdrawing substituent. Sulfonic acid group is a deactivating group, which decreases the electron density. Hence, it is possible that the nitro group in nosyl group can behave like a good leaving group and can compete for the fluoride ion. Such a side reaction has also been reported in the synthetic procedures involving p-nitrobenzenesulfonamides [216]. The ability of nosylate to be an efficient leaving group is dependant on the dihedral angle formed between the ribose ring and the sulphonyl group. As the sulphonyl group is pushed away from the axial position, its electron withdrawing effect at the 3' position is reduced and, hence, the nucloephilic reaction is no longer efficient at this position [204]. The denitrofluorination of aromatic compounds by [^{18}F]fluoride has also been reported in literature [62]. They had concluded that for the nitro group to be an efficient leaving group, the electron density at the reaction center had to be decreased. To study the possible structural effects leading to such a scenario, the electron donating effect of hindered and unhindered anisoles were studied as a model case. It was observed in anisoles that in case of unhindered compounds the methoxy group tends to lie in the plane of the aromatic compound and the lone pair of oxygen is in conjugation with the aromatic ring. This increases the electron density at the para position. However, when the methoxy group is sterically hindered, the oxygen lone pair is forced out of plane and adapts a sp3 type of hybridization which reduces the electron density at the para position and reduces the reactivity at the nitro group. By a similar logic, it would appear that the presence of the trityl group probably induces the aromatic ring of the nosyl group to be

twisted out of plane and hence reduces the reactivity at the 3' position of the furanosyl ring. Similar effects on the nucleofugicity of the nitro group were also reported during the radiofluoriniation of aromatic compounds [217, 218].

The nucleophilic fluorination reaction was carried out on nosyl chloride under identical conditions to [^{18}F]FLT synthesis and the product was analyzed by TLC and HPLC. The TLC scan [**Fig. 6.8.**] shows two radiolabeled products one at the origin and the

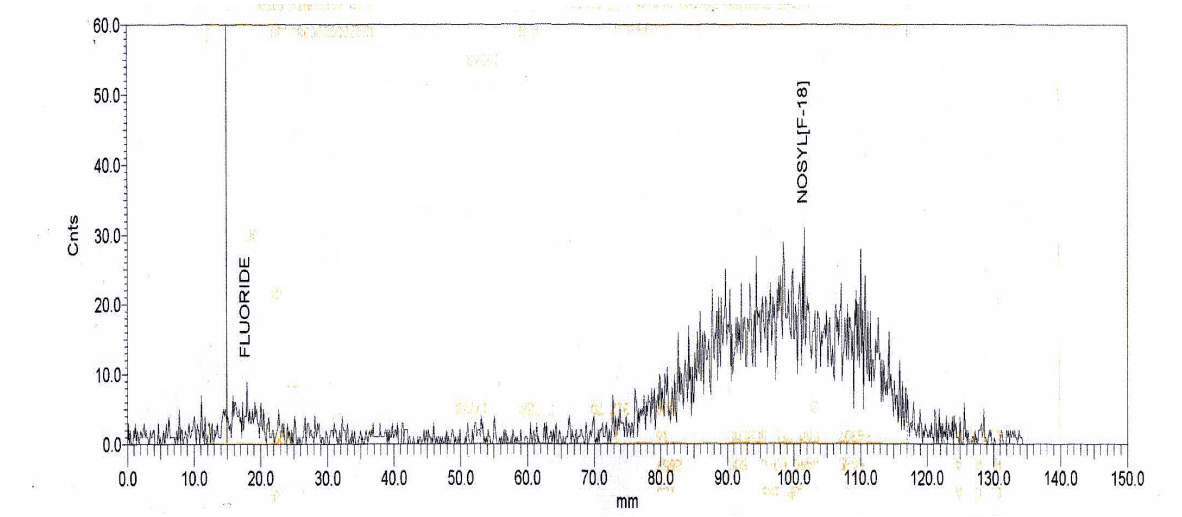

Fig.6.8. *Radio TLC of radiofluorinated nosyl chloride in 95:5 MeCN/H_2O*

other at the solvent front. These correspond to the free fluoride and to the fluorinated nosyl derivative. The compound is non-polar and moves along with the solvent front. Similarly, in the HPLC [**Fig.6.9.**] it is observed that the compound is eluted with a retention time of 6.95 min, which is similar to that of the impurity obtained in case of [^{18}F]FLT. There is a corresponding UV absorption peak at 7.05 min, which indicates that the fluorinated compound is also UV absorbing. Confirmation of the origin of the product was carried out by the HPLC analysis of standard nosyl chloride which shows a retention time of 7.65 min [**Fig. 6.10.**].

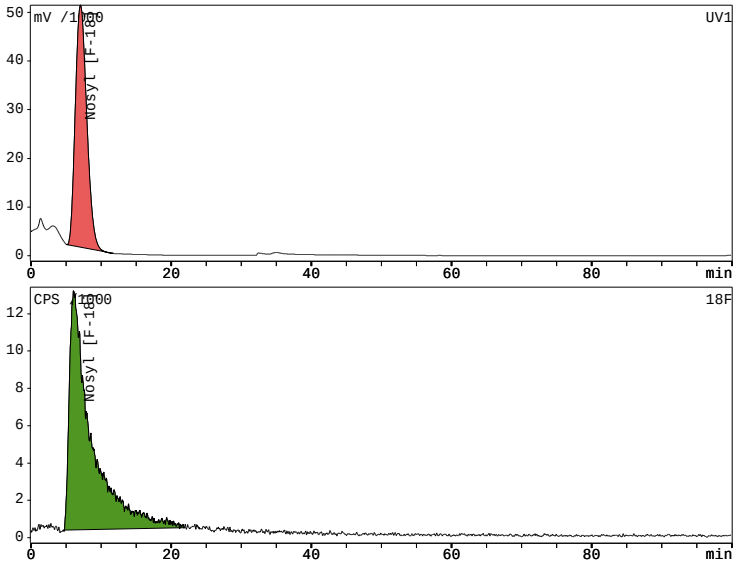

Fig. 6.9. *HPLC chromatogram [radioactive as well as UV (λ = 254 nm)] of radiofluorinated nosyl chloride (Green = Radioactive peak, Red = UV)*

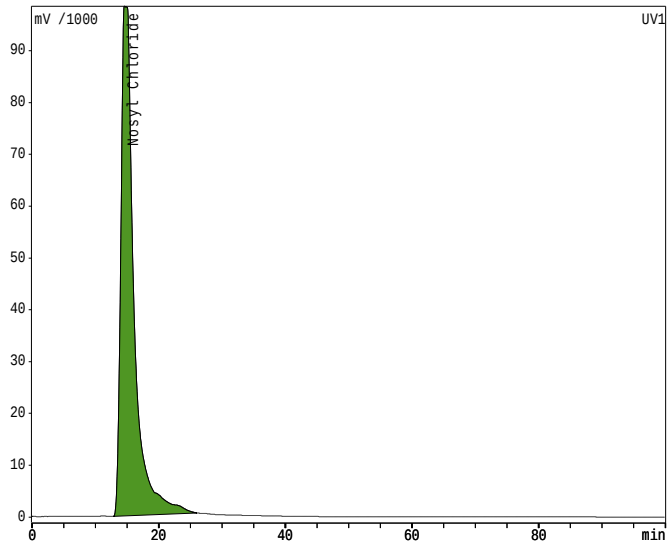

Fig.6.10. *HPLC chromatogram of nosyl chloride (UV, λ = 254 nm)*

Mass spectral analysis

The mass spectrum of the final product [**Fig.6.11.**] obtained by Electron spray ionization (ESI-MS) displays a major peak at m/z 242. This corresponds to the molecular ion peak of nosyl chloride and is confirmed by the mass spectrum of standard nosyl chloride. The mass spectrum of the hydrolyzed precursor [**Fig.6.12.**] displays a major peak at m/z 289 in addition to the peaks at 275 and 303 m/z. The peak at 303 m/z corresponds to the dimethyl trityl ion and the sequential

loss of two methyl groups leads to the formation of 289 and 275 m/z. The final product does not show any of the peaks arising from the DMT moiety and hence further confirms the presence of nosyl chloride as the chemical impurity which is obtained during the synthesis of [^{18}F]FLT.

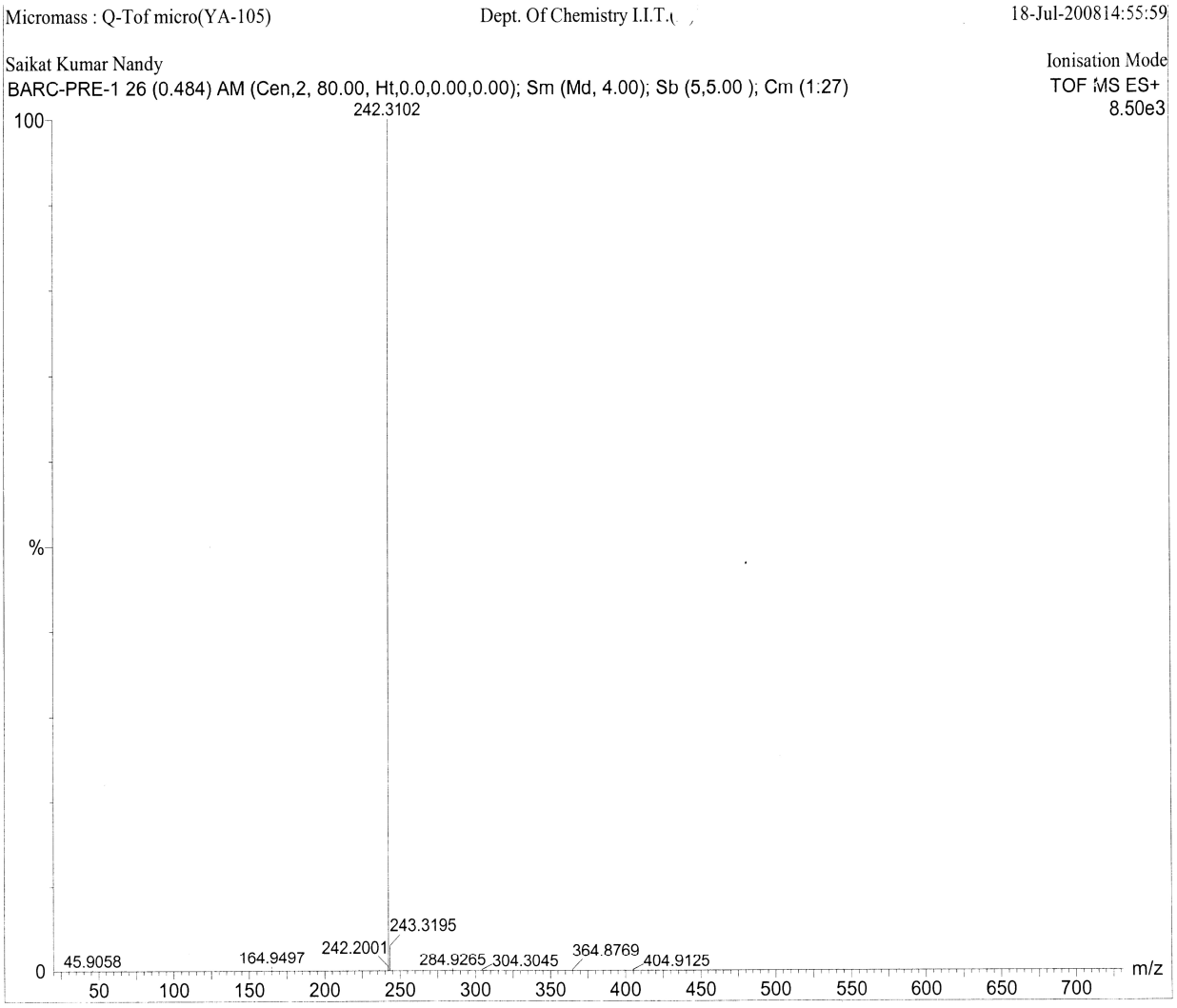

Fig.6.11. *Mass spectrum of decayed [^{18}F]FLT sample*

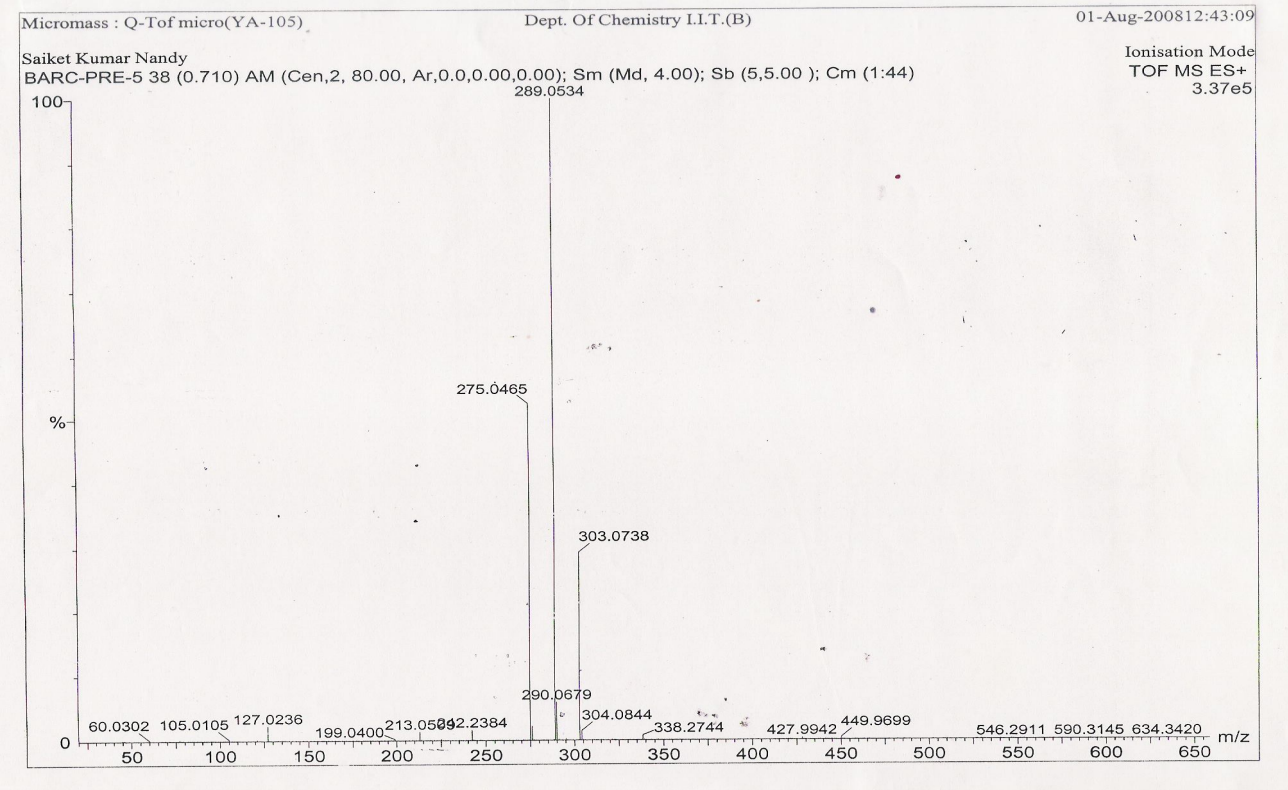

Fig.6.12. *Mass spectrum of acid hydrolyzed FLT-BOC precursor*

PET imaging

Radiofluorinated nosyl chloride was injected in a rabbit and the images obtained are given in **Fig. 6.13**. From the image it is clearly observed that there is bone uptake. However, a similar uptake is not observed when [^{18}F]FLT [**Fig. 6.14.**] is injected, presumably because of very low concentration of radiofluorinated nosyl chloride in the injected dose. This is a significant observation since it indicates that the radiofluorination occurs at two different sites in the BOC precursor, one at the 3' position by substituting the nosylate group and the second at the 4-position of the nosyl group by substituting the nitro group. There could be two possible explanations for the enhanced bone uptake. The fluorinated compound can undergo rapid defluorination and generate free fluoride which explains the bone uptake. However, this is possible only when the compound is 4-nitrosulfonyl fluoride. This can be ruled out since it is

well known that sulphonyl fluorides rapidly generate fluoride ion in aqueous solutions. This will then be trapped on

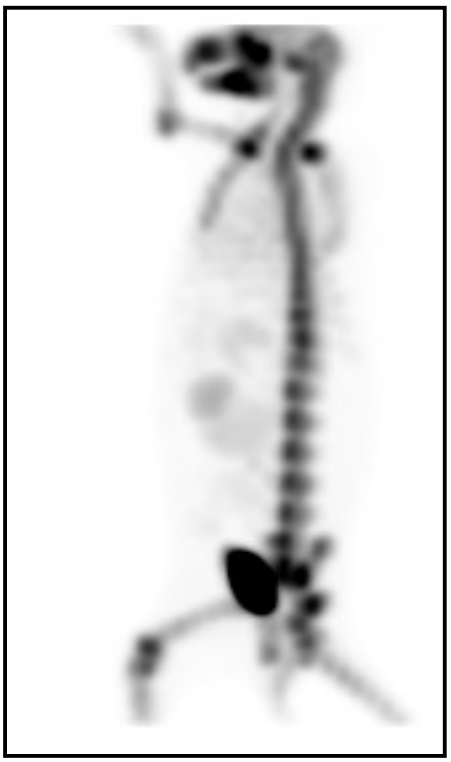

Fig.6.13. *PET scan of rabbit with [^{18}F]FBSA*

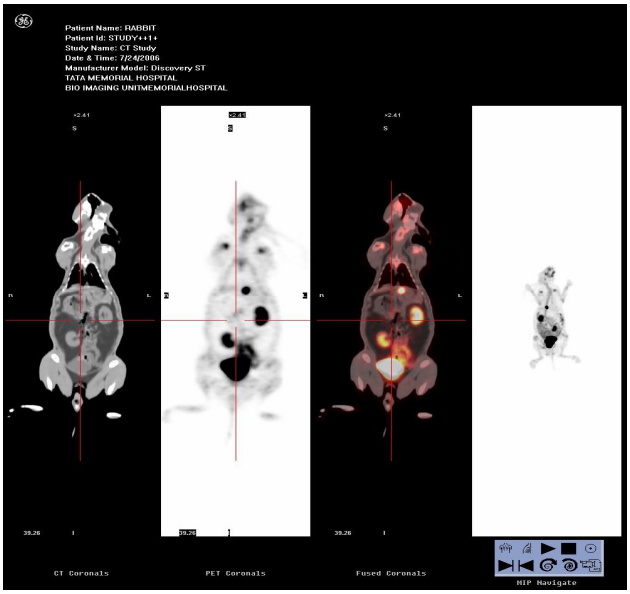

Fig.6.14. *PET/CT scan of rabbit with [^{18}F] FLT*

an alumina column and, hence, will not be observed in the final product. The alternative is the nucleophilic substitution reaction on nosyl group. This could be explained by **Scheme 6.I.2**. In case of the precursor, the fluorination takes place with nitro as the leaving group. On subsequent hydrolysis we obtained [^{18}F] FBSA. In case of nosyl chloride also, the radiofluorination takes place at 4 position to yield [^{18}F] FBSA which can easily bind to free hydroxyl group of calcium hydroxyl apatite by sulphonic ester formation.

6.I.4 Conclusion

In this study, it is confirmed that a radioactive byproduct, [^{18}F]FBSA is present, in the [^{18}F]FLT produced, using the FLT-BOC-precursor and combination-column composed of neutral alumina and anion exchanger, Ps-HCO_3 as a purification cartridge. The compound is probably formed by the competitive fluorination of the precursor with the nitro group acting as a leaving group. The quantity of this by-product is quite small and does not impair the image quality, yet it may not be acceptable radio pharmacologically. It is evident that the use of a combination column is not sufficient to synthesize radiochemically and chemically pure [^{18}F]FLT. The possibility of such a purification procedure, which can be conveniently adapted to [^{18}F]FDG synthesis modules, can be tried with other precursors like anhydrothymidine although the yields are lower.

PART-II

Fully automated and simplified radiosynthesis of [^{18}F]3'-Deoxy-3'-Fluorothymidine ([^{18}F]FLT) Using Anhydro Precursor and Single Neutral Alumina Column Purification

6.II.1.

Introduction

The synthesis methods for [^{18}F]FLT reported so far (listed in PART-I) show a common approach. HPLC purification is required only to remove the impurity products arising from the leaving groups used in the precursor in the radiofluorination step or the blocking groups in the hydrolysis step. If these products can be avoided, [^{18}F]FLT synthesis could be achieved with column purification technique very similar to [^{18}F]FDG. A precursor with minimum-blocking groups holds the key to an HPLC-free radiosynthesis procedure.

The PART-I of this chapter is ended with the important conclusion that the use of a combination column is not sufficient to synthesize radiochemically and chemically pure [^{18}F]FLT from FLT-BOC precursor. The possibility of such a purification procedure, which can be conveniently adapted to [^{18}F]FDG synthesis modules, can be tried with other precursors like anhydrothymidine although the yields are lower.

In this chapter, the fully automated radiosynthesis procedure of [^{18}F]FLT starting from 5'-O-(4,4'-dimethoxytriphenylmethyl)-2,3'-anhydrothymidine (DMTThy), a precursor in which the –OH group is protected by the 4,4'-dimethoxytriphenylmethyl substituent (**Scheme 6.II.1.**) and single neutral alumina column purification is described in details which is an outcome of the idea concluded in PART-I. Analysis of radioactive and non-radioactive impurities was carried out along with biodistribution by PET imaging study in normal rabbit in order to verify the

localization of the tracer in the highly proliferating tissues like bone marrow, guts etc. This fully automated radiosynthesis procedure can be readily implemented in any [^{18}F]FDG synthesis module without the need for additional automation for the semi preparative HPLC purification.

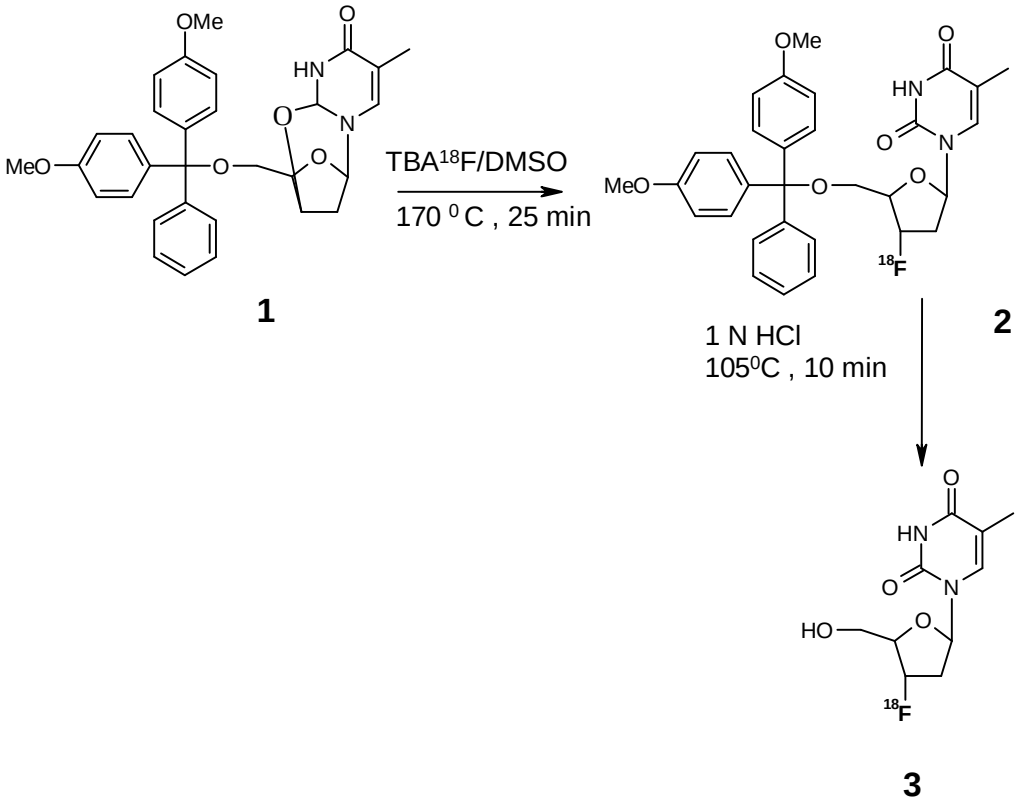

5'-O-(4,4'-dimethoxytriphenylmethyl)-2,3-anhydro-thymidine (DMTThy, **1**)
5'-O-(4,4'-dimethoxytriphenylmethyl)-3'-deoxy-3'-[^{18}F]fluorothymidine (**2**)
3'-deoxy-3'-[^{18}F]fluorothymidine ([^{18}F]FLT, **3**)

Scheme 6.II.1. *Schematic representation of synthesis of [^{18}F]FLT starting from anhydro precursor, DMTThy*

6.II.2 Materials & Methods

6.II.2. a. Reagents and apparatus

5'-O-(4,4'-dimethoxytriphenylmethyl)-2,3'-anhydrothymidine (DMTThy), precursor for synthesis, Fluorothymidine standard, $TBAHCO_3$ solution (75 mM), molecular-grade anhydrous acetonitrile, ^{18}F trapping column (Ps-HCO_3), 10% NaCl, 1.0 M HCl, 1.0 M NaH_2PO_4 buffer, sterile and pyrogen-free water for injection and pharmaceutical grade ethanol were procured from ABX Advanced Biochemical Compounds, Germany. Dimethoxytrityl chloride, di-methyl sulfoxide (DMSO), thymidine and thymine were obtained from Aldrich, USA. Aluminum oxide (neutral, Activity I-II) was purchased from Merck, India. Evacuated 10 ml vials certified for sterility and pyrogen free were obtained from ACILA AG, Germany. Minisart 0.2μ filters were purchased from Sartorius. Sterility testing was carried out in-house using standard protocol as described in earlier chapter. Pyrogen testing was done by LAL test using Endosafe Reagent Kits from Charles River Laboratory, USA (US License No. 1197). Radioactivity was measured using a calibrated ion chamber (Capintec CRC-15R).

Alizarin Red S Was procured from Sigma. Aluminium-Test Kit, Merckoquant® (Detection limit: 10-250 mg/l Al) and Microquant ®(Detection limit: 0.1-6 mg/l Al) were purchased from Merck, India. All other chemicals used were of HPLC and AR grade.

HPLC analysis was carried out using a Knauer HPLC system equipped with a variable wavelength UV detector and a radiometric detector. The analysis was carried out using a C-18 reverse phase analytical column (LIChroCART ® 250-4, HPLC cartridge, LIChrospher® 100, RP-18, 5 μm). The elution profile was monitored at a wavelength of 254 nm. Radiochemical purity was evaluated by Thin layer chromatography (Silica gel 60, Merck) using acetonitrile/water (95:5) as the mobile phase and the radiochromatogram acquired and analyzed

using a RayTest TLC scanner (Model No. BGO-V-Detector) and GINA® software provided with the scanner. Additionally, the radiochemical and chemical purity were also determined by reverse phase HPLC. The elution was carried out using ethanol/water (7.5:92.5) solvent at a flow rate of 0.5 ml/min.

6.II.2.b. Automated Radiosynthesis of [^{18}F]FLT

Radiofluorination and conversion of DMTThy to [^{18}F]FLT was carried out using our adapted general-purpose fluorination module described in details in Chapter 2. The fully automated radiosynthesis of [^{18}F]FLT consisted of three different steps as summarized in the **Table 6.II. 1**. At the end of the synthesis, [^{18}F]FLT in buffered saline was sent to an automated dispensing unit and dispensed into different vials in a class 100 area through 0.2μ filters. The radiochemical yield was expressed as the percentage of radioactivity finally obtained as [^{18}F]FLT compared with the total ^{18}F activity obtained in the reaction vessel without applying correction for radioactive decay.

6.II.2. c. [^{18}F]FLT Purification Column

The [^{18}F]FLT purification column [**Fig. 6.15.**] is a ready to use column composed of only neutral alumina, active, grade I-II (Brockmann). In brief, 7.7 g of neutral alumina (dry condition weight) was thoroughly washed with sterile deionised water to remove fine particles and then packed inside a polypropylene cartridge barrel [6.5 cm (L) x1.2 cm (W)] with luer connectors. Due care was taken to avoid formation of air bubbles in the packed column. The top and bottom of the column were having 20-μm-polyethylene frit to prevent leakage of alumina. The columns were conditioned before use by passing 10 ml of pure ethanol followed by 100 ml of sterile and bacterial endotoxin free water.

Table 6.II.1. Flow chart of [^{18}F]FLT radiosynthesis scheme

Step I: Nucleophilic fluorination of DMTThy
i) [^{18}F] fluoride trapped on a Chromafix 45-PS-HCO_3 anion exchange cartridge ii) [^{18}F] fluoride eluted from the column using 75mM $TBAHCO_3$ (0.5 ml, Vial V5) to the reaction vessel iii) Tetrabutyl ammonium fluoride [^{18}F] dried by azeotropic distillation with acetonitrile (1.0 ml, Vial V1) iv) DMTThy precursor (10 mg) dissolved in DMSO (1.0 ml, Vial V2) added to the reaction vessel. v) Radiofluorination (S_N2) reaction carried out at 170°C for 25 minutes
Step II: Deprotection
i) The reaction mixture was cooled to 50°C ii) 1N HCl (1ml, Vial V3) was added to the reaction vessel. iii) Acid hydrolysis carried out at 105°C for 10 minutes iv) Reaction mixture was cooled to 50°C
Step III: Purification through neutral alumina column
i) The reaction mixture is passed through a single combination column ii) The reaction vessel was rinsed with 10% ethanol (1.5ml, Vial V4) and the column was first washed with this solvent. iii) [^{18}F]FLT was eluted using 10% ethanol (12ml, Vial V6) and is collected in the product vial containing 10% NaCl (1.7ml) and 1M NaH_2PO_4 (0.7ml)

Fig.6.15. *Neutral alumina purification and ^{18}F trapping columns*

6.II.2. d. Quality Control

The synthesized [^{18}F]FLT was checked for clarity, colour and presence of any suspended particle. The pH was checked with pH test paper strip. The radiochemical purity was first checked by radio-TLC. The radiochemical purity was also checked by analytical HPLC. Twenty-five micro liter of the test solution was injected into the HPLC column and the eluate was

monitored by UV absorbance (λ = 254 nm) as well as radioactivity profile. The eluate consisted of 7.5% EtOH (solvent A) and 92.5% Water (solvent B) with 0.5ml/min flow rate in an isocratic system. The presence of non-radioactive impurities was also checked under the same HPLC conditions. Finally, the [^{18}F]FLT prepared was confirmed by comparing the retention time of the UV peak of reference standard FLT with the radioactive peak of the test solution.

6.II.2. e. Test of Aluminium ions

The aluminum ion (Al^{3+}) concentration in the product was measured by the Alizarin Red S method as described by Nakao *et al*. [158]. The samples were also analyzed by Microquant® Al test kit according to the instructions given in the manual.

6. II.2.f. Sterility and Bacterial Endotoxin Tests

Sterility tests were performed in accordance with Indian Pharmacopoeia: IP, 1996: IP, addendum 2005 protocol. In this test, 1 ml of the [^{18}F]FLT sample, post radioactive decay, was inoculated in fluid thioglycollate medium at 37°C for 14 days to observe the growth of aerobic and anaerobic bacteria. Similarly, 1 ml of the [^{18}F]FLT sample was also inoculated in soyabean casein digest medium at 22-25°C for 14 days to detect fungal growth.

The bacterial endotoxin test was performed in accordance with USP XXV. The test was based on the formation of gel clot in the sample by Limulus Amoebocyte Lysate (LAL) reagent having a sensitivity of 0.125 EU/ml.

6.II.2. g.i. PET Imaging Studies in rabbits

The bio-distribution of [^{18}F]FLT in normal healthy rabbits was studied using the GE Advanced PET scanner. Rabbits (~2.5 Kg) were maintained in our animal house and fed standard animal house diet. The animals were administered [^{18}F]FLT (~ 111 MBq / 2.0 ml) intravenously through the marginal ear vein. The rabbits were given standard anesthesia and PET images were acquired at 30, 60 and 200 min post injection.

6.II.2.g.ii Comparison study of [^{18}F]FDG and [^{18}F]FLT in inflammation model

[^{18}F]FLT is said to localize preferentially in rapidly growing tumors but not in inflammation. Since, [^{18}F]FDG PET is reported to be poorly differentiate tumors from inflammatory formations, the utility of [^{18}F]FLT to differentiate pyogenic infection sites and compare it to that of [^{18}F] FDG using a rabbit model is studied.

Method: Two New Zealand rabbits chosen for this study were pre-sensitized with *S.aureus* antigens by standard immunization methods. These were then injected with $3X10^8$ and $1X10^9$ cfu of *Staphylococcus aureus – Cowan I Strain* at various location subcutaneously on dorsal aspect. These are then serially screened at Day 1, 3, 7 & 10 for evaluation of lesion appearance and size [**Fig.6.16.**]. These were also imaged with [^{18}F]FLT on these days and [^{18}F]FDG PET on Day 2, 6 & 9. Both, early (30-45 min post injection) and delayed (2-3 hours) images were obtained on each occasion.

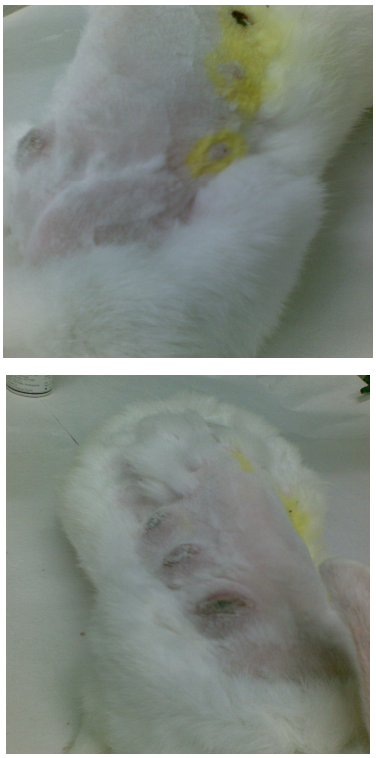

Fig.6.16. *S.aureus induced pyogenic lesion in rabbit*

6.II. 2.h. Patients Study

PET/CT images of a number of cancer patients of different origin as well as variety of brain tumors, were studied using approximately 74-111 MBq of [^{18}F]FLT per patient. Images were taken one hour post injection. For performing the clinical trials in patient, regulatory clearance from the Tata Memorial Hospital (TMH) Ethics Committee was obtained (This was a collaborative project with the Bio-Imaging Unit, TMH where the clinicians of the particular unit were also involved).

6. II.3 Results and Discussion

Starting from the precursor, DMTThy, [^{18}F]FLT was synthesized as per **Scheme 6.II.1** and purified by passing the reaction mixture through a single neutral alumina column. The radiochemical yield (without radioactive decay correction) was 8.48 ± 0.93 % (**Table.6.II.2**) in a total synthesis time of 68 ± 3 min. The optimization of reaction parameters for synthesizing [^{18}F] FLT starting from the precursor, DMTThy was systematically done by Machulla et al. [203]. According to their published data, the radiochemical yield of

Table 6.II.2. Radiochemical yield of [^{18}F]FLT

Sr. No	^{18}F in the reaction vessel (MBq)	[^{18}F]FLT produced (MBq)	% Yield*
1	10,804	851	7.88
2	8,880	722	8.13
3	15,572	1,550	9.95
4	16,280	1,247	7.65
5	16,576	1,458	8.80

* Without decay correction

[^{18}F]FLT was a function of the amount of DMTThy used as starting material and the maximum yield was obtained starting with 25 mg DMTThy (n = 2, 11.0 ± 0.4, decay corrected). But in

their procedure, they had included a Sep-Pak purification of the acid hydrolyzed reaction mixture to achieve good HPLC purification; and further studied with 10 mg DMTThy. The most probable reason was to avoid the saturation of the HPLC column. The method of single neutral alumina column purification developed does not restrict the initial precursor to be started with but to make the process much more economic, we have carried out our experiments with 10 mg of DMTThy. Starting with 10 mg DMTThy, three different radiofluorination temperatures (140ºC, 160°C and 180°C respectively) were monitored including the optimization of the duration of radiofluorination .The maximum yield they have reported was 14.3 ± 3.3 % (n = 9) with the radiofluorination at 160°C for10 min. But at the same time, after HPLC purification, only 1.3 GBq of [^{18}F] FLT could be prepared from 20 GBq of [^{18}F]fluoride within 90 mins. A simple calculation will reveal that the overall yield was only 6.5 % (decay corrected). The overall yield (without decay correction), we have reported is much higher and the total synthesis time is also less. The synthesized [^{18}F]FLT was clear, colourless and free of suspended or colloidal particles. The pH was in the range of 6.5-7.0. The radio TLC of the radio fluorinated DMTThy showed the presence of free [^{18}F]fluoride with R_f (max) of 0.01 whereas the radio fluorinated DMTThy moved as a broad peak starting from R_f of 0.4 to 1.0 [**Fig. 6.17.**]. The TLC of the final purified [^{18}F]FLT showed a very prominent peak at R_f (max) of 0.64 [**Fig. 6.18.**]. The HPLC chromatogram of the synthesized [^{18}F]FLT doped with reference standard FLT is shown in [**Fig. 6.19.**]. From this figure it is observed that the eluate displays a single radioactive peak at 47.17 min, but shows two UV-absorbing peaks. One at 15.83 min (Peak1) and the other at 48.53 min (Peak 2). Peak 2 corresponds to the reference standard FLT as confirmed by HPLC separately [**Fig.6.20.**].

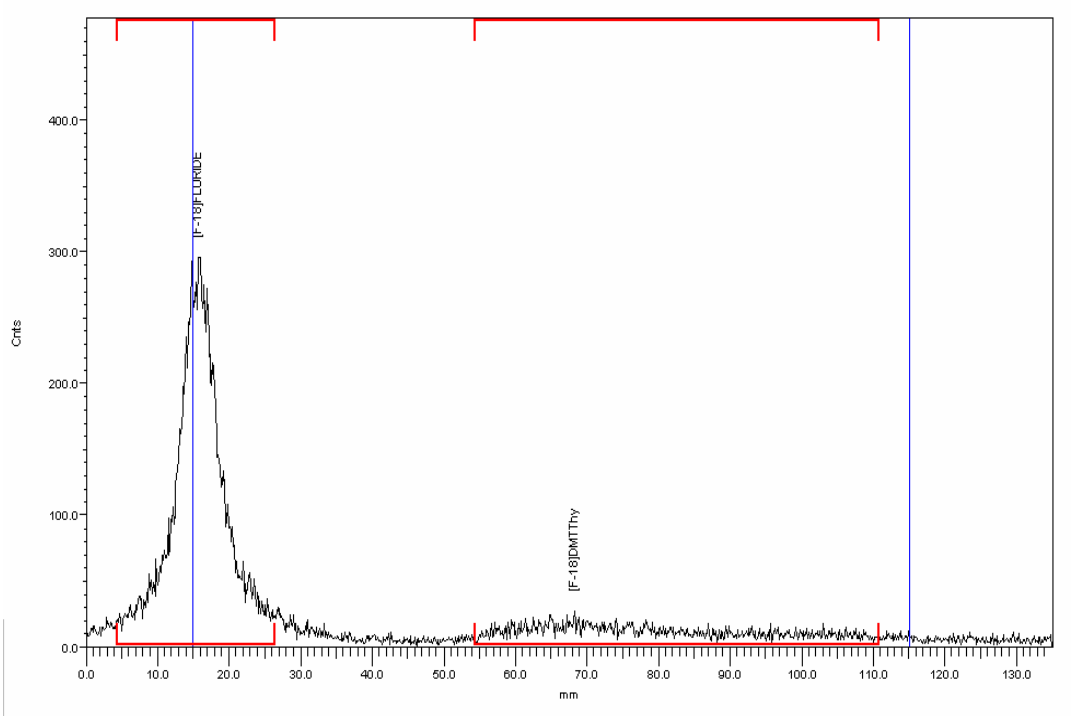

Fig.6.17. *Radio TLC of radiofluorinated DMTThy in 95/5 MeCN/H_2O*

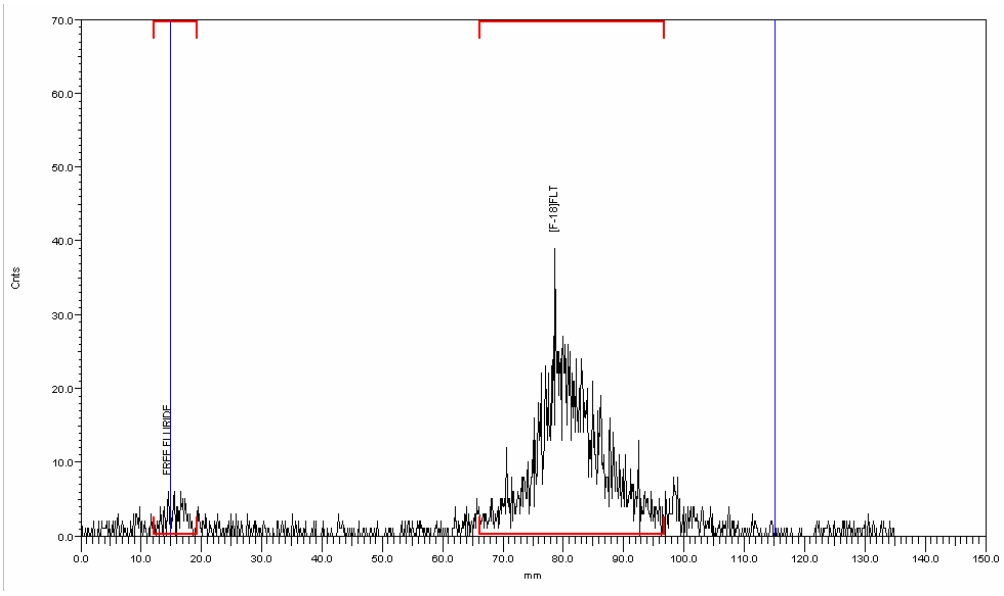

Fig.6.18. *Radio TLC of [^{18}F]FLT in 95/5 MeCN/H_2O*

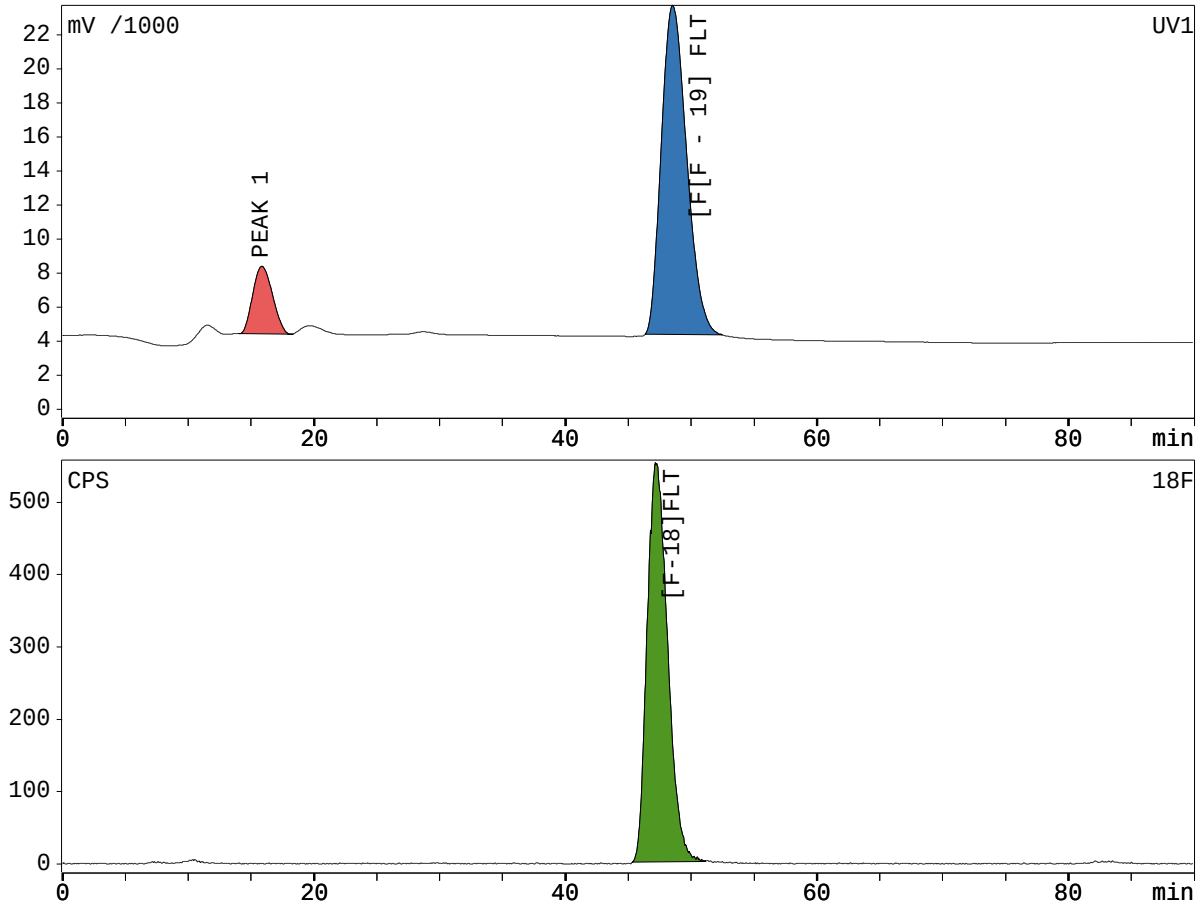

Fig. 6.19. *HPLC chromatogram of [^{18}F]FLT doped with reference standard FLT*

The co-elution of the radioactivity peak along with the UV peak of the reference standard FLT confirmed that the single radioactive peak corresponds to [^{18}F]FLT. Peak 1 in UV appears to be that of DMSO since other possible impurities originating from the precursor are thymidine, DMT and thymine. Of these, DMT is a highly colored compound, which absorbs strongly at 498 nm [196]. UV-VIS absorbance of the final product doesn't show any absorbance corresponding to this wave length which rules out the presence of DMT. Pure thymidine elutes out around 27 min under identical HPLC condition. The HPLC chromatogram of the [^{18}F]FLT does not show any UV peak around 27 min. So the presence of thymidine is also ruled out. Pure thymine is not at all soluble in the eluting solvent i.e. 10% ethanol containing water. So the co-elution of pure thymine with [^{18}F]FLT from the alumina column is not practically possible. DMSO is a high boiling liquid with a boiling point of 189°C [219]. The maximum reaction temperature, in this

synthesis is 170°C. So it is logical to expect vapours of DMSO to be carried forward into the subsequent steps and finally eluted out with [^{18}F]FLT in the eluting solvent, as it is highly miscible with water. It is also a known fact that DMSO exhibits UV-VIS absorption in the wavelength range of 220 nm-350 nm, maximum absorption at 265 nm [219, 220].

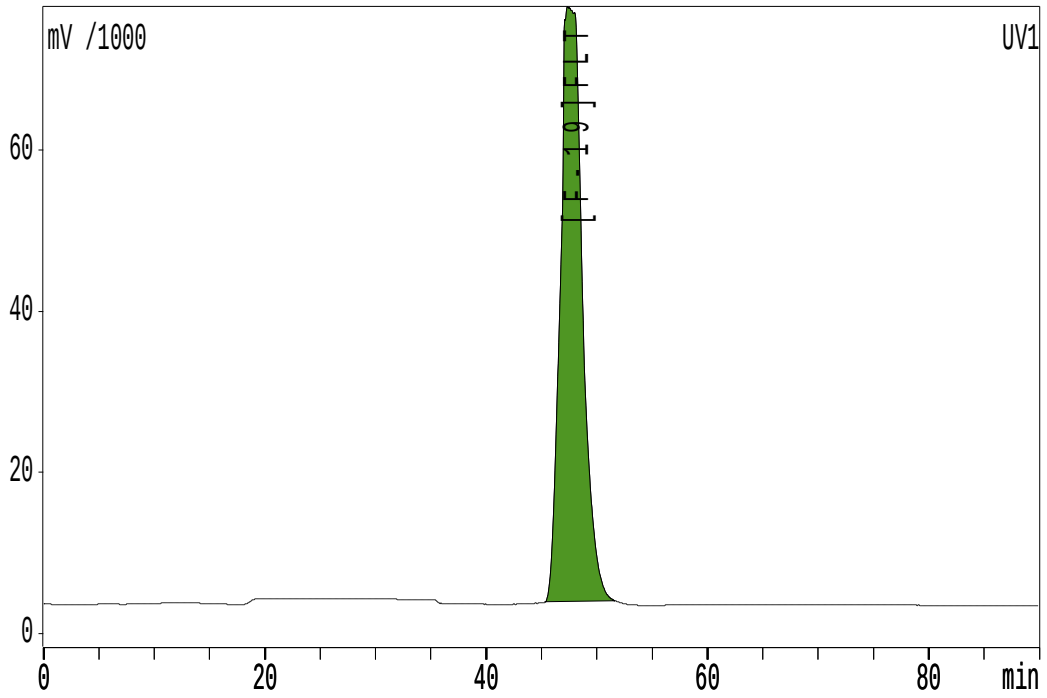

Fig. 6.20. *HPLC chromatogram of reference standard FLT (UV, λ = 254 nm)*

So we expect a UV peak in the HPLC chromatogram of [^{18}F]FLT as the monitoring wavelength is 254nm. This explains the origin of the small UV peak at 15.83 min. This was further confirmed by analytical HPLC of pure DMSO and UV-Vis spectroscopy. DMSO belongs to solvents in Class 3 (Solvents with Low Toxic Potential) according to The European Agency for the Evaluation of Medicinal products (EMEA 2000) and the acceptable limit as residual solvent is 5000 ppm or higher [178]. The oral rat LD_{50} is also very high (14,500mg/Kg). Considering 185 MBq (5 mCi) [221] as the standard injectable dose, the level of DMSO will be much lower than the acceptable limit.

The Alizarin Red S method, detects Al^{3+} on the basis of colour development reaction between aluminium hydroxide (formed from Al^{3+} in the presence of ammonium hydroxide) and alizarin Red S. The detection limit with unaided eye for this method is 5μg/ml, which is also the permissible limit [158]. [^{18}F]FLT samples after radioactive decay, analyzed by this showed Al^{3+} below detectable levels.Further analysis with Microquant® test kit (sensitivity 0.1-6.0 μg/ml) based on Chromazurol S Method confirmed that the Al^{3+} concentration in [^{18}F]FLT was in the range of 2-3μg/ml.

Sterility was achieved by 0.2 μ filtration, since autoclaving of [^{18}F]FLT is not possible due to the thermal instability of [^{18}F]FLT, leading to increase in the free ^{18}F content.

PET imaging in rabbits

PET images showing the bio-distribution of [^{18}F]FLT in normal rabbits at different time points are given in **Fig. 6.21**. The images demonstrated progressive selective uptake in the marrow, a tissue with a high proliferative rate. High retention of [^{18}F]FLT in nose, submandibular lymph node and guts indicates the presence of proliferative cell in these regions. FLT is known to excrete through the kidneys and collect in the urinary bladder. We have observed accumulation of radioactivity in these organs. FLT has low uptake in brain and none of our rabbits' images showed any uptake in brain. Additionally, there was no significant bone uptake, which suggests that the amount of free $^{18}F^-$ in the synthesized [^{18}F]FLT was insignificant. The observations on rabbit imaging with [^{18}F]FLT were in very good agreement with the results on normal dog as well as dog with non-Hodgkin's lymphoma reported by Shields et al. [193].

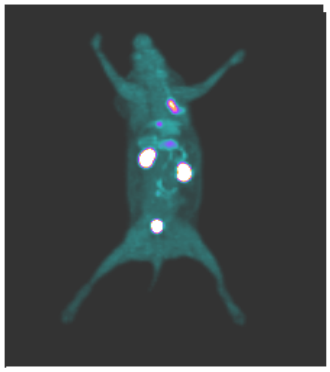

(a)

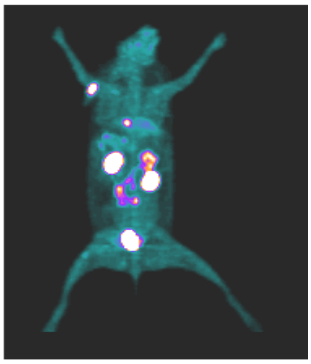

(b)

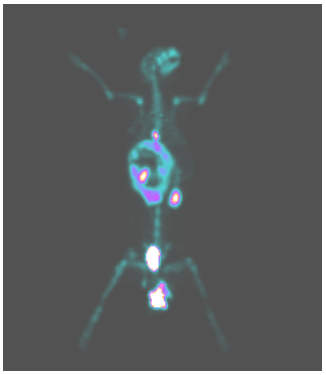

(c)

Fig.6.21. *PET scan of rabbit following (a) 30 min post injection (b) 60 min post injection and (c) 200 min post injection*

Comparison study of [^{18}F]FDG and [^{18}F]FLT in inflammation model

The [^{18}F]FDG images of the rabbits showed significant uptake of [^{18}F]FDG at the infection sites [**Fig.6.22.**] and proves its inability to differentiate tumors from infection as well as inflammation. Whereas the [^{18}F]FLT PET images [**Fig.6.23.**] did not show any tracer uptake in the infection sites showing its superiority over [^{18}F]FDG in differentiating tumors from infection as well as inflammation.

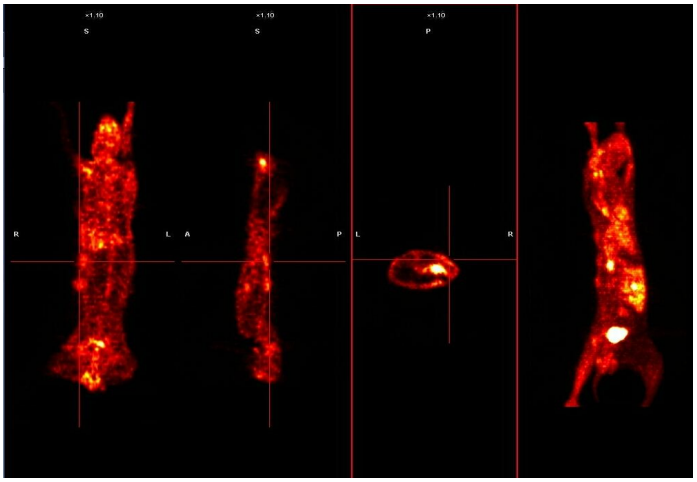

Mild uptake of [^{18}F]FDG on pyogenic lesion site (Early Image)

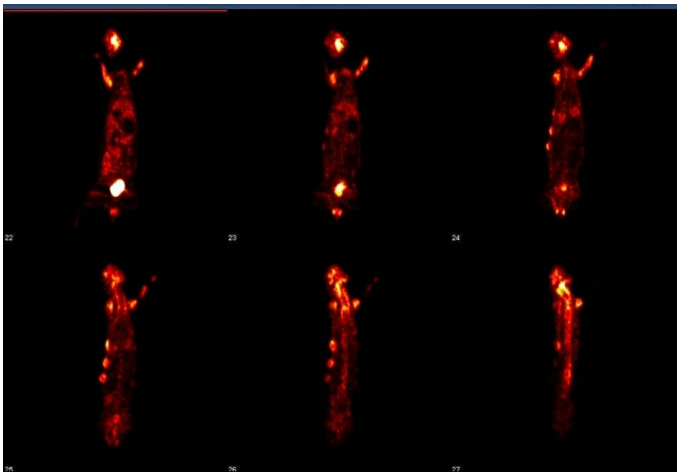

High uptake of [^{18}F]FDG on pyogenic lesion site (Delayed Image)

Fig.6.22. *[^{18}F]FDG PET images showing tracer uptake in the lesion sites which are non-tumorous*

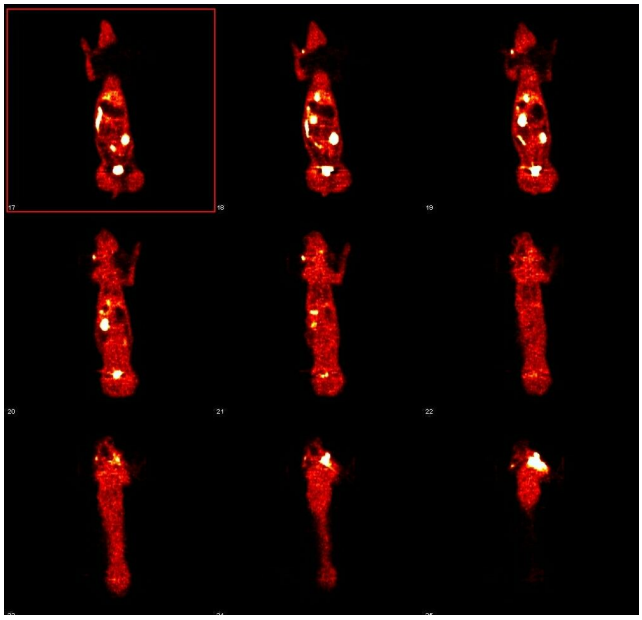

Early (25 minute post injection) [^{18}F]FLT image of the model rabbit. No uptake in pyogenic lesion site, brain and bone. Uptake in gall bladder, two kidneys, guts and in the urinary bladder.

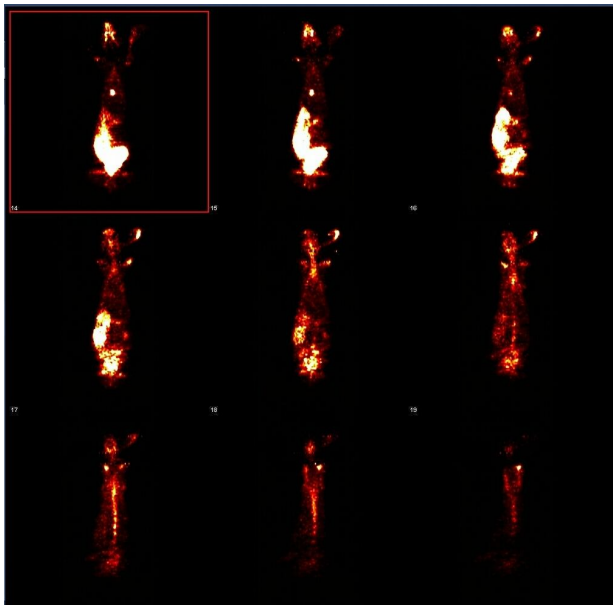

Delayed (2 hours post injection) [^{18}F]FLT image of the model rabbit. No uptake in the pyogenic lesion site. Prominent uptake in marrow, nose and jaws. High uptake in the gut due to the presence of highly proliferating endothelial cells. Expected tracer accumulation in the bladder due to normal excretion.

Fig. 6.23. *[^{18}F]FLT images of the rabbit*

Patients Study

The clearance for regular clinical use and commercial production using the method developed was obtained in January 2010 and the routine production as well as clinical use started from May 2010. Normal healthy volunteer [**Fig. 6.24.**] as well as a variety of patients having history of brain tumors which is commonly difficult to image using [^{18}F]FDG because of high background resulting from the normally intense uptake of [^{18}F]FDG in brain were studied [**Fig. 6.25., 6.26., 6.27.**).

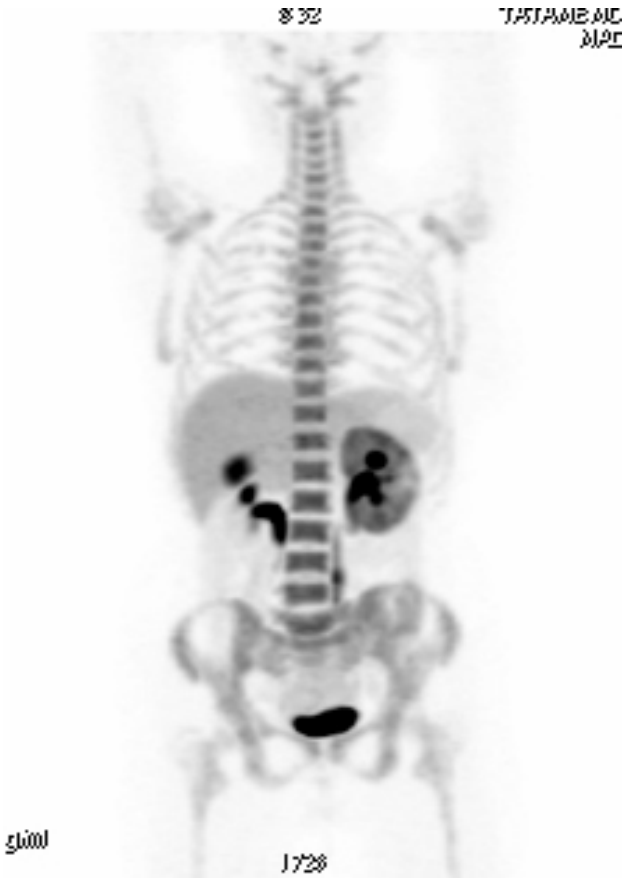

Fig.6.24. *[^{18}F]FLT scan of a healthy volunteer. Showing good uptake in bone marrow (tissue with highly proliferative cells), kidney and bladder (normal excretory channel), no uptake in brain which is advantageous in comparison to [^{18}F]FDG for imaging brain tumor patients*

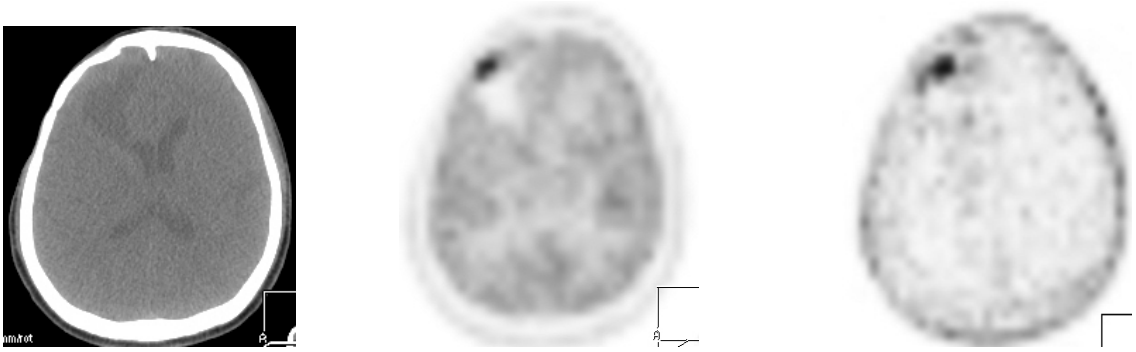

CT **[^{18}F]FDG PET** **[^{18}F]FLT PET**

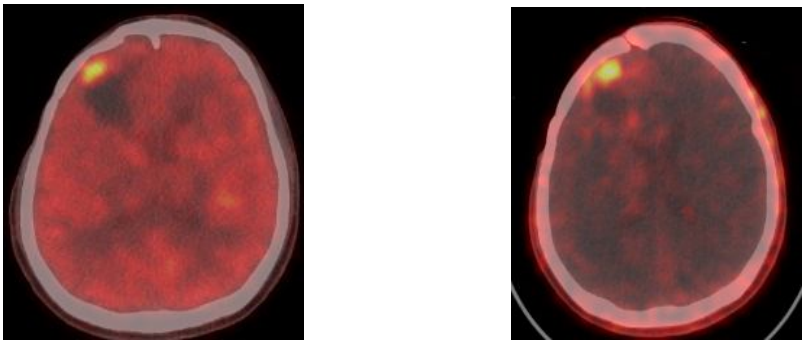

[^{18}F]FDG PET/CT **[^{18}F]FLT PET/CT**

Fig. 6.25. *Comparison of [^{18}F]FDG and [^{18}F]FLT scan of a 43 Year Old, Male Glioma patient. In case of [^{18}F]FDG scan, the background is very high due to normal [^{18}F]FDG uptake but in the [^{18}F]FLT scan, there is no such back ground. In this case, in both the scans, the uptake of the tracer in glioma is clearly visible as the size of the glioma is bigger*

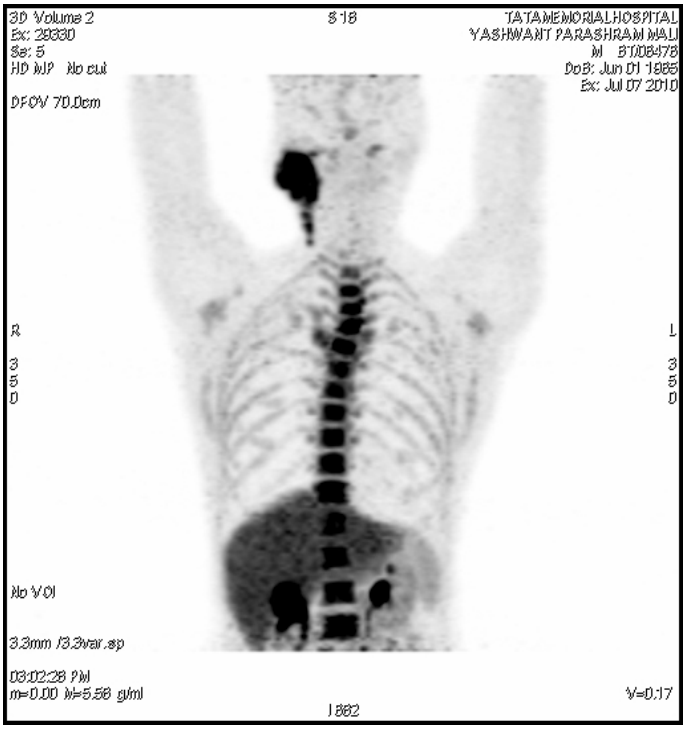

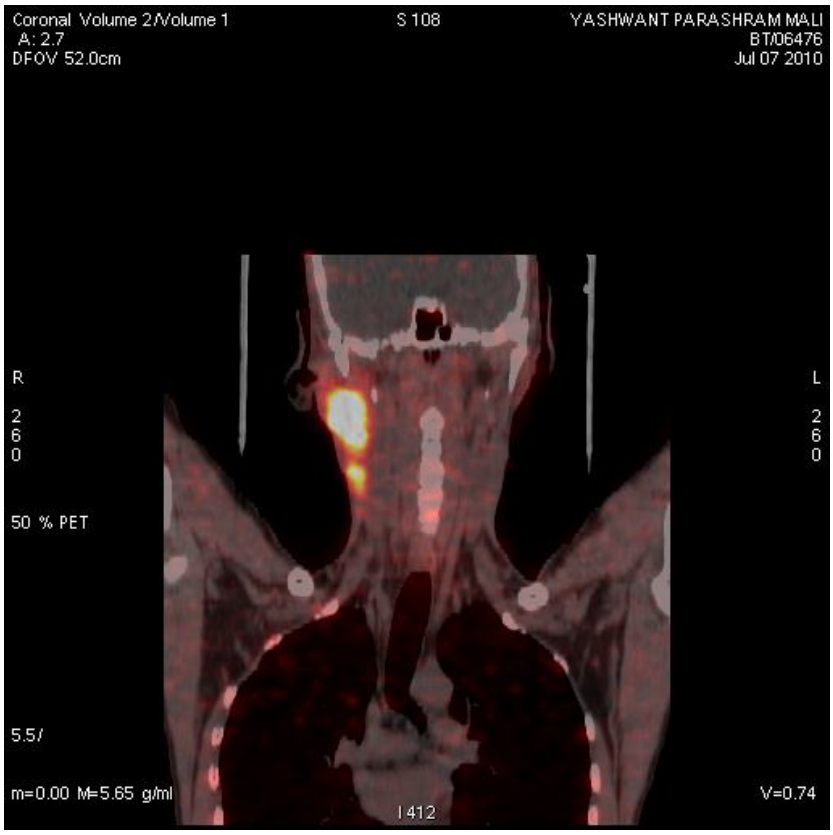

Fig. 6.26. *[^{18}F]FLT Scan, Positive for metastasis*

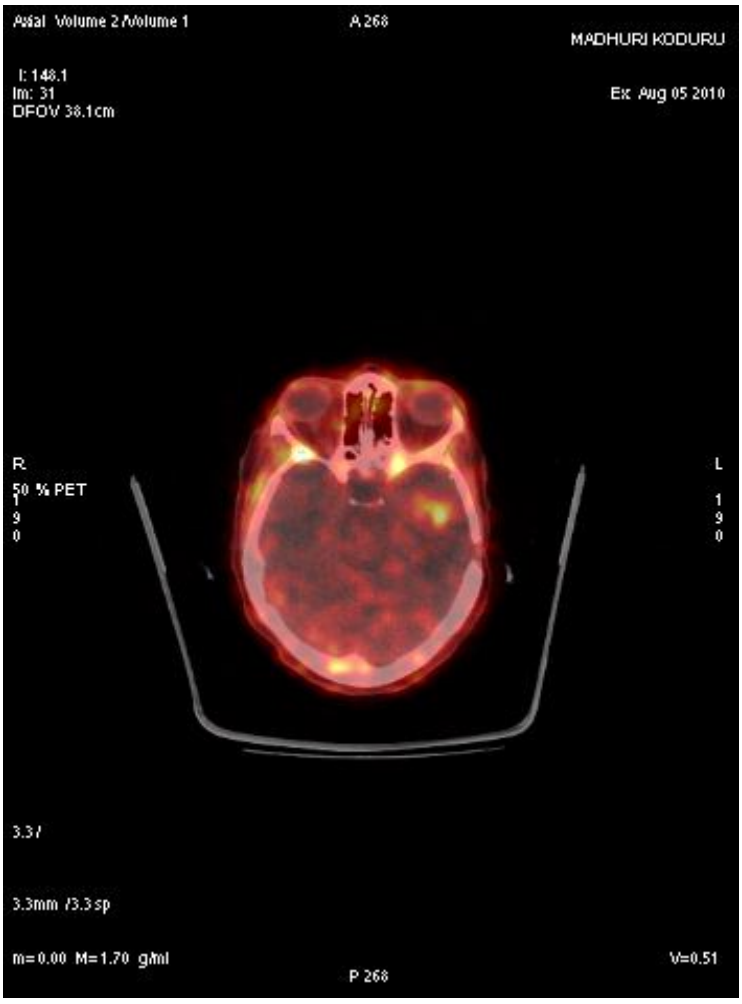

Fig.6.27. *Astrocytoma Recurrence Patient, [^{18}F]FLT Scan*

6.II.4. Conclusion

A simple, fully automated, radiosynthesis procedure for the synthesis of [^{18}F]FLT starting form the anhydro precursor, DMTThy, followed by purification using a single neutral alumina column purification is developed instead of semi preparative HPLC purification. The synthesized [^{18}F]FLT is radiochemically pure and DMSO is the only chemical impurity but well below the permissible limit in the synthesized [^{18}F]FLT [222]. This is achieved in a general purpose fluorination module similar to that for FDG synthesis like the GE TRACERlab FX_{FDG} with

considerable yield of 8.48 ± 0.93 % (n = 5) without decay correction in 68 ± 3 min. The synthesis procedure is very simple, fast, reliable and very similar to [^{18}F]FDG synthesis procedure with consistent radiochemical yield. The regulatory clearance for the routine production for distribution to hospitals and clinical use was obtained in January 2010 and from May 2010, routine production and clinical use is started. This new procedure can easily be used for the routine production of [^{18}F]FLT using commercially available FDG synthesis modules from different vendors.

CHAPTER 7

Fully automated radiosynthesis of 16-α-[^{18}F] Fluoroestradiol ([^{18}F]FES), using a single neutral alumina column-cartridge for purification

7.1. Introduction

The estrogen receptors (ER) PET imaging of metabolic activity in breast tumors with [^{18}F]fluorodeoxyglucose (FDG) is now a well-established procedure [223], and FDG-PET can be used to monitor tumor response to therapy [223-228]. The ability to predict whether a patient is likely to respond to hormone therapy would be beneficial in instances where the ER status of breast tumors is unclear, such as in cases of recurrent or metastatic breast cancers inaccessible to biopsy or in the presence of multiple sites of disease development [229-231]. Estrogen receptor imagings with PET or SPECT are potential tools being evaluated for this purpose in several centers [232].The PET tracer, 16-α-[^{18}F]Fluoroestradiol ([^{18}F]FES) has been shown to be a specific tracer of estrogen receptors in normal breast tissues and in breast cancer [233-238] and the uptake of [^{18}F]FES in breast tumors correlates with *in vivo* estrogen receptor content of tumors, as assessed by in vitro radioligand assays [238]. [^{18}F]FES was first synthesized by nucleophilic displacement of the aliphatic triflet 3, 16β-bis (trifluoromethane sulfonyloxy) estrone using tetrabutyl ammonium [^{18}F]fluoride, followed by acid hydrolysis and ketone reduction. The overall radiochemical yield of [^{18}F]FES of 30% was reported in about 90 min using high performance liquid chromatography (HPLC) purification [235]. This process when automated gave only an overall yield of 6% in 80 min and the low yield was reported to be due to certain operations that could not be carried out

as efficiently as in the manual procedure [239]. A one-pot synthesis of [^{18}F]FES has been described by the nucleophilic fluorination of 3-methoxymethyl-16β,17β-epiestriol-O-cyclic sulfone with an overall radiochemical yield of 30-45% in 60-120 minutes with a specific activity of about 37GBq/μmol (1 Ci/μmol) [240]. However, the reported procedure is particularly complex due to the necessity of HPLC purification of the intermediate as well as the final product. The fully automated synthetic procedure becomes much more complicated as three separate hydrolysis steps are required to ensure complete removal of the protecting groups ending up in the final crude product [241-243]. Oh et al. [244] have reported an automated method of [^{18}F]FES production using a commercial FDG module (GE TracerLab MX) and a modified disposable cassette system, resulting in consistently high radiochemical yields. The purification was achieved by semi-preparative HPLC. Recently, a fully automated synthesis procedure for large-scale production of [^{18}F]FES for clinical use has been reported using a minimal amount of precursor, reduced number of hydrolysis steps and a single terminal purification by HPLC [245] and an in-house modified commercial automatic synthesis unit (ASU) purchased from Advanced Cyclotron Systems (Richmond, British Columbia, Canada).The total synthesis time is reported to be 73 min with very high radiochemical purity (>99%) but with a wide range of decay corrected yield (15-35%). The summary of the available radiosynthesis procedure indicates that none of them can straightway be adapted to our general purpose fluorination module which in principle is very similar to GE TRACERlab FX_{FDG}. The main practical difficulty is that, to become successful, a single column or cartridge purification method has to be developed based on combination column or SEP-PAK® cartridges. Guided by this idea, a fully automated radio synthesis procedure for [^{18}F]FES by the nucleophilic fluorination of the MMSE precursor and subsequent purification using a neutral alumina column-cartridge has been developed.This

chapter describes in details the fully automated radiosynthesis procedure developed by us including the quality control analysis of the synthesized [^{18}F]FES, analysis of radiochemical and chemical impurities and bio-distribution study by PET/CT imaging of healthy female rabbit showing localization of radioactivity in the target organ (mammary gland). The ultimate benefit of this work is that this important PET RP will be available for the service of patients as it can quite easily be made in most centres that make [^{18}F]FDG.

7. 2. Materials & Methods

7.2.1. Reagents and apparatus

The precursor of [^{18}F]FES synthesis i.e. 3-O-methoxymethyl-16β,17β-O-sulfuryl-estra-1, 3,5(10)-triene-3,16β,17β-triol (MMSE), FES reference standard, 75mM $TBAHCO_3$ solution, DNA grade acetonitrile, 10% NaCl, 1M HCl, 1M NaH_2PO_4 buffer, sterile and pyrogen-free water for injection and pharmaceutical grade ethanol were procured from ABX Advanced Biochemical Compounds, Germany. Fluorine-18 separation cartridge, Chromafix 45-PS-HCO_3, was obtained from Marcherey-Nagel, Germany. Aluminium oxide active (neutral, activity I-II) for column chromatography was procured from MERCK, India. Evacuated 10 ml vials (sterile and pyrogen free) were obtained from ACILA AG, Germany. Minisart 0.2μ filters (Sartorius®) were purchased locally. Sterility tests were carried out in-house using standard protocol. Radioactivity was measured using a dose calibrator (Capintec CRC-15R). Radiofluorination and conversion of MMSE to [^{18}F]FES was carried out in a Nuclear Interface Module (Munster, Germany) configured for general-purpose fluorination and extensively used for [^{18}F]FDG production. Radio-HPLC analysis was carried out in a Knauer system (Germany) with a tunable UV absorption detector and a radiometric detector system using a C-18 reverse phase analytical column (Nucleosil, 5μM, 250 × 4 mm). The UV absorption was monitored at 254 nm. Radio

TLC was carried out on Silica Gel 60, 20 × 20 and Silica Gel 60 F_{254}, 20 × 20 (Merck, Germany) and scanned using a RayTest TLC scanner with a BGO scintillation detector and the spectrum was analyzed with GINA® software. Mass spectra were recorded by Electron spray ionization-Mass spectrometry (ESI-MS) (Q-TOF micro YA-105, Micromass). Aluminium-Test Kit, Microquant® (Detection limit: 0.1-6 mg/l) were procured from Merck, India. All other chemicals used were of either HPLC or analytical grade and procured locally. All animal experiments were carried out as per guidelines set for animal experiments and after approval from the BARC Animal Ethics Committee.

7.2.2. [^{18}F]FES purification column-cartridge

The [^{18}F]FES purification column-cartridge is a ready to use one and is composed of neutral alumina, active, grade I-II (Brockmann) and made in-house. In brief, 6g of neutral alumina (dry weight) was thoroughly washed with sterile, de-ionized water to remove fine particles. After removal of fine particles, it was soaked into water for 6-7 hours. Then, dried with the application of vacuum. When it becomes free flowing, it was packed inside a polypropylene cartridge barrel (6.5 cm × 1.2 cm) very firmly avoiding the formation of any kind of air bubbles or looseness. The top and bottom of the column-cartridge were attached with 20-µm-polyethylene frits. The column-cartridge was washed thoroughly by passing 20 ml of sterile and bacterial endotoxin free water just before use.

7.2.3. Fully Automated radiosynthesis of [^{18}F]FES

The most commonly followed route for the synthesis of [^{18}F]FES, is the nucleophilic substitution at the 16β position of MMSE by [^{18}F]fluoride followed by hydrolysis of the protecting groups [**Fig.7.1.**] The fully automated synthesis of [^{18}F]FES was based on this scheme and consists of three main steps. 1) Nucleophilic fluorination of MMSE 2) Deprotection and 3) Purification

through a neutral alumina column. [^{18}F]fluoride from the cyclotron was first trapped on a Chromafix 45-PS-HCO_3 anion exchange cartridge. This is then eluted from the column using 75mM $TBAHCO_3$ (0.4 ml) to the reaction vessel. The [^{18}F]TBAF fluoride was then dried by azeotropic distillation with acetonitrile (0.8 ml). To the dry [^{18}F]TBAF, the MMSE precursor (2mg) dissolved in acetonitrile (0.6 ml) was added and the S_N2 fluorination reaction carried out at 115°C for 15 min. The acetonitrile was then evaporated from the reaction mixture and acid hydrolysis was carried out by the addition of 1N HCl (1 ml) at 120°C for 15 min. The reaction mixture was cooled to 50°C and then loaded on the neutral alumina column-cartridge. The reaction vessel was rinsed with 5% ethanolic water (1.5 ml) and this was passed through the column-cartridge directing the eluent to the waste. [^{18}F]FES was then eluted from the column using 15% aqueous ethanol solution (14ml) and was collected in the product vial containing 10% NaCl (1.7 ml) and 1M NaH_2PO_4 (0.7 ml). The alcohol content was brought to the permissible limit by further diluting with 10 % NaCl. [^{18}F]FES collected in the product vial is then transferred to an automated dispensing unit and dispensed into different vials in a class 100 area through a 0.2 μM filter. The [^{18}F]FES was obtained as a clear, colorless solution, free of any suspended particles.

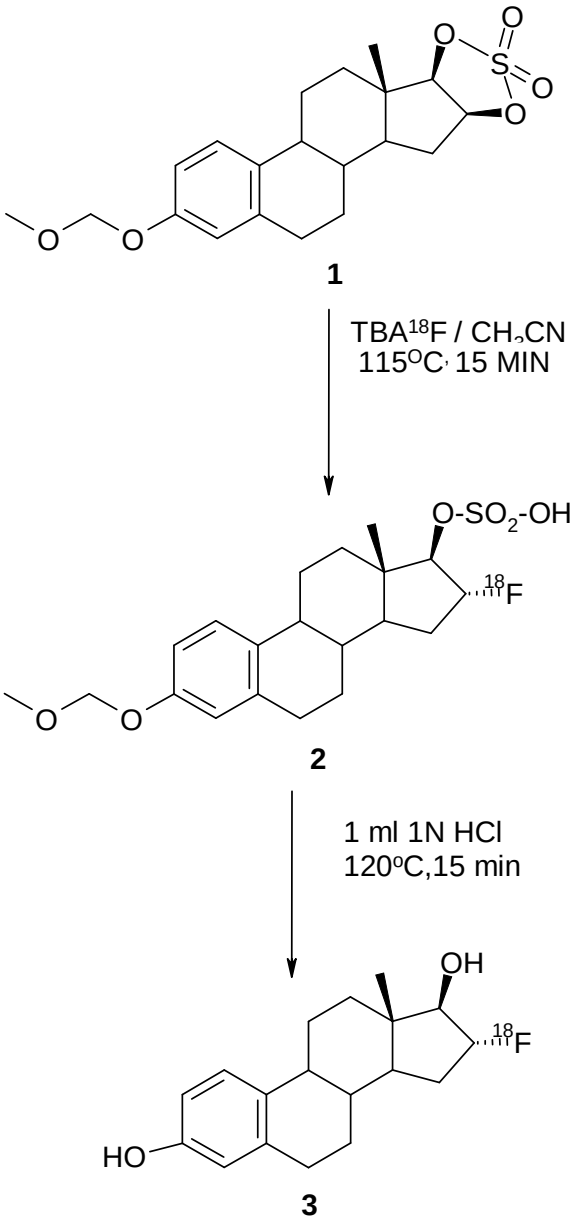

1. 3-O-methoxymethyl-16-beta-17-beta-O-sulfuryl-estra-1,3,5(10)-triene-3,16-beta,17-beta-triol(MMSE)
2. 3-O-methoxymethyl-16-alpha-[^{18}F]fluoro-estra-1,3,5(10)-triene-3,17-beta-diol-17-beta-sulfate
3. 16-alpha-[18F]fluoroestradiol([18F]FES)

Fig. 7.1. *Schematic representation of [^{18}F]FES synthesis from MMSE*

7.2.4. Quality control

The pH of [^{18}F]FES was checked with pH test paper strip. The radiochemical purity was first checked by radio-TLC using a silica gel 60-coated plate developed in methanol/ammonia (95:5, v/v) solvent system. TLC of the reference standard FES was also developed in the same solvent and stained with iodine vapour for comparison. Additionally the chemical and radiochemical purity were also analyzed using an analytical HPLC (Sample volume: 25 µl) by monitoring the UV absorbance (λ = 254 nm) as well as the radioactivity profile. The mobile phase consisted of 90% MeOH and 10% water and HPLC was done with an isocratic system at a flow rate of 0.5 ml/min. The presence of non-radioactive impurities was also verified under similar HPLC conditions by analyzing pure MMSE, reference-standard FES and a mixture of the two. Finally [^{18}F]FES prepared was confirmed by co-eluting peaks (radioactive as well as UV) in HPLC analysis and comparing the UV peak of [^{18}F]FES with that of cold reference standard of FES.

7.2.5. Test for aluminum ions

The samples were analyzed by Microquant® Al test kit as per standard protocol, to check if any dissolved aluminium, from the alumina column-cartridge is transmitted in the final synthesized [^{18}F]FES and quantify.

7.2.6. Sterility and Bacterial Endotoxin Tests

Sterility tests were performed in accordance with the Indian Pharmacopoeia, 1996 and addendum 2005 protocol. In this test, 1 ml of the [^{18}F]FES sample after radioactive decay was inoculated in fluid thioglycollate medium at 37°C for 14 days to observe the growth of aerobic and anaerobic bacteria. Similarly, 1 ml of the [^{18}F]FES sample was also inoculated in soyabean casein digest medium at 22-25°C for 14 days to detect fungal growth.

The bacterial endotoxin test was performed in accordance with USP XXV. The test was based on the formation of gel clot in the sample by Limulus Amoebocyte Lysate (Sensitivity: 0.125 EU/ml) reagent.

7.2.7. PET-CT imaging

The normal biodistribution of [^{18}F]FES was studied by PET/CT (Discovery ST, GEMS, GE, USA) imaging of normal healthy female rabbit (~2.5 Kg).[^{18}F]FES (~111 MBq / 1.0 ml) was injected intravenously through the ear vein. Images were recorded 2 hrs post injection after the rabbit was suitably anesthetized.

7. 3. Results & Discussion

Starting from the precursor, MMSE, [^{18}F]FES was prepared in a synthesis module configured for [^{18}F]FDG synthesis. Purification was achieved using a single neutral alumina cartridge-column. The radiochemical yield obtained (without decay correction) was 11.5 ± 1.6% (n = 5) (**Table 7.1.**). The radiochemical yield was expressed as the percentage

Table 7.1. Radiochemical yield of [^{18}F] FES

Sr. No	^{18}F in the reaction vessel (MBq)	[^{18}F]FES produced (MBq)	% Yield*
1	**3,700**	**340.4**	**9.2**
2	**12,950**	**1,665**	**12.86**
3	**24,050**	**2,590**	**10.77**
4	**27,010**	**3,145**	**11.64**
5	**29,600**	**3,885**	**13.13**

* Without decay correction

of radioactivity finally obtained as [^{18}F]FES compared with the total ^{18}F activity obtained in the reaction vessel without applying decay correction. Early in 1980s, after considering [^{18}F]FES as a suitable imaging agent for estrogen receptor, Kieswetter et al. [234, 246] first synthesized 16α-[^{18}F]FES with a radiochemical yield of 30-60% within a total synthesis period of 70-110 min using bis-triflate of 16β-hydroxyestrone as a precursor coupled with HPLC purification. Lim et al. [240] first demonstrated the synthesis of [^{18}F]FES using MMSE as a precursor with an overall radiochemical yield of 50-60% within a synthesis period of 60 min. In this case also, complicated and time consuming HPLC purification was the purification procedure utilized. Later on many reports came out finding difficulties in the hydrolysis step to achieve the final [^{18}F]FES. Römer et al. [243] thus extensively studied the radio synthesis of [^{18}F]FES and tried to solve out the difficulty in hydrolyzing the protecting groups. According to them, heating in a closed bulb at 135°C for 15 min with 1ml 1M HCl, after the MeCN was evaporated from the radio-fluorinated reaction mixture, formed 16α-[^{18}F]fluoroestradiol in high yield. But the semi-preparative HPLC was the choice of purification process. Oh et al. [244] reported a high yield radio synthesis procedure based on specially and extensively modified GE TRACERlab MX [^{18}F]FDG module and modified disposable cassette system for [^{18}F]FDG. They have reported a decay corrected radiochemical yield of 45.3 ± 2.8% with 2 mg of precursor, MMSE. In this study also, HPLC is the purification procedure and the eluted [^{18}F]FES is to be again re-trapped in C-18 column to reduce the alcohol content in the final injectable and then to be re-eluted with 1 ml EtOH and 4 ml of 0.9% NaCl. The procedure is quite complicated in comparison to [^{18}F]FDG synthesis using solid phase extraction (SPE) cartridges using GE TRACER lab FX_{FDG} module. The main interest of the present study is to develop a radio-synthesis procedure very similar to above mentioned [^{18}F]FDG synthesis which can be easily executed with very simple GE

TRACERlab FX_{FDG} module ensuring the economic use of costly automated synthesis module. Additionally, the possibility of using a single neutral alumina column for purification is explored out. The final [^{18}F]FES obtained was clear, colourless and free of any suspended particles as confirmed by visual checking. The pH was in the range of 6.5-7.0. The entire synthesis was monitored by TLC at the three important steps, viz (1) after radiofluorination of the precursor, MMSE (2) after acid hydrolysis of the ^{18}F-substituted MMSE and finally (3) after purification through the neutral alumina cartridge and elution with 15% ethanolic water. The TLC of the radiofluorinated MMSE showed the presence of free [^{18}F]fluoride with a R_f of 0.04 whereas the radiofluorinated MMSE was observed as a broad peak with a R_f of 0.5 as shown in [**Fig. 7.2.**]. The radio-TLC pattern of acid hydrolyzed radiofluorinated MMSE was having an extra peak at R_f of 0.7 in addition to the two peaks at R_f of 0.05 and 0.5 which corresponds to free [^{18}F]fluoride and another to radiofluorinated MMSE [**Fig.7.3.**]. If we critically analyze the results obtained in these two TLCs, it is very clear that the additional radioactivity peak corresponds to the presence of [^{18}F]FES in the hydrolyzed reaction mixture. The TLC of the final purified [^{18}F]FES showed only one peak with an R_f of 0.69 as shown in [**Fig. 7.4(a).**] which confirms the absence of free [18F]fluoride The difference in the R_f values of the radiofluorinated reaction product of MMSE ([^{18}F]MMSE) and [^{18}F]FES were in accordance with their polarity. The presence of [^{18}F]FES was further verified by comparison with a reference standard FES by TLC under identical conditions. Visualization of the spots was achieved by iodine staining. The R_f value of [^{18}F]FES exactly matched with that of reference standard FES [**Fig.7.4(b).**].This confirms the radiochemical purity of the synthesized [^{18}F]FES. The HPLC chromatogram of [^{18}F]FES doped with reference standard FES is

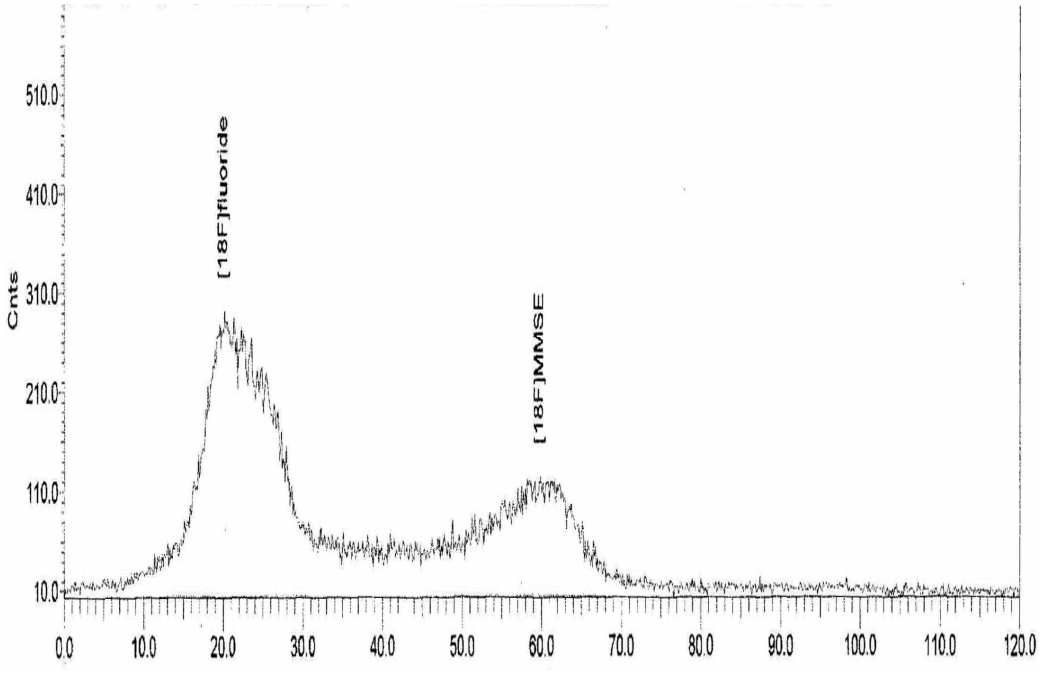

Fig.7.2. *Radio-TLC of radiofluorinated MMSE. Two peaks with R_f values of 0.04 (corresponding to free $^{18}F^{-}$) and 0.5 (Radiofluorinated MMSE).*

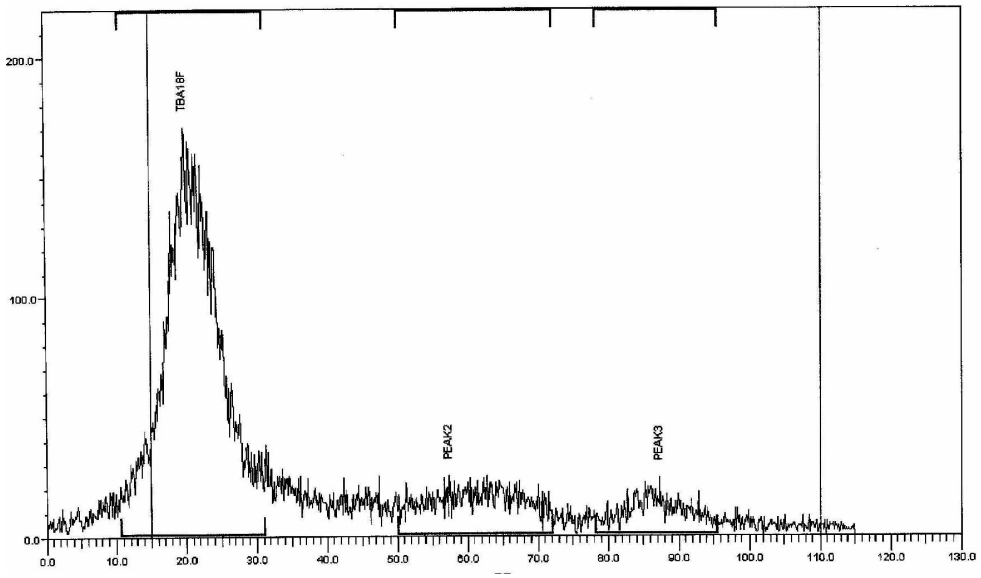

Fig.7.3. *TLC of acid hydrolyzed radiofluorinated MMSE, showing three different peaks with R_f values of 0.05 (free $[^{18}F]F^{-}$), 0.5 (radiofluorinated MMSE) and 0.7($[^{18}F]$FES)*

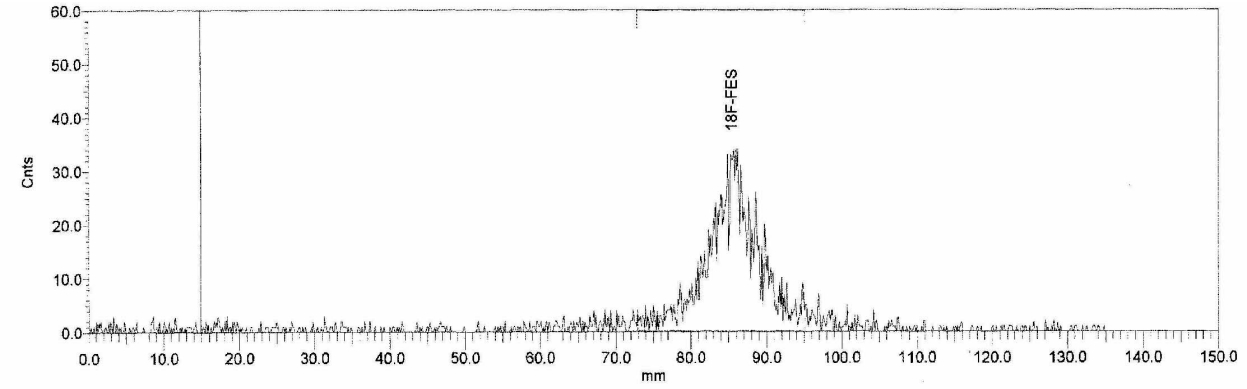

No	Name	Max.Pos mm	Pos mm-mm	rf_center	rf_max	I Cnts	%s %	%t %
1	18F-FES	85.6	72.9-95.1	0.69	0.71	1784.0	100.00	75.63
	Total					2359.0	132.23	100.00
	Sum					1784.0	100.00	75.63
	Rem					575.0	32.23	24.37

(a)

(b)

Fig. 7.4. *(a) RadioTLC of [^{18}F]FES (b) TLC scan of the reference standard [^{19}F]FES developed in the same solvent and stained by iodine vapour, R_f range: 0.68-0.76*

shown in **Fig. 7.5(a).**. From the chromatogram it is seen that the retention time of [^{18}F]FES is 10.75 min and the corresponding retention time from the UV chromatogram is 11.58 min. The difference in the retention times of radioactivity and UV peak was due to the fact that in our HPLC system, the sample after injection, faces the radioactivity detector first and then the UV detector and the connecting tubing length of these two detectors is quite long. The retention time of [^{18}F]FES was validated using a reference FES standard **Fig. 7.5(b).** under identical HPLC condition**.** The presence of UV active non-radioactive

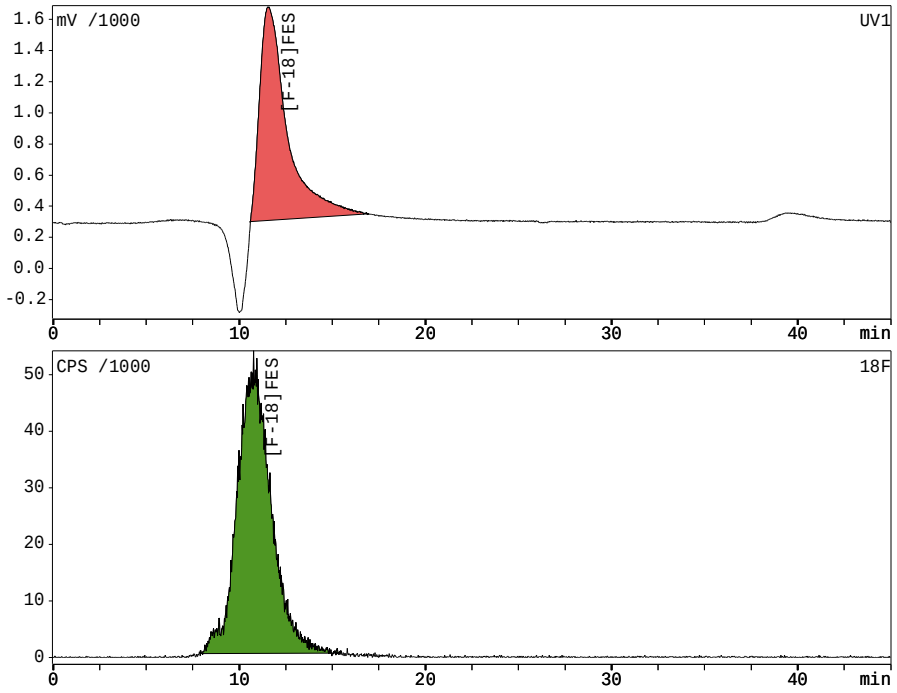

(a)

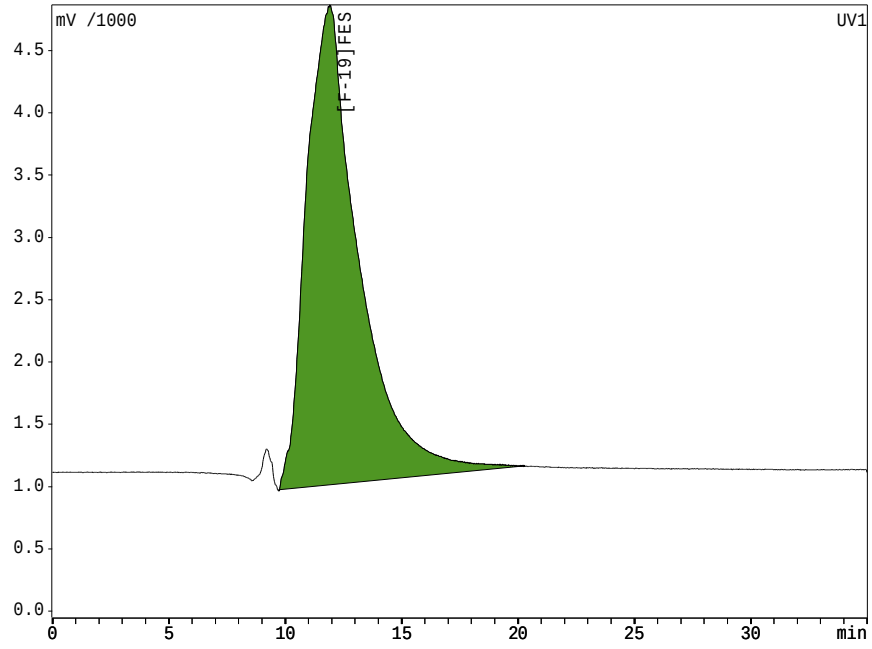

(b)

Fig. 7.5. *(a) Radio HPLC of [^{18}F]FES doped with reference standard [^{19}F]FES (green peak = radioactive peak, red peak = UV peak) (b) HPLC of reference standard FES (UV peak, λ = 254 nm)*

impurities were also examined. The precursor, MMSE shows a retention time of 17.03 min. When a mixture of MMSE and reference standard FES were analyzed two well resolved peaks were obtained at 11.00 min (FES) and 15.03 min (MMSE) respectively [**Fig.7.6.**].

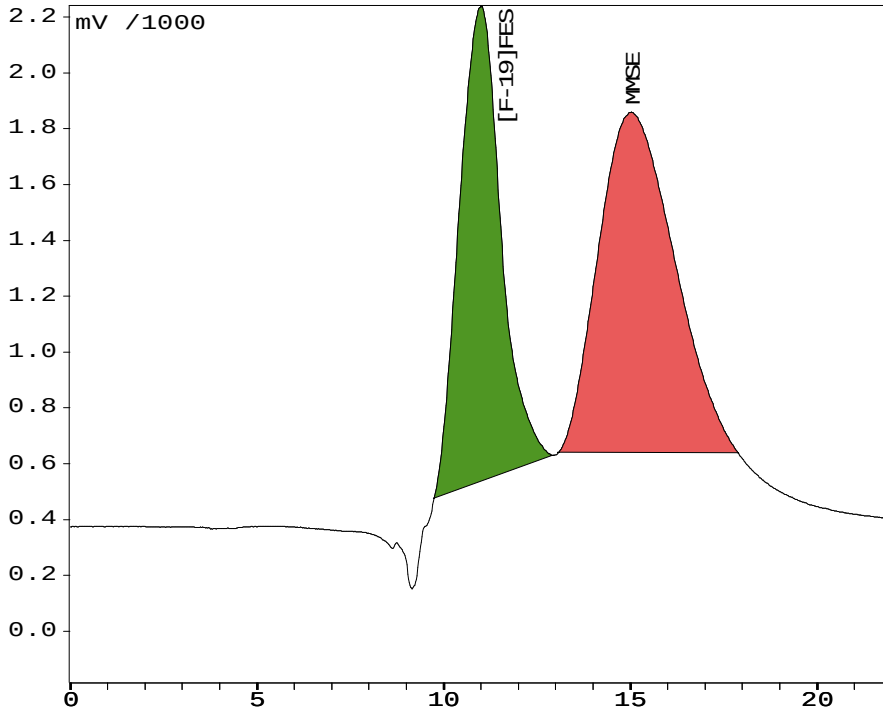

Fig. 7.6. *HPLC chromatogram of a mixture of MMSE and reference standard FES (UV, λ = 254 nm)*

No 17-β-estradiol is present in the synthesized [^{18}F]FES which if present would have been observed as an extra UV peak with a retention time of 13.53 [**Fig.7.7.**] min under identical HPLC conditions. The mass spectrum of the decayed sample of [^{18}F]FES [**Fig.7.8.**] obtained by Electron Spray Ionization (ESI-MS) displays a major peak at *m/z* 242.2362. This corresponds most probably to TBA^+ cation [$(C_4H_9)_4N^+$] or due to molecular ion peak of a chemical structure where the carbon skeleton of the steroid remains intact and one – OH group is attached to the 3 position of the aromatic ring [**Fig. 7.9. (a)**]. This may be formed when the cyclic sulphate

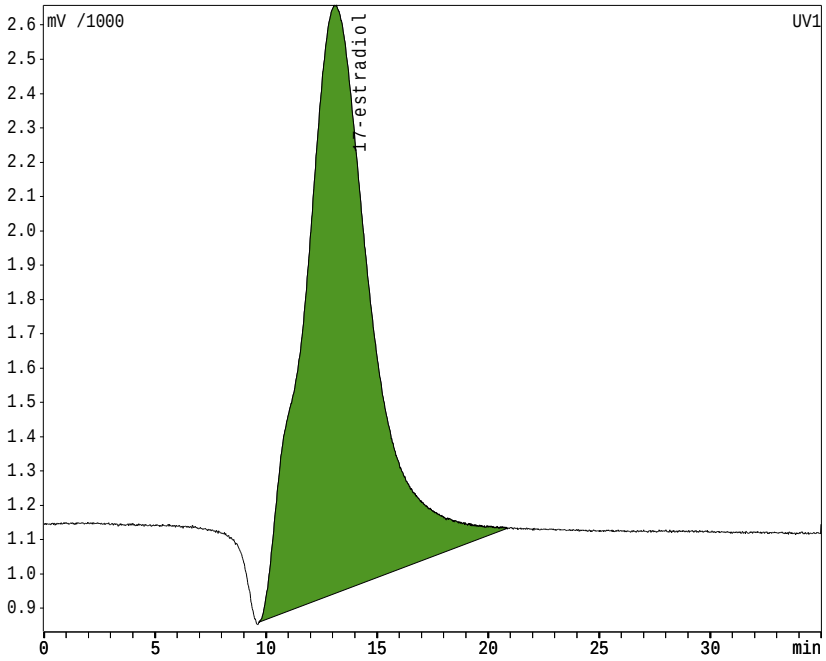

Fig. 7.7. *HPLC chromatogram of 17-β-estradiol [UV (λ = 254 nm), R_t : 13.53 min*

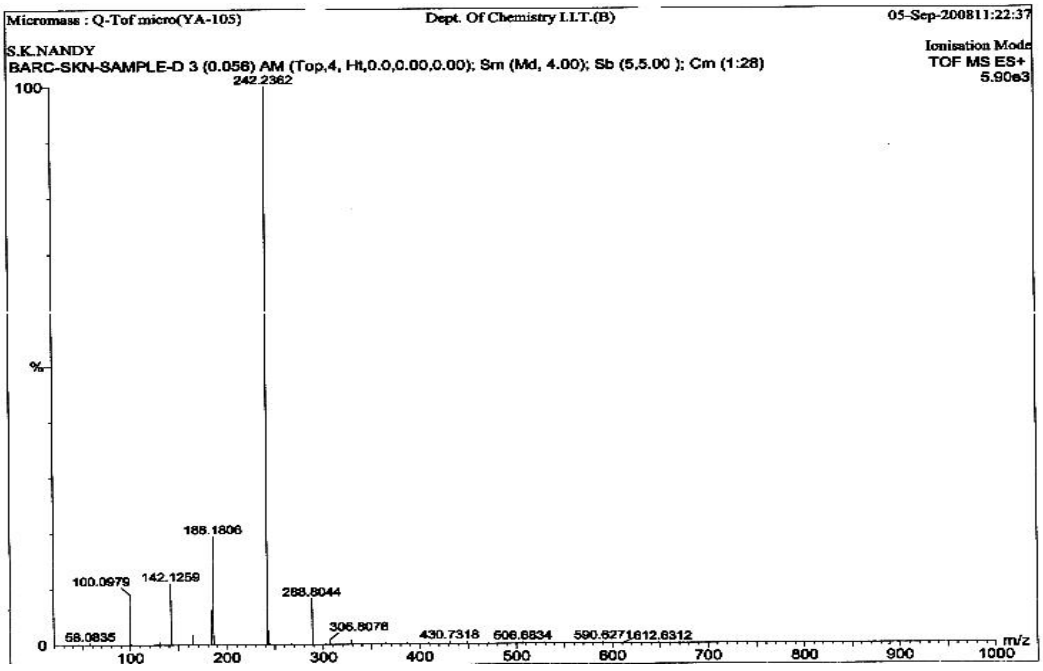

Fig.7.8. *Mass spectrum (ESIMS) of decayed sample of [^{18}F]FES*

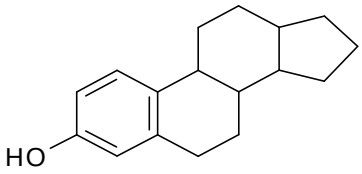

(a)

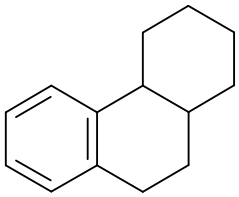

(b)

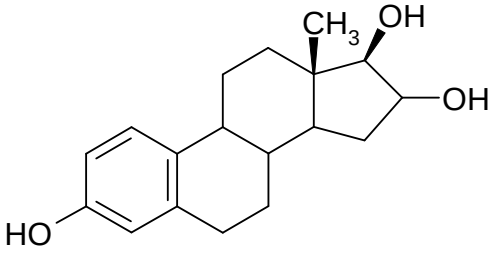

(c)

Fig. 7.9. *Probable structures correspond to m/z values*

ring is totally knocked out from the precursor MMSE under drastic synthesis conditions. The mass spectrum also confirms that the synthesized [^{18}F]FES does not contain any 17-β-estradiol (natural estradiol) as an impurity since no molecular ion peak is seen at *m/z* 272.38. This is important since it can saturate the receptors thereby reducing the uptake of [^{18}F]FES. This is a strong supportive proof of the radio HPLC analysis of the synthesized [^{18}F]FES. There are four more peaks at *m/z* 100.0979, 142.1259, 186.1806 and 288.8044. The first two of them may correspond to sulphuric acid and sulphate salts. The peaks of *m/z* 186.1806 and 288.8044 correspond to structures as shown in **Fig. 7.9(b).** and epistrol **7.9(c)**. The presence of this compound within the synthesized [^{18}F]FES may have an adverse effect if it can saturate over

expressed ER in ER+ breast tumor thereby reducing the uptake of [^{18}F]FES. This part needs further evaluation.

Analysis with Microquant® Al^{3+} test kit (sensitivity 0.1-6µg/ml) based on Chromazurol S method confirmed that Al^{3+} in the final [^{18}F]FES was in the range of 3-4µg/ml, which was within the permissible levels-as applicable for $^{99m}TcO_4^-$ eluting from ^{99}Mo - ^{99m}Tc alumina generator. PET/CT images of the female rabbit were recorded two hours post injection and are shown in **Fig. 7.10(a)** and **7.10(b)**. Distinct localization of radioactivity was observed in the mammary gland of the rabbit, which is known to have estrogen receptors. This indirectly proves once again the radiochemical purity of the synthesized [^{18}F]FES. No uptake in bone confirmed the absence of free [^{18}F]fluoride.

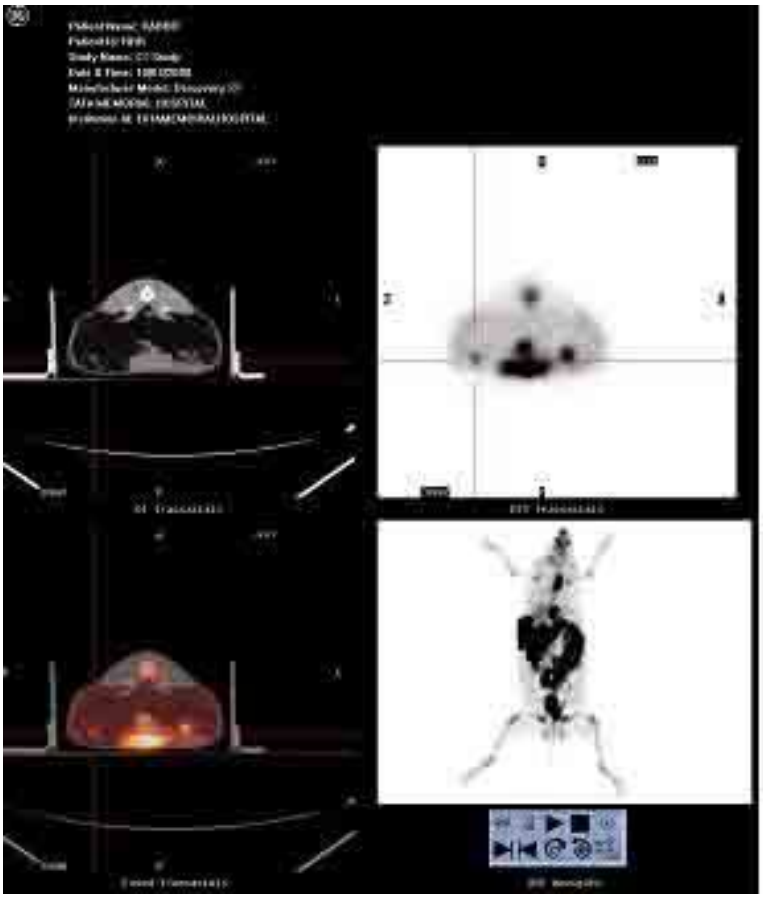

7.10(a)

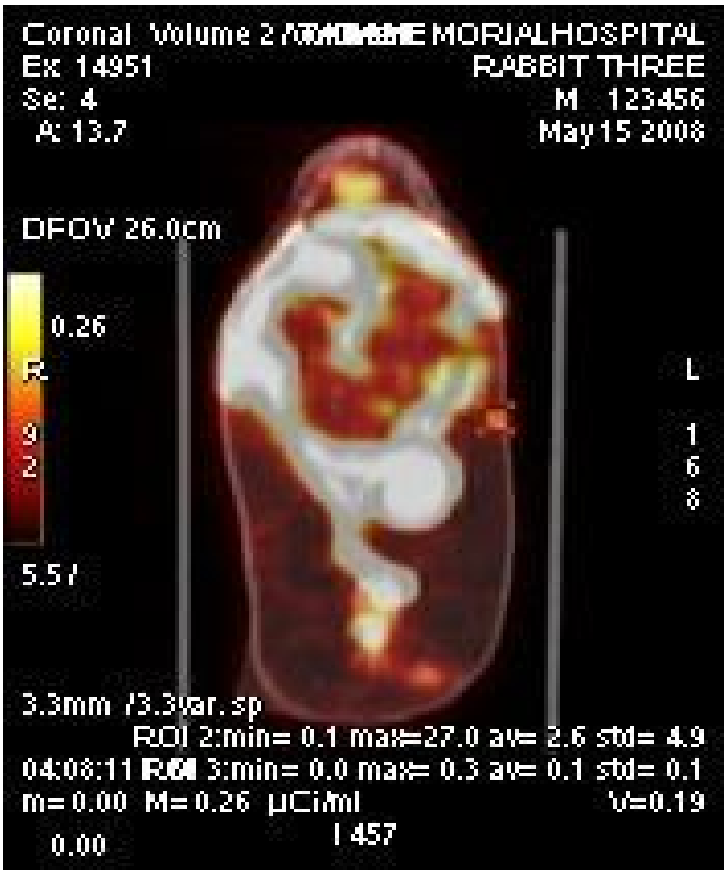

7.10(b)

Fig. 7.10. (a & b). *PET/CT Scan of female rabbit following [^{18}F]FES injection showing distinct uptake in mammary gland which are known to have high ER concentration (Two Hours Post Injection)*

Neutral alumina is a known to be good adsorber of fluoride ions. As noticed in the radio TLC of the reaction mixture of MMSE after hydrolysis, free [^{18}F]F$^-$ is the main radioactive impurity which can be easily trapped by using sufficient quantity of neutral alumina. Further, from the radio TLC mentioned above, it is very clear that only a percentage of the ^{18}F-labeled MMSE is getting hydrolyzed under the hydrolysis condition which is the main reason of its low yield also. Since ^{18}F-labeled MMSE is much more lipophilic in comparison to [^{18}F]FES, it will have a strong interaction with neutral alumina. So, if the eluting solvent volume as well as composition

is cleverly chosen, [^{18}F]FES can be selectively eluted out and in the present case, 25 % ethanol containing water serve the purpose.

7.4. Conclusion

A fully automated radio synthesis procedure of [^{18}F]FES utilizing our general purpose fluorination module very similar in configuration to GE TRACERlab FX_{FDG} is developed. Considering the unavailability of a synthesis module equipped with semi-preparative HPLC purification facility, an alternate purification procedure based on single neutral alumina column-cartridge purification has been attempted so that the developed method can easily be applied with any standard FDG synthesis module, making this important PET RP available to the patient. The overall radiochemical yield 11.5 ± 1.6 % (n = 5) without decay correction is less in comparision to the reported procedures using semi-preparative HPLC but the use of using single neutral column for purification makes the radiosynthesis process very user friendly. The total synthesis time is 65 ± 1 minutes.

CHAPTER 8

A Simple, column purification technique for the fully automated radiosynthesis of ethyl [^{18}F]Fluoroacetate ([^{18}F]EFA) as a proradiotracer of [^{18}F]fluoroacetate ([^{18}F]FA) for the measurement of *glial metabolism by PET*

8.1 Introduction

Glial cells are the main effector cells of innate immune responses to neuronal damage in the central nervous system (CNS). Microglia and astrocytes are strongly activated in response to neuronal damage, producing an array of inflammatory mediators and performing phagocytic functions. Therefore, selective imaging of glial cell activity may be a valuable method to determine the extent and progress of disease and to access a therapeutic intervention [247]. Furthermore, changes in glial metabolism in brain ischemia, Alzheimer's disease, depression, schizophrenia, epilepsy and manganese neurotoxicity have been reported. Undisputedly, the measure of glial metabolism *in vivo* for the elucidation and diagnosis of these diseases has significant importance [248].

Previous reports showed that radiolabeled acetate, ^{3}H-acetate, and its Fluoro analog, ^{3}H-fluoroacetate accumulated selectively in glial compartments and were proposed as potential tracers of glial oxidative metabolism [249]. Recently, 1-^{11}C-acetate was successfully used for PET detection and characterization of gliomas [250, 251]. 2-Fluoroacetate, a metabolic poison also known as compound 1080, has attracted considerable attention as a specific inhibitor of glial cell metabolism, and it has been extensively used in brain metabolism studies [252-254]. 2-Fluoroacetate is selectively transported to the glial metabolic compartment [249] and converted to fluoroacetyl-CoA and then to 2-fluorocitrate in the Krebs cycle [255].

Radiolabeled 2-fluoroacetate was proposed as a metabolic tracer for the CNS more than 20 years ago [249], and its toxicity is not an issue when a minute amount of no-carrier added (n.c.a.) radiotracer is used [256], [^{18}F]FAC has also been evaluated as an alternative to 1-^{11}C-acetate for imaging of prostate carcinomas in mouse model [257] and in human patients [258]. In a very recent study [247], the use of [^{18}F] FAC as a specific PET tracer of glial cell metabolism in rodent models of glioblastoma, stroke, and ischemia-hypoxia has been reported with very encouraging result. Howevr, for brain studies, the low blood-brain barrier (BBB) permeability of anionic form like FA is a fundamental problem.

To resolve this problem, two approaches have recently been reported. One approach using 1-^{11}C – octanoate has been reported by Kuge et al. [259, 260] and Yamazaki et al [261]. The strategy was to use a highly lipophilic fatty acid for blood-brain barrier (BBB) permeability and to measure β-oxidation activity in astrocytes. Another approach was a proradiotracer concept reported by Inoue et al. [262] and Momosaki et al. [263]. Here, the BBB permeability is achieved by combining radiolabeled acetate with a highly lipophilic group, and then this proradiotracer is cleaved to radiolabeled acetate and the lipophilic group in brain by carboxyesterase. However, both approaches have limited use because of the 20 min $T_{1/2}$ of carbon -11.

It is well known that ethyl acetate easily enters the brain and is then hydrolyzed to acetate rapidly *in vivo*. Based on these characteristics, [^{18}F]ethyl fluoroacetate [^{18}F]EFA, ethyl-ester of FA, was first proposed by Mori et al. [264] in 2007 as a potential PET tracer of oxidative metabolism in the brain and later evaluated as a proradiotracer by the same workers in 2009 for the measurement of glial metabolism by investigating membrane permeability, ester hydrolysis in the brain and plasma, and PET imaging in common marmosets [248]. Additionally, the longer half-life (110 min)

of Fluorine–18 offers more convenience for the synthesis and metabolism studies of PET radiopharmaceuticals, which can also be applied commercially.

The only one method so far reported [248] for the synthesis of [^{18}F]EFA, isolates it from the reaction mixture after radiofluorination of the precursor, ethyl *O*-mesyl-glycolate by distillation under reduced pressure and then condensing the vapours in ice-cold alcohol with an overall yield of 28.6 ± 3.6 % (decay corrected) in a reasonably short synthesis time of 29 min.

In this study, a novel, straight-forward and fully automated radiosynthesis procedure for ethyl [^{18}F]fluoroacetate ([^{18}F]EFA) is developed, wherein, after the radiofluorination of the precursor, ethyl (p-tosyloxy) acetate, the radiofluorinated reaction mixture is directly trapped on a CHROMABOND® SET V cartridge-column (that is readily available since it is used for [^{18}F]FDG synthesis using alkali hydrolysis). The [^{18}F]EFA is selectively eluted out providing a radiochemical yield of 44.0 ± 1.5 % (n=5, without any decay correction) in a short synthesis time of 32 ±1 minutes using our synthesis module described in Chapter 2.

8. 2. Materials & Methods

8.2.1. Reagents and apparatus

Ethyl (p-tosyloxy) acetate ([^{18}F]EFA precursor), $TBAHCO_3$ solution (75 mM), molecular-grade anhydrous acetonitrile, ^{18}F trapping column (PS-HCO_3) , CHROMABOND® SET V cartridge-columns, pharmaceutical grade ethanol were procured from ABX, Advanced Biochemical Compounds, Germany. Evacuated 10 ml vials certified as sterile and pyrogen free were obtained from ACILA AG, Germany. Minisart 0.2μ filters were purchased from Sartorius. Sterility testing was carried out in-house using a standard protocol. Pyrogen testing was done by LAL test using Endosafe Reagent Kits from Charles River Laboratory, USA (US License No. 1197).

Radioactivity was measured using a calibrated ion chamber (Capintec CRC-15R). All other chemicals used were of HPLC and AR grade and procured locally.

Fig. 8.1. *Ethyl [^{18}F]Fluoro acetate ([^{18}F]EFA) purification column [CHROMABOND SET V, FDG-BASE-HYDR ® (920 mg Ps-H^{+} , 910 Ps-HCO$_3$- , 1520 mg ALOX-N, 680 mg HR-P)]*

The CHROMABOND® SET V has cation exchanger (PS-H^{+}, 920mg), anion exchanger (PS-HCO_3, 910 mg), neutral alumina (ALOX N, 1520 mg) and reverse phase (HR-P, 680 mg) [**Fig.8.1.**] The cartridge-columns were conditioned first by passing 20 ml ethanol followed by 100 ml of sterile and bacterial endotoxin free water before use.

HPLC analysis using a C-18 reverse phase analytical column (LiChroCART® 250-4, HPLC cartridge, LiChrospher® 100, RP-18, 5 μm) was done on a Knauer HPLC system equipped with a radiometric detector followed by a variable wavelength UV detector. Radiochemical purity was also evaluated by thin layer chromatography (Silica gel 60, Merck) using a RayTest TLC scanner (Model No. BGO-V-Detector) and GINA® software provided with the scanner.

8.2.2. Automated Radiosynthesis of [^{18}F]EFA

Radiofluorination and conversion of ethyl (p-tosyloxy) acetate to [^{18}F]EFA was carried out in our Nuclear Interface Module (Münster, Germany) configured for [^{18}F]FDG synthesis, very similar to GE TRACERlab FX_{FDG} module. The steps in the fully automated radiosynthesis of [^{18}F]EFA were summarized in **Table 8.1** and it is based on **Scheme 8.1**. Finally the synthesized

[^{18}F]EFA was sent to an automated dispensing unit and dispensed into vials in a class 100 area through a 0.2μ filter. The radiochemical yield was expressed as the percentage of radioactivity finally obtained as [^{18}F]EFA compared with the ^{18}F activity used without applying correction for radioactive decay during the synthesis. In order to determine the R_f values of the of the other radiofluorinated compounds expected after the radiofluorination of ethyl (p-tosyloxy) acetate, the reaction was terminated after the radio fluorination step and the reaction mixture was analyzed by radio-TLC.

8. 2.3. Quality Control

The synthesized [^{18}F]EFA was checked for clarity, colour and presence of any suspended particle. The pH was checked with pH-test paper strip. The radiochemical purity was first checked by radio-TLC followed by analytical HPLC. Thin layer chromatography was carried out using acetonitrile/water (95:5) as the mobile phase. The radio chromatograms were acquired at different steps of the synthesis procedure and analyzed. Twenty-five μl of the test solution was injected into the HPLC column and the eluate was monitored for radioactivity. The mobile phase for eluting consisted of 70% MeOH (solvent A) and 30% Water (solvent B) with 0.5ml/min flow rate in an isocratic system. The presence of non-radioactive impurities was also checked under the same HPLC conditions.

8.2.4. Sterility and Bacterial Endotoxin Tests

Sterility tests were performed in accordance with the Indian Pharmacopoeia, 1996 and addendum 2005 protocol. In this test, 1 ml of the [^{18}F]EFA sample, after radioactive decay, was inoculated in 25 ml fluid thioglycollate medium and incubated at 37°C for 14 days to observe the growth of aerobic and anaerobic bacteria. Similarly, 1 ml of the [^{18}F]EFA sample was also inoculated in 25

ml of soyabean casein digest medium and incubated at 22-25°C for 14 days to detect fungal growth.

The bacterial endotoxin test was performed in accordance with USP XXV. The test was based on the formation of gel clot in the sample by Limulus Amoebocyte Lysate (Sensitivity: 0.125 EU/ml) reagent.

Table 8.1. Flow chart of [^{18}F]EFA radiosynthesis scheme

Step I: Nucleophilic fluorination of ethyl (p-tosyloxy) acetate
i) [^{18}F] fluoride trapped on a Chromafix 45-PS-HCO_3 anion exchange cartridge ii) [^{18}F] fluoride eluted from the column using 75mM $TBAHCO_3$ (0.5 ml, Vial V5) to the reaction vessel iii) Tetrabutyl ammonium fluoride [^{18}F] dried by azeotropic distillation with acetonitrile (1.0 ml, Vial V1) iv) Ethyl (p-tosyloxy) acetate (10 mg) dissolved in MeCN (1.0 ml, Vial V2) added to the reaction vessel. v) S_N2 fluorination reaction carried out at 105°C for 7 minutes
Step II: Purification through Chromabond® SET V Column
i) The reaction mixture was cooled to 65°C ii) The reaction mixture was passed through the Combination Column iii) The reaction vessel was rinsed with ethanol containing water (2 ml, Vial V4) and pass through the column. iv) [^{18}F]EFA was eluted from the column using ethanol (12ml, Vial V6) and is collected in the product vial.

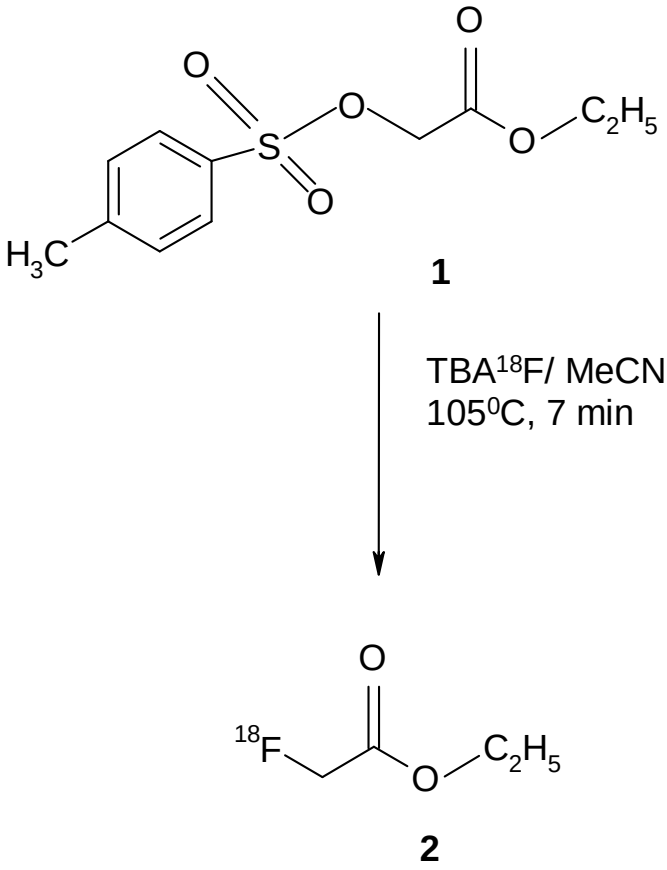

1. Ethyl (p - tosyloxy) acetate
2. Ethyl [^{18}F]fluoro acetate ([^{18}F]EFA)

Scheme 8.1. *Schematic representation of synthesis of [^{18}F]EFA starting from the precursor, Ethyl (p-tosyloxy) acetate*

8.3 Results and Discussion

Starting from the precursor, ethyl (p-tosyloxy) acetate (compound **1** in **Scheme 8.1**), [^{18}F]EFA was synthesized and purified by passing the reaction mixture after radiofluorination through a single combination column, CHROMABOND® SET V. The total synthesis time was 32 ± 1 min and gave a radiochemical yield (without decay correction) of 44.0 ± 1.5 % (n = 5) (**Table 8.2**). The synthesized [^{18}F]EFA was colourless,

Table 8.2. Radiochemical yield of [^{18}F]EFA

S. No	^{18}F in the reaction vessel (MBq)	[^{18}F]EFA produced (MBq)	% Yield*
1	2775	1224.7	44.1
2	2960	1239.5	41.9
3	3515	1554.0	44.2
4	3774	1739.0	46.1
5	17,575	7696.0	43.8

* Without decay correction

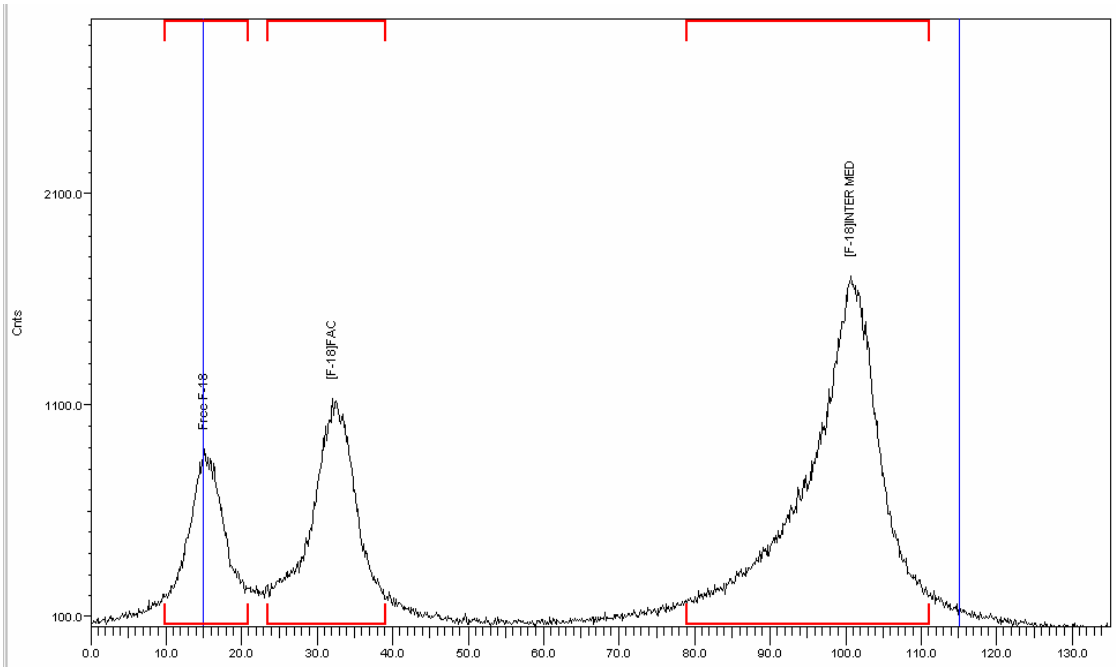

Fig.8.2. *Radio TLC of the radiofluorinated reaction mixture in 95:5 MeCN/H_2O.Three radioactive peaks. Free [^{18}F]F^- with an R_f value of 0.0, [^{18}F]Fluoroacetate with an R_f value of 0.17 and the radio fluorination intermediate, ethyl[^{18}F]fluoroacetae with an R_f value of 0.9.*

clear (free of any suspended or colloidal particle) and had a pH of 7.0. The radio-TLC of the raadio-fluorinated precursor, ethyl (p–tosyloxy) acetate in 95:5 (MeCN: H_2O) solvent showed three peaks. The first one at an R_f (max) of 0.0, the second one with an R_f (max) of 0.17 and the

last one with an R_f (max) of 0.9 [**Fig. 8.2.**]. The first peak is due to the unreacted [^{18}F]fluoride as confirmed by developing separate radio-TLC of TBA^{18}F in the same solvent system. The second peak with a R_f of 0.17 corresponds to [^{18}F]Fluoroacetate ([^{18}F]FAC) [257] and the third radiolabeled peak suggests that it is due to a non-polar compound, which is ethyl [^{18}F] fluoroacetate (compound **2** in **Scheme 8.1**), our target radiolabeled compound [264]. The formation of [^{18}F]FAC though not expected in the radiofluorination, may probably be explained by partial hydrolysis of ethyl-[^{18}F]-fluoroacetate *in situ* by TBAOH, present in small quantities, in the reaction mixture. The TLC of the final purified [^{18}F]EFA showed a single very prominent peak at R_f (max) of 0.9-1.0 (RCP > 95%) [**Fig. 8.3.**].The radio-HPLC chromatogram of the radiofluorinated

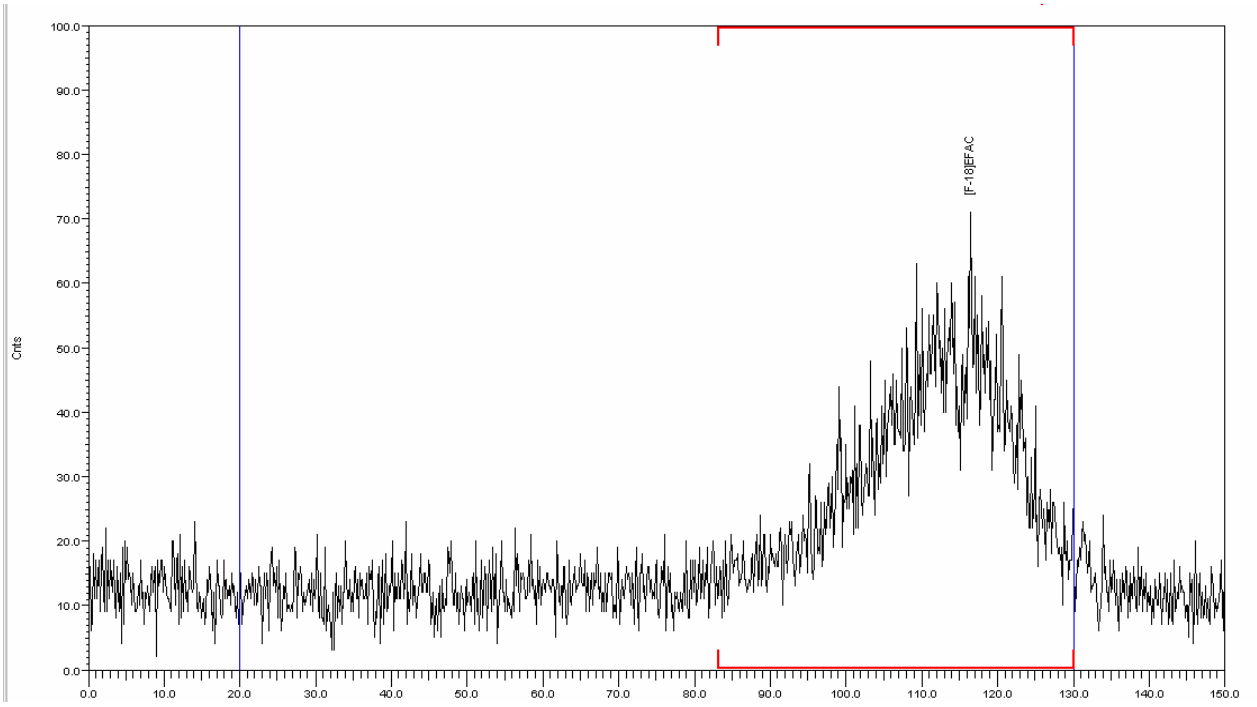

Fig. 8.3. *RadioTLC of Ethyl [^{18}F]Fluoroacetate in 95:5 MeCN: H_2O (R_f: 0.9 -1.0)*

reaction mixture displayed three radioactive peaks at 7.50 min, 29 min and 38.42 min having peak areas of 16.2 %, 77.07 % and 6.73 % respectively, whereas the radio-HPLC [**Fig.8.4.**] of

the final purified [^{18}F]EFA showed a single radioactive peak with a retention time 29.72 min confirming radiochemical purity. The comparison with reference standard ethyl fluoro acetate could not be done as the latter was not available.

The radiofluorination conditions (i.e. temperature and time) were optimized carrying out the radiofluorination of the precursor at different temperatures and different time periods, and analyzing the reaction mixture by radio-TLC (i.e. % area corresponding to the radioactive peak of ethyl [^{18}F]fluoroacetate).

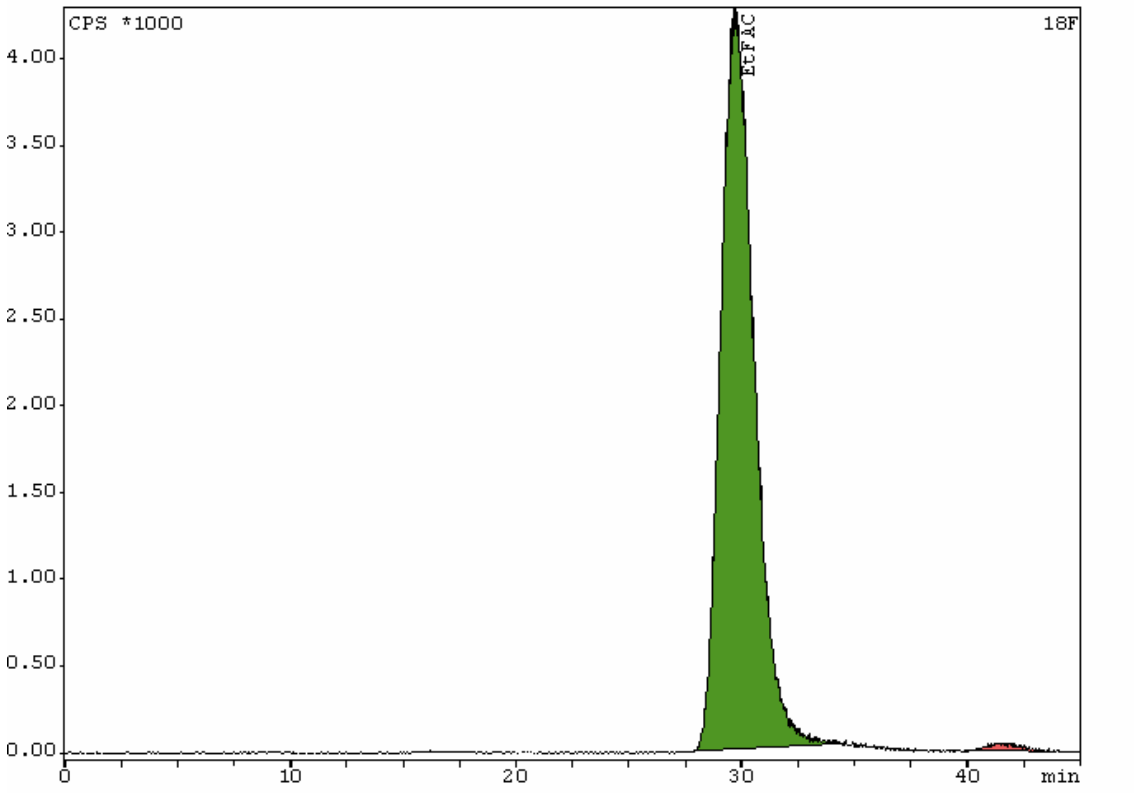

Fig. 8.4: *Radio HPLC chromatogram of Ethyl [^{18}F] fluoroacetate, Retention time: 29.72 min*

LiChroCART® 250-4, HPLC cartridge, LiChrospher® 100 RP-18 (5µm), 30/70 MeOH/H_2O solvent, 0.5 ml/min flow rate

In this work, different amounts of fluorine-18 radioactivity, ranging from 2.78 GBq to 17.58GBq (See **Table.8.2**) were used in the radiosynthesis. The data showed that the radiochemical yield of

the final product, ethyl [^{18}F]fluoroacetate was virtually independent of the amount of fluorine-18 radioactivity used since the precursor was in large excess.

The sterility and bacterial endotoxin tests were carried out and the synthesized [^{18}F]EFA was found to be sterile and endotoxin free. For purification, the CHROMABOND® SET V column is chosen as it is known to have cation exchanger (Ps-H^+) for trapping TBA^+, anion exchanger (Ps-HCO_3) and ALOX N for taking care of non-reacted [^{18}F]F^-, and reverse phase resin (HR-P) for taking care of lipophilic compounds. So, if the reaction mixture of the radiofluorinated precursor, ethyl (p-tosyloxy) acetate is loaded on this column and elute it with pure ethanol, the target radiolabeled compound, ethyl [^{18}F]fluoroacetate, being most lipophilic will selectively be eluted out with the desired radiochemical purity (> 95%).

8. 4. Conclusion

A fully automated radiosynthesis procedure for the synthesis of [^{18}F]EFA starting form the precursor, ethyl (p-tosyloxy) acetate and a commercially available combination purification cartridge-column has been developed. The radiochemical purity is more than 95%. Further, this development is done using our module configured for FDG synthesis. The yield is considerable; 44.2 ± 1.5 % (n = 5) without decay correction, and completed in 32 ± 1 min. The synthesis procedure is simple, quick, with consistent radiochemical yield. This method can easily be implemented in any regular [^{18}F]FDG synthesis module for large scale production of [^{18}F]EFA.

CHAPTER 9

A single combination-column purification technique for the fully automated radiosynthesis of [^{18}F]Fluoroacetate: a potential acetate analog for prostate tumor imaging

9.1 Introduction

Acetate is readily taken up by cells and is activated to acetyl-CoA in both the cytosol and mitochondria by acetyl-CoA synthetase. Acetyl-CoA is a common metabolic intermediate for synthesis of cholesterol and fatty acids, which are incorporated into membrane [265]. Acetyl-CoA is also oxidized in mitochondria through the tricarboxylic acid (TCA) cycle pathway to CO_2 and water. Some of the acetate is converted to amino acids. In normal myocardium, acetate is metabolized to CO_2 *via* the TCA cycle as the dominant pathway. In contrast, tumor cells convert most of the acetate into fatty acid by a key enzyme fatty acid synthetase, which is over expressed in cancer cells [266]. Acetate is predominantly incorporated into intracellular phosphatidycholine membrane microdomains that are important for tumor growth and metastasis [267].

PET with [^{11}C]acetate has a high sensitivity for detection of prostate cancer and several other cancers that are poorly detected by [^{18}F]FDG. [^{11}C]Acetate has been used as a positron emission tomography (PET) tracer for studying myocardial oxidative metabolism and regional myocardial blood flow [268] and for imaging renal, pancreatic, and prostate tumors [269]. However, the potential for widespread use of [^{11}C]acetate is limited for its 20.4 min $T_{1/2}$ of ^{11}C. Even with high yield synthesis, only one to three patients can be studied from a single-batch production. [^{18}F]Fluoroacetate ([^{18}F]FAC) is an analog of acetate with a longer $T_{1/2}$ of 110 min, is metabolized to fluoroacetyl-CoA and then fluorocitrate, which can not further metabolized to

CO_2 and water [270, 254]. Therefore, fluoroacetate is trapped in the cell in proportion to oxidative metabolism. [^{18}F]FAC has been evaluated as a PET agent for imaging prostate cancer [257].

To realize the potential of sodium [^{18}F]FAC in PET imaging, an automated synthesis that can be carried out in a short period and with a high yield is necessary. Synthesis of [^{18}F]FAC was reported by several groups [271-273]. However, all of these needed a long synthesis time (>60 min) and provided a low radiochemical yield (< 34 %). As a result, these methods are unlikely to fulfill the high demand for the radiopharmaceutical if used routinely. The chemical steps for the synthesis of sodium [^{18}F]FAC are quite similar to those used to prepare [^{18}F]-2-fluoro-deoxyglucose (FDG) and hence, the synthesis module used for the latter could be used to produce sodium [^{18}F]FAC [274, 61]. Many automated [^{18}F]FDG synthesizers are commercially available today, each with individual characteristics. Sun et al. [275] and Ponde et al.[257] recently reported an automated synthesis of [^{18}F]FAC with a modified commercially available cassette based 2-[^{18}F]FDG synthesizer. If we analyze their method critically, it is clear that the radiofluorinated reaction mixture containing the intermediate, ethyl-[^{18}F]fluoro acetate is first trapped into Oasis HLB plus cartridges, washed thoroughly with large volume of water (30 ml) to get rid off unreacted [^{18}F]fluoride and alkali hydrolysis was performed on the cartridges. Elution of [^{18}F]FAC from the Oasis HLB plus cartridges and further purification gave useable [^{18}F]FAC. In the routine production of [^{18}F]FDG, either acid or alkali hydrolysis is used after which, the hydrolyzed reaction mixture is loaded to a single combination-column or a set of Sep Pak® cartridges and finally, [^{18}F]FDG is directly eluted from the purification column by passing adequate volume of water.

In this study, an attempt has been made to develop a novel fully automated radiosynthesis procedure for [^{18}F]fluoroacetate ([^{18}F]FAC) using a single combination-column composed of

neutral alumina and reverse-phase resin, for purification, TBA^{18}F as nucleophile and ethyl (p-tosyloxy) acetate as the precursor. The developed procedure is very similar to [^{18}F]FDG synthesis and the synthesis has been carried out in our adapted synthesis module very similar to GE TRACERlab FX_{FDG} module.

9. 2. Materials & Methods

9.2.1. Reagents and apparatus

Ethyl (p-tosyloxy) acetate ([^{18}F]FAC precursor), potassium fluoro acetate reference standard, $TBAHCO_3$ solution (75 mM), molecular-grade anhydrous acetonitrile, ^{18}F trapping column (PS-HCO_3), 10% NaCl, 1.0 M NaH_2PO_4, sterile and pyrogen-free water for injection and pharmaceutical grade ethanol were procured from ABX, Advanced Biochemical Compounds, Germany. Neutral Alumina and sodium hydroxide pellets (NaOH) were obtained from Aldrich, USA. Evacuated 10 ml vials, certified for sterility and pyrogen free were obtained from ACILA AG, Germany. Minisart 0.2μ filters were purchased from Sartorius. Sterility testing was carried out in-house using standard protocol. Pyrogen testing was done by LAL test using Endosafe Reagent Kits from Charles River Laboratory, USA (US License No. 1197). Radioactivity was measured using a calibrated ion chamber (Capintec CRC-15R). All other chemicals used were of HPLC and AR grade.

The combination-column used for purification is made in our laboratory and composed of neutral alumina (ALOX N, 3350 mg) and reverse phase (HR-P, 680 mg) [**Fig.9.1.**]. The column is conditioned first by passing 20 ml ethanol followed by 100 ml of sterile and bacterial endotoxin free water before use.

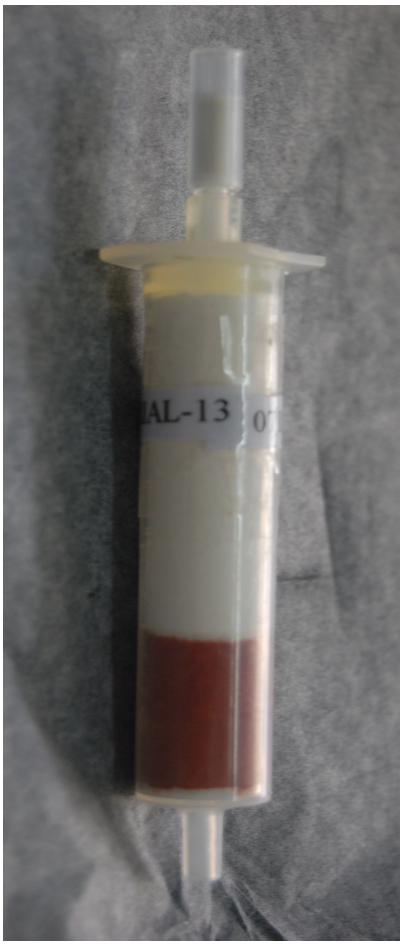

Fig.9.1. *[^{18}F]Fluoro acetate ([^{18}F]FAC) purification column composed of ALOX N and HR-P (Reverse Phase Resin). At the top, the small column attached is the ^{18}F trapping column , 45-Ps-HCO_3*

HPLC analysis using a C-18 reverse phase analytical column (LIChroCART® 250-4, HPLC cartridge, LIChrospher® 100, RP-18, 5 μm) was carried out on a Knauer HPLC system equipped with a radiometric detector followed by a variable wavelength UV detector. Radiochemical purity was also evaluated by thin layer chromatography (Silica gel 60, Merck) using a RayTest TLC scanner (Model No. BGO-V-Detector) and GINA® software provided with the scanner.

9.2.2. Automated Radiosynthesis of [^{18}F]FAC

Radiofluorination and conversion of ethyl-(p-tosyloxy) acetate to [^{18}F]FAC was carried out in a Nuclear Interface Module (Munster, Germany) configured for [^{18}F]FDG synthesis and in

principle is very similar to GE TRACERlab FX $_{FDG}$ module (Described in detail in Chapter 2). The steps in the fully automated radiosynthesis of [^{18}F]FAC were summarized in **Table 9.1** and it is based on **Scheme 9.1**. Finally the synthesized [^{18}F]FAC in buffered saline was sent to an automated dispensing unit and dispensed into vials through a 0.2μ filter in a class-A clean area. The radiochemical yield was expressed as the percentage of radioactivity finally obtained as [^{18}F]FAC compared to the ^{18}F activity used without applying correction for radioactive decay during the synthesis. In order to determine the R_f value of the [^{18}F] fluorinated intermediate, ethyl [^{18}F] fluoroacetate, the reaction was terminated after the radio fluorination step and the reaction mixture was analyzed by radio-TLC.

9.2.3. Quality Control

The synthesized [^{18}F]FAC was checked for clarity (presence of any suspended particle(s)) and colour. The pH was checked with pH-test paper strip. The radiochemical purity was first checked by radio-TLC followed by analytical HPLC. Thin layer chromatography was carried out using acetonitrile/water (95:5) as the mobile phase. The radio chromatograms were acquired at different steps of the synthesis procedure and analyzed. Twenty-five μl of the test solution was injected into the HPLC column and the eluate was monitored for UV (λ = 210 nm) absorbance as well as radioactivity. The mobile phase for eluting consisted of 70% MeOH (solvent A) and 30% water (solvent B) with 0.5ml/min flow rate in an isocratic system. The presence of non-radioactive impurities was also checked under the same HPLC conditions. Finally, [^{18}F]FAC prepared was confirmed by comparing the retention time of the radioactive peak of the test solution with the UV peak of reference standard [^{19}F]fluoroacetate.

Table 9.1. Flow chart of [^{18}F]FAC radiosynthesis scheme

Step I: Nucleophilic fluorination of ethyl (p-tosyloxy) acetate i) [^{18}F] fluoride trapped on a Chromafix 45-PS-HCO_3 anion exchange cartridge ii) [^{18}F] fluoride eluted from the column using 75mM $TBAHCO_3$ (0.5 ml, Vial V5) to the reaction vessel iii) Tetrabutyl ammonium fluoride [^{18}F] dried by azeotropic distillation with acetonitrile (1.0 ml, Vial V1) iv) Ethyl (p-tosyloxy) acetate (10 mg) dissolved in MeCN (1.0 ml, Vial V2) added to the reaction vessel. v) S_N2 fluorination reaction carried out at 105°C for 7 minutes
Step II: Deprotection i) The reaction mixture was cooled to 65°C ii) 0.7 M NaOH (1.5 ml, Vial V3) was added to the reaction vessel. iii) Base hydrolysis carried out at 65°C for 10 minutes iv) Reaction mixture was cooled to 50°C
Step III: Purification through Alumina and Reverse Phase Combination Column i) The reaction mixture was passed through the Combination Column ii) The reaction vessel was rinsed with 15% ethanol containing water (1.5 ml, Vial V4) and the column was first washed with this solvent. iii) [^{18}F]FAC was eluted using 15% ethanol containing water (12ml, Vial V6) and is collected in the product vial containing 10% NaCl (1.7ml) and 1M NaH_2PO_4 (0.7ml)

9.2.4. Sterility and Bacterial Endotoxin Tests

Sterility tests were performed in accordance with the Indian Pharmacopoeia, 1996 and addendum 2005 protocol. In this test, 1 ml of the [^{18}F]FAC sample after radioactive decay was inoculated in 25 ml fluid thioglycollate medium and incubated at 37°C for 14 days to observe

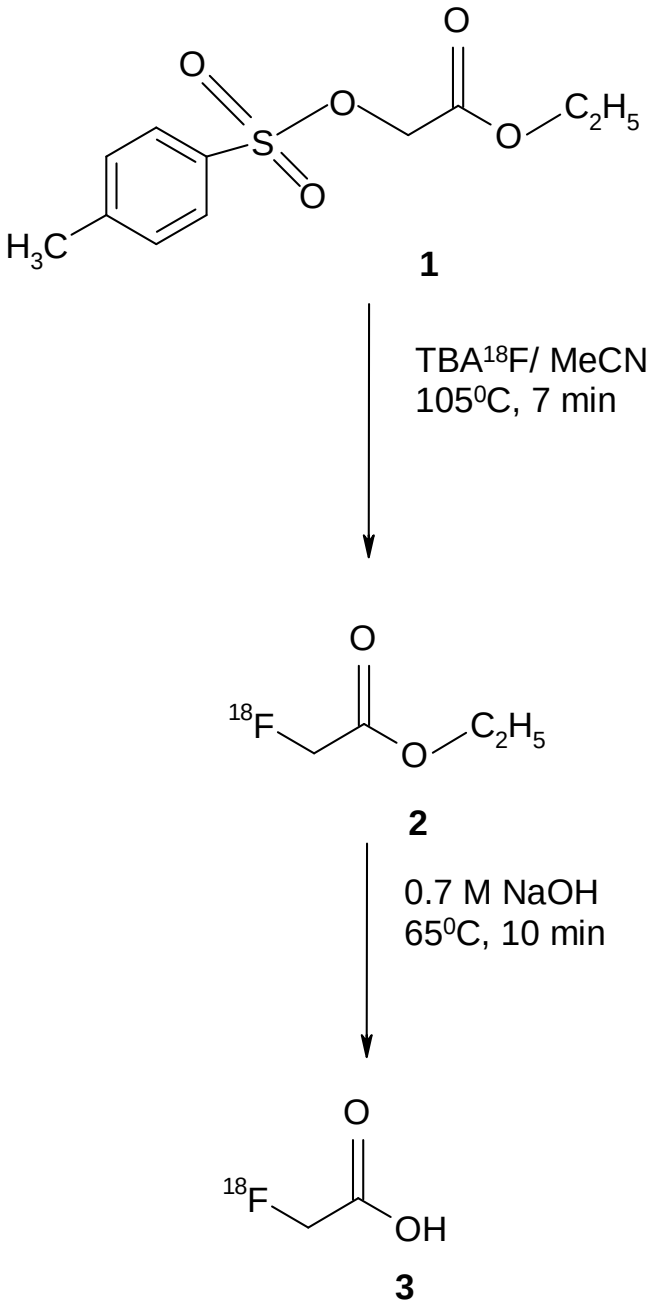

1. Ethyl (p - tosyloxy) acetate
2. [^{18}F]fluorinated intermediate, Ethyl [^{18}F]fluoro acetate
3. [^{18}F]fluoro acetic acid ([^{18}F]FAC)

Scheme. 9.1. *Schematic representation of synthesis of [^{18}F] FAC starting from the precursor, Ethyl (p-tosyloxy) acetate*

the growth of aerobic and anaerobic bacteria. Similarly, 1 ml of the [^{18}F]FAC sample was also inoculated in soyabean casein digest medium and incubated at 22-25°C for 14 days to detect fungal growth.

The bacterial endotoxin test was performed in accordance with USP XXV. The test was based on the formation of gel clot in the sample by Limulus Amoebocyte Lysate (Sensitivity: 0.125 EU/ml) reagent.

9.3 Results and Discussion

Starting from the precursor, ethyl (p-tosyloxy) acetate (compound **1** in **Scheme 9.1**), [^{18}F]FAC was synthesized and purified by passing the reaction mixture after hydrolysis step through a single combination column. The total synthesis time was 40 ± 1 min and the radiochemical yield (without decay correction) was 47.2 ± 3.0 % (n = 5) (**Table 9.2**). The synthesized [^{18}F]FAC was clear (free of any suspended or colloidal particle), colourless and had a pH

Table 9.2: Radiochemical yield of [^{18}F]FAC

S. No	^{18}F in the reaction vessel (MBq)	[^{18}F]FAC produced (MBq)	% Yield*
1	2275	1224.7	44.1
2	2886	1383.8	50.4
3	2590	1143.4	44.1
4	5550	2645.5	47.7
5	13,505	6734.0	49.8

* Without decay correction

between 7.0 to 7.5. Prior to deprotection, the radio-TLC of the radio-fluorinated precursor of FAC in 95:5 (MeCN: H_2O) solvent showed three peaks with R_f of 0.0, 0.17 and 0.9 respectively [**Fig. 9.2**.]. The first peak is due to the unreacted [^{18}F]fluoride, as confirmed by developing a separate radio-TLC of TBA^{18}F in the same solvent system. The peak with a R_f of 0.17

corresponds to [^{18}F]FAC [257] and the third peak with a R_f of 0.9 suggests that a non-polar compound elutes there, and is the [^{18}F]fluorinated intermediate, ethyl [^{18}F] fluoroacetate (compound **2** in **Scheme 9.1**)[275]. The formation of [^{18}F]FAC though not expected in the radiofluorination, but may probably, be explained by partial hydrolysis of ethyl [^{18}F] fluoroacetate *in situ* by TBAOH present in the reaction mixture in a small quantity. The radio-TLC of the reaction mixture after hydrolysis in the same solvent system showed two radioactive peaks. One with the R_f (max) 0.05 and the other with R_f (max) of 0.32 [**Fig. 9.3.**]. The third radioactive peak corresponding to ethyl [^{18}F]Fluoro acetate completely disappeared indicating 100% hydrolysis. The TLC of the final purified [^{18}F]FAC (compound **3** in Scheme 1) showed a single very prominent peak at R_f (max) of 0. 43 (RCP > 95%) [**Fig. 9. 4.**].

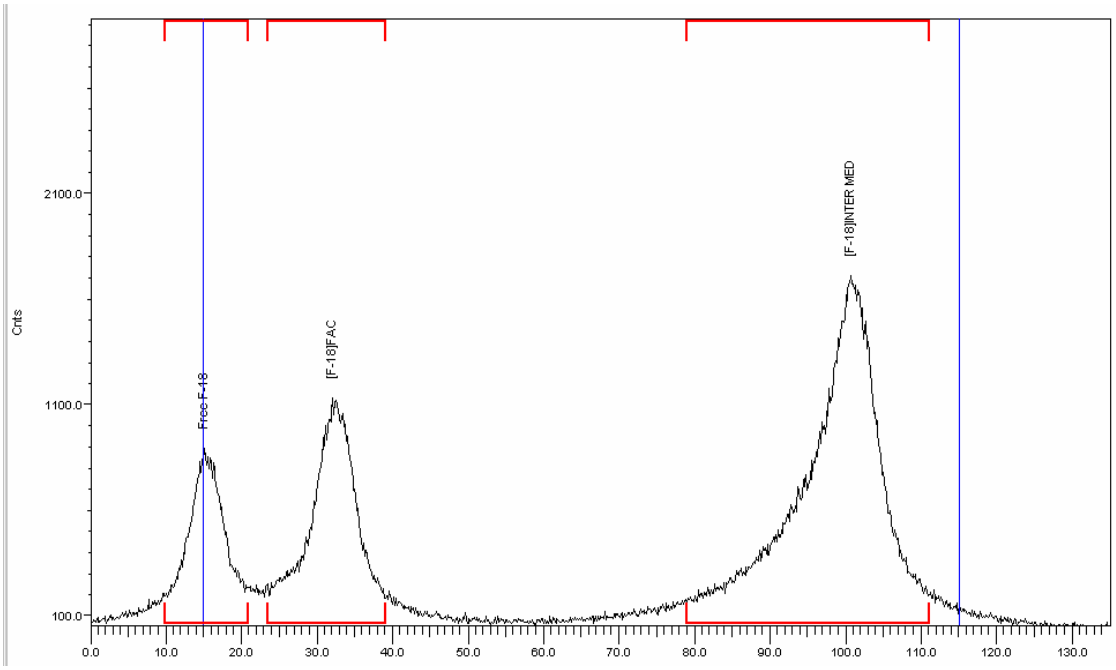

Fig.9.2. *Radio TLC of the radiofluorinated reaction mixture in 95:5 MeCN/H_2O.Three radioactive peaks. Free [^{18}F]F$^-$ with an R_f value of 0.0, [^{18}F]Fluoroacetate with an R_f value of 0.17 and the radio fluorination intermediate, ethyl[^{18}F]fluoroacetae with an R_f value of 0.9.*

The radio-HPLC chromatogram of the radiofluorinated reaction mixture displayed three radioactive peaks eluting at 7.50 min, 28.97 min and 38.42 min, with area under peak being 16.2 %, 77.07 % and 6.73 % respectively, whereas the radio-HPLC [**Fig.9.5.**] of the final purified [^{18}F]FAC showed a single radioactive peak with a retention time 7.15 min confirming radiochemical purity. Chemical purity was also assessed by HPLC, but no specific peaks were found showing that no impurities were present.

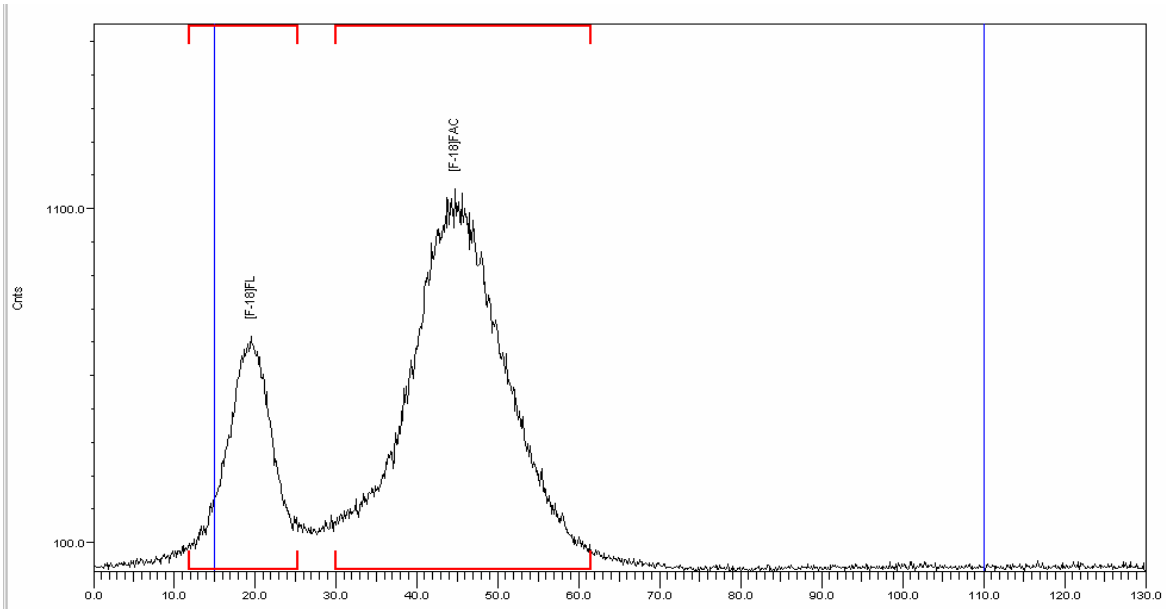

Fig.9.3. *Radio TLC of the alkali hydrolyzed reaction mixture in 95:5 MeCN/H_2O.Two radioactive peaks. Free [^{18}F]F$^-$ with an R_f value of 0.05 (% area 23.08), [^{18}F]Fluoroacetate with an R_f value of 0.32 (% area 76.92).The third radioactive peak of the radiofluorinated intermediate, ethyl[^{18}F]fluoroacetate is completely absent ensuring complete hydrolysis*

The radiofluorination conditions, viz., temperature and time were optimized by carrying out the radiofluorination of the precursor at different temperatures for different time periods and analyzing the radio-TLC (i.e. % area corresponding the radioactive peak of ethyl [^{18}F]fluoroacetate) of the reaction mixture. For hydrolysis of ethyl [^{18}F]fluoroacetate to obtain [^{18}F]FAC, both acid hydrolysis as well as alkali hydrolysis were studied. Alkali hydrolysis emerged as the preferable one, as it could be done at a comparably low temperature, resulting in

a shortened synthesis time, thereby minimizing the radioactive decay loss. In this work, different amounts of fluorine-18 radioactivity, ranging from 2.59 GBq to 13.51GBq (Refer **Table.9.2**) were used in the radiosynthesis. The data indicate that the radiochemical yield of the final product, sodium [^{18}F]fluoroacetate did not depend much on the initial amount of fluorine-18 radioactivity.

The sterility and pyrogenicity tests were carried out on the synthesized [^{18}F]FAC and was found to pass the tests. Regarding the functioning of the purification column, neutral alumina is known to be very good adsorber of [^{18}F]fluoride while the radiofluorinated intermediate, ethyl [^{18}F]fluoroacetate and the unreacted precursor, ethyl (p-tosyloxy) acetate, will be trapped in the reverse phase resin (HR-P) because of their higher lipophilicity. Elution with a very polar solvent like water will result in all the hydrophilic components to elute out and this was observed in practice.

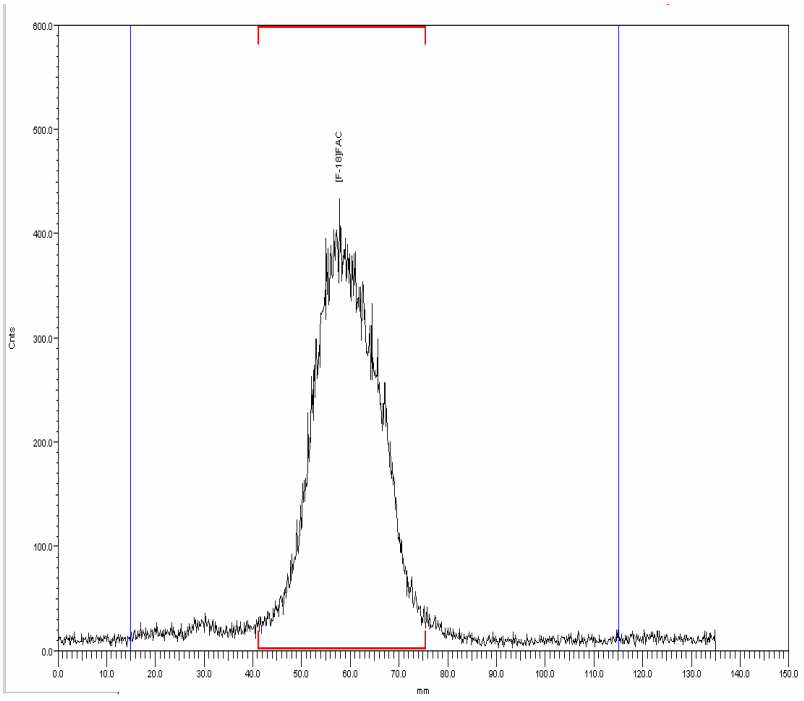

Fig. 9.4. *RadioTLC of [^{18}F]Fluoroacetate in 95:5 MeCN: H_2O (R_f : 0.32)*

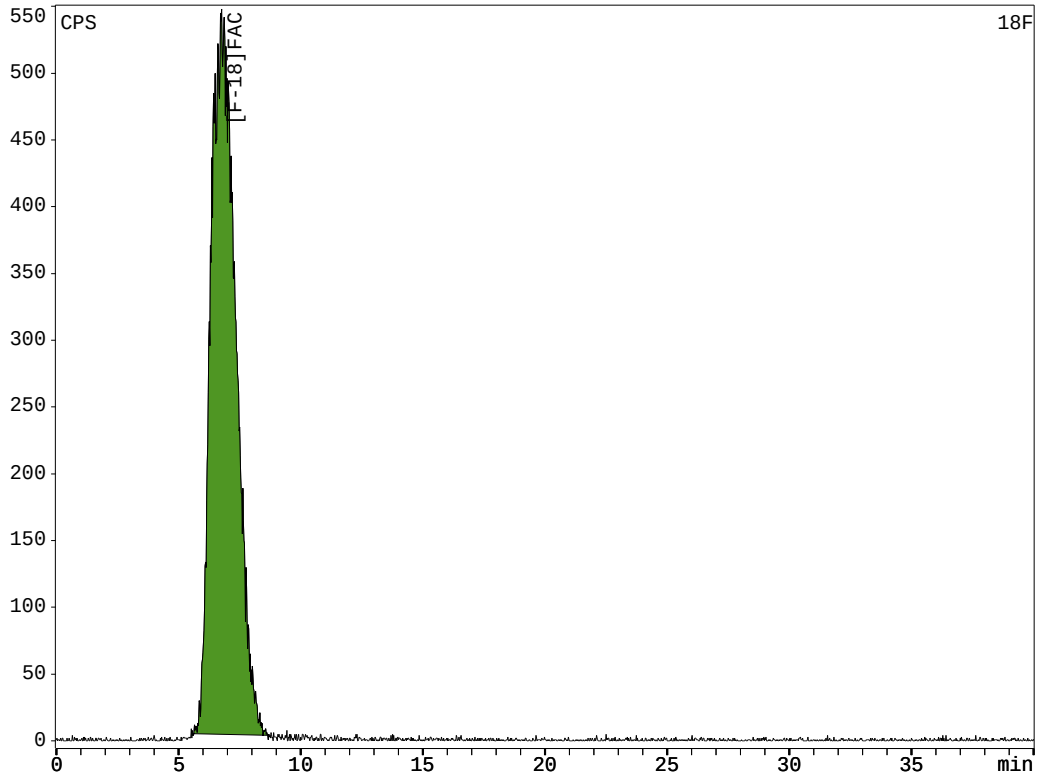

Fig.9.5. *Radio HPLC chromatogram of [^{18}F]fluoroacetate, Retention time: 7.15 min LiChroCART® 250-4, HPLC cartridge, LiChrospher® 100 RP-18 (5µm), 30/70 MeOH/H_2O solvent, 0.5 ml/min flow rate*

When the column was eluted with water, and the radio-TLC was analyzed, it showed an almost 50/50 mixture of free [^{18}F]F^- and [^{18}F]FAC. Hence, this gave a clue for the composition of the eluting solvent so that preferentially [^{18}F]FAC can only be eluted over free [^{18}F]F^-. So it was decided to increase the lipophilicity of the eluting solvent by adding ethanol to pure water and 15% ethanol in water was emerged to be the desired eluting solvent ensuring the radiochemical purity more than 95%.

9.4. Conclusion

A, novel, fully automated radiosynthesis procedure for the synthesis of [^{18}F]FAC starting form the precursor, ethyl (p-tosyloxy) acetate and single combination purification column has been developed. The radiochemical purity of the synthesized [^{18}F]FAC is more than 95% and is free

of any non-radioactive impurity. Further, the method is developed using our fluorination module configured for FDG synthesis with good radiochemical yield of 47.2 ± 3.0 % (n = 5) without decay correction in 40 ± 1 min. The synthesis procedure is very simple, fast, reliable and very similar to [^{18}F]FDG synthesis procedure with consistent radiochemical yield. This new radiosynthesis procedure can easily be implemented in any regular [^{18}F]FDG synthesis module.

CHAPTER 10
A fully automated radiosynthesis of 4-[^{18}F] fluorobenzaldehyde: a synthon for amine-oxi peptide labelling

10.1
Introduction

The fact that many human tumors overexpress a variety of receptors for regulatory peptides and peptide hormones [276] constitutes the basis of peptide receptor-targeted diagnostic imaging in nuclear medicine. Intense research has therefore been directed toward the development of small radiolabeled neuropeptide analogs with nuclear and pharmacokinetic properties suitable for high-contrast localization of human neoplasms. Of the imaging techniques available, PET represents the standard of excellence with respect to sensitivity, resolution, and the possibility for quantification. However, although several peptide analogs labeled with SPECT radionuclides such as ^{99m}Tc and ^{111}In have entered clinical studies [277, 278] or even clinical routine [279, 280], only a limited number of receptor-targeted peptides has been labeled with PET radionuclides such as ^{18}F, ^{68}Ga, ^{64}Cu and also ^{86}Y (for dosimetry); of these, only a small fraction has been applied for *in vivo* receptor imaging in patients [281 -284].

However, rapid and direct no-carrier-added (n.c.a.) ^{18}F-labeling of complex biomolecules such as peptides is not possible except using radio-metallation. For the n.c.a nucleophilic introduction of $^{18}F^-$, basic conditions are necessary which lead to proton abstraction from the precursor molecules and the formation of [^{18}F]HF as well as denaturing of sensitive organic substrates. Thus, various ^{18}F- labeling prosthetic groups have been developed [285, 286] and applied for conjugation labeling of biomolecules. The most frequently used method is ^{18}F-acylation [287-289],

which has been applied for ^{18}F-labeling of octreotide [290, 291], α-melanocyte-stimulating hormone [292], (Arg^{15}, Arg^{21}) vasoactive intestinal polypeptide [293], an RGD-containing glycopeptide [294], human C-peptide [295], and neurotensin [283-288, 296]. In most cases, this methodology entails time-consuming, moderate-yield, multistep radiosynthesis of the ^{18}F-labeled prosthetic groups. So far, only one 1-step preparation of an n.c.a. ^{18}F-fluoroacylation agent has been described [297]. However, comparably low yields of N-succinimydyl 4-([^{18}F] fluoromethyl) benzoate [**Fig. 10.1.**] (18 %- 25% within 30 min) as well as defluorination [298] prevented routine application of this ^{18}F-labeled prosthetic group.

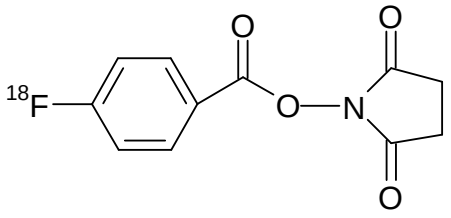

[^{18}F]SFB

N-succinimydyl 4-[^{18}F]-fluorobenzoate ([^{18}F]SFB)

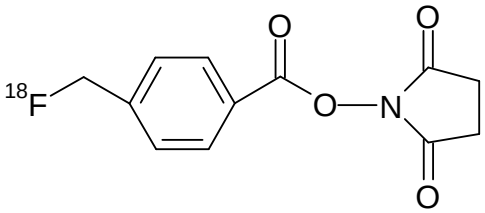

[^{18}F]SFMB

N-succinimidyl-4-[^{18}F]-(fluoromethyl) benzoate ([^{18}F]SFMB)

Fig.10.1. *Popular [^{18}F] Fluorinating agents for [^{18}F]-labeling of peptides*

A further disadvantage of the ^{18}F-fluoroacylation methodology consists of the necessity to use protected peptide precursors for conjugation with the prosthetic group, which in turn requires subsequent deprotection.

More recently, a new fast and straight forward strategy has been published that allows one-step, high-yield, synthesis of [^{18}F]Fluoride-labelled prosthetic group with stability against in vivo

defluorination and fast, one-step, chemoselective conjugation with unprotected peptides in aqueous media. The synthesis consists in chemoselective oxime formation between an amino-oxy peptide and 4-[^{18}F]Fluoro Benzaldehyde [299] [**Fig. 10. 2.**].

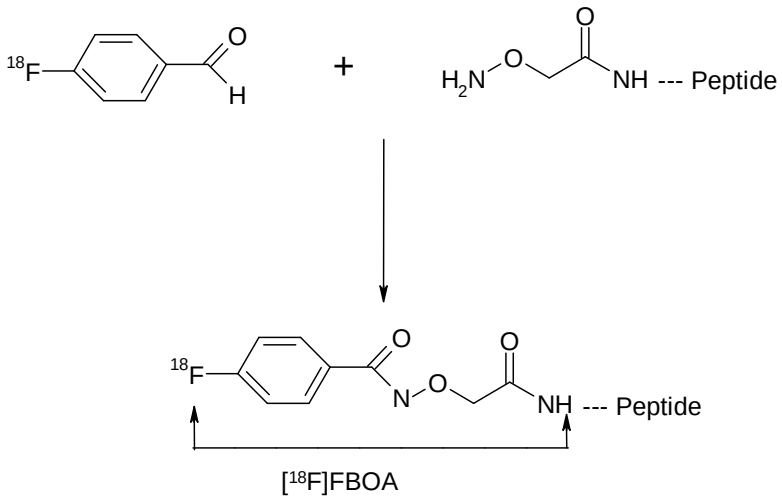

Conjugation of 4-[^{18}F]fluoro-benzaldehyde to aminoxy-functionalized peptides via oxime formation {[^{18}F]FBOA = N-(4-[^{18}F]fluorobenzylidene)oxime}

Fig. 10.2. *4-[^{18}F]Fluorobenzaldehyde as a synthon for amine-oxy peptide labeling*

This methodology has been developed bearing in mind the objective of labeling large [^{18}F]Fluoride-labelled peptides for routine clinical application. In order to implement this idea, large scale production of [^{18}F]Fluoride-labelled prosthetic group for the radiofluorination of peptides using commercially available automatic synthesis modules is now possible. Mading et al. [300] have reported an assisted synthesis of [^{18}F]SFB with Tracerlab^{TM} FX_{FDG} (General Electric Medical System, A module designed for the production of two batches of [^{18}F]FDG one by one (presently this type of module is discontinued). An automated preparation of 4-[^{18}F]fluorobenzoic acid as well as N-succinimidyl-4-[^{18}F]Fluorobenzoate using a CPCU (Siemens/CTI) has been described [301]. Very recently, Antonio Speranza et al.[302] have reported a fully automated synthesis procedure of 4-[^{18}F]fluorobenzaldehyde using GE Tracerlab^{TM} FX_{FN} module. They have replaced HPLC purification procedure with commercially available Sep Pak®

columns and used a handmade purification device (HPD) in connection with the commercial synthesizer for complete synthesis.

If we look at the synthesis scheme of 4-[^{18}F] Fluorobenzaldehyde [**Fig.10.3.**], this is a single step radiofluorination of the precursor 4-Formyl-N, N, N-Trimethylanilinium Triflate [303, 304] and subsequently purification by semi preparative HPLC or commercially available cartridges.

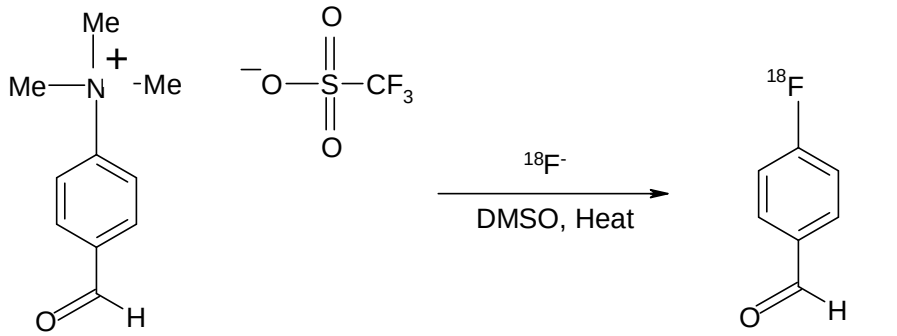

4- Formyl -N,N,N -trimethylanilinium triflate

4-[^{18}F]fluorobenzaldehyde

N.C.A (no carrier added) radiosynthesis scheme of 4-[^{18}F]fluorobenzaldehyde

Fig.10.3. *4-[^{18}F]fluorobenzaldehyde radiosynthesis scheme*

But alternatively, [^{18}F]fluorobenzaldehyde is typically prepared in a high yield by radiofluorination of *o*- or *p*- nitrobenzaldehyde using [^{18}F]fluoride activated with Kryptofix 2.2.2./K^+ as a complexing agent [305, 306] [**Fig. 10.4.**]. In this chapter, the development of a fully automated radiosynthesis procedure of 4-[^{18}F]fluorobenzaldehyde starting from 4-nitrobenzaldehyde, a commercially available, low cost, of the shelf chemical using a Nuclear Interface Fluorination Module similar to GE TRACERlab FX_{FDG} is described in detail. For purification, the possibility of a single neutral alumina column is explored. Optimization of the amount of starting material (lowest possible), radiofluorination temperature and duration to obtain maximum radiochemical yield within a short synthesis period are also studied.

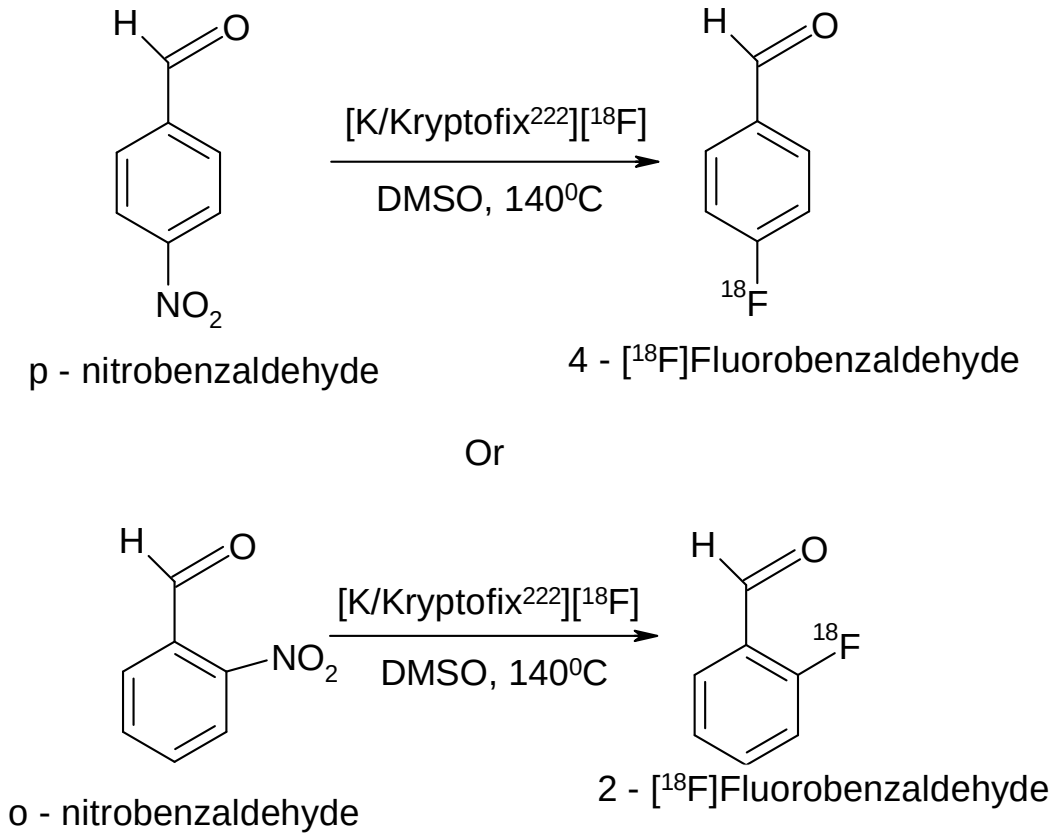

Fig.10.4. *Radiosynthesis scheme of [^{18}F]fluorobenzaldehydes starting from respective nitro benzaldehydes*

10. 2. Materials & Methods

10.2.1. Reagents and apparatus

4-nitro benzaldehyde (AR Grade, purity >99%), 4-fluoro benzaldehyde (GC grade, purity > 99%) are procured from Sigma Aldrich. $TBAHCO_3$ solution (75 mM), molecular-grade anhydrous acetonitrile, ^{18}F trapping column (PS-HCO_3), sterile and pyrogen-free water for injection and pharmaceutical grade ethanol were procured from ABX, Advanced Biochemical Compounds, Germany. Neutral Alumina used for preparing the purification column were procured from Aldrich, USA. Evacuated 10 ml vials, certified for sterility and pyrogen free were obtained from ACILA AG, Germany. Minisart 0.2μ filters were purchased from Sartorius.

Radioactivity was measured using a calibrated ion chamber (Capintec CRC-15R). All other chemicals used were of HPLC and AR grade.

HPLC analysis using a C-18 reverse phase analytical column (LIChroCART® 250-4, HPLC cartridge, LIChrospher® 100, RP-18, 5 μm) was carried out on a Knauer HPLC system equipped with a radiometric detector followed by a variable wavelength UV detector. Radiochemical purity was also evaluated by thin layer chromatography (Silica gel 60, Merck) using a RayTest TLC scanner (Model No. BGO-V-Detector) and GINA® software provided with the scanner.

10.2.2. Neutral Alumina Purification Column

The purification column used is made in-house and is composed of activated neutral alumina, active, grade I-II (Brockmann). In brief, 6g of neutral alumina (dry weight) was thoroughly washed with sterile, de-ionized water to remove fine particles. After removal of fine particles, it was soaked into water for 6-7 hours. Then, dried with the application of vacuum. When it becomes free flowing, it was packed inside a polypropylene cartridge barrel (6.5 cm × 1.2 cm) firmly avoiding the formation of any kind of air bubbles or cavities. The top and bottom of the column-cartridge were attached with 20-μm-polyethylene frits. The column-cartridge was washed thoroughly by passing 20 ml of sterile and bacterial endotoxin free water just before use.

10.2.3. Automated Radiosynthesis of 4 - [^{18}F]Fluorobenzaldehyde

Radiofluorination and conversion of 4-nitro benzaldehyde to 4-[^{18}F]Fluorobenzaldehyde was carried out in a Nuclear Interface Module (Munster, Germany) configured for [^{18}F]FDG synthesis similar to TRACERlab FX $_{FDG}$ module . The steps in the fully automated radiosynthesis of 4-[^{18}F]Fluorobenzaldehyde were as given in **Table 10.1,** which is as per **Fig. 10.4.**

Table 10.1. Flow chart of 4- [^{18}F]Fluorobenzaldehyde radiosynthesis

Step I: Radiofluorination of *p*–Nitro Benzaldehyde
i) [^{18}F] fluoride trapped on a Chromafix 45-PS-HCO_3 anion exchange cartridge ii) [^{18}F] fluoride eluted from the column using 75mM $TBAHCO_3$ (0.5 ml, Vial V5) to the reaction vessel iii) Tetrabutyl ammonium fluoride [^{18}F] dried by azeotropic distillation with acetonitrile (1.0 ml, Vial V1) iv) p-nitro benzaldehyde dissolved in DMSO (1.0 ml, Vial V2) added to the reaction vessel. v) Radiofluorination of p-nitro benzaldehyde is carried out at 150°C for 15 minutes
Step II: Purification through Single Neutral Alumina Column
i) The reaction mixture was cooled to 65°C ii) The reaction mixture was pumped through the Neutral Alumina Column iii) The reaction vessel was rinsed with 5 % ethanol containing water (1.5 ml, Vial V4) and the column was first washed with this solvent. iv) 4-[^{18}F]Fluorobenzaldehyde was eluted using 80 % ethanol containing water (8 ml, Vial V6) and is collected in the product vial.

The radiochemical yield was expressed as the percentage of radioactivity finally obtained as 4-[^{18}F]Fluorobenzaldehyde compared to the ^{18}F activity used without applying correction for radioactive decay during the synthesis. Optimization of the amount of starting material i.e. 4-nitro benzaldehyde to be started with, radiofluorination temperature and duration of radiofluorination have been studied using our adapted fluorination module. For doing so, the radiofluorinated reaction mixture was taken out and RadioTLC was developed in suitable solvent. The area under the radioactive peak corresponding to 4-[^{18}F] fluorobenzaldehyde (The R_f value is verified by developing TLC of reference standard 4-[^{18}F] Fluorobenzaldehyde and staining with iodine vapour) is directly expressed as the radiofluorination percentage.

10.2.4. Quality Control

The synthesized 4-[^{18}F] Fluorobenzaldehyde was checked for clarity and colour. The pH was checked with pH-test paper strip. The radiochemical purity was first checked by radio-TLC followed by analytical HPLC. Thin layer chromatography was carried out using acetonitrile/water (95:5) as the mobile phase. The radio-chromatograms were acquired at different steps of the synthesis procedure and analyzed. Twenty-five µl of the test solution was injected into the HPLC column and the eluate was monitored for UV (λ = 254 nm) absorbance as well as radioactivity. The mobile phase for eluting consisted of 80% MeOH (solvent A) and 20% water (solvent B) with 0.5ml/min flow rate in an isocratic system. The presence of non-radioactive impurities was also checked under the same HPLC conditions. Finally, 4-[^{18}F]Fluoro- benzaldehyde prepared was confirmed by comparing the retention time of the radioactive peak of the test solution with the UV peak of reference standard 4-[^{19}F]fluorobenzaldehyde.

10. 3. Results and Discussion

Starting from the precursor, *p*-nitro benzaldehyde, 4-[^{18}F]Fluorobenzaldehyde was synthesized by single radiofluorination step and purified by passing the reaction mixture after radiofluorination through a single neutral alumina column. The total synthesis time was 35 ± 1 min and the radiochemical yield (without decay correction) was 30.1 ± 1.1 % (n = 5) (**Table 10.2.**). The synthesized 4-[^{18}F]Fluorobenzaldehyde was clear (free of any suspended or colloidal particle), orange yellow in colour and had a pH between around 7.0.

Table 10.2. Radiochemical yield of 4-[^{18}F]Fluorobenzaldehyde

S. No	^{18}F in the reaction vessel (MBq)	[^{18}F]EFA produced (MBq)	% Yield*
1	5550	1739	31.3
2	7400	2355	31.8
3	3700	1110	30.0
4	4255	1319	31.0
5	8100	2349	29.0

*** Without decay correction**

The radio-TLC of the radio-fluorinated *p*- nitro benzaldehyde in 95:5 (MeCN: H_2O) solvent showed two peaks with R_f of 0.09 and 0.9 respectively [**Fig. 10.5.**]. The first peak is due to the unreacted [^{18}F]fluoride, as confirmed by developing a separate radio-TLC of TBA^{18}F in the same solvent system. The peak with R_f of 0.9 suggests the presence of an [^{18}F]labeled non-polar compound and in this case our desired radiolabeled compound, 4-[^{18}F]Fluorobenzaldehyde which is formed by nucleophilic aromatic substitution of the leaving group, i.e. $–NO_2$ from substrate *p*-nitrobenzaldehyde activated by the presence of an strong electron withdrawing group, -CHO in the *para* position to the leaving group, $-NO_2$. The TLC of the final purified 4-[^{18}F]Fluorobenzaldehyde showed a single very prominent peak at R_f (max) of 0.9 (RCP > 99%) [**Fig.10.6.**]. That the radioactive peak with R_f equal to 0.9 to 1.0 was really correspond to 4-[^{18}F]Fluorobenzaldehyde was verified by developing the TLC of reference standard 4-[^{19}F]Fluorobenzaldehyde in the same solvent system and staining with iodine vapour [**Fig.10.7.**].

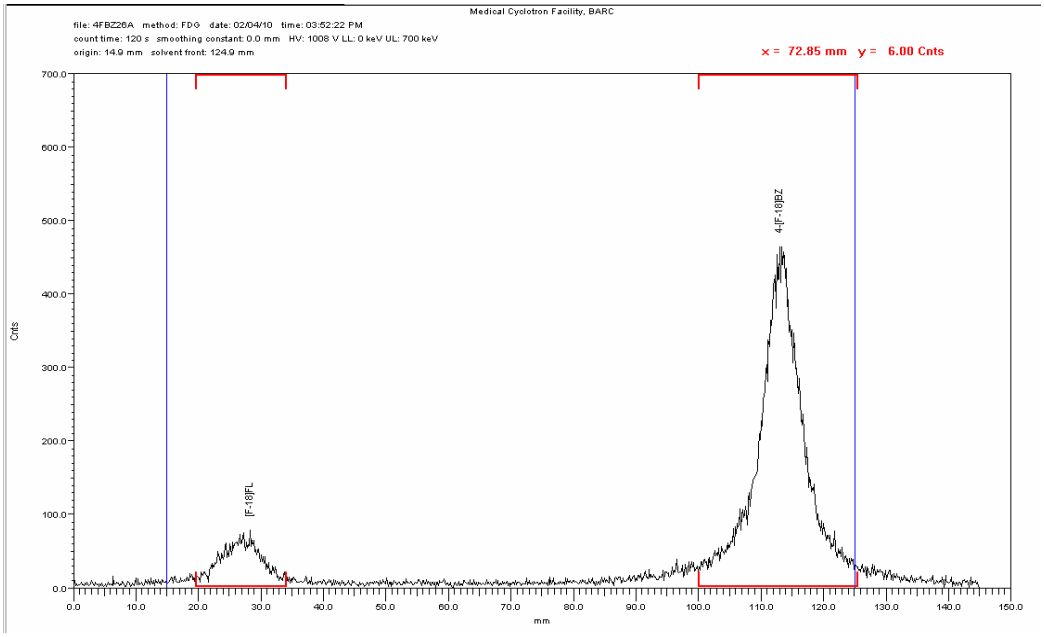

Fig.10.5. *Radio-TLC of the radiofluorinated reaction mixture of p – nitro Benzaldehyde in MeCN: H_2O (95:5). First radioactive peak corresponds to free [^{18}F]F^- with an R_f of 0.09 and the other radioactive peak corresponds to 4-[^{18}F]Fluorobenzaldehyde with an R_f of 0.9.*

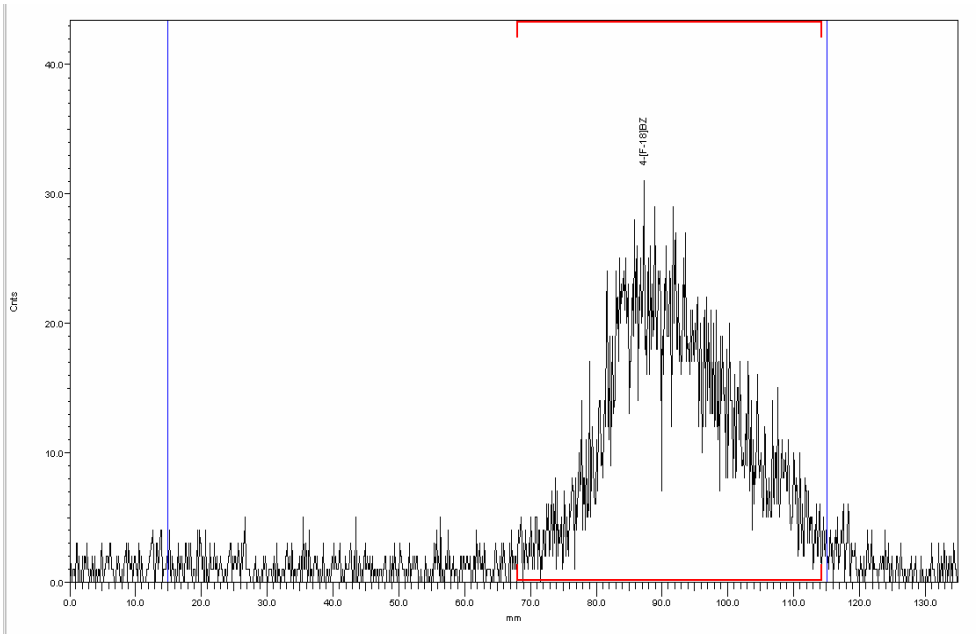

Fig.10.6. *Radio-TLC of 4-[^{18}F]Fluorobenzaldehyde in MeCN: H_2O (95:5), R_f value of 4-[^{18}F]Fluorobenzaldehyde is 0.85*

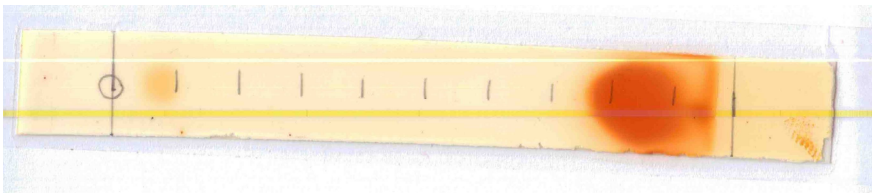

Fig.10.7. *TLC of reference standard 4-Fluorobenzaldehyde in MeCN: H_2O (95:5) Coloured by iodine vapour, R_f (range): 0.8-0.9*

The HPLC chromatogram of the synthesized 4-[^{18}F]Fluorobenzaldehyde doped with reference standard 4-fluorobenzaldehyde is shown in **Fig. 10.8**. From this figure it is observed that the radiochromatogram displays single radioactive peak at 12.50 min, and a single UV peak at 12.53 min. The HPLC chromatogram (UV, λ = 254 nm) of only reference standard 4-fluorobenzaldehyde [**Fig.10.9.**] shows a single peak with a retention time of 12.5 min.

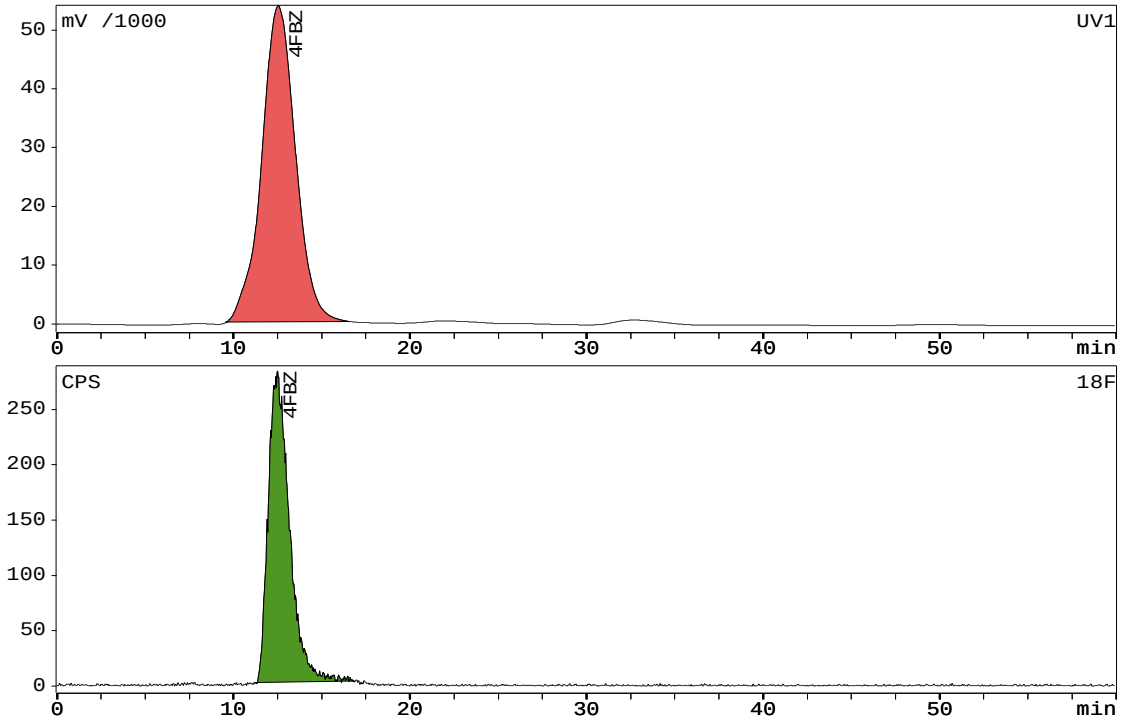

Fig. 10.8. *HPLC Spectrum of 4-[^{18}F] Fluoro Benzaldehyde doped with reference standard 4-Fluoro-Benzaldehyde (Red Peak = UV peak of reference standard, Green peak = radioactivity peak of 4-[^{18}F]-BZ, Radioactivity Peak, R_t = 12.50 min, UV (λ = 254 nm) Peak, R_t: 12.53 min) [C-18 RP (LiChroCART® 250-4), 0.5 ml/min flow rate, 80/20 Methanol/Water solvent]*

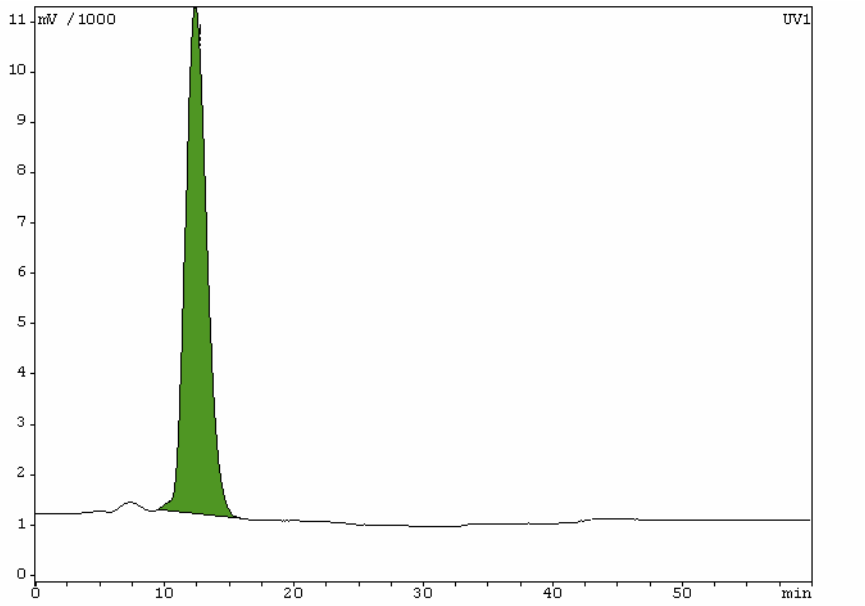

Fig.10.9. *HPLC chromatogram of reference standard 4-Fluorobenzaldehyde (UV, λ = 254 nm). R_t = 12.5 min [C-18 RP (LiChroCART® 250-4), 0.5 ml/min flow rate, 80/20 Methanol/Water solvent]*

The co-elution of the radioactivity peak along with the UV peak of the reference standard 4-fluorobenzaldehyde confirmed that the single radioactive peak corresponds to 4-[^{18}F]Fluorobenzaldehyde.

The radiofluorination conditions, viz., temperature and time were optimized by carrying out the radiofluorination of the precursor at different temperatures for different time periods and analyzing the radio-TLC (i.e. % area corresponding the radioactive peak of 4-[^{18}F]fluorobenzaldehyde) of the reaction mixture but conditions as suggested by Lemaire et al.[305, 306]. They have reported to achieve a good yield (> 50%) when they have carried out the radiofluorination reaction within a temperature range of 130°C-140°C for 20 minutes in DMSO with a substrate concentration of 15mg/ml. It is also been reported that under this experimental conditions the substrates were very stable and no fluorination by products such as [^{18}F]fluorobenzoic acid was observed by oxidation with DMSO [306]. Considering the design of our synthesis module, a little bit higher reaction temperature i.e. 150°C was proved to be the best

with a relative shorter synthesis time of 15 minutes. To achieve the highest specific activity, it is always desirous to have the maximum radiochemical yield starting with the lowest amount of precursor. In order to optimize that, keeping the radiofluorination temperature and duration fixed, radiofluoritation was carried out starting with different amount of *p*-nitro benzaldehyde i.e. 2.5, 5.0, 7.5, 10.0, 15.0 mg and then the percentage of radiofluorination was calculated directly from the area of the radioactive peak corresponding to 4-[^{18}F] Fluorobenzaldehyde in the radio TLCs. It is observed that 2.5 mg is too less to have a good overall radiochemical yield after purification. Higher degree of radiofluorination was observed when the amount of starting material was increased from 2.5 mg but reached a plateau after 7.5 mg. The overall radiochemical yield was not too different when started with 5 mg and 7.5 mg. With the intention of having highest specific activity, 5 mg was chosen as the optimized amount. Regarding the functioning of the purification column, neutral alumina is known to be very good adsorber of [^{18}F]fluoride and if we observe the radio TLC of the reaction mixture, the substrate, p-nitro benzaldehyde shows a very high degree of radiofluorination leaving a very less percentage of free unreacted [^{18}F]F^{-} to be trapped in the purification column to obtain high radiochemical purity. Since the desired compound i.e. 4-[^{18}F]Fluoro benzaldehyde is the lipophilic component in the reaction mixture, a highly lipophilic solvent (80% ethanol containing water) is chosen to selectively elute it out with high radiochemical purity (> 95 %).

10.4. Conclusion

A, novel, fully automated radiosynthesis procedure for the synthesis of 4-[^{18}F]Fluoro benzaldehyde starting form the low cost starting material, p-nitrobenzaldehyde ethyl (p-tosyloxy) acetate and single combination purification column has been developed. The radiochemical

purity of the synthesized 4-[^{18}F]Fluorobenzaldehyde is more than 95% and is free of any non-radioactive impurity. Further, the method is developed using a module configured for FDG synthesis with good radiochemical yield of 30.1 ± 1.1 % (n = 5) without decay correction in 35 ± 1 min. The synthesis procedure is very simple, fast, reliable and very similar to [^{18}F]FDG synthesis procedure with consistent radiochemical yield. This new radiosynthesis procedure can easily be implemented in any regular [^{18}F]FDG synthesis module.

CHAPTER 11

Studies on a rapid radio synthesis procedure for [^{18}F] FHBG using non-HPLC purification technique

11.1 Introduction

Gene therapy is expected to have significant potential in treating several common cancers using a variety of viral and non-viral vectors and there have been several attempts in this area with some success [307-313]. Among these, herpes simplex virus thymidine kinase (HSV-tk) has been used as a key prodrug-converting enzyme for a number of anticancer gene therapy approaches [314, 315]. The enzyme has a broad substrate specificity and can convert less toxic ganciclovir (GCV, 9-[(1, 3 – dihydroxy-2-propoxy) methyl]-guanine) or penciclovir (PCV, 9-[4-hydroxy-3(hydroxyl-methyl) butyl]-guanine) into toxic compounds that results in cell death [316]. The 5- substituted analogue of thymidine 1-(2'-deoxy-2'-fluoro-β-D-arabinofuranosyl)-5-iodouracil (FIAU) is the substrate for thymidine kinase and is incorporated in to DNA [317-320]. Imaging of HSV-tk expression is reliant on the use of enzyme imaging agents, fluorinated (fluorine-18) or iodinated (iodine-124, iodine-125 and iodine-131) prodrugs such as fluorinated GCV and PCV analogues 8-[^{18}F]Fluoroganciclovir ([^{18}F]FGCV), 9-[(3-[^{18}F]fluoro-1-hydroxy-2-propoxy)methyl]guanine ([^{18}F]FHPG), 8-[^{18}F]fluoropenciclovir ([^{18}F]FPCV), 9-(4-[^{18}F]fluoro-3-hydroxymethylbutyl)guanine ([^{18}F]FHBG); and radio-fluorinated and radio-iodinated FIAU analogues [^{18}F]FIAU, [^{124}I]FIAU and [^{125}/^{131}I]FIAU, coupled with biomedical imaging technique positron emission tomography (PET) or single photon emission tomography (SPECT) [**Fig.11.1.**] [321-342]. Both acyclovir and ganciclovir have been used as antiviral agents [343-347] and exploited in

gene therapy.

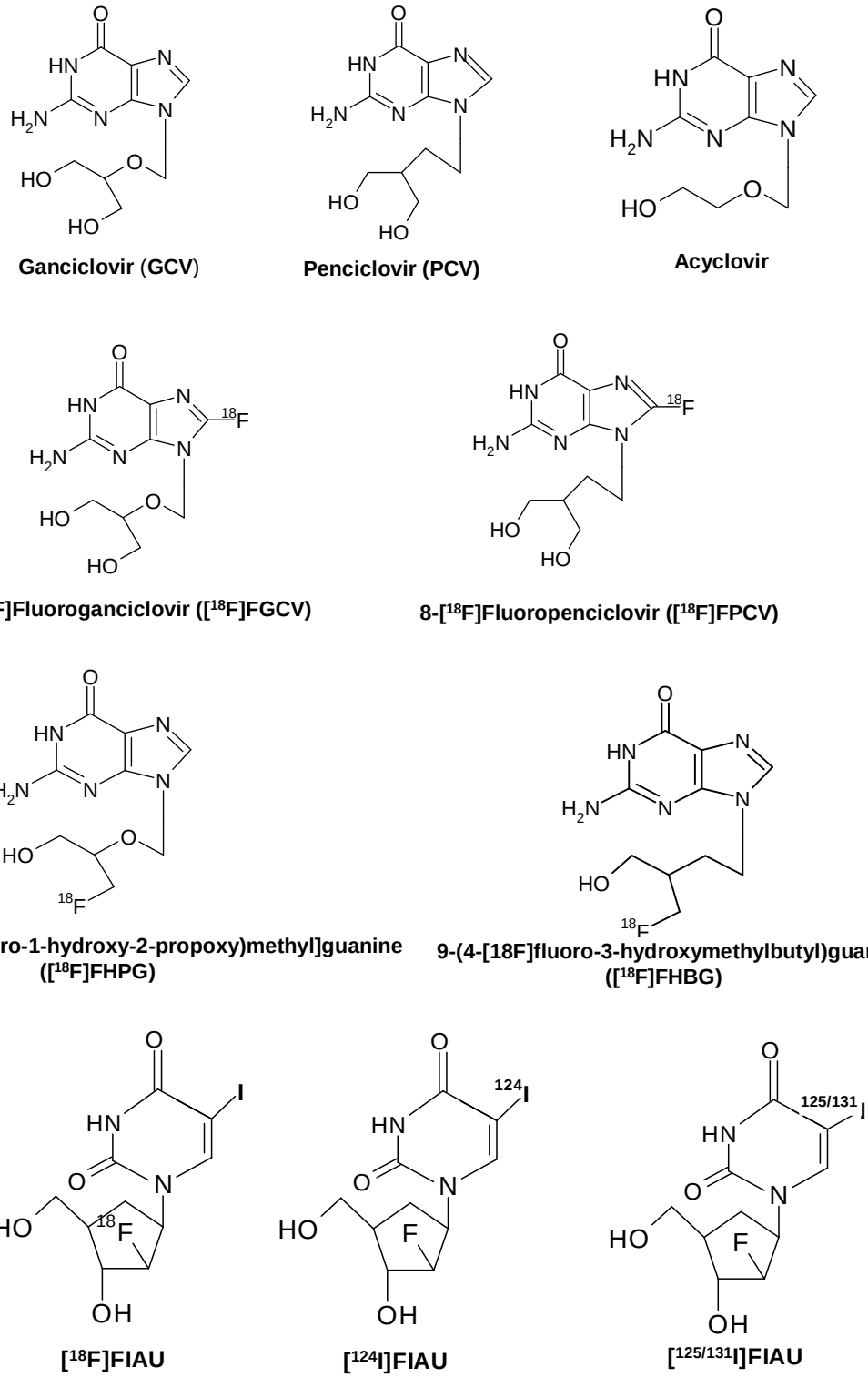

Fig. 11.1. *Chemical structures of Ganciclovir (GCV), Penciclovir (PCV), Acyclovir, [^{18}F]FGCV, [^{18}F]FPCV, [^{18}F]FHPG, [^{18}F]FHBG, [^{18}F]FIAU, [^{124}I]FIAU, and [$^{125/131}$I]FIAU*

These anti-viral agents are phosphorylated by the viral kinase to their monophosphates and metabolically trapped in cells. Absence of viral kinase in non-infected cells minimizes phosphorylation of these viral agents. Cellular retention of radioactivity is therefore an indicator of HSV-TK gene expression. The ganciclovir analog, 9-[(3-fluoro-1-hydroxy-2-propoxy) methyl] guanine (FHPG) is biologically active and is phosphorylated by the viral kinase to its monophosphate at 67 % the rate of thymidine [336]. Its potency against HSV (F-strain) in the cell culture (ID_{50} 7 mM) is only 14-fold lower than that of ganciclovir. Hence, fluorine -18 labeled FHPG and structurally closely related penciclovir analog, 9-(4-[^{18}F] fluoro-3-hydroxymethylbutyl) guanine ([^{18}F]FHBG) were found to be potential radio tracers in assessing the efficiency of gene therapy. Comparison among acyclovir, ganciclovir and penciclovir [344, 348] reveals the following – (a) the phosphorylation rate by viral kinase followed by host kinase to form triphosphate of penciclovir is 12 times higher than ganciclovir, and 120 times higher than acyclovir in 4 hour incubation ; (b) the intracellular stability of the triphosphate of penciclovir is 7 times higher than acyclovir and 3 times higher than ganciclovir; and (c) inhibition of DNA polymerase by the penciclovir triphosphate is equal or higher than acyclovir, and is 10 to 30 times higher than ganciclovir. This comparison suggests that the radio-labeled fluoro analogue of penciclovir, FHBG, might be more suitable than the fluoro analogue of ganciclovir, FHPG, or radio labeled acyclovir [349, 350] for imaging of viral infection and transfected cells by PET [321]. This probe has been used clinically for human pharmacokinetic and dosimetry studies [341].

In the past few years, several research groups have reported [^{18}F] FHBG production through different approaches [321, 338, 351-353]. However, most of these syntheses required a long synthesis time (> 55 min) and provided a low, unstable radiochemical yield [354]. More recently, Chang et al. [351] reported a robotic system for the automated production of [^{18}F]FHBG

with a high uncorrected radiochemical yield (19%). However, this two-step two-pot procedure still required a long synthesis time (80 min). Fully automatic production of [^{18}F]FHBG is essential for preclinical and clinical applications to reduce radiation exposure during preparation and to offer a reliable high radiochemical yield. Kang, S.H. et al. [356] reported a comparison of two fully automatic synthesis methods using the Tracerlab MX (Cassette based module from GE Healthcare for [^{18}F] FDG production) and Explora RN Module. They reported a radiochemical yield of 21.0 ± 3.8 % (n = 5, decay corrected) in a synthesis time 63.0 ± 5.0, including HPLC purification with a radiochemical purity of 98.0± 0.9 % (n = 5) using Tracerlab MX chemistry module. While using Explora RN module, they have reported to have a radiochemical yield of 32.0 ± 1.2 % (n = 5, decay corrected) in a synthesis time of 38.0 ± 2.0 min including HPLC purification steps with a radiochemical purity of 99.0 ± 0.6 % (n = 5). Tang et al. [354] reported a simplified one-pot automated synthesis of [^{18}F]FHBG using a substantially modified Tracerlab FX $_{F-N}$ module using SEP-PAK® cartridge purification instead of high performance liquid purification (HPLC) with a radiochemical yield of 8-14% (decay uncorrected, n =10) within a short synthesis time of 40 minutes. However, these reported procedures are very difficult to put to practice because of some practical difficulties since it requires a specialized synthesis module with second reaction vessel as well more reagent reservoirs to wash out the impurities from the purification cartridges. So, it is decided to develop our own synthesis procedure and in this chapter, the results of preliminary attempts to develop a fully automated method of radio synthesis of [^{18}F]FHBG within a much shorter synthesis time with a good radiochemical yield using a non-HPLC general purpose fluorination module is described. During this process, in order to avoid cumbersome HPLC purification process, the possibility of purification using

combination purification cartridge composed of neutral alumina and anion exchanger as well as commercially available SEP-PAK® cartridges are explored.

11.2. Materials & Methods

11.2.1. Reagents and apparatus

FHBG precursor, Tosyl-FHBG, reference standard FHBG, $TBAHCO_3$ solution (75 mM), molecular-grade anhydrous acetonitrile, 1N hydrochloric acid (1N HCl), 10% NaCl solution, 1M NaH_2PO_4 buffer ^{18}F trapping column (PS-HCO_3), Ps-HCO_3 anion exchanger for preparing the combination purification cartridge, sterile and pyrogen-free water for injection and pharmaceutical grade ethanol were procured from ABX, Advanced Biochemical Compounds, Germany. Neutral Alumina used for preparing the purification column were procured from Aldrich, USA. Sep Pak® cartridges were procured from Water, USA. Evacuated 10 ml vials, certified for sterility and pyrogen free were obtained from ACILA AG, Germany. Minisart 0.2µ filters were purchased from Sartorius. Radioactivity was measured using a calibrated ion chamber (Capintec CRC-15R). All other chemicals used were of HPLC and AR grade.

HPLC analysis using a C-18 reverse phase analytical column (Machery Nagel®, 5µm, 250X8X4 mm) was carried out on a Knauer HPLC system equipped with a radiometric detector followed by a variable wavelength UV detector. Radiochemical purity was also evaluated by thin layer chromatography (Silica gel 60, Merck) using a RayTest TLC scanner (Model No. BGO-V-Detector) and GINA® software provided with the scanner. Thin layer chromatography (TLC) of the refernce standard FHBG was carried out using Silica Gel 60, F254, Merck TLC plates.

11.2.2. Combination Purification Cartridge

The purification cartridges used were made in house whenever required. The cartridges were mainly composed of cation exchanger (Ps-H^+), anion exchanger (Ps-HCO_3) and neutral alumina, active, grade I-II (Brockmann). To determine the optimum combination purification cartridge, a variety of compositions of these three materials was tried out to obtain good radiochemical purity (>95%). Among all the permutation and combinations tested, the best radiochemical purity (~ 80 %) was obtained when a combination cartridges is composed of very little amount of cation exchanger, equal amount of anion exchanger and neutral alumina. Neutral alumina, before use, was thoroughly washed with sterile, de-ionized water to remove fine particles. After removal of fine particles, it was soaked into water for 6-7 hours. Then, dried with the application of vacuum. When it becomes free flowing, it was used to prepare the combination cartridges. Inside a polypropylene cartridge barrel (6.5 cm × 1.2 cm), one 20-µm-polyethylene frit was first placed at the bottom. 2.5g of conditioned neutral alumina was first poured into it. One frit is placed on neutral alumina and tightly packed without allowing formation of any kind of air bubbles or looseness. On that, 2.5 g Ps-HCO_3 anion exchanger is added and again one frit is placed and tightly packed. On the top, 700 mg Ps-H^+, cation exchanger is packed and a conditioned by passing first 20 ml ethanol and then 100 ml of sterile and bacterial endotoxin free water.

Since combination cartridge purification gave only around 80 % RCP, we tried to develop a better purification process using commercially available singe use SEP-PAK® cartridges. Different combinations of the SEP-PAK® cartridges were tried out. QMA Accell Plus, C18 RP Plus, ALUMINA N Plus, Oasis® WAX (Weak Anion Exchanger) Sep-Pak cartridges were used in the trials. Each type of SEP-PAK® cartridges must be conditioned before use for its ultimate efficacy. In this case also, the combination of two ALUMINA N Plus and two Oasis® WAX

Sep-Pak cartridges combination gave good radiochemical purity (~ 92%). ALUMINA N Plus Sep-Pak® cartridges were conditioned by passing 10 ml of water and then mildly dried by passing helium, but it is ensured that they remain wet. Oasis® WAX Sep-Pak cartridges were conditioned first by passing 5 ml of absolute ethanol and then washed by passing 50 ml of water.

11. 2.3. Automated Radiosynthesis of [^{18}F]FHBG

Radiofluorination and conversion of the precursor, Tosyl FHBG to [^{18}F]FHBG was carried out in a Nuclear Interface Module (Munster, Germany) configured for [^{18}F]FDG synthesis and in principle is very similar to GE TRACERlab FX $_{FDG}$ module . The steps in the fully automated radiosynthesis of [^{18}F]FHBG were summarized in **Table 11.1** as per reaction steps shows in **Fig. 11.2**. Optimization of radio- fluorination temperature and duration of radio-fluorination have been studied using our adapted fluorination module. For doing so, the radio-fluorinated reaction mixture was taken out at different steps of the radiosynthesis and Radio-TLC was developed in suitable solvent (95/5 MeOH/NH_3). The area under the radioactive peak corresponding to [^{18}F]FHBG [The R_f value is verified by developing TLC of reference standard FHBG in Silica Gel 60, F254 TLC plate (The whole plate shows light green fluorescent under UV and the compound spot is visualized by pink coloured spot development)] is directly expressed as the radio-fluorination percentage.

Table 11.1. Flow chart of [^{18}F]FHBG Radiosynthesis

Step I: Radiofluorination of FHBG precursor, Tosyl-FHBG
i) [^{18}F] fluoride trapped on a Chromafix 45-PS-HCO_3 anion exchange cartridge
ii) [^{18}F] fluoride eluted from the column using 75mM $TBAHCO_3$ (0.5 ml, Vial V5) to the reaction vessel
iii) Tetrabutyl ammonium fluoride [^{18}F] dried by azeotropic distillation with acetonitrile (1.0 ml, Vial V1)
iv) Tosyl FHBG (25 mg) dissolved in DMSO (1.0 ml, Vial V2) added to the reaction vessel.
v) Radiofluorination of Tosyl-FHBG is carried out at 135°C for 15 minutes
vi) The reaction mixture is cooled to 75˚C
vii) 1 ml 1N HCl is added to the reaction mixture from V3
viii) Acid hydrolysis was carried out at 125˚C for 6 min
ix) The reaction mixture is cooled to 65˚C
Step II: Purification using Sep Pak® cartridges
x) The reaction mixture is loaded on two conditioned ALUMINA N PLUS Sep Pak® and two Oasis® WAX cartridges stacked together (Alumina N Plus Sep Pak® → Alumina N Plus Sep Pak® → Oasis® WAX→ Oasis® WAX, TOP→ BOTTOM) and the effluent is directed to waste.
xi) 2 ml 80 % ethanol containing water is added to the reaction vessel, rinsed and the cartridges were washed and finally directed to waste.
xii) [^{18}F]FHBG is eluted with 12 ml 25% ethanol containing water.

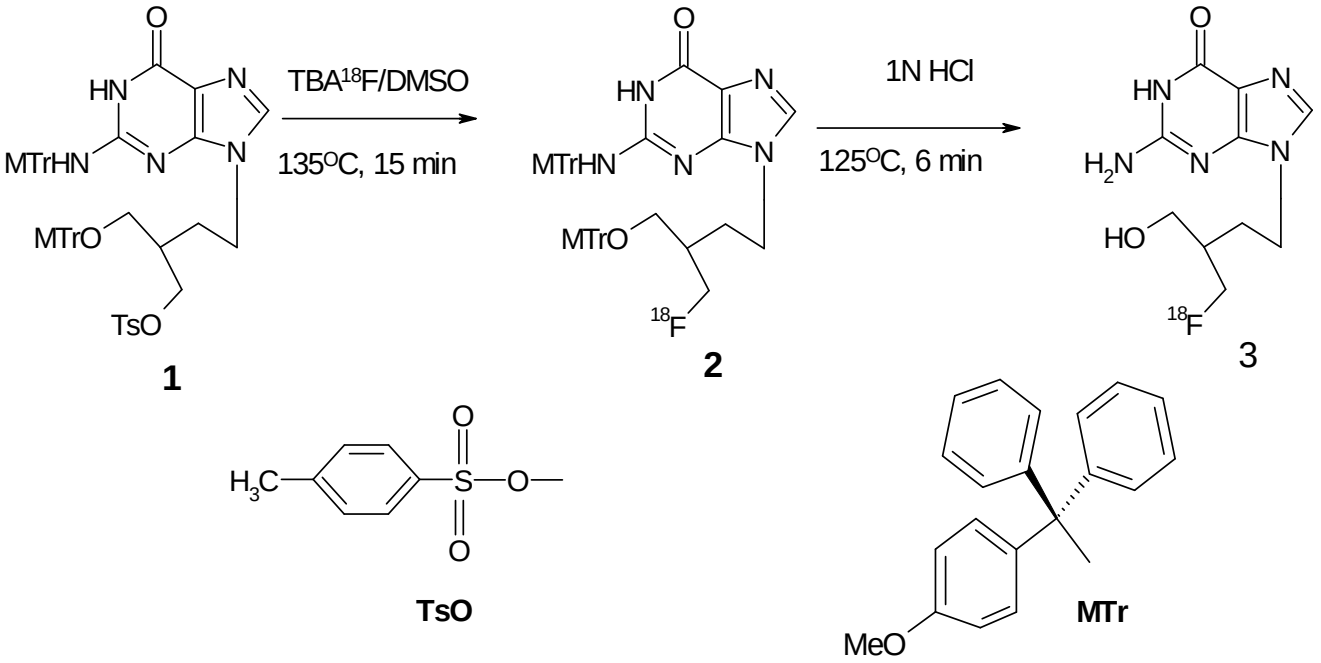

1. N^2-(p-anisyldiphenylmethyl)-9-[(4-tosyl)-3-p-anisyldiphenylmethoxy-methylbutyl] guanine
2. N^2-(p-anisyldiphenylmethyl)-9-[(4-[^{18}F]fluoro)-3-p-anisyldiphenylmethoxy-methylbutyl] guanine
3. 9-[(4-[^{18}F]fluoro)-3-hydroxymethylbutyl]guanine ([^{18}F]FHBG)

Fig.11.2. *Radiosynthesis scheme of [^{18}F]FHBG*

11.2.4. Quality Control

The synthesized [^{18}F]FHBG was checked for clarity (presence of any suspended particle(s)) and colour. The pH was checked with pH-test paper strip. The radiochemical purity was first checked by radio-TLC followed by analytical HPLC. Thin layer chromatography was carried out using methanol/ammonia (95:5) as the mobile phase. The radio chromatograms were acquired at different steps of the synthesis procedure and analyzed. Twenty-five µl of the test solution was injected into the HPLC column and the eluate was monitored for UV (λ = 254 nm) absorbance as well as radioactivity. The mobile phase for eluting consisted of 85% MeCN (solvent A) and 15%

water (solvent B) with 1.0ml/min as well as 2.0ml/min flow rate in an isocratic system. The presence of non-radioactive impurities was also checked under the same HPLC conditions. Finally, [^{18}F]FHBG prepared was confirmed by comparing the retention time of the radioactive peak of the test solution with the UV peak of reference standard [^{19}F]FHBG.

11. 3. Results and Discussion

Starting from the precursor, *Tosyl-FHBG*, [^{18}F]FHBG was synthesized in two steps (radio fluorination and acid hydrolysis) process and purified using Sep Pak® cartridges. The total synthesis time was 35 ± 1 min and the radiochemical yield (without decay correction) was 19.5 ± 1.6 % (n = 5) (**Table 11.2**). The synthesized [^{18}F]FHBG was clear (free of any suspended or colloidal particle), and had a pH between between 5.5-6.0.

Table 11.2. Radiochemical yield of [^{18}F]FHBG

S. No	^{18}F in the reaction vessel (MBq)	[^{18}F]FHBG produced (MBq)	% Yield*
1	555	118.4	21.3
2	1850	329.3	17.8
3	2200	399.6	18.0
4	3700	721.5	19.5
5	3885	813.6	20.9

*** Without decay correction**

The radio-TLC of the radio-fluorinated *Tosyl-FHBG* in 95:5 (MeOH: NH_3) solvent showed two peaks with R_f of 0.09 and 0.6 respectively. The first peak is due to the unreacted [^{18}F]fluoride, as confirmed by developing a separate radio-TLC of TBA^{18}F in the same solvent system. The peak with R_f of 0.6 represents the presence of an ^{18}F-labelled intermediate, Tosyl-[^{18}F]FHBG compound and which is formed by nucleophilic substitution of the leaving group, i.e. –OTs from the precursor , Tosyl FHBG . The TLC of the final purified [^{18}F]FHBG showed a single very prominent peak at R_f (max) of 0.7 (RCP ~ 95%) [**Fig.11.3.**]. That the radioactive peak with R_f

equal to 0.7 was really correspond to [^{18}F]FHBG was verified by developing the TLC of reference standard 4-[^{19}F]FHBG in the same solvent using UV F254 TLC plates [**Fig.11.4.**].

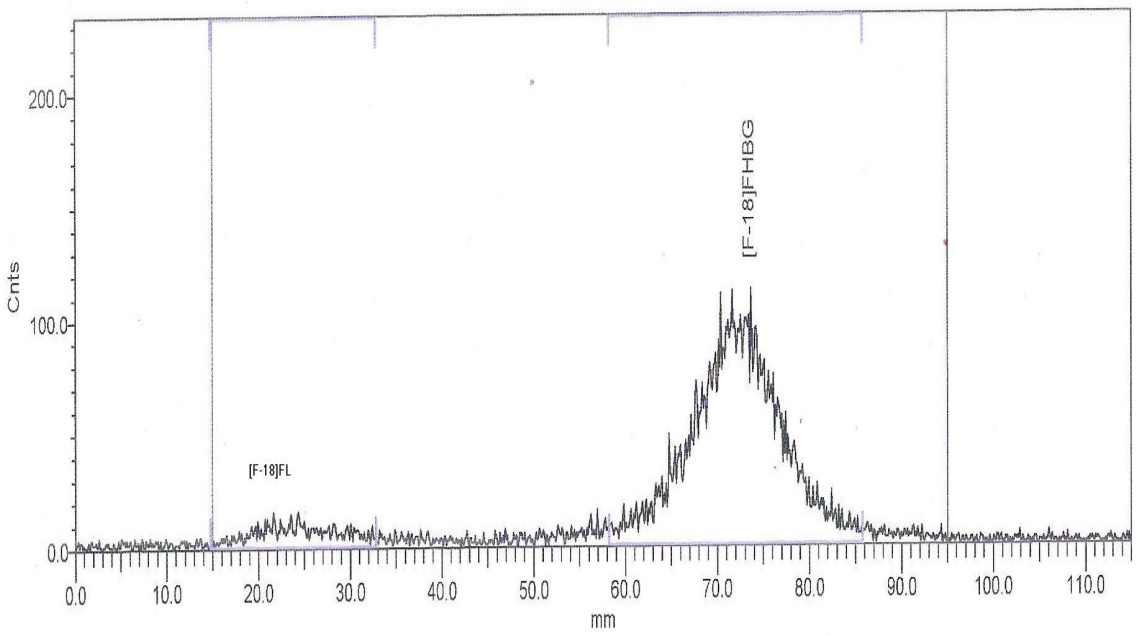

Fig.11.3. *Radio-TLC of [^{18}F]FHBG in MeOH: NH_3 (95:5), R_f value of [^{18}F]FHBG is 0.7*

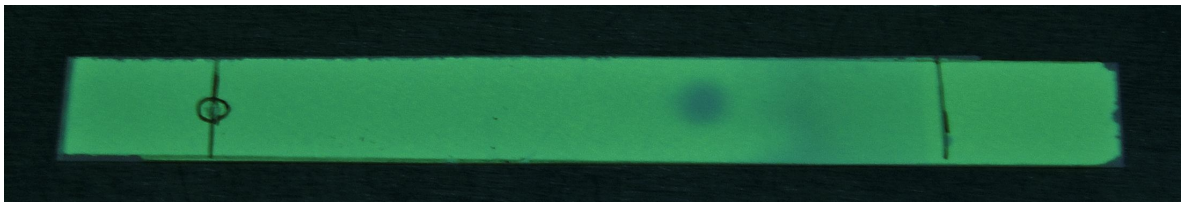

Fig. 11. 4. *TLC of reference standard [^{19}F]FHBG in MeOH: NH_3 (95:5) in Silica Gel 60, F254 TLC plate. The whole TLC plate shows yellow fluorescence under the influence of UV. The compound spot can easily be seen by characteristic violet colour. R_f of [^{19}F]FHBG is 0.65.*

The HPLC chromatogram of the synthesized [^{18}F]FHBG doped with reference standard [^{19}F]FHBG is shown in **Fig. 11.5**. From this figure it is observed that the radio HPLC chromatogram displays single radioactive peak at 1.9 min, and a single UV (λ = 254 nm) peak at

2.13 min. The HPLC chromatogram (UV, λ = 254 nm) of only reference standard [^{19}F]FHBG [**Fig. 11.6.**] shows a single peak with a retention time of 12.5 min.

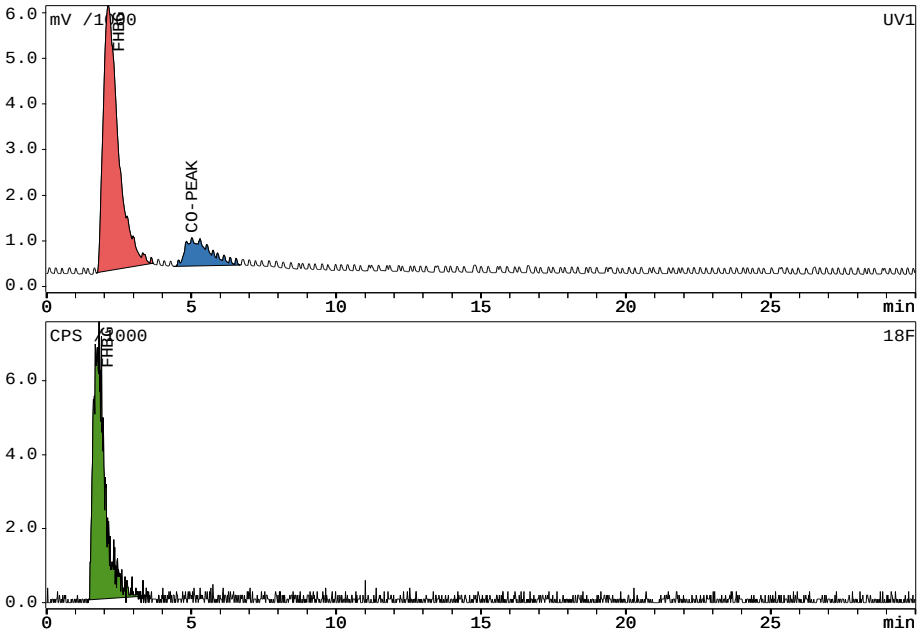

Fig.11.5. *HPLC of [^{18}F]FHBG doped with Ref. Std. FHBG. t_R (FHBG) = 2.13 min, t_R ([^{18}F]FHBG) = 1.8 min, Flow Rate = 1.9 ml/min. C-18 Reverse Phase (5μm, 250x8x4 mm) Solvent : MeCN/H_2O (85/15), UV (λ = 254 nm)*

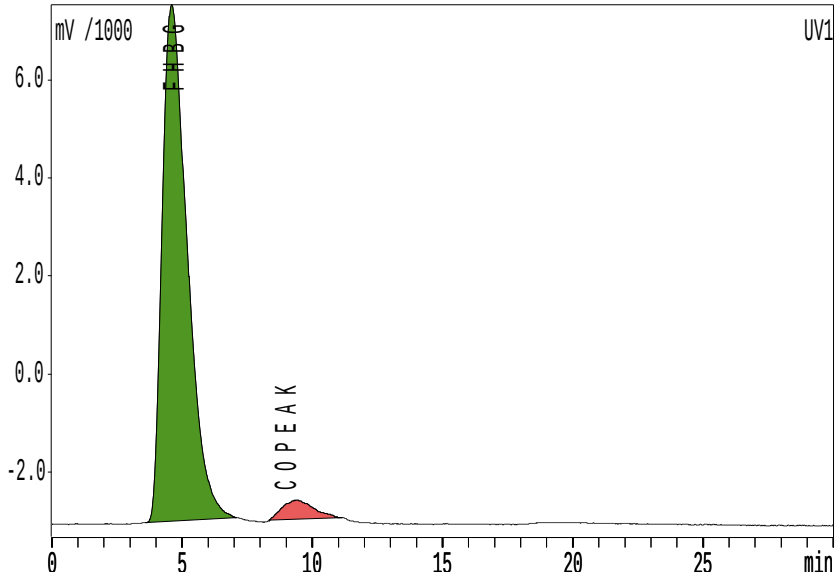

Fig.11.6. *HPLC chromatogram of reference standard [^{19}F]FHBG (UV, λ = 254 nm) t_R = 4.6 min (green peak, the small red peak most probably originates from some impurity present in the reference standard [^{19}F]FHBG) [C-18 RP (5μm, 250x8x4 mm), 1.0 ml/min flow rate, 85/15 MeCN/H_2O solvent]*

The co-elution of the radioactivity peak along with the UV peak of the reference standard [^{19}F]FHBG confirmed that the single radioactive peak corresponds to [^{18}F]FHBG. The difference in the retention times of the radioactivity peak and UV peak is due to the dead volume of the tubing connecting the lead-shielded radioactivity detector attached externally, to the UV detector in the HPLC.

The presence of UV active non-radioactive impurities was also examined. The precursor, Tosyl-FHBG shows a retention time of 9.53 min [**Fig.11.7**.]. The precursor, tosyl-FHBG and reference standard [^{19}F]FHBG are very clearly separated under identical HPLC conditions [**Fig.11.8.**]. Any other UV peak except the peak of the reference standard [^{19}F]FHBG was observed. So, it may be assumed that the synthsized [^{19}F] FHBG is free of any significant non-radioactive impurities.

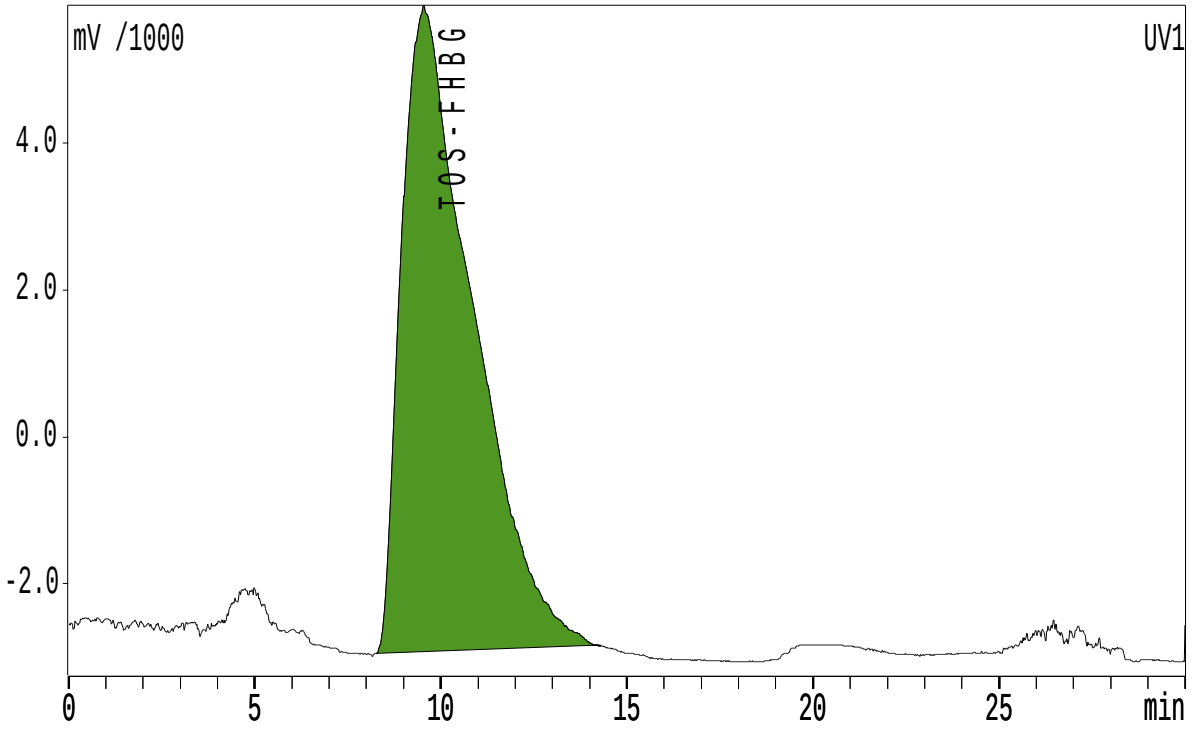

Fig.11.7. *HPLC chromatogram of Tosyl-FHBG (UV, λ = 254 nm) t_R = 9.6 min [C-18 RP (5μm, 250x8x4 mm), 1.0 ml/min flow rate, 85/15 MeCN/H_2O solvent]*

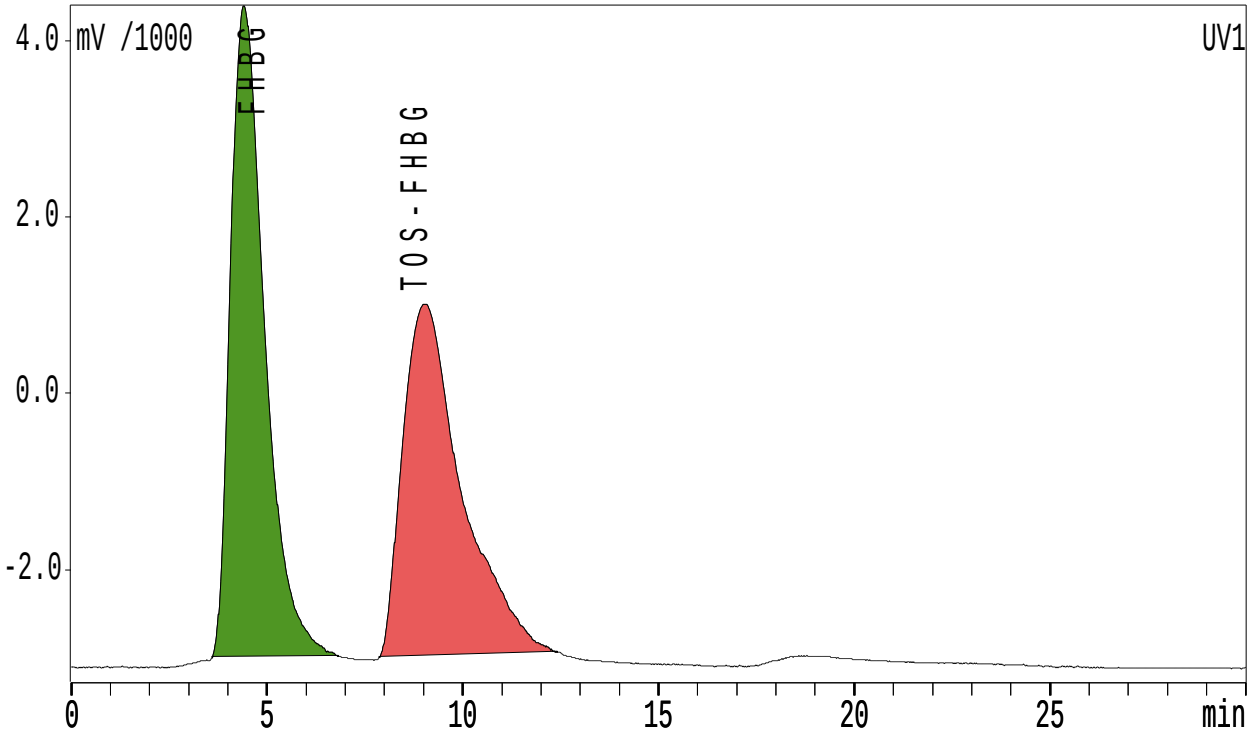

Fig.11.8. *HPLC chromatogram of a mixture of Tosyl-FHBG & reference standard [^{19}F]FHBG (UV, λ = 254 nm), t_R (Ref. Std FHBG) = 4.4 min, t_R (Tosyl FHBG) = 9.1 min [C-18 RP (5μm, 250x8x4 mm), 1.0 ml/min flow rate, 85/15 MeCN/H_2O solvent]*

11.4. Conclusion

A, novel, fully automated radiosynthesis procedure for the synthesis of [^{18}F]FHBG starting form the precursor, Tosyl-FHBG and Sep Pak® purification has been developed. The radiochemical purity of the synthesized [^{18}F]FHBG is around 95% and is free of any non-radioactive impurity. Further, the method is developed using a synthesis module configured for FDG synthesis with good radiochemical yield of 19.5 ± 1.6 % (n = 5) without decay correction in 35 ± 1 min. The synthesis procedure is very simple, fast, reliable and very similar to [^{18}F]FDG synthesis

procedure with consistent radiochemical yield. This new radiosynthesis procedure can easily be implemented in any regular [^{18}F]FDG synthesis module.

References

1. Choppin G.R.; Rydberg J. in Nuclear Chemistry: Theory and Applications; Pergamon Press, Oxford 1980

2. Hevesy G. de. *Biochem J.*, **1923**, *17*, 439.

3. Stöcklin G. in Ullmanns Enzyclopädie der technischen Chemie, Bd. 20: Erzeugung künstillcher Radionuklide; VCH Weinheim **1981**, 25-42.

4. Stöcklin G.; Qaim S. M.; Rösch F. *Radiochim. Acta*., **1995,** 70*/71,* 249.

5. Schicha H.; Schober O. Nuklearmedizin (Compact Lehrbuch), 3. Aufl. Schattenauer Verlag , Stuttgart. **1997.**

6. Quim S. M. *Radiochim.Acta*., **2001**, *89,* 223.

7. Quim S. M. *Radiochim.Acta.*, **2001**, *89,* 297.

8. Bremer K. H. in Ullmanns Enzyclopädie der technischen Chemie, Bd. 20: Erzeugung künstillcher Radionuklide; VCH Weinheim **1981**, 59-64.

9. Wüstenberg T.; Jordan K.; Giesel F. L.; Villringer A. *Der Radiologe*. **2003**, *7*, 552.

10. Stöcklin G. *Nachr. Chem. Tech. Lab.*, **1986**, *34,* 1057.

11. Wienhard, K.; Wagner, R.; Heiss, W. D. in PET-Grundlagen und Anwendung der Positronen Emissions Tomographie, Springer Verlag Heidelberg ,**1989**.

12. Coenen, H. H. *Der Nuklearmadiziner*, **1994**, *17*, 203.

13. Coenen H. H. in Clinical Molecular Anatomic Imaging: PET, PET/CT and SPECT/CT, Ch. 16, PET-radiopharmaceuticals: fluorinated compounds; Lippincott & Wilkins, **2003**.

14. Herzog H. *Radiochim Acta.*, **2001**, *89*, 203**.**

15. Henrich E.; Ebert K.H. *Angew. Chem*., **1992**, *104,* 1310.

16. Ache H. J. *Angew. Chem.*, **1972**, *84*, 234.

17. Pauleit D.; Floeth F.; Hamacher K.; Reimenschneider M. J.; Reifenberger G.; Müller H. –

W.; Zilles K.; Coenen H. H.; Langen K. –J. *Brain*, **2005**,*128*,678.

18. Weber S.; Herzog A.; Cremer M.; Engels R.; Hamacher K.; Kehren F.; Mühlensiepen H., Ploux L.; Reinartz R.; Reinhart P.; Rongen F.; Sonnenberg F.; Coenen H.H.; Halling H. *IEEE Trans. Nucl. Sci.*, **1999**, *46*, 1177.

19. Weber S.; Bauer A.; Herzog A.; Kehren F.; Mühelnisiepen H.; Vogelbruch J.; Coenen H. H.; Zilles K., Halling H. *IEEE Trans. Nucl. Sci.*, **2000**, *47*, 1665.

20. Missimer J.; Madi Z.; Honer M.; Keller C.; Schubiger P. A., Ametamey, S.M. *Phys. Med. Biol.*, **2004**, *49*, 2069.

21. Woody C.; Kriplani A.; O'Connor P.; Pratte J.-F.; Radeka V.; Rescia S.; Schlyer D.; Shokouhi S.; Stoll S.; Vaska P., Villaneuva A.; Volkow N.; Yu B. *Nuc. Inst. and Meth. A* **2004**, *527*, 166.

22. Flower J. S.; Wolf, A.P. *Nuclear Science Series (NAS-NS-3201)*, **1982**.

23. Längström B.; Anderson Y.; Antoni G.; Axelson S.; Bjurling P.; Fasth K.J.; Ge A.; Kihlberg, T.; Ullin J.; Watanabe Y. *Acta. Radiol. Suppl*., **1991**, *376*, 31.

24. Holschbach M.; Schirrmacher R.; Solbach C.; Hamkens W.; Coenen, H.H. *J Label Compds Radiopharm.*, **1997**, *40*, 762 .

25. Längström B.; Antoni G.; Gullberg P.; Halldin C.; Malmborg P.; Någren K.; Rimland A.; Svärd, H. *J Nucl Med.*,**1987**,*28*, 1037.

26. Ehrin E.; Gawell L.; Högberg T.; de Paulis T.; Ström P. *J Label Compounds Radiopharm*. **1987**, *24*, 931.

27. Coenen H.H.; Moerlein S.M.; Stöcklin G. *Radiochim Acta*., **1983**, 34, 47.

28. Pagani M.; Stone-Elander S.; Larsson S.A. *Eur J Nucl Med.*,**1997**, 1302..

29. Plenevaux A.; Guillaume M.; Brihaye C.; Lamaire C.; Cantineau R.*Appl Radiat Isot.*, **1990**,

41, 829.

30. Emert J.; Blum T.; Hamacher K.; Coenen H.H. *Radiochim Acta*., **2001**, *89*, 863.

31. Coenen H. H.; Kling P.; Stöcklin G. *J Nucl Med*., **1989**, 41, 829.

32. Wester H. J.; Hertz M.; Weber W.; Heiss P.; Senekowitsch-Schmidtke R.; Schwaiger M.; Stöcklin, G. *J Nucl Med*.,**1999**, 40, 205.

33. Pauleit D.; Stoffels G.; Schaden W.; Hamacher K.; Bauer D.; Tellimann L.; Herzog H.; Bröer S.; Coenen H. H.; Langen K. –J. *J. Nucl. Med.*, **2005**, *46*, 411..

34. Weckesser M.; Langen K.–J.; Rickert C.H.; Kloska S.; Straeter R.; Hamacher K.; Kurlemann G.; Wassmann H.; Coenen H.H.; Schober O. *Eur J Nucl Med Mol Imaging*. **2005**, *32*, 422 .

35. Reivich M.; Kuhl D.; Wolf A.; Greenberg J.; Phelps M.; Ido T.; Casella V.; Flower J.; Hoffmann E.; Aalavi A.; Som P.; Sokoloff L. *Circ. Res*. **1979**, *44*, 127.

36. Gallagher B.M.; Flower J. S.; Gutterson N. I.; McGregor R. R.; Wan C. N.; Wolf, A. P. *J Nucl. Med.*, **1978**, *19*, 1154.

37. Coleman R. E. *Nucl Med Biol*., **2000**, *27*, 689.

38. Stöcklin, G. *Eur J Nucl Med.*, **1992**, *19*, 527.

39. Knapp F. F.; Mirzadeh S. *Eur J Nucl Med*., **1992**, *21*, 1151.

40. Gould K.L.; Goldstein R. A., Mullani N.A., Kirkeeide R. L.; Wong W.H.; Tewson T.J.; Berridge M.S.; Bolomey L. A.; Hartz R. K.; Smalling R. W.; Facc F. F.; Nishikawa A. *J. Am. Coll. Cardiol.*, 1986, *7*, 775.

41. Quim S. M.; Stöcklin G. *Radiochim Acta.*, **1983**, *34*, 25.

42. Guillaume M.; Luxen A.; Nebeling B.; Argentini M.; Clark J. C.; Pike V. W. *Appl Radiat Isot.*, **1991**, *42* , 749.

43. Hess E.; Takács S.; Scholten B.; Tárkányi F.; Coenen H. H.; Quim, S.M. *Radiochim. Acta.*, **2001**,*89*, 357.

44. Casella V.; Christman D. R.; Ido T.; Wolf A. P. *Radiochim. Acta*., **1978**, *25*, 17.

45. Tilbury R. S.; Dahi J. R. *Radiat. Res*., **1979**, *79*, 22.

46. Retz-Schmidt T.; Weil J.L. *Phys. Rev*., **1960**, *119*, 1079.

47. Leiser K. H. *Einführung in die Kernchemie*, Verlag Chemie, Weinheim **1980**.

48. Atkins P. W. *Physikalische Chemie*, VCH, Weinheim **1990.**

49. Kim D. W.; Ahn D.S.; Oh Y. H.; Lee S.; Kil H.S.; Oh S.J.; Lee S.J.; Kim J.S.; Ryu J.S., Moon D.H.; Chi D. Y. *J Am Chem Soc*., **2006**, *128*, 16394.

50. Lee S.J.; Oh J.; Chi D.Y.; Kil H. S.; Kim E. N.; Ryu J.S.; Moon D.H. *Eur J Nucl Med Mol Imaging*.**2007**,*34*, 1406.

51. Moon B.S.; Lee K.C.; An G.I.; Chi D.Y.; Yang S.D.; Choi C.W.; Lim S.M.; Chun K.S. *J Label Compds Radiopharm.*, **2006**, *49*, 287.

52. Lee S.J.; Oh S.J.; Chi D.Y.; Lee B.S.; Ryu J.S.; Moon D.Y. *J Label Compds Radiopharm*., **2008**, *51*, 80.

53. Coenen H.H. in Synthesis and Application of Isotopically Labelled Compounds (Baille, T.A.; Jones, J.R. (eds.)), No-carrier-added ^{18}F-chemistry of Radiopharmaceuticals, Elsevier Publ. Amsterdum **1989**, 433-448.

54. Coenen H.H.; Klatte B.; Knöchel A.; Schüller M.; Stöcklin G. *J Label Compds Radiopharm*., **1986**, *23*, 455.

55. Block D.; Klatte B.; Knöchel A.; Beckmann R.; Holm U. *J Label Compds Radiopharm.*, **1986**, *23*, 468.

56. Block D.; Coenen H. H.; Stöcklin G. *J Label Compds Radiopharm*., **1987**, *24*, 1029.

57. Coenen H.H. in Progress in Radiopharmacy Development in Nuclear Medicine 10 (Cox, Mather, Sambson, Lazarus, eds.). New radiohalogenation methods: An overview, Martinus Nijhoff Publishers, Dordrecht, **1986**, 196-220.

58. Kilbourn M. R. Fluorine-18 Labelling of Radiopharmaceuticals, *Nuclear Science Series NAS-NS-3203*, National Academy Press Washington D. C.,**1990**.

59. DeGrado T.R.; Wang S.; Holden J.E.; Nickles R.J.; Taylor M.; Stone C.K. *Nucl Med Biol*. **2000a**, *27*, 221.

60. Takahashi T.; Ido T.; Iwata R. *Appl Radiat Isot.*, **1991**, *42*, 801.

61. Hamacher K.; Coenen H.H.; Stöcklin G. *J. Nucl. Med.*, **1986**, *27*, 235.

62. Ding Y.S.; Shiue C.Y.; Flower J.S.; Wolf A.P.; Plenevaux A. *J Fluorine Chem.*, **1990**, *48*, 189.

63. Attina M.; Cacace F.; Wolf A.P. *J Chem Soc Chem Comn*., **1983**, 108.

64. Angelini G.; Speranza M.; Wolf A.P. Shiue, C.Y. Flower J.S.; Watanable M. *J Label Compds Radiopharm.*, **1984**, *21*, 1223.

65. Angelini G.; Speranza M.; Wolf A.P. Shiue C.Y. *J Fluorine Chem.*, **1985**, 27, 177.

66. Coenen H.H. in PET Chemistry-The Driving Force in Molecular Imaging (Chapter 2: Fluorine -18 Labelling Methods: Features and Possibilities of Basic Reactions, pp 15) (Schubiger, Lehmann and Friebe Ed), Springer, **2007**.

67. Snyder S.E.; Kilbourn M.R. in Handbook of Radiopharmaceuticals (Chapter 6: Chemistry of fluorine-18 radiopharmaceuticals, pp 195-227) (Welch, M.J. and Redvanly, C. S. Ed), Wiley, **2003**.

68. Lemaire C.; Cantineau M.G.; Plenevaux A.; Christianens L. *J Nucl Med*., **1991**, *32*, 2266.

69. Katsifis A.; Hamacher K.; Schnitter J.; Stöcklin G. *App. Radiat Isot*., **1993**, *44*, 1015.

70. Shiue C.Y.; Salvadori P.A.; Wolf A.P.; Flower J.S.; MacGregor R.R. *J Nucl Med*, **1982**, 13, 899.

71. Jewett D.M.; Potocki J.F. Ehrenkauffer R. *J Fluorine Chem*., **1984**, *24*, 477.

72. Ehrenkauffer R.; Potocki J.F.; Jewett D.M. *J Nuc. Med.*,**1984**, *25*, 333.

73. Bida G.T.; Satyamurthy N.; Barrio J.R. *J Nucl Med*., **1984**, 25, 1327.

74. Adam M.J.; Abeysekaera B.F.; Ruth T.J.; Jivan S.; Pate B.D. *J Label Compd Radiopharm*., **1984**, *21*, 1227.

75. Coenen H.H.; Moerlein S.M. *J Fluorine Chem*., **1987**, *36*, 63.

76. Hess E.; Sichler S.; Kluge A.; Coenen H.H. *Appl Radiat Isot*., **2002**, 57, 185 .

77. Coenen H.H.; Franken F.; Metwally S.; Stöcklin G. *J Label Compds Radiopharm*.,**1986**, *23*, 1179.

78. Coenen H.H.; Franken F.; Kling P.; Stöcklin G.*Appl Radiat Isot*., **1988**, *39*, 1243.

79. Namavari M.; Bishop A.; Satyamurthy N.; Bisa G.; Barrio J.R. *Appl Radiat Isot.*, **1992**, *43*, 989.

80. de Vries E.F.J.; Luurtsema G.; Brüssermann M.; Elsinga P.H.; Vaalburg W. *Appl Radiat Isot.*, **1999**, 51, 389.

81. Wagner M.F.; Ermert J.; Coenen H.H. *J Nucl Med*., **2009**, *50*, 1724.

82. Block D.; Coenen H.H.; Stöcklin G. *J Label Compds Radiopharm*., **1987,** *24*, 1029.

83. Block D.; Coenen H.H.; StöcklinG. *J Label Compds Radiopharm*., **1988**, *25*, 201.

84. Kilbourn M.R.; Dence C.S.; Welch M.J.; Mathias C.J. *J Nucl Med*., **1987**, *28*, 462.

85. Block D.; Coenen H.H.; StöcklinG. *J Label Compds Radiopharm*., **1988**, *25*, 185.

86. Shai Y.; Kirk K. L.; Channing M.A.; Dunn B.B.; Lesniak M.A.; Eastman R.C.; Finn R.D.; Roth J.; Jacobson K.A. *Biochem*., **1989**, *28*, 4801.

87. Coenen H.H.; Laufer P.; Stöcklin G.; Wienhard K.; Pawlik G.; Böcker-Schwarz H.G.; Heiss W.D.*Life Sciences*, **1987**, *40* , 81.

88. Moerlein S.M.; Perlmutter J.S. *Neurosci. Lett.*, **1991**, *123*; 23.

89. Moerlein S.M.; Perlmutter J.S.*Eur J Pharmacol*., **1992**, *218*, 109.

90. Wilson A.A.; Dasilva J.N., Houle S. *Appl Radiat Isot*. **1995**, *46*, 765.

91. Jelinski M.; Dissertation Unversität zu Köln, Berichte des Forschungszentrum Jülich, JÜL, **2003**, 4044.

92. Guhlke S.; Coenen H.H.; Stöcklin G. *J Nucl Med*.; **1991**, *32*; 1009.

93. Guhlke S.; Wester H.J.; Bruns C.; Stöcklin G. *Nucl Med Biol*., **1994**, *21*. 819.

94. Balu M.; Ganatra R., Bender M.A. *Semin Nucl Med*., **1972**, *2*, 31.

95. Grant F.D.; Fahey F.H.; Packard A.B., Davis R.T.; Alavia Treves, S.T. *J Nucl Med*., **2008**, *28*,68 .

96. Balu M.; Nagler W., Bender M.A. *J Nucl Med*., **1962**, *3*, 332.

97. Thrall J.H. *CRC Crit Rev Clin Radiol Nucl Med*., **1976**, *8*, 1.

98. Davis M.A.; Jones, A.G. *Semin Nucl Med*., **1976**, *6*, 19.

99. Blake G. M.; Park-Holoan S.J.; Cook G.J.R., et al. *Semin Nucl Med*., **2001**, *1*, 28.

100. Wootton R.; Dore C. *Clin Physiol Meas*., **1986**, *7*, 333.

101. Hoh C. K.; Hawkins R.A.; Dahlbom, M., et al. *J Comput Assist Tomogr*., **1993**,17, 34.

102. Toegel S.; Hoffmann O.; Wadsak W., et al. *Eur J Nucl Med Mol Imaging*., **2006**, *33*, 491.

103. Ishiguro K.; Nakagaki H.; Tsuboi S., et al. *Calcif Tissue Int.*, **1993,** *52*, 278.

104. Hockley B.J.; Scott P.J.H. *Appl Radiat Isot*., **2010**, *68*, 117.

105. Even-Sapir E.; Mishani E.; Flusser G.; Metser Ur. *Semin Nucl Med*., **2007**, *37*, 462.

106. Fogelman I.; Cook G.; Israel O.; Van der Wall H. *Semin Nucl Med*., **2005**, *34*, 224.

107. Hetzel M**.;** Arslandemir C.; König H.H.; et al. *J Bone Miner Res*., **2003**,*18*, 2206 .

108. Even-Sapir E, Metser U, Flusser G, et al. *J Nucl Med*., **2004**, *45*: 272.

109. Couturier, Oliver**,**Luxen, André, Chatal, Jean-François; Vuillez, Jean-Philippe, Rigo, Pierre; Hustinx, Roland. *Eur J Nucl Med Mol Imaging*., **2004**, *31*, 1182.

110. Nandy S.K., Rajan M.G.R., Soni P.S. *Indian J Nucl Med*., 2006, 21.

111. Nandy S.K., Rajan M.G.R., Soni P.S., Rangarajan V. *BARC Newsl*., **2007,** *281*, 16.

112. United States Pharmacopoeia (USP). Sodium fluorine F 18 injection. 31.ed. The NF.26.ed.Rockville: The United States Pharmacopoeia Convention, **2008**.p.2195.

113. Avila-Rodriguez M.A., Wilson S.J., McQuarrie A.S.*Appl Radiat Isot*., **2008**, *66*, 1775.

114. Gillies M.J., Najim N**.,** Zweit J. *Appl Radiat Isot*., **2006**, *64*, 431.

115. Timerbaev A.R. *J Chromatogr A*., **1996**, 756, 300 .

116. Spinks J.W.T., Woods R.J., An Introduction to Radiation Chemistry, 2nd. Edn., John Wiley, New York ,**1976**.

117. Solin O., Bergman J., Haaparanta M., Reissell A. *Appl. Radiat Isot*., **1988,** *39*, 1065..

118. ICRP Publication 53: Radiation Dose to patients from Radiopharmaceuticals. Stockholm, Sweden: International Commission on Radiological Protection: **1987**.

119. ICRP Publication 80: Radiation Dose to patients from Radiopharmaceuticals. Stockholm, Sweden: International Commission on Radiological Protection: **1999**.

120. Chang C. W., Chou T.K., Liu R.S., Wang S.J., Lin W.J., Chen C.H., Wang H.E. *Appl Radiat Isot.*,**2007**, 65, 682.

121. www.dnai.org.

122. Rasey J.S., Koh W.J., Grierson J.R., Grunbaum Z., Krohn K.A. *Int J Radiat Oncol Biol Phys.*, **1989**,*17*, 985.

123. Adams G.E., Dewey D.L. *Biochem Biophys Res Commun.*, **1963**, 12, 473.

124. Wiebe L. I. *International Congress Series*., **2004**, *1264*, 53.

125. Rasey J.S., Nelson N.J., Chin L., Evans M.L., Grunbaum, Z. *Radiat Res*., **1990**, 122, 301.

126. Hodgkiss R. *Anti-Cancer Drug Design*., **1998**,*13*, 687.

127. Startford I. and Workman P. *Anti-Cancer Drug Design*., **1998**, *13*, 519.

128. Machulla, H. J. (Ed.); Imaging of Hypoxia-Tracer Developments. Kluwer Academic Publisher, Dordreght, Netharlands, **1999**.

129. Yang D.J., Wallace S., Cherif A, Gretzer M.B., Kim E.E., Podoloff D.A., Li C. *Radiology*., **1995**, *194*, 795.

130. Jerabek P.A., Patrick T.B., Kilbourn M.R., Dischino D.D., Welch M.J. *Int J Rad Appl Instrum [A]*. **1986,** 37, 599.

131. Rasey J.S., Grunbaum Z., Magee S., Nelson N.J., Olive P.L., Durand R.E., Krohn K.A.; *Radiat Res*., **1987**, *111*, 292.

132. Koh W.J., Rasey J.S., Evans M.L., Grierson J.R., Lewellen T.K., Graham M.M., Krohn, K.A., Griffin T.W. *Int J Radiat Oncol Biol Phys*., **1992**, *22*, 199.

133. Martin G.V., Caldwell J.H., Graham M.M., Grierson J.R., Kroll K., Cowan M.J., Lewellen, T.K., Rasey J.S., Casciari J.J., Krohn K.A. *J Nucl Med*., **1992**, *33*, 2202.

134. Rasey J.S., Koh W.J., Evans M.L., Peterson L.M., Lewellen T.K., Graham M.M., Krohn, K.A. *Int J Radiat Oncol Biol Phys*., **1996**, *36*, 417.

135. Varagnolo L., Stokkel M.P., Mazzi U., Pauwels E.K. *Nucl Med Biol.*, **2000**, *27*, 103.

136. Grönross T., Eskola O., Lehtiö K., Minn H., Marjamäki P., Bergman J., Haaparanta M., Forsback S., Solin O. *J Nucl Med*., **2001**, *42*, 1397.

137. Lehtiö K., Oikonen V., Nyman S., Grönross T., Roivainen A., Eskola O., Minn H. *Eur J Nucl Med Mol Imaging.*, **2003**, *30*, 101.

138. Iuliana Toma-Dasu, Alexandru Dasuu and Anders Brahmeu. . Quantifying tumor hypoxia by PET imaging- A theoretical Analysis. Advances In Experimantal Medicine and Biology, ISSN 0065-2598, **2009**, 267-272.

139. Eary J.F., Krohn K.A. *Eur J Nucl Med*., **2000**, *27*, 1737.

140. Valk P.E., Mathis C.A., Prados M.D., Gilbert J.C., Budinger T.F. *J Nucl Med*., **1992**, *33*, 2133.

141. Rajendran J.G., Wilson D.C., Conrad E.U., Peterson L.M., Bruckner J.D., Rasey J.S., Chin, L.K., Hofstrand P.D., Grierson J.R., Eary J.F., Krohn K.A. *Eur J Nucl Med Mol Imaging*., **2003,***30,* 695.

142. Couturier O., Luxen A., Chatal J.C., Vuillez J.P., Rigo P., Hustinx R. *Eur J Nucl Med Mol Imaging.* , **2004**, *31*, 1182.

143. Rajendran J.G., Hendrickson K.R.G., Spence A.M., Muzi M., Krohn K.A., Mankoff D.A. *Eur J Nucl Med Mol Imaging* ., **2006**, *33*, S44-S53 .

144. Rasey J.S., Hofstrand P.D., Chin L.K. Tewson T.J. *J Nucl Med*., **1999**,*40*, 1072.

145. Kachur A.V., Dolbier W.R. Jr, Evans S.M., Shiue C.Y., Shiue G.G., Skov K.A., Baird I.R., James B.R., Li A.R., Roche A., Koch C.J. *Appl Radiat Isot.,* **1999**, *51*, 643.

146. Dolbier W.R. Jr, Li A.R., Koch C.J., Shiue C.Y., Kachur A.V. *Appl Radiat Isot.*, **2001**, *54*, 73.

147. Komar G., Seppänen M., Eskola O., Lindholm P., Grönroos T.J., Forsback S., Sipilä H., Evans S.M., Solin O., Minn H. *J Nucl Med*., **2008**, *49*, 1944.

148. Mahy P., De Bast M., Gillart J., Labar D., Grégoire V. *Eur J Nucl Med Mol Imaging.,* **2006**, *33*, 553.

149. Kumar P., Wiebe L.I., Asikoglu M., Tandon M., McEwan A.J. *Appl Radiat Isot*., **2002**, *57*,

697.

150. Kämäräinen E.L., Kyllonen T., Nihtila O., Bjork H., Solin O. *J Labelled Comp Radiopharm*., **2004**, *47*, 37.

151. Patt M., Kuntzsch M., Machulla H.J. *J Radioanal Nucl Chem*.**1999**, *240*, 925.

152. Tang G., Wang M., Tang X., Gan M., Luo L. *Nucl Med Biol*. **2005**, *32*, 553.

153. Lim J.L., Berridge M.S. *Appl Radiat Isot*., **1993**, *44*, 1085.

154. Nandy S.K., Rajan M.G.R., Korde A., Soni P.S. IAEA-CN-157/025, International conference on Clinical PET and Molecular Nuclear Medicine (IPET 2007), Bangkok, 10-14 November, **2007**.

155. Nandy S.K., Rajan M.G.R., Korde A., Soni P.S. *Quarterly Journal of Nuclear Medicine and Molecular Imaging*, **2008**, *52* (supplement 1)**,** 14th European Symposium on Radiopharmacy and Radiopharmaceuticals (ESRR'08).

156. Nandy Saikat, Rajan M.G.R., Korde A., Krishnamurthy N.V. *Appl Radiat Isot.*, **2010**, *68*, 1937.

157. Channing M.A., Huang B.X., Eckelmann W.C. *Nucl Med Biol*., **2001**, *28*, 469.

158. Nakao R., Kida T., Suzuki K. *Appl Radiat Isot.*, **2005**, *62*, 889.

159. Wu H., Chen L., Gao G., Zhang Y., Wang T., Guo S. *Nano Biomed. Eng.*, **2010**, *2*, 231.

160. Tang Y., Guan X., Su T., Gao N., Wang J. *Colloids and Surfaces A*: *Physiochem Eng.* Aspects., **2009**, 337, 33.

161. Nandy S.K., Rajan M.G.R. *J Radioanal Nucl Chem*. **2010**, *286*, 241.

162. Graeber T.G., Osmanian C., Jacks T., Housman D. E., Koch C.J., Lowe S. W. *Nature*., **1996**, *379*, 88.

163. Rischin, D., Hicks R. J., Fischer R., Binns D., Corry J., Porceddu S. *J Clin Oncol*., **2006**,

24, 2098.

164. Chapman J. D. N. *Engl J Med*. **1979**, *301*, 1429.

165. Rajendran J. G., Mankoff D. A., O'Sullivan F., Peterson L. M., Schwartz D. L., Conrad, E.V., Spence A. M., Muzi M., Farwell D.G., Krohn K.A. *Clin Cancer Res*. **2004**, *10*, 2245.

166. Reischl G., Ehrlichmann W., Bieg C., Solbach C., Kumar P., Wiebe L. I., Machulla H. –J. *Appl Radiat Isot*., **2005**, *62*, 897.

167. Parliament M. B., Chapman J. D., Urtasun R. C. *Br J Cancer*., **1992**, *65*, 90.

168. Groshar D., McEwan A. J. B., Parliament M. B., Urtasun R. C., Golberg L. E., Hoskinson M., Mercer J. R., Mannan R. H., Wiebe L. I., Chapman J. D. *J Nucl Med*., **1993**, 34, 885.

169. Kumar P., Stypinski D., Xia H., McEwan A. J., Machulla H. –J., Wiebe L. I. *J Labelled Compds Radiopharm.* **1999**, 42, 3.

170. Piert M., Machulla H. –J., Reischl G., Ziegler S., Kumar P., Wiebe L.I., Schwaiger M. *J Nucl. Med.* **2002**, 43, 278 .

171. Piert M., Machulla H. -J., Picchio M., Reischl G., Zeigler S., Kumar P., Wester H. –J., Beck R., McEwan A.J.B., Wiebe L.I., Schwaiger M. *J Nucl Med*., **2005**, *46*, 106.

172. Sorger D., Patt M., Kumar P., Wiebe L.I., Barthel H., Seese A., Dannenberg C., Tannaphel A., Kluge R., Sabri O. *Nucl Med Biol*., **2003**, *30*, 317.

173. Kumar P., Emami S., McEwan A.J.B., Wiebe L.I. *Letters in Drug Design & Discovery*. **2009**, *6*, 82.

174. Yuasa M., Yoshida H., Hara T. *Appl Radiat Isot*., **1997**, *48*, 201.

175. Gomzina N.A., Vasil'ev D.A., Karsikova, R.N. *Radiochemistry*. **2002**, *44*, 366.

176. Karsikova R. PET Chemistry: The driving force in molecular imaging. Springer Berlin

Heidelberg Publisher. **2007**, 289-316.

177. Nandy S.K., Rajan M.G.R. *Appl Radiat Isot*. **2010**, *68*, 1944.

178. Impurities: Residual Solvents in New Veterinary Medicinal Products, Active Substances and Excipients, VICH Topic GL18 (Impurities Solvents), June 2000 (Recommended for Implementation at Step 7 of the VICH Process).

179. Kostakoglu L., Agress H., Goldsmith S.J. *RadioGraphics.***, 2003,** *23***:** 315.

180. Mercer J.R. *J Pharm Pharmaceut Sci.,* **2007**, *10*, 180.

181. Mottaghy F.M., Reske S.N. *Pituitary.,* **2006,** *9***,** 237.

182. Adams S., Baum R., Rink T., Schumm-Drager P.M., Usadel K.H., Hor G. *Eur J Nucl Med*., **1998,** *25***,** 79.

183. Adams S., Baum R.P., Hartel A., Schumm-Drager, P.M. Usadel, K.H., Hor G. *Nucl. Med Commun.* **1998,** *19***,** 641.

184. Lee J.D., Yang W.I., Park Y.N**.,** Kim K.S., Choi J.S., Yun M., Ko D., Kim T.S., Cho A.E., Kim H.M., Han K.H., Im S.S., Ahn Y.H., Choi C.W., Park J.H. *J Nucl Med***., 2005,** *46***,** 1753.

185. Torizuka T., Tamaki N., Inokuma T., Magata Y., Sasayama S., Yonekura Y., Tanaka A., Yamaoka Y., Yamamoto K., Konishi J. *J Nucl Med*., **1995**, *36***,** 1811.

186. Zhuang H., Alavi A. *Semin. Nucl Med*., **2002**, *32*, 47.

187. Chang J.M., Lee H.J., Goo J.M., Lee H.Y., Lee J.J., Chung J.K., Im J.G. *Korean J. Radiol***.,** **2006,** 7**,** 57.

188. United States, National Library of Medicine- national Institute of Health, 8600 Rockville

Pike, Bethesda, MD 20894. **Url: http:// www.nlm.nih.gov/**

189. Nanni C., Rubello D., Al-Nahhas A., Fanti S. *Nucl Med Commun*., **2006**, *27*, 685.

190. Shiue C.Y., Welch M.J. *Radiol Clin North Am*., **2004**, *42***,** 1033.

191. Christman D.; Crawford E.J., Friedkin M., Wolf A.P. *Proc Natl Acad Sci. U.S.A***., 1972,** *69***,** 988.

192. Wells P., Gunn R.N., Alison M., Steel C., Golding M., Ranicar A.S., Brady F., Osman S., Jones T., Price P. *Cancer Res.***, 2002,** *62***,** 5698.

193. Shields A.F., Grierson J.R., Dohmen B.M., Machulla H. -J., Stayannoff J.C., Lawhorn-Crews J.M., Obradovich J.E., Muzik O. Mangner T.J. *Nature Medicine*, **1998,** *4***,** 1334.

194. Muzi M., Spence A.M., O'Sullivan F., Mankoff D.A., Wells J.M., Grierson J.R., Link J.M., Krohn K.A. *J Nucl Med*., **2006**, 47**,** 1612.

195. Grierson J.R., Shields A.F. *Nucl Med Biol*., **2000**, *27***,** 143.

196. Mankoff D.A., Shields A.F., Krohn K.A. *Radiol Clin North Am*., **2005**, *43***,** 153.

197. Toyohara J., Waki A., Takamatsu S., Yonekura Y., Magata Y., Fujibayashi Y. *Nucl Med Biol*., **2002**, *29***,** 281.

198. Rasey J.S., Grierson J.R., Wiens L.W., Kolb P.D., Schwartz J.L. *J Nucl Med*., 2002, *43*, 1210.

199. Barthel H., Perumal M., Latigo J., He Q., Brady F., Luthra S.K., Prince P.M., Aboagye E.O. *Eur J Nucl Med Mol Imaging*., **2005**, *32*, 257.

200. Wilson I. K., Chatterjee S., Wolf W. *J Fluor Chem*., **1991**, *55*, 283.

201. Wodarski C., Eisenbarth J., Naber K., Henze M., Haberkorn U., Eisenhut M. *J Labelled Comp Radiopharm* ., **2000**, *43*, 1211.

202. Martin S.J., Eisenbarth J.A., Wagner – Utermann U., Mier W., Henze M., Prizkow H.,

Haberkorn U., Eisenhut M. *Nucl Med Biol*., **2002**, 29, 263.

203. Machulla H.J., Blocher A., Kuntzsch M., Piert M., Wei R., Grierson J.R. *J Radioanal. Nucl Chem.*, **2000**, *243*: 843.

204. Windhorst A.D., Klein P.J., Eisenbarth J., Oeser T., Kruijer P.S., Eisenhut M. *Nucl Med Biol.*,**2008,** *35*, 413.

205. Nandy S.K., Rajan M.G.R., Korde A., Chawdhary P.R. *J Labelled Comp. Radiopharm*., **2007**, *50*, S121.

206. Yun M., Oh S.J., Ha H.J., Ryu J.S., Moon D.H. *Nucl Med Biol.*, **2003**, *30***,**151.

207. Agarwal H.K., Parang K. *Nucleosides Nucleotides Nucleic Acids.***, 2007,** *26*,317.

208. Demirtas I., Buyukkidan B., Elmastas M. *Turk J Chem*., **2002**, *26***,** 889.

209. Rengan R., Chakraborty P.K., Kilbourn M. *J Labelled Comp. Radiopharm.***, 1990,** *33***,** 563.

210. Binkley E.R., Binkley R.W. *Preparative Carbohydrate Chemistry*, Marcel Dekker, New York, **1997**, 88.

211. Tewson T.J., Paulsen A., and el-Shafie F. *J Labelled Comp. Radiopharm*., **2003**, *46***,** S222.

212. Kaul S., Dandekar K.A., Schilling B.E., Barbhaiya R.H. *Drug Metab. Dispos.*, **1999**, *27*, 1.

213. Suehiro M., Vallabhajosula S., Goldsmith S.J., Ballon D.J. *Appl Radiat Isot*., **2007**, *65***,** 1350.

214. Bourgeois M., Mougin-Degraef M., Leost F., Cherel M., Gerstein J.F., Le Bars D., Barbet J. Faivre-Chauvet A. *J Pharm Biomed Anal.*, **2007**,*45*,154.

215. Beck J.R. *Tetrahedron.*, **1978**, *34***,** 2057.

216. Wuts P.G.M., Northuis J.M. *Tet Lett.***, 1998,** *39*, 3889.

217. Attina A., Cacae F., Wolf A.P. *J Labelled Comp Radiopharm*., **1983**, *20*, 501.

218. Vlasov V.M. *Russ Chem Rev*., **2003**, *72*, 681.

219. www.sigmaaldrich.com/catalogue (Product CAS Number: 67-68-5)

220. Choi M.F., Hawkins P. *Spectrochimica Acta*., **1995**, *51A* ,579..

221. Salskov A., Tammisetli S., Grierson J., Vesselle H. *Semin Nucl Med*., **2007**, 37, 429

222. Nandy S.K., Krishnamurthy N.V., Rajan M.G.R. *J Radioanal Nucl Chem*., **2009**, DOI. 10.1007/s 10967-0322-1.

223. Bombardieri E.; Crippa F. *Q J Nucl Med*., **2001**, *45*, 245.

224. Wahl R.L.; Zasadny K.; Helvie M.; Hutchins G.D.; Weber B.; Cody R. *J Clin Oncol*. **1993**, *11*, 2101.

225. Mortimer J.E.; Dehadashti F.; Siegel B.A.; Trinkaus K.; Katzenellenbogen J.A.; Welch, M.J. *J Clin Oncol*. **2001**,*19*, 2797.

226. Stafford S.E.; Gralow J.R.; Schubert E.K.; Rinn K.J.; Dunnwald L.K.; Livingston R.B.; Mankoff D.A. *Acad Radiol*., **2002**, *9*, 913.

227. Burcombe R.J.; Makris A.; Pittam M.; Lowe J.; Emmott J.; Wong W.L. *Eur J Cancer*. **2002**, *38*, 375.

228. Mankoff D.A.; Dunnwald L.K.; Gralow J.R.; Ellis G.K.; Charlop A.; Lawton T.J.; Schubert E.K.; Tseng J.; Livingston R.B. *J Nucl Med*., **2002**, *43*, 500.

229. Rose C.; Thorpe S.M.; Andersen K.W.; Pedersen B.V.; Mouridsen H.T.; Blichert-Toft M.; Rasmussen B.B. *Lancet*., **1985**, *1*, 9.

230. Bertelsen C.A.; Giuliano A.E.; Kern D.H.; Mann B.D.; Roe D.J.; Morton D.L. *J Surg Res*., **1984,** *37*, 257.

231. Clark G.M.; Sledge G.W. Jr; Osborne C.K.; McGuire W.L. *J Clin Oncol*., **1987**, *5*, 55.

232. Van de Wiele C.; De Vos F.; Slegers G. ; Van Belle S. ; Dierckx R.A. *Eur J Nucl Med*., **2000**, *27*, 1421.

233. Dehdashti F., Mortimer J.E., Siegel B.A., Landis K.G., Thomas J.B., Maureen J.F., Diana D.D., Duffy Cutler P., Katzenellenbogen J.A., Welch M.J. *J Nucl Med*.,**1995**,36,1766.

234. Katzenellenbogen J.A., Mathias C.J., Vanbrocklin H.F., Brodack J.W. Welch M.J. *Nucl Med Biol.*, **1993**, 20, 735.

235. Kiesewetter D.O., Kilburn M.R., Landvatter S.W., Heiman D.F., Katzenellenbogen J.A., Welch M.J. *J Nucl Med*.**1984**, *25*,1212.

236. Mathias C.J., Welch M.J., Katzenellenbogen J.A., Brodack J.W., Kilburn M.R., Carlson K.E., Kiesewetter D.O. *Nucl Med Biol.* **1987**,*14:*15.

237. McCurie A.H., Dehdashti F., Siegel B.A., Lyss A.P., Brodak J.W., Mathias C.J., Mintun M.A., Katzenellenbogen J.A, Welch M.J. *J Nucl Med*.,**1991**, *32*, 1526.

238. Mintun M.A., Welch M.J, Siegel B.A., Mathias C.J., Brodak J.W., McCurie A.H., Katzenellenbogen J.A. *Radiology*.,**1988**, *169*, 45.

239. Brodack J.W., Kilburn M.R., Welch M.J., Katzenellenbogen J.A. *J Nucl Med.***1986**, *27*, 714.

240. Lim J.L., Zheng L., Berridge M.S., Tewson T.J. *Nucl Med Biol.*,**1996**, *23*, 911.

241. Berridge M.S., Rosenfold P., Franceschini M.P., Tewson T.J. *J Org Chem*.,**1990**, *55*, 1211.

242. Tewson T.J., Mankoff D.A., Peterson L.M., Woo I., Petra P. *Nucl Med Biol.*,**1999**, *26*, 905.

243. Romer J., Steinbach J., Kasch H. *Appl Radiat. Isot.*,**1996**, *47***,** 395.

244. Oh S.J., Chi, D.Y., Mosdzianowski, C., Kil H.S., Ryu J.S., Moon D.Y. *Appl Radiat. Isot.*, **2007**, *65*, 676.

245. Kumar P., Mercer J., Doerkson C., Tonkin K., McEwan A.J.B. *J Pharm Pharmaceut Sci*.,**2007**, *10***,**256s-265s.

246. Kiesewetter D.O., Katzenellenbogen J.A., Kilburn M.R. and Welch M.J. *J Org Chem*. **1984**, *49,* 4900.

247. Matrik J, Ogasawara A, Martin-McNulty B, Ross J, Flores J E, Gill H S., Tinianow J N, Vanderbilt AN, Nishimura M, Peale F, Pastuskovas C, Greve J. M. *J Nucl Med*., **2009**, *50* , 982.

248. Mori T, Li-Q S, Kobayashi M, Kiyono Y, Okazawa H, Furukawa T, Hidekazu Kawashima, Welch M J, Fujibayashi Y. *Nucl Med Biol*., **2009**, *36*: 155.

249. Muir D.; Berl S.; Clarke D.D. *Brain Res*., **1986.,** *380*: 336.

250. Liu R.S.; Chang C.P.; Chu L.S. et al. *Eur J Nucl Med Mol Imaging.*, **2006**, *33*: 420.

251. Tsuchida T.; Takeuchi H.; Okazawa H.; Tsujikawa T.; Fujibayashi Y. *Nucl Med Biol*., **2008**, *35*, 171.

252. Fonnum F.; Johnsen A.; Hassel B.*Glia.*, **1997**, *21*, 106.

253. Lear J.L.; Ackermann R.F. *Metab Brain Dis*., **1990**, *5*, 45.

254. Clarke D.D. *Neurochem Res.***, 1991,** *16,*1055.

255. Peters R.; Wakelin R.W. *Proc R Soc Lond B Biol Sci*., **1953**, *140,*497.

256. Nishi R., Tong W., Wendt R III, Soghomonyan S., Mukhopadhyay U., Balatoni J., Mawlawi O., Bidaut L., Tinkey P., Brone A., Alauddin M., Gonzalez-Lepera C., Yang B., Gelovani J.G. *Mol Imaging Biol*., **2011**: DOI: 10.1007/s 11307-0110-0485-3

257. Ponde D.E.; Dence C.S.; Oyama N.; Kim J. ; Tai Y.C. ; Laforest R. ; Seigel B.A.; Welch M.J. *J Nucl Med*., **2007**, *48,* 420.

258. Matthies A.; Ezziddin S.; Ulrich E.M. et al. *Eur J Nucl Med Mol Imaging*., **2004**,*31*, 797.

259. Kuge Y.; Hikosaka K.; Seki K.; Ohkura K.; Nishijima K.; Tsukamoto E.; et al. *Nucl Med Biol.*, **2002**,*29*, 303.

260. Kuge Y.; Kawashima H.; Yamazaki S.; Hashimoto N.; Miyake Y. *Nucl Med Biol*., **1996**, *23*, 1009.

261. Yamazaki S.; Fukui K.; Kawashima H.; Kuge Y.; Miyake Y.; Kangawa K. *Ann Nucl Med.*, **1996**, *10*: 395.

262. Inoue O.; Hosoi R.; Momosaki S.; Yamamoto K.; Amitani M; Yamaguchi M. et al. *Nucl Med Biol.*, **2006,** *33*, 985.

263. Momosaki S.; Hosoi R.; Sanuki T.; Todoroki K.; Yamaguchi M.; Gee A. et al. *Nucl Med Biol.*, **2007**, *34*, 939.

264. Mori T, Li-Q S, Kobayashi M, Kiyono Y, Furukawa T, Okazawa H, Fujibayashi Y. *J Nucl Med*., **2007**, *48*, 302P.

265. Howard B.V.; Howard W.J. *Prog Biochem Pharmacol*., **1975**, *10* **,** 135.

266. Swinnen J.V.; Heemers H.; Deboel L.; Foufelle F.; Heyns W.; Verhoeven G. *Oncogene*., **2000**, *19* , 5173.

267. Swinnen J.V.; Van Veldhoven P.P.; Timmermans L.; De Schrijver E.; Brusselmans K.; Vanderhoydonc F.; Van de Sande T.; Heemers H.; Heyns W.; Verhoeven G.*Biochem Biophys Res Commun.*, **2003**, *302*, 898.

268. Visser F.C. *Coron Artery Dis.*, **2001**, *12*: S12-8.

269. Schoder H.; Larson S.M. *Semin Nucl Med*., **2004**, *34*, 274.

270. Patel S.S.; Walt D.R. *J Biol Chem*., **1987**, *262*, 7132.

271. Jeong J.M.; Lee D.S.; Chung J.K.; Lee M.C.; Koh C.S.; Kang S.S. *J Label Compd Radiopharm.,* **1997**, *39* **,** 395.

272. Sykes T.R.; Ruth T.J.; Adam M.J. *Int J Radiat Appl Instrum B.*, **1986**, ***13***, 497.

273. Bosch A.L.; Degrado T.R.; Gatley S.J. *Int J Radiat Appl Instrum A.*, **1986, *37,*** 305.

274. Fuchtner F.; Steinbach J.; Mading P.; Johannesen B. *Appl Radiat Isot.*, **1996,** 47, 61.

275. Sun L.Q.; Mori T.; Dence C.S.; Ponde D.E.; Welch M.J.; Furukawa T.; Yonekura Y.; Fujibayashi Y. *Nucl Med Biol.*, **2006**, *33*,153.

276. Reubi J.C.; Waser B. *Eur J Nucl Med Mol Imaging* **., 2003**, *30*, 781.

277. Behe M.; Behr T.M. *Biopolymers.*, **2002**, *66*, 399.

278. Gabriel M.; Decristoforo C.; Donnemiller E. et al. *J Nucl Med.*, **2003**,*44*, 708.

279. Krenning E.P. ; Kwekkeboom D.J. ; Bakker W.H. et al. *Eur J Nucl Med*., **1993**, *20*, 716.

280. Grewal R.K. ; Dadparvar S. ; Yu J.K. et al. *Cancer J.*, **2002**, *8*, 400.

281. Henze M. ; Schuhmacher J.; Hipp P. et al. *J Nucl Med*., **2001**, *42*, 1053.

282. Jamar F. ; Barone R. ; Mathieu I. et al. *Eur J Nucl Med Mol Imaging.*, **2003**, *30*, 510.

283. Anderson C.J.; Dehdashti F.; Cutler P.T. et al. *J Nucl Med*., **2001**, *42*, 213.

284. Wester H.J.; Schottelius M.; Scheidhauer K. et al. *Eur J Nucl Med.*, **2003**, 30, 117.

285. Stöcklin G.; Wester, H.J. Positron Emission Tomography: A Critical Assessment of Recent Trends. Dordrecht, The Netharlands: Kluwer Academic, **1998**, 57-90.

286. Okarvi S.M. *Eur J Nucl Med*., **2001**, *28*, 929.

287. Wester H.J.; Hamacher K.; Stöcklin G. *Nucl Med Biol.*, **1996**, *23*, 365.

288. Guhlke S.; Coenen H.H.; Stöcklin G. *Appl Radiat Isot.*, **1994**, *45*, 715.

289. Vaidyanathan G.; Zalutsky M.R. *Nucl Med Biol*., **1994**, *24*, 352.

290. Guhlke S.; Wester H.J.; Bruns C.; Stöcklin G. *Nucl Med Biol.*, **1994**, *21*, 819.

291. Wester H.J.; Brockmann J.; Rösch F. et al. *Nucl Med Biol.***1997**, *24*, 275.

292. Vaidyanathan G.; Zalutsky M.R. *Nucl Med Biol.*, **1997**, *24*, 171.

293. Moody T.W.; Leyton J.; Unsworth F.; John C.; Lang L.; Eckelman W. *Peptides.*, **1998**, *19*, 585.

294. Haubner R.; Wester H.J.; Weber W.A. et al. *Cancer Res.*, **2001**, *61*, 1781.

295. Fredriksson A.; Ekberg K.; Ingvar M.; Johansson B.L.; Wahren J.; Stone-Elander S. *Life Sci*., **2002**, *71*, 1361.

296. Bergmann R.; Scheunemann M.; Heiehert C. et al. *Nucl Med Biol.*, **2002**, *29*, 61.

297. Lang L.; Eckelmann W.C. *Appl Radiat Isot*., **1994**, *45*, 1155.

298. Magata Y.; Lang L.; Kiesewetter D.O.; Jagoda E.M.; Channing M.A.; Eckelman W.C. *Nucl Med Biol.*, **2000**, *27*, 163.

299. Poethko T.; Schottelius M.; Thumshim G. et al. *J Nucl Med*., **2004,** 45, 892.

300. Mading P.; Fuchter F.; Wust F. *Appl Radiat Isot*., **2005**, *63*, 329.

301. Maric J.; Sutcliffe I.J. *Appl Radiat Isot.*, **2007**, *65*, 199.

302. Speranza A.; Ortosecco G.; Castaldi E.; Nardelli A.; Pace L.; Salvatore M. *Appl Radiat Isot.*, **2009**, *67*, 1664.

303. Haka M.H.; Kilbourn M.R.; Watkins G.L.; Toorongian S.A. *J Labelled Compds Radiopharm.*, **1989**, *27*, 823.

304. Iwata R.; Pascali C.; Bogni A. et al. *Appl Radiat Isot.*, **2000**, *52*, 87.

305. Lemaire C.; Guillaume M.; Palmer A.J.; Cantineau R. *Appl Radiat Isot*., **1987**, *38*, 1033.

306. Lemaire C.; Damhaut P.; Plenevaux A.; Cantineau R.; Christiaens L.; Guillaume M. *Appl Radiat Isot.*, **1992**, *43*, 485.

307. Culver K.W.; Blaese R.M. *Trends Genet.*, **1994**,*10*, 174.

308. Culver K.W.; Ram Z.; Wallbridges S.; Ishii H.; Oldfield E.H.; Blasé R.M. *Science.* **1992**, *256*, 1550 .

309. Dranoff G.J. *J Clin Oncol.*, **1998**, *16*, 2548.

310. Hauber B.E.; Richard C.E.; Krenitski T.A. *Proc Natl Acad. Sci*. U.S.A., **1991**, 88, 8039.

311. Moolten F.L.; Wells J. M. *Natl Cancer Inst.*, **1990**, *82*, 297.

312. Moolten F.L.; Wells J.M.; Heyman R.A.; Evans R.M. *Human Gene Ther.*, **1990**, *1*, 125.

313. Vile R.G.; Hart I.R. *Cancer Res.*, **1993**, *53*, 3860.

314. Tjuvajev J.G.; Chen S. H .; Joshi A.; Joshi R.; Guo Z.S.; Balatoni J.; Ballon D.; Koutcher J.; Finn R.; Woo S.L.; Blasberg R.G. *Cancer Res.*, **1999**, *59*, 5186.

315. Balsberg R.; Tjuvajev J.G. *Quart J Nucl Med* ., **1999**, *43*, 163 .

316. Weissleder R.; Mahmood U. *Radiology.*, **2001**, *219*, 316 .

317. Robben J.; Reubi J.C.; Pollak Y.; Voorhout G. *Nucl Med Biol*., **2003**, *30*, 225 .

318. De A.; Lewis X .Z.; Gambhir S.S. *Mol Ther.*, **2003,** 7, 681.

319. Brust P.; Haubner R.; Friedrich A. Scheunemann M.; Anton M.; Koufaki O.N.; Hauses M.; Noll S.; Noll B.; Haberkorn U.; Schackert G.; Schackert H.K., Avril N.; Johannsen B. *Eur J Nucl Med.*,**2001,** *28*, 721.

320. Gambhir S.S.; Herschman H.R.; Cherry S.R.; Barrio J.R.; Satyamurthy N.; Toyokuni T.; Phelps M.E.; Larson S.M.; Balatoni J.; Finn R.; Sadelian M.; Tjuvajev J.; Blasberg R. *Neoplasia.*, **2000**, *2*, 118.

321. Alauddin M.M.; Conti P.S. *Nucl Med Biol.*, **1998**, 25, 175.

322. Alauddin M.M.; Conti P.S.; Mazza S.M.; Hamzeh F.M.; Lever J.R. *Nucl Med Biol*., **1996**, *23*, 287.

323. Alauddin M.M.; Shahinian A.;Gordon E.M.; Bading J.R.; Conti P.S. *J Nucl Med*., **2001**, *42*, 1682.

324. Alauddin M.M.; Shahinian A.; Kundu R.K.; Gordon E.M.; Conti P.S. *Nucl Med Biol*., **1999**, *26*, .

325. Yang H.; Berger F.; Tran C.; Gambhir S.S.; Sawyers C.L. *Prostate.*, **2003**, 55, 39.

326. de Vries E.F.; van Waarde A.; Harmsen M.C.; Mulder N.H.; Vaalburg W.L. Hospers G.A. *Nucl Med Biol.*, **2000** , *27*, 113..

327. Gambhir S.S.; Barrio J.R.; Herschman H.R.; Phelps M.E. *Nucl Med Biol*., **1999**, 26, 481.

328. Gambhir S.S.; Barrio J.R.; Phelps M.E.; Iyer M.; Namavari M.; Satyamurthy N. Wu L.; Green L.A.; Bauer E.; MacLaren D.C.; Nguyen K.; Berk A.J.; Cherry S.R.; Herschmann H.R. *Proc Natl Acad Sci.*, U.S.A., **1999**, *96*, 2333.

329. Gambhir S.S.; Bauer E.; Black M.E.; Liang Q.; Kokoris M.S.; Barrio J.R.; Iyer M.; Namavari M.; Phelps M.E.; Herschman H.R. *Proc Natl Acad Sci.*, U.S.A., **2000**, *97*, 2785 .

330. Hakimelahi G.H.; Khalafi-Nezhad A. *Helv Chim Acta*., **1989**, *72*, 1495.

331. Harnden M.R.; Jarvest R.L.; Bacon T. H.; Boyd M.R. *J Med Chem.*, **1987**, *30*, 1636.

332. Hospers G.A.; Calogero A.; van Waarde A.; Doze P.; Vaalburg W.; Mulder N.H.; de Vries E. F. *Cancer Res.*, **2000**, *60*, 1488 .

333. Hustinx R.; Shiue C.Y.; Alavi A.; McDonald D.; Shiue G.G.; Zhuang H.; Lanuti M.; Lambright E.; Karp J.S.; Eck S.L. *Eur J Nucl Med.*, **2001**, *28*, 5.

334. Inubushi M.; Wu J.C.; Gambhir S.S.; Sundaresan G.; Satyamurthy N.; Namavari M.; Yee S.; Barrio J.R.; Stout D.; Chatziioannou A.F.; Wu L.; Schelbert H.R. *Circulation.*, **2003**, *107*,326.

335. Iyer M.; Barrio J.R..; Namavari M.; Bauer E. ; Satyamurthy N. ; Nguyen K.; Toyokuni T.; Phelps M.E.; Herschman H.R.; Gambhir S.S. *J Nucl Med.*, **2001**, *42*, 96 .

336. Martin J.C.; McGee D.P.C.; Jeffrey G.A.; Hobbs D.W.; Smee D.F.; Mattews T. R.; Verheyden J.P.H. *J Med Chem.*, **1986**, *29*, 1384.

337. Pantuk A.J.; Berger F.; Zisman A.; Nguyen D.; Tso C.L., Matherly J.; Gambhir S.S.; Belldegrun A.S. *J Urol.*, **2002**, *168*, 1193.

338. Shiue G.G.; Shiue C.Y.; Lee R.L.; MacDonald D.; Hustinx R.; Eck S.L.; Alavi A.A. *Nucl. Med. Biol.*, **2001**, *28*, 875.

339. Tjuvajev J.G.; Doubrovin M.; Akhurst T.; Cai S.; Balatoni J.; Alauddin M.M., Finn R.; Bornmann W.; Thaler H.; Conti P.S.; Blasberg R.J. *J Nucl Med.*, **2002**, *43*, 1072 .

340. Wu J.C.; Inubushi M.; Sundaresan G.; Schelbert H.R.; Gambhir S.S. *Circulation.*, **2002**, 106, 180.

341. Yaghoubi S.; Barrio J.R.; Dahlbom M.; Iyer M.; Namavari M.; Satyamurthy N.; Goldman R.; Herschman H.R.; Phelps M.E.; Gambhir S.S. *J Nucl Med.*, **2001**,*42*, 1225.

342. Yaghoubi S.S.; Wu L.; Liang Q.; Toyokuni T. ; Barrio J.R.; Namavari M.; Satyamurthy N.; Phelps M.E.; Herschmsn H.R.; Gambhir S.S. *Gene Ther.*, **2001**, *8*, 1072.

343. Schaeffer H.J.; Bauchamp L.; De Marinda P.; Elion G. *Nature.*,**1978**, *272*, 583.

344. Smee D.F.; Boehme R.; Chernow M.; Binko B.P.; Matthews T.R. *Biochem Pharmacol*., **1985**, *34*, 1049.

345. Smee D.F.; Campbell N.J.; Matthews T.R. *Antiviral Res.*, **1985**, *5*, 259.

346. Smee D.F.; Martin J.C.; Verheyden J.P.H.; Matthews T.R. *Antimicrob Agents Chemother.*, **1983**, 23, 676.

347. Sterman D.H.; Treat J.; Litzky L.A.; Amin K.M.; Molnar-Limber K.L.; Wilson J.M.; Albelda S.M.; Kaiser L.R. *Hum Gene Ther.*, **1998**, 9, 2121.

348. Vere Hodge R.A. and Perkins R.M. *Antimicrob Agents Chemother*., **1989**, *33*, 223.

349. Barrio J.R.; Namavari M.; Satyamurthy N.; Srinivasan A.; Herschman H.; Gambhir S.S. et al. *J Nucl. Med.*, **1996**, *37*,193P.

350. Wilson A.A.; Conti P.S.; Dannals R.F.; Ravert H.T.; and Wagner Jr. H.N. *J Label Compd Radiopharm.*, **1991**, *29*. 765.

351. Penuelas I.; Boan J.F.; Marti-Climent J.M.; Barajas M.A.; Narviza I.; Satyamurthy N. et al. *Mol Imaging Biol.*, **2003**, *4*. 415.

352. Ponde D.E.; Dence C.S.; Schuster D.P.; Welch M.J. *Nucl Med Biol*., **2004**, *3*, 133 .

353. Wang J.; Zheng Q.; Fei X.; Mock B.H.; Hutchins G.D. *Bioorg Med Chem Lett.*, **2003**, *13*,3933.

354. Ganghua T.; Xiaolan T.; Hongsheng Li.; Mingfang W.; Baoyuan Li.; Mingqan L.; Hubing W.; Quanshi W. *Nucl Med Commun.*, **2010**, *31*, 211.

355. Chang C.W.; Lin M.; Wu S.Y.; Hsieh C.H.; Liu R.S.; Wang S.J. et al. *Appl Radiat Isot*., **2007**, *65*, 57.

356. Hun Kang S.; Oh S.J.; Lee S.J.; Kang K.W.; Kim S.K.; Lee H.; Lee S.J.; Kim I.H.; Lee, W.K. *Appl Radiat Isot.*, **2009**, *67*, 1758.

LIST OF PUBLICATIONS

Full Paper

1. Production of sterile [^{18}F] NaF for skeletal PET imaging.

S.K.Nandy, M.G.R. Rajan, P. S. Soni, V. Rangarajan.

BARC News Letter., **2007**, *Issue No. 281*, 14-27.

2. Evaluation of the radiochemical impurities arising during the competitive fluorination of nosyl group during the synthesis of 3'-deoxy-3'-fluorothymidine, [^{18}F]FLT.

S.K.Nandy, N.V. Krishnamurthy, M.G.R. Rajan.

Journal of Radioanalytical & Nuclear Chemistry., **2010**, *283*, 245-251.

3. Fully automated and simplified radio synthesis of [^{18}F] 3'-Deoxy-3'-Fluorothymidine using Anhydro Precursor and Single Neutral Alumina Column Purification.

S.K.Nandy, M.G.R.Rajan.

Journal of Radioanalytical & Nuclear Chemistry., **2010**, *283*, 741-748.

4. The possibility of a fully automated procedure for radiosynthesis of fluorine-18-labeled fluoromisonidazole using simplified single, neutral alumina column purification procedure.

Saikat Nandy, M.G.R.Rajan, A. Korde, N.V. Krishnamurthy.

Applied Radiation and Isotopes., **2010**, *68*, 1937-1943.

5. Fully automated radiosynthesis of [^{18}F]Fluoromisonidazole with single neutral alumina column purification: optimization of reaction parameters.

S.K.Nandy, M.G.R.Rajan.

Journal of Radioanalytical & Nuclear Chemistry.,**2010**, *286*, 241-248.

6. Simple, column purification technique for the fully automated radiosynthesis of [^{18}F]Fluoroazomycinarabinoside ([^{18}F]FAZA).

   S.K.Nandy, M.G.R.Rajan.

   Applied Radiation and Isotopes., **2010**, *68*, 1944-1949.

7. Chondroid hamartoma presenting as solitary pulmonary module: Results of dual time point ^{18}F-fluorodeoxyglucose-PET and comparision with ^{18}F-fluorothymidine PET and histiopathology.

   Basu S., **Nandy S**., Rajan M.G.R., Ramadar M., Moghe S.

   Hellenic Journal of Nuclear Medicine., **2011**, *14.(correspondence)*

International Journals (Abstracts)

1. Rapid synthesis of [^{18}F] Fluoro-L-Thymidine with simplified purification using a combination-column.

   S.K.Nandy, M.G.R.Rajan, A. Korde, P.R.Chaudhari & P.S.Soni.

   Journal of Labelled Compounds and Radiopharmaceiticals., **2007**, *50 (S1), pp S1-S510,* P 033.

2. Low cost combination-column for the purification of ^{18}F-FDG produced either by acid or alkali hydrolysis.

   S.K.Nandy, M.G.R.Rajan & P.S.Soni.

   Quarterly Journal of Nuclear Medicine and Molecular Imaging., **2008**, *52 (S1).*

3. Production of [^{18}F]Fluoromisonidazole with a single purification step using neutral alumina column: QC and Bio-distribution study:

S.K.Nandy, M.G.R.Rajan & P.S.Soni.

Quarterly Journal of Nuclear Medicine and Molecular Imaging., **2008**, *52 (S1)*.

4. Radiochemical Analysis of [^{18}F]Fluorothymidine produced from BOC-precursor and purified with a combination column of anion-exchanger and alumina.

S.K.Nandy, N.V. Krishnamurthy and R.M.Rajan.

Journal of Labelled Compounds and Radiopharmaceuticals., **2009**, *52 (S1), S256-S320,* P 202.

5. Fully automated radiosynthesis of [^{18}F] Fluoroestradiol by alkali hydrolysis and simplified column purification.

S.K.Nandy, R.M.Rajan.

Journal of Labelled Compounds and Radiopharmaceuticals., **2009**, *52 (S1),S256-S320*, P 203.

<u>Extended abstract in Inetrnational Atomic Energy Agency organized Symposium</u>

1. Synthesis of [^{18}F]Fluoromisonidazole using a general-purpose fluorination Module and combination purification column.

S.K.Nandy, M.G.R.Rajan, A.Korde & P.S.Soni

IAEA-CN-157/025, International conference on Clinical PET and Molecular Nuclear Medicine (IPET 2007), Bangkok, 10-14 November (2007).

2. Preliminary studies on a rapid radiosynthesis procedure for [^{18}F] FHBG using a Non-HPLC technique.

S.K.Nandy, M.G.R.Rajan, A.Korde & P.S.Soni.

IAEA-CN-157/025, International conference on Clinical PET and Molecular Nuclear Medicine (IPET 2007), Bangkok, 10-14 November (2007).

3. Multipurpose synthesis modules for preparing [F-18]-labeled compounds.

M.G.R.Rajan, **S.K.Nandy** & P.S.Soni.

IAEA-CN-157/025, International conference on Clinical PET and Molecular Nuclear Medicine (IPET 2007), Bangkok, 10-14 November (2007).

4. A simple and one pot fully automated synthesis of 3'-deoxy-3'-[^{18}F]fluorothymidine.

S.K.Nandy, M.G.R.Rajan.

IAEA-CN-185/148, International conference on Clinical PET and Molecular Nuclear Medicine (IPET 2011), Vienna, 8-11 November (2011).

5. A fully automated radiosynthesis of 4-[F-18]fluorobenzaldehyde: a synthon for amine-oxy peptide labelling.

S.K.Nandy, M.G.R.Rajan.

IAEA-CN-185/147, International conference on Clinical PET and Molecular Nuclear Medicine (IPET 2011), Vienna, 8-11 November (2011).

6. A single column purification technique for the fully automated radiosynthesis of [F-18] Fluoroacetate: a potential acetate analog for prostate tumor imaging.

S.K.Nandy, M.G.R.Rajan.

IAEA-CN-185/149, International conference on Clinical PET and Molecular Nuclear Medicine (IPET 2011), Vienna, 8-11 November (2011).

7. A single column purification technique for the fully automated radiosynthesis of [F-18]Ethyl Fluoroacetate([F-18]EFA) as a proradiotracer of [F-18]fluoroacetate([F-18]FA) for the measurement of glial metabolism by PET.

S.K.Nandy, M.G.R.Rajan.

IAEA-CN-185/163, International conference on Clinical PET and Molecular Nuclear Medicine (IPET 2011), Vienna, 8-11 November (2011).